

Nitrogen signaling and nuclear localization of the *Aspergillus nidulans* GATA transcription factor AreA.

by

Cameron Creighton Hunter

B.S., Kansas State University, 2011

AN ABSTRACT OF A DISSERTATION

submitted in partial fulfillment of the requirements for the degree

DOCTOR OF PHILOSOPHY

Interdepartmental Genetics Graduate Program
Department of Plant Pathology
College of Agriculture

KANSAS STATE UNIVERSITY
Manhattan, Kansas

2022

“There is nothing like looking, if you want to find something. You certainly usually find something, if you look, but it is not always quite the something you were after.”

-J.R.R. Tolkien

Abstract

Saprophytic fungi are responsible for the biodegradation and recycling of the majority of organic matter in nature; a process which allows for carbon and nitrogen to be reintroduced into the ecosystem. In order for this process to occur, fungi must have the ability to adapt quickly to changes in nutrient quality and availability within their environment. These rapid adaptations are achieved by the regulation of nutrient utilization gene expression. In *Aspergillus nidulans* the GATA transcription factor AreA activates transcription of nitrogen metabolic genes in response to nutrient availability. During nitrogen poor conditions (nitrogen sources other than ammonium and glutamine), AreA-dependent gene expression increases to activate alternative nitrogen nutrient utilization genes. When nitrogen sources become unavailable (nitrogen starvation conditions), expression of a subset of AreA-dependent genes greatly increases and AreA begins accumulating in the nucleus. Nuclear import of AreA appears to not be strongly regulated, unlike its *Saccharomyces cerevisiae* orthologs, Gln3p and Gat1p, which are regulated by Ure2p in response to sufficient intracellular nitrogen. In contrast, AreA nuclear localization is regulated by blocking its nuclear export via the exportin CrmA in response to nitrogen starvation. Previous research demonstrated that a hemagglutinin (HA) epitope-tagged AreA, AreA^{HA}, begins transitioning from the cytoplasm to the nucleus when cells become nitrogen starved, and after 4 hours of nitrogen starvation, AreA^{HA} is completely localized to the nucleus. This increase in nuclear localization parallels the activity increase observed during nitrogen starvation in AreA-dependent reporter gene assays. The research presented in this dissertation aims to understand the mechanisms and pathways involved in regulating the function and intracellular dynamics of the GATA transcription factor AreA as it pertains to nitrogen metabolism in *Aspergillus nidulans*. In Chapter 3, we identify the sequences within the AreA protein that are critical for import of AreA into the nucleus. We analyze the role of the six proposed Nuclear Localization Sequences (NLS)s within AreA in their native context by using in-frame deletions or point mutations of the NLSs separately and in combination. We also determine which NLSs are sufficient for nuclear localization when fused to Green Fluorescent Protein (GFP). Both of these approaches demonstrate that the multiple NLSs play redundant roles contributing to AreA nuclear localization. In Chapter 4, we move our

investigation to the mechanism of AreA nuclear accumulation by investigating the role of the α -importin KapA in AreA nuclear import and the effects SumO, the small ubiqutin-like modifier, has on the subcellular localization of both KapA and AreA. We also analyze the effects of nutrient signaling on AreA nuclear localization. We identify components of the Target of Rapamycin (TOR) signaling pathway as well as the autolysis pathway, via the transcription factor XprG which mediates aspects of starvation, that play roles in regulating AreA nuclear accumulation. In Chapter 5, we investigate how nitrogen is sensed by assessing the effects of ammonium concentration, the role AreA DNA binding mutants have on AreA nuclear accumulation, and how nitrogen metabolic mutants affect colonial growth and AreA nuclear accumulation on different nitrogen sources. Overall, this work advances our understanding of nitrogen regulation in fungi by the key transcription factor AreA by identifying key components that mediate and regulate AreA nuclear localization.

Nitrogen signaling and nuclear localization of the *Aspergillus nidulans* GATA transcription factor AreA.

by

Cameron Creighton Hunter

B.S., Kansas State University, 2011

A DISSERTATION

submitted in partial fulfillment of the requirements for the degree

DOCTOR OF PHILOSOPHY

Interdepartmental Genetics Graduate Program
Department of Plant Pathology
College of Agriculture

KANSAS STATE UNIVERSITY
Manhattan, Kansas

2022

Approved by:

Major Professor
Dr. Richard B. Todd

Copyright

© Cameron Hunter 2022.

Abstract

Saprophytic fungi are responsible for the biodegradation and recycling of the majority of organic matter in nature; a process which allows for carbon and nitrogen to be reintroduced into the ecosystem. In order for this process to occur, fungi must have the ability to adapt quickly to changes in nutrient quality and availability within their environment. These rapid adaptations are achieved by the regulation of nutrient utilization gene expression. In *Aspergillus nidulans* the GATA transcription factor AreA activates transcription of nitrogen metabolic genes in response to nutrient availability. During nitrogen poor conditions (nitrogen sources other than ammonium and glutamine), AreA-dependent gene expression increases to activate alternative nitrogen nutrient utilization genes. When nitrogen sources become unavailable (nitrogen starvation conditions), expression of a subset of AreA-dependent genes greatly increases and AreA begins accumulating in the nucleus. Nuclear import of AreA appears to not be strongly regulated, unlike its *Saccharomyces cerevisiae* orthologs, Gln3p and Gat1p, which are regulated by Ure2p in response to sufficient intracellular nitrogen. In contrast, AreA nuclear localization is regulated by blocking its nuclear export via the exportin CrmA in response to nitrogen starvation. Previous research demonstrated that a hemagglutinin (HA) epitope-tagged AreA, AreA^{HA}, begins transitioning from the cytoplasm to the nucleus when cells become nitrogen starved, and after 4 hours of nitrogen starvation, AreA^{HA} is completely localized to the nucleus. This increase in nuclear localization parallels the activity increase observed during nitrogen starvation in AreA-dependent reporter gene assays. The research presented in this dissertation aims to understand the mechanisms and pathways involved in regulating the function and intracellular dynamics of the GATA transcription factor AreA as it pertains to nitrogen metabolism in *Aspergillus nidulans*. In Chapter 3, we identify the sequences within the AreA protein that are critical for import of AreA into the nucleus. We analyze the role of the six proposed Nuclear Localization Sequences (NLS)s within AreA in their native context by using in-frame deletions or point mutations of the NLSs separately and in combination. We also determine which NLSs are sufficient for nuclear localization when fused to Green Fluorescent Protein (GFP). Both of these approaches demonstrate that the multiple NLSs play redundant roles contributing to AreA nuclear localization. In Chapter 4, we move our

investigation to the mechanism of AreA nuclear accumulation by investigating the role of the α -importin KapA in AreA nuclear import and the effects SumO, the small ubiqutin-like modifier, has on the subcellular localization of both KapA and AreA. We also analyze the effects of nutrient signaling on AreA nuclear localization. We identify components of the Target of Rapamycin (TOR) signaling pathway as well as the autolysis pathway, via the transcription factor XprG which mediates aspects of starvation, that play roles in regulating AreA nuclear accumulation. In Chapter 5, we investigate how nitrogen is sensed by assessing the effects of ammonium concentration, the role AreA DNA binding mutants have on AreA nuclear accumulation, and how nitrogen metabolic mutants affect colonial growth and AreA nuclear accumulation on different nitrogen sources. Overall, this work advances our understanding of nitrogen regulation in fungi by the key transcription factor AreA by identifying key components that mediate and regulate AreA nuclear localization.

Table of Contents

List of Figures	xiii
List of Tables.....	xv
Acknowledgements	xvii
Dedication	xix
Chapter 1 - Introduction & Objectives	1
1.1 Transcription factors in fungi	1
1.2 <i>Aspergillus nidulans</i> as a model for studying nitrogen regulation	2
1.3 Nitrogen regulation by AreA	3
1.4 Research Objectives	7
Chapter 2 - Experimental Procedures.....	9
2.1 Strains	9
2.2.1 <i>Aspergillus nidulans</i> strains.....	9
2.2.2 <i>Escherichia coli</i> strains.....	9
2.2 Methods	18
2.2.1 <i>A. nidulans</i> strains, media, and growth conditions	18
2.2.2 Bacterial media and growth conditions.....	18
2.2.3 FGSC gene knockout strains	18
2.3 Molecular techniques	19
2.3.1 DNA manipulation.....	19
2.3.2 Polymerase Chain Reaction	19
2.3.3 Southern Blot.....	20
2.3.4 β -galactosidase assays.....	20
2.3.5 5-FOA selection for loss of <i>Afp_{pyrG}</i> deletion cassettes.....	20
2.3.6 Sequence analysis.....	20
2.3.7 Immunostaining, Immunofluorescence, and GFP Microscopy.....	21
2.3.8 Abbreviations of varying degrees of usefulness	23
Chapter 3 - Nuclear Localization of the GATA transcription factor AreA	25
3.1 Abstract.....	25
3.2 Contribution statement	26

3.3 Introduction.....	27
3.4 Materials and Methods	31
3.4.1 Strain Construction.....	31
Construction of <i>gpd(p)areA^{HA}</i> NLS mutants via two-step gene replacement	31
Mutation of the bipartite NLS	31
NLS mutant combinations.....	31
Construction of GFP-NLS fusions.....	33
GFP strains	34
3.4.2 <i>Aspergillus nidulans</i> strains used in Chapter 3.....	35
3.4.3 Oligonucleotides used in this study.....	38
3.5 Results.....	39
3.5.1 AreA has multiple conserved Nuclear Localization Signals.....	39
3.5.2 Effects of mutation of AreA classical NLSs on AreA activity	41
3.5.3 Analysis of the effects of NLS mutations in AreA	44
3.5.3.a Analysis of AreA classical NLS mutations on nuclear accumulation	44
3.5.3.b A non-canonical bipartite NLS in AreA is conserved with mammalian GATA-4	44
3.5.4 Identification of AreA NLSs sufficient for nuclear localization.....	47
3.5.4.a Construction of the GFP-NLS fusion proteins.....	47
3.5.4.b Analysis of GFP-NLS fusions	49
3.5.5 Construction and preliminary analysis of a <i>gpd(p)gfp::areA</i> fusion protein.....	51
3.6 Discussion	54
Chapter 4 - Regulation of AreA nuclear accumulation	57
4.1 Abstract.....	57
4.2 Introduction.....	59
4.2.1 Overview of the nuclear pore and the general mechanisms of nuclear import....	59
4.2.2 The α -Importin KapA	61
4.2.3 SumO modification and its role in nuclear localization	61
4.2.4 The TOR Signaling Pathway	62
4.2.5 Autolysis and Autophagy in <i>A. nidulans</i>	64
4.2.6 Regulation of AreA nuclear import.....	64

4.3 Materials and Methods	65
4.3.1 Strain construction.....	65
FGSC gene knockout strains	65
4.3.2 Molecular techniques.....	68
4.3.3 Immunostaining, immunofluorescence, and direct fluorescence microscopy	68
4.4 Results.....	69
4.4.1 The α -importin KapA aids in AreA nuclear localization.....	69
4.4.1.a Subcellular co-localization of KapA::GFP and AreA ^{HA}	69
4.4.1.b Construction of the <i>kapA</i> ^{S111F} point mutant.....	71
4.4.1.c Effects of <i>kapA</i> ^{S111F} on AreA subcellular localization.....	75
4.4.1.d Effects of <i>kapA</i> ^{S111F} on AreA NLSs::eGFP.....	77
4.4.1.e KapA overexpression leads to loss of AreA ^{HA} nuclear accumulation.....	78
4.4.2 The Relationship between SumO, AreA, and KapA.....	80
4.4.2.a Effects of <i>sumO</i> Δ and SumO overexpression on <i>A. nidulans</i> growth and AreA ^{HA} subcellular localization.....	80
4.4.2.b Effects of <i>sumO</i> Δ on KapA::GFP subcellular localization	83
4.4.2.c Effects of <i>sumO</i> overexpression on KapA::GFP subcellular localization	85
4.4.2.d Effects of <i>kapA</i> overexpression on AreA ^{HA} subcellular localization in a <i>sumO</i> Δ mutant.....	88
4.4.3 TOR signaling pathway components regulate AreA nuclear accumulation.....	90
4.4.3.a Rapamycin Inhibits AreA nuclear accumulation.....	90
4.4.3.b Identifying a functional homologue for Ure2p: the Gln3p cytoplasmic anchor	92
4.4.3.b.i <i>gstA</i> does not inhibit AreA nuclear accumulation	92
4.4.3.b.ii AN3255 Δ URE2.....	93
4.4.3.c Analysis of TOR pathway deletions on AreA ^{HA} nuclear localization.....	95
4.4.3.d XprG links Autolysis and regulation to AreA.....	97
4.5 Discussion	99
The role of KapA and SUMO in AreA nuclear accumulation	99
The role of the TOR pathway in AreA nuclear accumulation	102
Chapter 5 - Nitrogen sensing and AreA nuclear accumulation in <i>Aspergillus nidulans</i>	105

5.1 Abstract.....	105
5.2 Introduction.....	106
5.3 Materials and Methods	109
5.3.1 Strain Construction.....	109
5.3.2 Molecular techniques.....	113
5.3.3 Construction of <i>gpd(p)areA102^{HA}</i>	113
5.3.4 Construction of <i>gpd(p)areA217^{HA}</i>	114
5.3.5 Immunostaining, and Immunofluorescence Microscopy.....	114
5.4 Results.....	116
5.4.1 The effects of ammonium concentration on AreA nuclear accumulation	116
5.4.2 The effects of DNA-binding domain mutants on nitrogen sensing in <i>A. nidulans</i>	118
5.4.2.a The classical <i>areA</i> zinc finger DNA-binding domain mutants alter colonial growth of <i>A. nidulans</i> on alternative nitrogen sources	118
5.4.2.b Analysis of DNA-binding mutants on the nuclear accumulation of AreA ^{HA} .	123
5.4.2.c Construction of a strain with wild-type <i>areA</i> at <i>wA</i> and <i>gpd(p)areA217^{HA}</i> at the native <i>areA</i> locus.....	128
5.4.2.d Analysis of wild-type <i>areA</i> targeted to <i>wA</i> in a <i>gpd(p)areA217^{HA}</i> strain.....	131
5.4.3 The role of nitrogen metabolic mutants on nitrogen sensing via AreA ^{HA} nuclear accumulation.....	133
5.5.1 The effects of ammonium concentration on colonial growth and AreA ^{HA} nuclear accumulation.....	137
5.5.2 The role of DNA-binding mutants on nitrogen sensing and AreA nuclear accumulation.....	138
5.5.3 The role of metabolism in nitrogen sensing.....	140
Chapter 6 - Discussion and Future Directions	143
References	147
Appendix A - Hunter <i>et al.</i> , 2014	166

List of Figures

Figure 1.1 Overview of nitrogen metabolism regulation	6
Figure 3.1 Nuclear Localization Signals in AreA.....	39
Figure 3.2 AreA NLS protein sequence alignment	40
Figure 3.3 Effects of the mutations of AreA NLSs on <i>A. nidulans</i> growth.....	42
Figure 3.4 Effects of mutation of AreA NLSs on AreA-dependent gene expression.....	43
Figure 3.5 The effects of mutating the AreA NLSs on AreA ^{HA} nuclear accumulation	46
Figure 3.6 <i>gpd(p)::egfp::areANLS</i> fusion gene construct.....	48
Figure 3.7 Subcellular distribution of GFP-NLS proteins	50
Figure 3.8 Strategy for construction of a <i>gfp::areA</i> fusion gene.....	52
Figure 3.9 Construction of a functional GFP-AreA ^{HA} fusion protein	53
Figure 4.1 General overview of nuclear import and export.....	60
Figure 4.2 Rudimentary TOR signaling pathway in <i>S. cerevisiae</i>	63
Figure 4.3 Co-localization of AreA ^{HA} and KapA::eGFP	70
Figure 4.4 <i>kapA</i> ^{S111F} two-step gene replacement strategy.....	73
Figure 4.5 <i>kapA</i> ^{S111F} growth phenotype	74
Figure 4.6 Localization of AreA ^{HA} in a <i>kapA</i> ^{S111F} mutant	76
Figure 4.7 Localization of GFP::NLSs in a KapA ^{S111F} mutant strain.....	77
Figure 4.8 Loss of AreA ^{HA} nuclear accumulation in a <i>kapA</i> overexpression strain.....	79
Figure 4.9 Colonial growth of <i>sumO</i> Δ strains.....	81
Figure 4.10 AreA ^{HA} subcellular localization in <i>sumO</i> Δ and overexpression strains	82
Figure 4.11 Co-localization of AreA ^{HA} and KapA::eGFP in a <i>sumO</i> Δ background.....	84
Figure 4.12 Subcellular localization of AreA ^{HA} and KapA::eGFP in a <i>sumO</i> overexpression strain on 1% glucose	86
Figure 4.13 Subcellular localization of AreA ^{HA} and KapA::eGFP during <i>sumO</i> overexpression on 1% xylose	87
Figure 4.14 <i>kapA</i> overexpression in a <i>sumO</i> Δ mutant.....	89
Figure 4.15 Localization of AreA ^{HA} in the presence of rapamycin.....	91
Figure 4.16 Localization of AreA ^{HA} in a <i>gstA</i> Δ and a <i>gstA</i> overexpression strain	92

Figure 4.17 Clustal-Ω sequence alignment of GstA and AN3255 to <i>S. cerevisiae</i> URE2p	93
Figure 4.18 Subcellular distribution of AreA ^{HA} in an AN3255Δ strain.....	94
Figure 4.19 Localization of AreA ^{HA} in TOR pathway deletion mutants	96
Figure 4.20 Effects of the <i>atgHΔ</i> , <i>xprG2</i> , and <i>xprGΔ</i> mutations on AreA ^{HA} nuclear accumulation	98
Figure 4.21 Working model of TOR pathway control of AreA nuclear import	103
Figure 5.1 Wild type <i>A. nidulans</i> colony growth and AreA ^{HA} subcellular localization on decreasing ammonium concentrations.....	117
Figure 5.2 Construction and growth phenotypes of <i>gpd(p)areA102^{HA}</i>	120
Figure 5.3 Construction and growth phenotypes of <i>gpd(p)areA217^{HA}</i> mutants.....	121
Figure 5.4 Growth of DNA-binding mutants on decreasing ammonium concentrations	122
Figure 5.5 Mutations in the <i>areA</i> DNA-binding mutants	124
Figure 5.6 Nuclear localization of the classical AreA ^{HA} DNA-binding mutants on a range of nitrogen sources	126
Figure 5.7 Nuclear localization of the AreA ^{HA} DNA-binding mutants on a range of nitrogen sources.....	127
Figure 5.8 Two-step PCR fusion strategy	130
Figure 5.9 Colonial growth and nuclear localization of AreA217 ^{HA} in a <i>gpd(p)areA217^{HA}</i> mutant expressing wild type <i>areA</i> at the <i>wA</i> locus.....	132
Figure 5.10 Nitrogen assimilation in <i>A. nidulans</i>	133
Figure 5.11 Colonial growth and AreA ^{HA} localization in nitrogen metabolic mutants	135
Figure 5.12 Colonial growth of the <i>glnAΔ</i> mutant in comparison to wild-type <i>areA^{HA}</i> and <i>areAΔ</i> strains on various nitrogen sources and concentrations	136

List of Tables

Table 2.1 “Michael Hynes” <i>Aspergillus nidulans</i> strains.....	10
Table 2.2 “Richard Todd” <i>Aspergillus nidulans</i> strains constructed by others.....	12
Table 2.3 “Richard Todd” <i>Aspergillus nidulans</i> strains constructed by Hunter	13
Table 3.1 Survey of NLSs experimentally confirmed in <i>A. nidulans</i>	28
Table 3.2 AreA ^{HA} strains and strains used for construction in Chapter 3.....	35
Table 3.3 Oligonucleotides used in this study	38
Table 4.1 <i>Aspergillus nidulans</i> strains used in Chapter 4.....	65
Table 4.2 Identification of the TOR pathway genes.....	91
Table 5.1 <i>Aspergillus nidulans</i> strains used in Chapter 5.....	109

It's dangerous to go alone.

Take this.

Acknowledgements

I find myself wondering where to begin as I sit here at the end gazing back towards the past. This journey has been complicated with many twists and turns. Many people have had a significant impact on me completing this journey. Some which have offered a helping hand at the right time, some who chose to be my companion for a season or two, and some real lunatics who saw the chaos of my adventures, smirked, grabbed their gear, and have been fighting dragons and demons alongside of me while reciting epic poems of our adventures ever since. To all of you, Thank you. You have all meant so much to me. I needed all of the kindness that was given, all of the laughter, and all of the love bestowed. Some of you deserve more than this small gesture, for those, I am sorry. I hope this gesture can be viewed with eyes unclouded and be known. To the lunatics, you stood beside me and laughed as the storms rolled through. You provided a guiding light for me when the night was darkest. I would truly be lost without you.

I can't put words to the appreciation and gratitude that I have for my advisor, Richard Todd. This has been an interesting chapter in our lives. You took a chance on me. I know it hasn't been an easy road, but it is one I would travel with you again. You have taught me how to be a scientist. You showed me what true passion and dedication looks like. You made me part of your family. Thank you. I am eternally grateful.

To my committee Barbara Valent, Revathi Govind, and Kathrin Schrick, thank you for all of your guidance and encouragement. You have been advisors, supporters, confidants, and you have always challenged me to keep learning and growing. I am truly blessed to have had each one of you on my committee.

I want to thank the members of the Todd Lab and the Plant Pathology Department. Kendra, Grethel, Damien, Brandon, Anna, and Joel. You were all amazing. You made my days in the lab some of the happiest and most interesting days of my life. Jen, thanks for the endless kindness, support, and guidance through the hoops of academia. Dr. Leslie, Dr. Draper, and Dr. Kennelly, thank you for going out of your way to make sure I felt safe and secure during the most uncertain times of my research.

I want to thank my family. I love you all. Mom, Dad, and Laurisa, you taught me to be inquisitive, to be passionate, to work hard, be smart, and have fun. You encouraged me to strive for more and to never give up. Grandma Jean, you showed me the importance of education and self improvement as a life-long concept. Thank you for all of your enthusiasm and encouragement during my studies.

Lastly, I want to thank my wife. Kari, I love you. None of this would have been possible without you. You have been the queen of my merry band of lunatics. The seas have been rough, but we did it! You fill my life with happiness. You inspire me. I can't wait to see where our next adventure leads us.

Dedication

This work is a dedication in three parts:
Jean Hunter, Kari Hunter, and Jim Weaver.

Jean,

For being a model for the pursuit of education as a life-long concept. Thank you for all of our lovely conversations. I am looking forward to the next one.

Kari,

In this life and all the rest.

Jim,

For I believe that real promises should be kept.
Dangerous ideas or not.

Your best is all you can give
and all the world needs. XO

Chapter 1 - Introduction & Objectives

1.1 Transcription factors in fungi

Fungi have a remarkable ability to adapt quickly to changes in their environment. This is achieved in large part by extensive networks of transcriptional gene regulation. In eukaryotes, transcription is regulated by proteins called transcription factors, which interact with specific DNA sequences in the promoter region upstream of a gene to activate or to repress transcription (LATCHMAN 1997). There are many different classifications of transcription factors, which have been comprehensively studied. They have been organized by the sequence similarity of their DNA binding domains (DBDs). C2H2 zinc fingers, basic-region leucine zipper (bZIP), zinc binuclear cluster, and GATA are just a few of the different DNA binding domains (WEIRAUCH AND HUGHES 2011). Transcription factor genes are abundant in fungal genomes and control a wide range of processes (TODD *et al.* 2014). Fungal members of the GATA family, for example, are involved in regulation of photoinduction, circadian regulation, siderophore production, and nitrogen metabolism (WILSON AND ARST 1998). Transcription factors bind specific sequences using their DBDs. The upstream DNA binding site recognition motif in promoters conforms to a general sequence structure according to the type of DNA binding domain; a few examples of recognizable motifs are TATA motifs, CCAAT motifs, and GATA motifs.

In general, transcription factors bind to a DNA binding motif in the promoter region upstream of the coding sequence of the regulated gene. Then other proteins, which are part of the general transcription machinery, are recruited to the promoter along with RNA Polymerase II to form a transcriptional complex, and transcription is initiated. Once the gene has been transcribed, the RNA is transported from the nucleus and into the cytoplasm to the protein synthesis machinery to be translated into a protein.

Transcription factors, like other proteins, are synthesized in the cytoplasm. This leads to a problem of logistics, where the transcription factor needs to be transported into the nucleus in order to promote transcription. The nucleus has a double membraned structure known as the nuclear envelope which keeps the contents inside the nucleus separated from

cytoplasm. In order to get into the nucleus, the nuclear envelope is covered in nuclear pore complexes (NPCs) in which molecules smaller than about 30 kDa are capable of passive transport through (ROUT AND AITCHISON 2000). Most nuclear proteins including transcription factors must have a nuclear localization signal (NLS) and nuclear export signal (NES) to be actively transported into the nucleus by an importin or out of the nucleus by an exportin (CHANG AND HSIA 2020). Several types of NLSs are known including the classical monopartite lysine and arginine rich sequence originally identified in the Large SV40 T-antigen, classical bipartite NLSs, as well as other non-canonical bipartite or tripartite NLSs (POKORSKA *et al.* 2000; PHILIPS *et al.* 2007). This process can be regulated by intra and inter molecular masking of the NLS/NES, modulation of binding affinities between transporter and cargo, and cytoplasmic/nuclear sequestration [reviewed in POON AND JANS (2005); BAUER *et al.* (2015)]. The regulation of nucleocytoplasmic transport will be discussed in greater detail in the following chapters.

1.2 *Aspergillus nidulans* as a model for studying nitrogen regulation

Aspergillus nidulans is a homothallic, filamentous ascomycete that was chosen after an exhaustive survey of molds as the “most suitable” mold for use as a model organism (PONTECORVO *et al.* 1953). *A. nidulans* is a very adaptable and easy to manipulate model organism. Unlike many other fungi, *A. nidulans* has contact inhibition whereby growth of adjacent colonies is restricted to maintain individuality, so it is possible to grow multiple independent colonies per plate. It also exhibits a 2-day vegetative growth period during its asexual cycle. This leads to the ability for fast screening of progeny growth phenotypes. The sexual cycle takes approximately 10 days and produces ascospores inside of a cleistothecium, which can be cleaned and physically separated from the asexual spores for genetic analysis of progeny (TODD *et al.* 2007b). *A. nidulans* has both a haploid and diploid life cycle and is typically in the haploid stage which allows for quick phenotype to genotype analysis (TODD *et al.* 2007a). A strain has now been constructed (*nku4Δ*) that is defective in nonhomologous integration of introduced sequences during transformation allowing high efficiency gene-targeting (NAYAK *et al.* 2006). In 2003, the *A. nidulans* genome was sequenced by the Broad Institute and in 2005, Nature published an annotated genome (GALAGAN *et al.* 2005). The genome is ~30 Mbp, has 8 chromosomes, and the sequence has been annotated.

A whole-genome knockout construct collection is available at the Fungal Genetics Stock Center (DE SOUZA *et al.* 2014). *A. nidulans* can utilize a wide range of nitrogen-containing nutrients and has complex global and pathway-specific regulatory systems that interact to control expression of genes for uptake and break down of nitrogen sources to allow efficient nitrogen assimilation (ARST JR AND COVE 1973; TODD 2016). Due to its excellent genetics, *A. nidulans* is used as a model for various important plant and human pathogens, such as *Aspergillus fumigatus*, *Aspergillus flavus*, and *Aspergillus clavatus*, as well as the significantly important citric acid producer, *Aspergillus niger*. In contrast to *A. nidulans*, many of the other aspergilli lack a defined sexual cycle, making them more difficult to study genetically. Furthermore, genomes of many other *Aspergillus* species have been sequenced facilitating comparative analysis (DE VRIES *et al.* 2017; KJÆRBØLLING *et al.* 2020). The foundational research, classical genetics, rapid growth, ease of use, and comparability to both pathogens and industrial relevant fungi make *A. nidulans* an important model organism for filamentous ascomycetes.

1.3 Nitrogen regulation by AreA

The regulation of nitrogen metabolism has been studied extensively in fungi for more than 70 years. The best studied systems are *S. cerevisiae*, *A. nidulans*, *Neurospora crassa*, and *Fusarium fujikuroi* (MARZLUF 1997; WONG *et al.* 2008a; TUDZYNSKI 2014; TODD 2016). Regulation of fungal nitrogen metabolism genes occurs primarily at the level of transcription, and the key regulators and many of the regulatory mechanisms are conserved throughout the Ascomycete fungi. Generally, fungi show a preference in nitrogen nutrient utilization such that ammonium and glutamine are preferred over alternative nitrogen sources (ARST JR AND COVE 1973). Consequently, the genes for uptake and metabolism of alternative nitrogen nutrients are repressed when preferred nitrogen sources are available, and repression is relieved in the absence of preferred nitrogen sources. This process is called nitrogen metabolite repression (NMR) or ammonium repression. The key factor that mediates relief from repression are orthologs of the transcription factor AreA (WONG *et al.* 2008a). AreA acts broadly to activate nitrogen metabolism genes in the absence of preferred nitrogen sources, in conjunction with pathway-specific transcription activators that activate uptake and

metabolism genes for specific alternative nitrogen-containing compounds when they are available (TODD 2016).

In the early 1970's the field of nitrogen metabolite repression in *A. nidulans* was in its infancy and was being studied by multiple research groups. Each of these groups were analyzing mutants that showed derepression of nitrogen repressible activities; a few researchers also saw carbon catabolite repression phenotypes of their mutants (COHEN 1972; HYNES 1972; ARST JR AND COVE 1973). As could be expected, this led to each group giving their mutants different names including *amdT*, *xprD1*, and *areA* (COHEN 1972; HYNES 1972; ARST JR AND COVE 1973). These mutants eventually were determined to be alleles of the same gene locus and the consensus was to call the gene *areA* (ARST JR AND COVE 1973). Over the next fifteen years more mutant screens were conducted and the extensive regulation of nitrogen metabolism by *areA* was characterized. It was postulated that AreA was responsible for positive regulation of nitrogen metabolite repressed genes by regulation of both nitrogen metabolic enzymes and proteases. AreA was cloned in 1986 and sequence analysis revealed a GATA zinc finger DNA binding domain (CADDICK *et al.* 1986; KUDLA *et al.* 1990). The crystal structure of the DNA binding domain was determined and showed that AreA is capable of binding to CGATAG sites as well as the consensus (A/T)GATA(A/G) sites (STARICH *et al.* 1998).

AreA is responsible for global regulation of nitrogen utilization and uptake genes, which makes the regulation of AreA itself important to understand. The activity of AreA is highly regulated by multiple control mechanisms that act transcriptionally, post-transcriptionally, by interaction with other proteins, and by subcellular localization. These regulatory strategies will be briefly discussed and summarized below.

Under nitrogen poor or nitrogen starvation conditions the *areA* gene is subject to autogenous transcriptional regulation by AreA, activating its own expression (LANGDON *et al.* 1995). During nitrogen sufficient conditions, *areA* mRNA transcript stability is affected by deadenylation leading to an increased rate of degradation (PLATT *et al.* 1996a). This was shown to be slowed by mutation of *ccr4* and *caf1* deadenylase genes (MOROZOV *et al.* 2010). Deletion of the *areA* 3'UTR (untranslated region) increased mRNA stability leading to partial derepression of AreA-regulated genes, and the *areA* 3'UTR decreased stability of other

transcripts when inserted into the 3' region of other transcripts (MOROZOV *et al.* 2010). Deletion of the C-terminus region of AreA also showed partial derepression of AreA (PLATT *et al.* 1996a; PLATT *et al.* 1996b).

There are multiple proteins that interact with AreA which lead to both positive and negative regulation of NMR. The co-repressor NmrA interacts directly with AreA, inhibiting function during nitrogen repressing conditions (ANDRIANOPOULOS *et al.* 1998). The regulation of NmrA has also been characterized and its transcription is activated by the bZIP transcription factor MeaB during nitrogen repressing conditions (WONG *et al.* 2007), and the NmrA protein is degraded by PnmB protease during derepressing conditions (LI *et al.* 2021) (Figure 1.1).

AreA activation is also modulated during derepressing conditions. The coactivator TamA positively interacts with AreA to upregulate gene expression (DAVIS *et al.* 1996; SMALL *et al.* 1999; DOWNES *et al.* 2014), whereas the GATA zinc finger transcription factor AreB negatively regulates AreA by promoter competition (WONG *et al.* 2008a). Finally, subcellular localization also regulates AreA activity. In the presence of non-preferred nitrogen sources (not ammonium or glutamine), AreA activity is increased, in part due to the transcript being more stable, and also by AreA not being repressed by NmrA, and AreA cycles in and out of the nucleus. During nitrogen starvation, the export of AreA from the nucleus is blocked, and AreA accumulates in the nucleus resulting in AreA-dependent gene expression two to three-fold higher than when AreA is cycling in and out of the nucleus (TODD *et al.* 2005; HUNTER *et al.* 2014)(Figure 1.1).

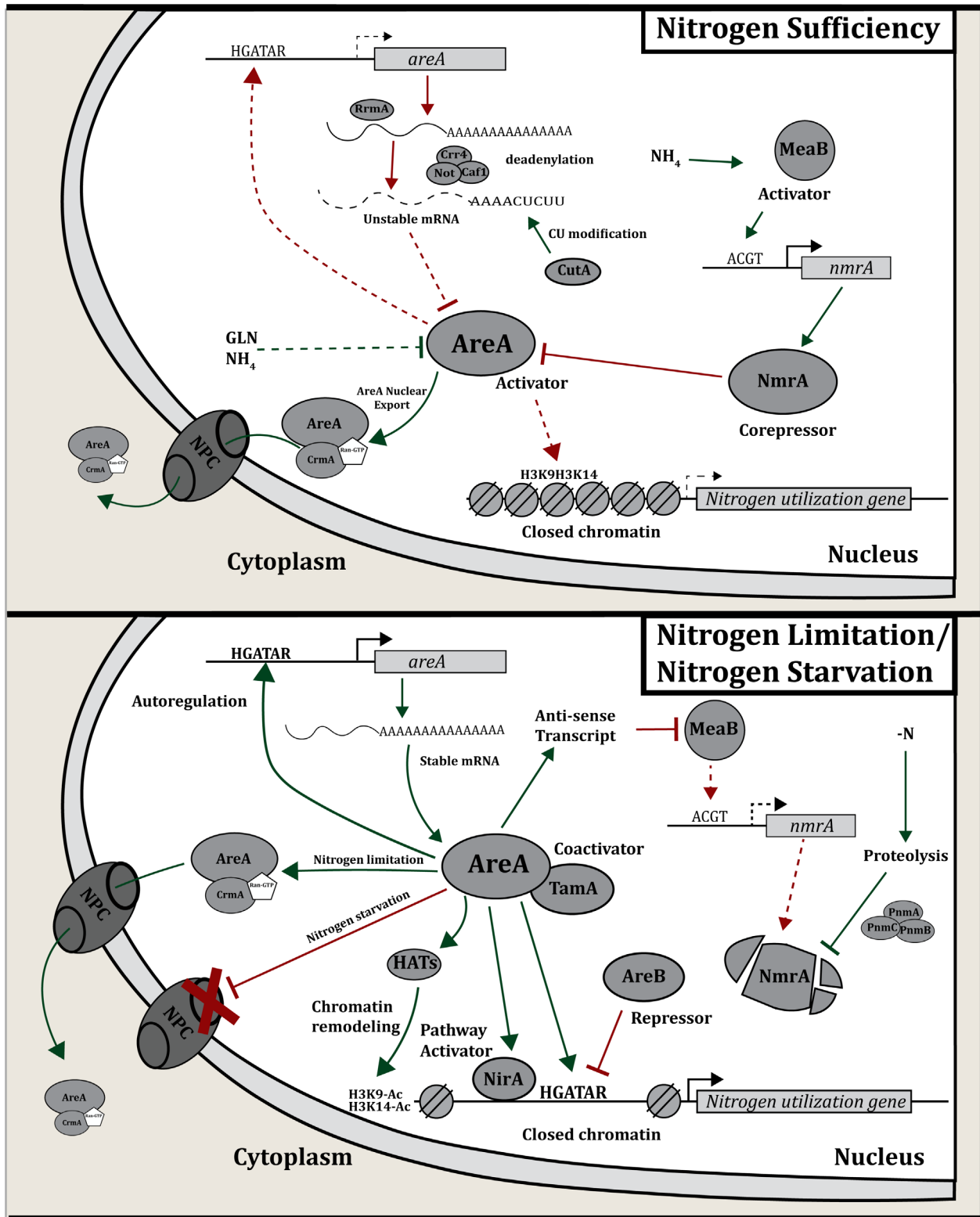


Figure 1.1 Overview of nitrogen metabolism regulation

Model for regulation of nitrogen metabolism adapted from TODD (2016).

1.4 Research Objectives

This dissertation focuses on nitrogen signaling and nuclear localization of the *A. nidulans* GATA transcription factor AreA. The objective of Chapter 3 is to understand nuclear localization of AreA by identification and characterization of the nuclear localization sequences (NLSs) within the AreA protein that direct AreA to the nucleus. The two main approaches are to: (i) mutate the predicted NLSs within AreA and determine their effects on AreA nuclear localization and AreA-dependent gene expression, and (ii) fuse the predicted NLSs to Green Fluorescent Protein (GFP) and assess the ability to direct GFP to the nucleus. The objective of Chapter 4 is to understand the mechanisms and regulation of AreA nuclear accumulation. We examine the role of the KapA alpha-importin, the small ubiquitin-like modifier SumO, the Target of Rapamycin (TOR) signaling pathway, and the transcription factor XprG in regulation of nuclear accumulation of AreA. The objective of Chapter 5 is to determine how nitrogen availability is signaled in *A. nidulans*. We analyze mutants with altered AreA DNA-binding activity to determine if nuclear accumulation is dependent on DNA binding and to dissect the role of AreA DNA binding in nitrogen signaling. We also assess the effects of several nitrogen metabolic mutations on signaling of AreA nuclear accumulation.

We can handle anything together.

Chapter 2 - Experimental Procedures

2.1 Strains

2.2.1 *Aspergillus nidulans* strains

A. nidulans strains used in this study that were constructed in the Hynes-Davis lab at The University of Melbourne are listed in Table 2.1 using conventional annotations from CLUTTERBUCK (1973). Strains constructed in the Todd lab at Kansas State University or supplied to the Todd lab are listed in Table 2.2, and strains constructed by C.C. Hunter are listed in Table 2.3. All strains contain the *veA1* mutation. Detailed descriptions of strain construction are provided in the relevant chapters.

2.2.2 *Escherichia coli* strains

General plasmid manipulation utilized the *E. coli* strain NM522 [F' *proA*⁺*B*⁺ *lacI*^qΔ(*lacZ*)M15/Δ(*lac-proAB*) *glnV thi-1* Δ(*hdsS-mcrB*)5] (GOUGH *et al.* 1983). Details of plasmid construction are provided in the relevant chapters.

Table 2.1 “Michael Hynes” *Aspergillus nidulans* strains

Strain	Genotype^a
MH1	<i>biA1</i>
MH50	<i>yA adE20 su(adE20) areA102 pyroA4 riboB2</i>
MH54	<i>biA1 niiA4</i>
MH764	<i>wA3 riboB2 facB101</i>
MH5699	<i>yA1 adE20 su(adE20) areAΔ::riboB⁺ pyroA4 riboB2</i>
MH8767	<i>yA1 pabaA1 amdR44 argB::amdS-lacZ areA217 riboB2</i>
MH9883	<i>wA3 gpd(p)areA^{HA} riboB2 facB101</i>
MH9922	<i>wA3 areA::riboB(5') riboB2 facB101</i>
MH9949	<i>biA1 gpd(p)areA^{HA} amdS-lacZ</i>
MH9962	<i>yA1 glnAΔ::riboB⁺ amdS-lacZ areA102 pyroA4</i>
MH10041	<i>wA3 gpd(p)areA^{HA,Δ60-423} pyroA4</i>
MH10244	<i>yA1 wA1 riboB2</i>
MH10266	<i>wA3 gpd(p)areA^{HA}::riboB(3') riboB2 facB101</i>
MH10267	<i>wA3 gpd(p)areA102^{HA} riboB2</i>
MH10504	<i>yA2 pabaA2 acuE201</i>
MH10609	<i>biA1 wA3 gpd(p)areA102^{HA}</i>
MH10653	<i>yA1 pabaA1 amdR44 argB::amdS-lacZ areA217 niiA4 riboB2 [amdR-tamA ectopic]</i>
MH10665	<i>yA1 gpd(p)areA^{HA} pyroA4 prn-309</i>
MH10696	<i>yA1 pabaA1 amdR44 argB::amdS-lacZ areA217::riboB⁺(5') niiA4 riboB2 [amdR-tamA ectopic]</i>
MH10798	<i>yA1 pabaA1 gpd(p)areA217^{HA} amdR44 argB::amdS-lacZ niiA4 riboB2 [amdR-tamA ectopic]</i>
MH10827	<i>yA1 pabaA1 gpd(p)areA217^{HA} pyroA4</i>
MH10897	<i>yA1 pabaA1 gpd(p)areA^{HA} fmdS-lacZ</i>
MH10967	<i>yA1 areAΔ::riboB fmdS-lacZ pyroA4 riboB2 facB101</i>
MH11050	<i>yA1 pabaA1 gpd(p)areA^{HA}::riboB(3') fmdS-lacZ</i>
MH11052	<i>yA1 pabaA1 gpd(p)areA^{HA} fmdS-lacZ niiA4</i>

^a All strains carry the *veA1* mutation.

Table 2.1 “Michael Hynes” *A. nidulans* strains (continued)

Strain	Genotype^a
MH11072	<i>yA1 pabaA1 gpd(p)areA^{HA}::riboB(3') fmdS-lacZ pyroA4 nkuAΔ::Bar</i>
MH11099	<i>yA1 pabaA1 gpd(p)areA^{HA.Δ609-615} fmdS-lacZ pyroA4 nkuAΔ::Bar</i>
MH11131	<i>yA1 pabaA1 gpd(p)areA^{HA} pyroA4 nkuAΔ::argB⁺</i>
MH11186	<i>yA1 pabaA1 gdhAΔ::riboB gpd(p)areA^{HA} fmdS-lacZ pyroA4</i>
MH11263	<i>yA1 gpd(p)areA^{HA} fmdS-lacZ sumOΔ::Bar</i>
MH11432	<i>gpd(p)areA^{HA.Δ60-423} fmdS-lacZ pyroA4 nkuAΔ::Bar</i>
MH11457	<i>gpd(p)areA^{HA.Δ60-423} pyroA4 nkuAΔ::Bar</i>
MH11481	<i>gpd(p)areA^{HA} amdS-lacZ pyroA4 sumOΔ::Bar::xylP(p)sumO</i>
MH11668	<i>yA1 pabaA1 gpd(p)areA^{HA.Δ811-816} pyroA4 fmdS-lacZ nkuAΔ::Bar</i>
MH11967	<i>yA1 pabaA1 gpd(p)areA^{HA.Δ609-615.Δ811-816} fmdS-lacZ pyroA4 nkuAΔ::Bar</i>
MH12068	<i>yA1 pabaA1 gpd(p)areA^{HA.Δ703-712} pyroA4 nkuAΔ::argB</i>
MH12226	<i>yA1 pabaA1 gpd(p)areA^{HA} pyroA4 nkuAΔ::argB kapA::xylP(p)kapA-AfpyroA</i>
MH12236	<i>yA1 pabaA1 gpd(p)areA^{HA} amdS-lacZ nkuAΔ::argB kapA::xylP(p)kapA-AfpyroA sumOΔ::Bar</i>
MH12318	<i>gpd(p)areA^{HA} amdS-lacZ pyroA4 kapA::kapA::GFP-Afribob</i>
MH12328	<i>pabaA1 gpd(p)areA^{HA} amdS-lacZ kapA::kapA::GFP-Afribob sumOΔ::Bar</i>

^a All strains carry the *veA1* mutation.

Table 2.2 “Richard Todd” *Aspergillus nidulans* strains constructed by others

Strain	Genotype^a
RT49	<i>yA1 pabaA1 gpd(p)areA^{HA}-bip pyroA4 nkuAΔ::argB⁺</i>
RT52	<i>pyrG89 gpd(p)areA^{HA} fmdS-lacZ pyroA4 nkuAΔ::Bar</i>
RT210	<i>pyrG89 gpd(p)areA^{HA} fmdS-lacZ pyroA4 nkuAΔ::Bar kapA^{S111F}</i>
RT211	<i>pyrG89 gpd(p)areA^{HA} fmdS-lacZ pyroA4 nkuAΔ::Bar kapA^{S111F}</i>
RT212	<i>gpd(p)areA^{HA.Δ60-423.Δ811-816} fmdS-LacZ</i>
RT214	<i>gpd(p)areA^{HA.Δ60-423.R685A,R686A,R720A,R722A} fmdS-lacZ pyroA4</i>
RT216	<i>gpd(p)areA^{HA.Δ60-423.Δ609-615} fmdS-lacZ</i>
RT235	<i>gpd(p)areA^{HA} fmdS-lacZ pyroA4 nkuAΔ::Bar kapA^{S111F}</i>
RT238	<i>pyrG89 wA::gpd(p)gfp::areANLS4-Afpyro gpd(p)areA^{HA} fmdS-lacZ pyroA4 nkuAΔ::Bar crmA^{T525C}::pyrG⁺</i>
RT268	<i>yA1 pabaA1 gpd(p)areA^{HA-H704A} pyroA4 nkuAΔ::argB⁺</i>
RT269	<i>yA1 pabaA1 gpd(p)areA^{HA-H704A} pyroA4 nkuAΔ::argB⁺</i>
RT270	<i>yA1 pabaA1 gpd(p)areA^{HA-H704A} pyroA4 nkuAΔ::argB⁺</i>
RT271	<i>yA1 pabaA1 gpd(p)areA^{HA-H704A} pyroA4 nkuAΔ::argB⁺</i>
RT490	<i>pyrG89 gpd(p)areA^{HA} fmdS-lacZ pyroA4 nkuAΔ::Bar AN1923Δ::AfpyrG</i>
RT491	<i>pyrG89 gpd(p)areA^{HA} fmdS-lacZ pyroA4 nkuAΔ::Bar AN1923Δ::AfpyrG</i>
RT492	<i>pyrG89 gpd(p)areA^{HA} fmdS-lacZ pyroA4 nkuAΔ::Bar AN1923Δ::AfpyrG</i>
RT493	<i>pyrG89 gpd(p)areA^{HA} fmdS-lacZ pyroA4 nkuAΔ::Bar AN1923Δ::AfpyrG</i>

^a All strains carry the *veA1* mutation.

Table 2.3 “Richard Todd” *Aspergillus nidulans* strains constructed by Hunter

Strain	Genotype^a
RT121	<i>yA1 pabaA1 gpd(p)areA^{HA.Δ609-615.R685A,R686A,R720A,R722A} fmdS-lacZ pyroA4 nkuAΔ::argB⁺</i>
RT123	<i>yA1 pabaA1 gpd(p)areA^{HA.Δ609-615.R685A,R686A,R720A,R722A.Δ811-816} fmdS-lacZ pyroA4 nkuAΔ::argB⁺</i>
RT129	<i>yA1 pabaA1 gpd(p)areA^{HA.Δ60-423.Δ609-615.R685A,R686A,R720A,R722A} fmdS-lacZ pyroA4</i>
RT131	<i>yA1 pabaA1 gpd(p)areA^{HA.Δ60-423.Δ609-615.R685A,R686A,R720A,R722A.Δ811-816} fmdS-lacZ pyroA4</i>
RT132	<i>yA1 pabaA1 gpd(p)areA^{HA.Δ60-423.Δ609-615.Δ811-816} fmdS-lacZ</i>
RT134	<i>yA1 pabaA1 gpd(p)areA^{HA.R685A,R686A,R720A,R722A} fmdS-lacZ pyroA4 nkuAΔ::argB⁺</i>
RT248	<i>yA1 gpd(p)areA^{HA.Δ60-423.R685A,R686A,R720A,R722A.Δ811-816} fmdS-lacZ pyroA4</i>
RT273	<i>yA1 pabaA1 gpd(p)areA^{HA}-bipΔNLS5 fmdS-lacZ</i>
RT289	<i>pyrG89 biA1 wA::gpd(p)gfp::AfpyroA gpd(p)areA^{HA} fmdS-lacZ pyroA4 nkuAΔ::Bar crmA^{T525C}::pyrG⁺</i>
RT290	<i>pyrG89 biA1 wA::gpd(p)gfp::AfpyroA gpd(p)areA^{HA} fmdS-lacZ pyroA4 nkuAΔ::Bar crmA^{T525C}::pyrG⁺</i>
RT291	<i>pyrG89 biA1 wA::gpd(p)gfp::areA^{102zf}::AfpyroA gpd(p)areA^{HA} fmdS-lacZ pyroA4 nkuAΔ::Bar crmA^{T525C}::pyrG⁺</i>
RT292	<i>pyrG89 biA1 wA::gpd(p)gfp::areA^{102zf}::AfpyroA gpd(p)areA^{HA} fmdS-lacZ pyroA4 nkuAΔ::Bar crmA^{T525C}::pyrG⁺</i>
RT293	<i>pyrG89 biA1 wA::gpd(p)gfp::areA^{102zf}::AfpyroA gpd(p)areA^{HA} fmdS-lacZ pyroA4 nkuAΔ::Bar crmA^{T525C}::pyrG⁺</i>
RT331	<i>wA::gpd(p)gfp::areA^{NLS102zf}::AfpyroA areAΔ::riboB⁺ pyroA4</i>
RT332	<i>wA::gpd(p)gfp::AfpyroA areA::riboB⁺ pyroA4</i>
RT334	<i>pyrG89 wA::gpd(p)gfp::areA^{NLS123}::AfpyroA gpd(p)areA^{HA} fmdS-lacZ pyroA4 nkuAΔ::Bar kapA^{S111F} crmA^{T525C}::pyrG⁺</i>
RT335	<i>pyrG89 wA::gpd(p)gfp::areA^z::AfpyroA gpd(p)areA^{HA} fmdS-lacZ pyroA4 nkuAΔ::Bar kapA^{S111F} crmA^{T525C}::pyrG⁺</i>
RT336	<i>pyrG89 biA1 wA::gpd(p)gfp::areA^{zfbip}::AfpyroA gpd(p)areA^{HA} fmdS-lacZ pyroA4 nkuAΔ::Bar kapA^{S111F} crmA^{T525C}::pyrG⁺</i>
RT337	<i>pyrG89 biA1 wA::gpd(p)-gfp::areA^{NLS5}::AfpyroA gpd(p)areA^{HA} fmdS-lacZ pyroA4 nkuAΔ::Bar kapA^{S111F} crmA^{T525C}::pyrG⁺</i>

^a All strains carry the *veA1* mutation.

Table 2.3 “Richard Todd” *A. nidulans* strains constructed by Hunter (continued)

Strain	Genotype^a
RT338	<i>pyrG89 biA1 wA::gpd(p)gfp::AfpYROA gpd(p)areA^{HA} fmdS-lacZ pyroA4 nkuAΔ::Bar kapA^{S111F} crmA^{T525C}::pyrG⁺</i>
RT339	<i>pyrG89 gpd(p)areA^{HA} fmdS-lacZ pyroA4 nkuAΔ::Bar kapA^{S111F} crmA^{T525C}::pyrG⁺</i>
RT373	<i>pyrG89 biA1 wA::gpd(p)gfp::areANLS217zf AfpYROA gpd(p)areA^{HA} fmdS-lacZ pyroA4 nkuAΔ::Bar crmA^{T525C}::pyrG⁺</i>
RT401	<i>pyrG89 biA1 wA::gpd(p)-gfp::areANLS123+5::AfpYROA gpd(p)areA^{HA} fmdS-lacZ pyroA4 nkuAΔ::Bar kapA^{S111F} crmA^{T525C}::pyrG⁺</i>
RT402	<i>pyrG89 wA::gpd(p)-gfp::areANLS123+5::AfpYROA gpd(p)areA^{HA} fmdS-lacZ pyroA4 nkuAΔ::Bar kapA^{S111F} crmA^{T525C}::pyrG⁺</i>
RT407	<i>pyrG89 yA1 pabaA1 areA(5'Δ)::riboB fmdS-lacZ pyroA4 AN0504Δ::AfpYrG</i>
RT408	<i>pyrG89 yA1 pabaA1 areA(5'Δ)::riboB fmdS-lacZ AN0504Δ::AfpYrG</i>
RT409	<i>pyrG89 areA(5'Δ)::riboB fmdS-lacZ AN0504Δ::AfpYrG</i>
RT410	<i>pyrG89 areA(5'Δ)::riboB fmdS-lacZ pyroA4 AN0504Δ::AfpYrG</i>
RT433	<i>gpd(p)areA^{HA} fmdS-lacZ AN0504Δ::AfpYrG</i>
RT434	<i>yA1 pabaA1 gpd(p)areA^{HA} fmdS-lacZ pyroA4 AN0504Δ::AfpYrG</i>
RT435	<i>yA1 pabaA1 amdR44 argB::amdS-lacZ areA217 riboB2</i>
RT436	<i>yA1 pabaA1 amdR44 argB::amdS-lacZ areA217 riboB2</i>
RT467	<i>pyrG89 jipAΔ::AfpYrG⁺ gpd(p)areA^{HA} fmdS-lacZ pyroA4 nkuAΔ::Bar</i>
RT468	<i>pyrG89 jipAΔ::AfpYrG⁺ gpd(p)areA^{HA} fmdS-lacZ pyroA4 nkuAΔ::Bar</i>
RT469	<i>pyrG89 areA(5'Δ)::riboB pyroA4 atmAΔ::AfpYrG⁺</i>
RT470	<i>gpd(p)areA^{HA} pyroA4 nkuAΔ::argB atmAΔ::AfpYrG⁺</i>
RT471	<i>pabaA gpd(p)areA^{HA} pyroA4 nkuAΔ::argB atmAΔ::AfpYrG⁺</i>
RT480	<i>pyrG89 yA1 pabaA1 areA(5'Δ)::riboB fmdS-lacZ pyroA4 AN0103Δ::AfpYrG⁺</i>
RT481	<i>pyrG89 areA(5'Δ)::riboB fmdS-lacZ pyroA4 AN0103Δ::AfpYrG⁺</i>
RT482	<i>pyrG89 yA1 pabaA1 areA(5'Δ)::riboB fmdS-lacZ AN0103Δ::AfpYrG⁺</i>
RT496	<i>pyrG89 gpd(p)areA^{HA} fmdS-lacZ pyroA4 AN0103Δ::AfpYrG⁺</i>
RT497	<i>pyrG89 yA1 gpd(p)areA^{HA} fmdS-lacZ pyroA4 AN0103Δ::AfpYrG⁺</i>
RT509	<i>pyrG89 pyroA4 nkuAΔ::Bar AN6026Δ1::AfpYrG⁺</i>

^a All strains carry the *veA1* mutation.

Table 2.3 “Richard Todd” *A. nidulans* strains constructed by Hunter (continued)

Strain	Genotype^a
RT510	<i>pyrG89 AN6026Δ2::Afp_{pyrG}⁺ pyroA4 nkuAΔ::Bar</i>
RT511	<i>pyrG89 AN6027Δ2::Afp_{pyrG}⁺ pyroA4 nkuAΔ::Bar</i>
RT512	<i>pyrG89 AN6027Δ8::Afp_{pyrG}⁺ pyroA4 nkuAΔ::Bar</i>
RT513	<i>pyrG89 AN6028Δ1::Afp_{pyrG}⁺ pyroA4 nkuAΔ::Bar</i>
RT514	<i>pyrG89 AN6028Δ3::Afp_{pyrG}⁺ pyroA4 nkuAΔ::Bar</i>
RT515	<i>pyrG89 AN6029Δ2::Afp_{pyrG}⁺ pyroA4 nkuAΔ::Bar</i>
RT516	<i>pyrG89 AN6029Δ3::Afp_{pyrG}⁺ pyroA4 nkuAΔ::Bar</i>
RT517	<i>pyrG89 AN6029Δ4::Afp_{pyrG}⁺ pyroA4 nkuAΔ::Bar</i>
RT518	<i>pyrG89 AN11221Δ1::Afp_{pyrG}⁺pyroA4 nkuAΔ::Bar</i>
RT519	<i>pyrG89 AN11221Δ6::Afp_{pyrG}⁺pyroA4 nkuAΔ::Bar</i>
RT553	<i>yA1 gpd(p)areA^{HA} fmdS-lacZ prn309</i>
RT554	<i>yA1 pabaA1 gpd(p)areA^{HA} fmdS-lacZ pyroA4 prn-309</i>
RT555	<i>yA1 glnAΔ::riboB⁺ gpd(p)areA^{HA} fmdS-lacZ pyroA4</i>
RT556	<i>yA1 pabaA1 gpd(p)gfp::areA(A2) fmdS-lacZ pyroA4 nkuAΔ::Bar</i>
RT557	<i>yA1 pabaA1 gpd(p)gfp::areA(A13) fmdS-lacZ pyroA4 nkuAΔ::Bar</i>
RT558	<i>yA1 pabaA1 gpd(p)gfp::areA(A16) fmdS-lacZ pyroA4 nkuAΔ::Bar</i>
RT559	<i>yA1 pabaA1 gpd(p)gfp::areA(A19) fmdS-lacZ pyroA4 nkuAΔ::Bar</i>
RT560	<i>yA1 pabaA1 gpd(p)gfp::areA(A21) fmdS-lacZ pyroA4 nkuAΔ::Bar</i>
RT561	<i>yA1 pabaA1 gpd(p)gfp::areA(A23) fmdS-lacZ pyroA4 nkuAΔ::Bar</i>
RT564	<i>pyrG89 AN3846Δ2::Afp_{pyrG}⁺ pyroA4 nkuAΔ::Bar</i>
RT565	<i>pyrG89 AN3846Δ3::Afp_{pyrG}⁺ pyroA4 nkuAΔ::Bar</i>
RT575	<i>biA1 wA3 gpd(p)areA102 niaD15</i>
RT576	<i>biA1 gpd(p)areA102 niaD15</i>
RT580	<i>yA1 pabaA1 gpd(p)areA^{HA.Δ703-712} pyroA4 sumOΔ::Bar</i>
RT581	<i>yA1 pabaA1 gpd(p)areA^{HA.Δ703-712} fmdS-lacZ pyroA4 sumOΔ::Bar</i>
RT582	<i>yA1 pabaA1 gpd(p)areA^{HA.Δ703-712} amdS-lacZ kapA::xylP(p)kapA sumOΔ::Bar</i>
RT583	<i>yA1 pabaA1 gpd(p)areA^{HA.Δ703-712} amdS-lacZ kapA::xylP(p)kapA sumOΔ::Bar</i>
RT588	<i>pyrG89 pyroA4 nkuAΔ::Bar AN1730Δ2::Afp_{pyrG}⁺</i>

^a All strains carry the *veA1* mutation.

Table 2.3 “Richard Todd” *A. nidulans* strains constructed by Hunter (continued)

Strain	Genotype^a
RT589	<i>pyrG89 pyroA4 nkuAΔ::Bar AN1810Δ4::AfpyrG⁺</i>
RT590	<i>pyrG89 pyroA4 nkuAΔ::Bar AN0454Δ6::AfpyrG⁺</i>
RT591	<i>pyrG89 pyroA4 nkuAΔ::Bar AN0454Δ7::AfpyrG⁺</i>
RT592	<i>pyrG89 pyroA4 nkuAΔ::Bar AN1731Δ4::AfpyrG⁺</i>
RT593	<i>pyrG89 AN6048Δ10::AfpyrG⁺ pyroA4 nkuAΔ::Bar</i>
RT594	<i>pyrG89 AN6048Δ11::AfpyrG⁺ pyroA4 nkuAΔ::Bar</i>
RT595	<i>pyrG89 AN6048Δ12::AfpyrG⁺ pyroA4 nkuAΔ::Bar</i>
RT596	<i>pyrG89 pyroA4 nkuAΔ::Bar AN1730Δ2::AfpyrG⁺ AN1810Δ5::AfpyrG⁺</i>
RT597	<i>biA1 wA1 gpd(p)areA^{HA} fmdS-lacZ niaD15</i>
RT598	<i>gpd(p)areA^{HA} fmdS-lacZ niaD15</i>
RT600	<i>AfpyrG-torA(p)::DLAP-torA(AN5982) pabaA1 wA3 gpd(p)areA217^{HA} pyroA4</i>
RT601	<i>AfpyrG-torA(p)::DLAP-torA(AN5982) wA3 gpd(p)areA217^{HA} pyroA4</i>
RT602	<i>yA1 gpd(p)areA^{HA} fmdS-lacZ pyroA4 kapA^{S111F} sumOΔ::Bar</i>
RT603	<i>gpd(p)areA^{HA} fmdS-lacZ pyroA4 kapA^{S111F} sumOΔ::Bar</i>
RT604	<i>yA1 gpd(p)areA^{HA} fmdS-lacZ kapA^{S111F} sumOΔ::Bar</i>
RT605	<i>gpd(p)areA^{HA} fmdS-lacZ kapA^{S111F} sumOΔ::Bar</i>
RT606	<i>yA1 gpd(p)areA^{HA.703-712Δ} pyroA4 kapA^{S111F}</i>
RT607	<i>gpd(p)areA^{HA.703-712Δ} pyroA4 kapA^{S111F}</i>
RT620	<i>gpd(p)areA^{HA} amdS-lacZ pyroA4 kapA::kapA::gfp-AfriboB sumO::xylP(p)sumO-Bar</i>
RT621	<i>gpd(p)areA^{HA} amdS-lacZ pyroA4 kapA::kapA::gfp-AfriboB sumO::xylP(p)sumO-Bar</i>
RT622	<i>yA1 pabaA1 gpd(p)areA^{HA.703-712Δ} pyroA4 kapA::xylP(p)kapA-AfpyroA</i>
RT623	<i>yA1 pabaA1 gpd(p)areA^{HA.703-712Δ} pyroA4 kapA::xylP(p)kapA-AfpyroA</i>
RT630	<i>AfpyrG-torA(p)::DLAP-torA(AN5982) gpd(p)areA^{HA} fmdS-lacZ pyroA4</i>
RT631	<i>pabaA1 AfpyrG-torA(p)::DLAP-torA(AN5982) gpd(p)areA^{HA} fmdS-lacZ pyroA4</i>
RT632	<i>yA1 gpd(p)areA^{HA} AfpyrG::torA(p)::DLAP-torA(AN5982) pyroA4</i>
RT624	<i>pyrG89 pyroA4 nkuAΔ::Bar AN1406Δ::AfpyrG⁺</i>
RT625	<i>pyrG89 pyroA4 nkuAΔ::Bar AN1406Δ::AfpyrG⁺</i>
RT626	<i>pyrG89 pyroA4 nkuAΔ::Bar AN1418Δ::AfpyrG⁺</i>

^a All strains carry the *veA1* mutation.

Table 2.3 “Richard Todd” *A. nidulans* strains constructed by Hunter (continued)

Strain	Genotype ^a
RT627	<i>pyrG89 pyroA4 nkuAΔ::Bar AN1418Δ::AfpyrG</i> ⁺
RT628	<i>pyrG89 pyroA4 nkuAΔ::Bar AN1420Δ::AfpyrG</i> ⁺
RT629	<i>pyrG89 pyroA4 nkuAΔ::Bar AN1420Δ::AfpyrG</i> ⁺
RT673	<i>yA1 pabaA1 wA::areA</i> ⁺ <i>gpd(p)areA217^{HA} pyroA4</i>

^a All strains carry the *veA1* mutation.

2.2 Methods

2.2.1 *A. nidulans* strains, media, and growth conditions

A. nidulans growth conditions and media were as described by (COVE 1966), with pH adjusted to 6.5. *Aspergillus* Nitrogen-free Minimal media (ANM) contained 1% (w/v) glucose as the carbon source and was appropriately supplemented for auxotrophic mutations. Nitrogen sources were added to a final concentration of 10mM unless otherwise stated. Genetic analysis was carried out using previously described techniques by CLUTTERBUCK (1974) and TODD *et al.* (2007b).

2.2.2 Bacterial media and growth conditions

Bacteria were grown on Luria broth (LB) agar supplemented with 50 µg/ml ampicillin to select for colonies containing ampicillin resistance plasmids, and 0.04 mM IPTG (isopropyl-β-D-thiogalactopyranoside) with 0.005% X-Gal (5-bromo-4-chloro-3-indolyl-β-D-galactoside) for blue-white colony selection as required (SAMBROOK *et al.* 1989).

2.2.3 FGSC gene knockout strains

A. nidulans gene knockout constructs (MCCLUSKEY *et al.* 2010; DE SOUZA *et al.* 2013) were obtained from the Fungal Genetics Stock Center, Manhattan, KS. Gene replacements were confirmed by PCR.

2.3 Molecular techniques

Standard molecular techniques were as described in (SAMBROOK AND RUSSELL 2001) or performed according to instructions from the manufacturer.

2.3.1 DNA manipulation

Plasmid DNA was isolated using Wizard Plus SV Miniprep DNA purification kit (Promega) following the manufacturer's instructions and *A. nidulans* genomic DNA isolated according to LEE AND TAYLOR (1990). PCR products and DNA fragments isolated from agarose gels were cleaned with the Wizard SV Gel and PCR Clean Up System (Promega) following the manufacturer's instructions. Digestion using restriction enzymes (Promega; New England Biolabs), dephosphorylation with Arctic Shrimp alkaline phosphatase (Promega), and ligations using T4 DNA ligase (Promega) were carried out following the manufacturers' instructions. DNA was separated on 1-2% agarose gels by electrophoresis in 1x TAE buffer. DNA was quantified using a Nanodrop 1000. Bacterial cells were rendered competent by treatment with calcium chloride (SAMBROOK *et al.* 1989) and stored at -80°C. DNA and 100 µl of competent cells were incubated on ice for 10 minutes followed by a 2-minute heat-shock at 37°C and returned to ice for 1-2 minutes before plating on LB agar media with 50 µg/ml ampicillin.

2.3.2 Polymerase Chain Reaction

PCR reactions used proof-reading enzymes: Pfu (Agilent), PfuTurbo (Stratagene), Phusion (Thermo Scientific) or Ex Taq (TaKaRa). Southern analysis to confirm gene replacements was performed using the DIG-High Prime DNA Labeling and Detection Starter Kit II (Roche). DNA polymerases according to the manufacturers' instructions. Templates were added approximately 1 ng for plasmid DNA and 100 ng *A. nidulans* genomic DNA. All reactions followed the recommended denaturing and annealing conditions with 33-36 amplification cycles. Oligonucleotide primers for PCR (IDT) are described in the relevant chapters.

2.3.3 Southern Blot

DNA samples were resolved in agarose gels and treated with 0.25M HCl for 12 minutes for depurination. DNA was then transferred to either Hybond N+ or XL positively charged membranes (Amersham) using 0.4M NaOH capillary transfer. Probe generation, hybridization (42°C overnight), and detection was carried out using the DIG (digoxigenin) High prime DNA labeling and detection starter kit II (Roche) following the manufacturer's instructions. Films exposed to Southern blots were developed in an Ecomax™ X-ray film processor (Protec).

2.3.4 β -galactosidase assays

Strains for *fmdS-lacZ* assays were constructed by meiotic crossing (TODD *et al.* 2007b). β -galactosidase assays were performed as described previously (DAVIS *et al.* 1988). Specific activity is expressed as $A_{420\text{nm}} \times 10^3 \text{ min}^{-1} \text{ mg}^{-1}$ of soluble protein. Protein concentrations were calculated as described in BRADFORD (1976) using Bio-Rad Protein Assay reagent (Bio-Rad) following the manufacturer's instructions.

2.3.5 5-FOA selection for loss of *AfpyrG* deletion cassettes

Uridine and uracil auxotrophs (*pyrG*⁻) after DNA-mediated transformation with wild type DNA fragments corresponding to deleted genes were selected using 1-2 mg/mL 5-fluoroorotic acid (5-FOA) (Zymo Research) added to protoplast media supplemented with 5 mM uracil and 10mM uridine and appropriate supplementation for other auxotrophies. Transformants containing the *pyrG*⁻ mutation, which leads to 5-FOA resistance were picked to selective media after two days incubation at 37°C.

2.3.6 Sequence analysis

Sanger DNA sequencing to confirm constructs and gene replacements was performed at the Kansas State University DNA Sequencing and Genotyping Facility. DNA sequence analysis was performed using Geneious Pro 5.3.4 (A. J. Drummond, B. Ashton, S. Buxton, M. Cheung, A. Cooper, C. Duran, M. Field, J. Heled, M. Kearse, S. Markowitz, R. Moir, S. Stones-Havas, S. Sturrock, T. Thierer, A. Wilson, 2011, available from <http://www.geneious.com/>).

The AreA protein sequence was examined for NLSs using PSORT II (NAKAI AND HORTON 1999), and manually to identify the non-canonical bipartite NLS conserved with GATA-4 (PHILIPS *et al.* 2007). Protein sequence alignments were done using ClustalW (THOMPSON *et al.* 2002) and protein sequences obtained from AspGD (<http://aspergillusgenome.org/>) (ARNAUD *et al.* 2012) or the GenBank database (<http://www.ncbi.nlm.nih.gov/genbank/>): *Aspergillus niger* AreA (CAA57524) (MACCABE *et al.* 1998), *Aspergillus oryzae* AreA (CAA05776) (CHRISTENSEN *et al.* 1998), *Aspergillus parasiticus* AreA (AAD37409) (CHANG *et al.* 2000), *A. nidulans* AreA (CAA36731) (LANGDON *et al.* 1995), *F. fujikuroi* AreA (CAA71897) (TUDZYNSKI *et al.* 1999), *Magnaporthe oryzae* NUT1 (AAB03415) (FROELIGER AND CARPENTER 1996), *N. crassa* NIT2 (P19212) (FU AND MARZLUF 1990), *Penicillium chrysogenum* Nre (AAA83400) (HAAS *et al.* 1995), *Penicillium roqueforti* NmC (CAA04815) (GENTE *et al.* 1999), *S. cerevisiae* Gat1p (P43574) (COFFMAN *et al.* 1996), *S. cerevisiae* Gln3p (P18494) (MINEHART AND MAGASANIK 1991), *S. cerevisiae* Dal80p (YKR034W) (CUNNINGHAM AND COOPER 1991), *S. cerevisiae* Gzf3p (YJL110C) (SOUSSI-BOUDEKOU *et al.* 1997), *A. nidulans* AreB beta (AN6221) (CONLON *et al.* 2001), *A. nidulans* LreA (AN3435) and LreB (AN3607) (PURSCHWITZ *et al.* 2008), *A. nidulans* SreA (AN0176) (HAAS *et al.* 1999), and *A. nidulans* NsdD (AN3152) (HAN *et al.* 2001), *Homo sapiens* GATA-1 (P15976) (TRAINOR *et al.* 1990; ZON *et al.* 1990), *H. sapiens* GATA-2 (P23769) (LEE *et al.* 1991; DORFMAN *et al.* 1992), *H. sapiens* GATA-3 (P23771) (HO *et al.* 1991; KO *et al.* 1991), *H. sapiens* GATA-4 (P43694) (HUANG *et al.* 1995), *H. sapiens* GATA-5 (NP_536721) (GAO *et al.* 1998), *H. sapiens* GATA-6 (Q92908) (SUZUKI *et al.* 1996) and mouse GATA-4 (Q08369) (ARCECI *et al.* 1993).

2.3.7 Immunostaining, Immunofluorescence, and GFP Microscopy

Immunostaining was conducted as described previously (TODD *et al.* 2005). Indirect UV immunofluorescence microscopy was performed using an Olympus BX51 upright biological reflected fluorescence microscope equipped with Nomarski Differential Interference Contrast (DIC), an EXFO X-Cite 120 Q fluorescence illumination system and a UPlanFLN Plan Semi Apochromat (Field Number FN26.5) Fluorite 100× oil objective with a numerical aperture of 1.30. Alexa-488 immunofluorescence was detected using a BrightLine Fluorescein Isothiocyanate (FITC) filter set (excitation wavelength band pass, 482/35 nm; dichroic mirror, 506 nm; emission 536/40 nm ZPIXEL). DAPI (4',6-diamidino-2-

phenylindole) fluorescence was detected using a BrightLine DAPI Hi Contrast filter set (excitation wavelength band pass, 387/11 nm; dichroic mirror, 409nm; ZPIXEL). For direct visualization of GFP, germlings were prepared for UV fluorescence microscopy as described previously (SMALL *et al.* 2001). GFP fluorescence was detected in fixed cells with the same microscope and camera as used for immunomicroscopy but using a BrightLine GFP filter set (excitation wavelength band pass 473/31, dichroic mirror, 495 nm; emission 483/32 nm ZPIXEL). At least 30 nuclei from each of two independent experiments were analyzed for each growth condition. Photomicrographs were captured using an Olympus DP72 12.8 Megapixel digital color camera and DP2-BSW digital camera software. Images were manipulated similarly within and between experiments using Adobe Photoshop CS2022. Images were cropped, and the tonal range was increased by adjusting highlights and shadows without altering the color balance. GFP or α -HA fluorescence was quantified with ImageJ (W. S. Rasband, ImageJ, U. S. National Institutes of Health, Bethesda, Maryland, USA, <http://imagej.nih.gov/ij/>, 1997-2012) using representative raw images. The nuclear fluorescence to cytoplasmic fluorescence ratio per unit area was calculated using the mean of 25 randomly paired ratios of nuclear to cytoplasmic regions, allowing the Standard Error of the Mean (SEM) to be calculated.

2.3.8 Abbreviations of varying degrees of usefulness

ANM – *Aspergillus* Nitrogen-free Minimal media

AspGD – *Aspergillus* Genome Database

FungiDB – Fungi Database

FGSC – Fungal Genetics Stock Center

SGD – *Saccharomyces* Genome Database

GFP – Green Fluorescent Protein

HA – Hemagglutinin

NLS – Nuclear Localization Signal

NES – Nuclear Export Signal

5-FOA – 5-fluoroorotic acid

NPC – Nuclear Pore Complex

-N – Nitrogen Starvation

OE – Overexpression

DBD – DNA-binding domain

ZF – Zinc finger

Even the smallest person can
change the course of the future.

Chapter 3 - Nuclear Localization of the GATA transcription factor AreA

3.1 Abstract

The *Aspergillus nidulans* GATA transcription factor AreA activates transcription of nitrogen metabolic genes in response to nitrogen limitation and is known to accumulate in the nucleus during nitrogen starvation. Sequence analysis of AreA revealed multiple nuclear localization signals (NLSs), five putative classical NLSs conserved in fungal AreA orthologs but not in the yeast functional orthologs Gln3p or Gat1p, and one putative non-canonical RRX₃₃RXR bipartite NLS within the DNA-binding domain. In order to identify the functional NLSs in AreA we constructed *areA* mutants affected in individual or combinations of putative NLSs as well as strains expressing Green Fluorescent Protein (GFP)-AreA NLS fusion genes. Deletion of all five classical NLSs individually or collectively did not affect utilization of nitrogen sources or AreA-dependent gene expression and did not prevent AreA nuclear localization. Mutation of the bipartite NLS conferred inability to utilize alternative nitrogen sources and abolished AreA-dependent gene expression, likely due to effects on DNA binding, but did not prevent AreA nuclear localization. Mutation of all six NLSs simultaneously prevented AreA nuclear accumulation. The bipartite NLS alone strongly directed GFP to the nucleus, whereas the classical NLSs collaborated to direct GFP to the nucleus. Therefore, AreA contains multiple conserved NLSs, which show redundancy and together function to mediate nuclear import. The noncanonical bipartite NLS is conserved in GATA factors from *Aspergillus*, yeast, and mammals, indicating an ancient origin.

3.2 Contribution statement

Cameron C. Hunter constructed the GFP-NLS fusion strains and performed GFP-NLS microscopy, constructed *fmdS-lacZ* strains and performed the reporter gene assays, constructed several *gpd(p)areA^{HA}* mutant strains and performed immunostaining and immunofluorescence microscopy. K. Siebert, K.H. Wong, S.D. Kreutzberger, J.A. Fraser, D.F. Clarke and R.B. Todd contributed to *gpd(p)areA^{HA}* variant strains construction. D.J. Downes conducted the growth tests and preparation of Figure 3.3 and contributed to immunofluorescence microscopy. R.B. Todd performed immunostaining and immunofluorescence microscopy. R.B. Todd, M.J. Hynes and M.A. Davis contributed to experimental design, data interpretation, and supervision. C.C. Hunter, R.B. Todd, and M.A. Davis wrote the manuscript.

Most of the work presented in this chapter is published as Hunter, C.C., Siebert, K.S., Downes, D.J., Wong, K.H., Kreutzberger, S.D., Fraser, J.A., Clarke, D.F., Hynes, M.J., Davis, M.A., and Todd, R.B. (2014) Multiple nuclear localization signals mediate nuclear localization of the GATA transcription factor AreA. ***Eukaryotic Cell***. **13**: 527-538. [KAES contribution: 14-064-]]

3.3 Introduction

Eukaryotic transcription factors are synthesized in the cytoplasm but function in the nucleus to regulate gene expression. This provides a logistical problem for these proteins, as they must be imported into the nucleus for function. Proteins enter the nucleus through the nuclear pore complex (NPC) (FELDHERR *et al.* 1984). Depending on the size of the protein, they can either passively diffuse through the pore (< 30 kDa), or they must be actively transported through the NPC (> 30 kDa) (MATTAJ AND ENGLMEIER 1998; TRAN *et al.* 2007). The NPC has been thoroughly studied in *Aspergillus nidulans* and is a dynamic structure of essential and nonessential proteins (DE SOUZA *et al.* 2003; DE SOUZA *et al.* 2004; OSMANI *et al.* 2006). Transport of large proteins through the NPC is facilitated by nuclear importins (karyopherins), which recognize short stretches of positively charged sequences on the cargo proteins that serve as nuclear localization signals (NLSs) (DINGWALL *et al.* 1982; KALDERON *et al.* 1984; JANS *et al.* 2000; PHILIPS *et al.* 2007). *A. nidulans* has 17 karyopherins to actively transport proteins between the cytoplasm and the nucleus (ARAUJO-BAZAN *et al.* 2009; MARKINA-INARRAIRAEGUI *et al.* 2011). There are two main types of classical NLSs found throughout eukaryotes, monopartite NLSs and bipartite NLSs. The monopartite NLSs conform to the classical SV40 Large T-antigen NLS and are the most commonly found NLS type (KALDERON *et al.* 1984). The classical bipartite NLSs comprise two distinct lysine-rich parts generally separated by 10 to 12 amino acids (ROBBINS *et al.* 1991). Other NLS types are known, including tripartite NLSs associated with the zinc binuclear clusters of *Saccharomyces cerevisiae* Lys14p, and *A. nidulans* PrnA, AlcR and NirA (EL ALAMI *et al.* 2000; POKORSKA *et al.* 2000; NIKOLAEV *et al.* 2003; BERGER *et al.* 2006), and a non-canonical arginine based bipartite NLS (RRX₃₃RXR) discovered in mammalian GATA-4 (PHILIPS *et al.* 2007).

Although most nuclear proteins contain a single NLS, some nuclear proteins lacking a NLS are thought to enter the nucleus by piggy-backing as a preassembled complex with a protein containing a NLS, as proposed for *A. nidulans* HapC and HapE, which associate with the NLS-containing protein HapB for nuclear import (STEIDL *et al.* 2004). In other cases, two or more NLSs occur within a single protein. Two NLSs were found in *A. nidulans* HapB, *S. cerevisiae* Gln3p, *S. cerevisiae* Mcm10p, human BCRA1, and human BCRA2 (CHEN *et al.* 1996; YANO *et al.* 2000; BURICH AND LEI 2003; CARVALHO AND ZHENG 2003; TUNCHEER *et al.* 2005),

whereas three NLSs were found in mammalian 5-lipoxygenase, human S1-1/RBM10, human Dot1a, and human Tra2 β (LUO *et al.* 2004; REISENAUER *et al.* 2010; LI *et al.* 2013; XIAO *et al.* 2013). From a literature survey of characterized NLSs in other transcription factors in *A. nidulans* we found most of these transcription factors appear to have between one and three NLSs, which makes the six NLSs in AreA an interesting and unique case (Table 3.1).

Table 3.1 Survey of NLSs experimentally confirmed in *A. nidulans*

Protein	NLS Type	Attributes	Location	Paper
PrnA	Tripartite		N-terminal	Pokorska, 2000
AmyR	Bipartite		N-terminal	Makita, 2009
HapB	2 Monopartite	NLS 2 in other <i>Aspergillus</i> , main NLS. NLS 1 does not appear to function.	C-terminal	Steidl, 2004 Goda, 2005
VeA	Classical Bip (KRX ₍₁₀₋₁₂₎ KRRK) KKX ₁₁ KRAR		N-terminal	Stinnett, 2007
AlcR	Five segment cluster part of the Zn ₂ Cys ₆ Cluster	NLS are independent of Zn ₂ Cys ₆ cluster. Can import without binding. Recognition of DNA binding sites with impaired nuclear targeting.	N-terminal	Nikolaev, 2003
NirA	3 motifs	K34 (8AA) upstream of Zn Cluster R46 within Zn Cluster R79 (9AA) downstream Zn Cluster	N-terminal	Berger, 2006
PacC	not reported	Cys2His2 zf-DBD 3 zf-protein It appears that the NLS(s) are in the ZF BDs.	N-terminal	Fernandez-Martinez, 2003

While localization to the proper subcellular compartment constitutes a logistical problem it also provides a platform for regulating protein function. A number of examples of regulated nuclear localization of transcription factors are known, e.g. *S. cerevisiae* Gln3p, Msn2p, and Mig1p (DE VIT *et al.* 1997; BECK AND HALL 1999), *Neurospora crassa* NUC1 (PELEG *et al.* 1996), and *A. nidulans* AmyR, PacC and NirA (MINGOT *et al.* 2001; BERGER *et al.* 2006; MAKITA *et al.* 2009). Regulated localization of nuclear proteins can be achieved by altering the balance of nuclear import and nuclear export using multiple mechanisms including direct covalent modification of targeting sequences to prevent or promote transport, cytoplasmic or nucleoplasmic anchoring, and by intramolecular or intermolecular masking of the NLS or nuclear export signal (NES) (POON AND JANS 2005). Covalent modification by phosphorylation and cytoplasmic anchoring both regulate nuclear import of *S. cerevisiae* Gln3p (BECK AND HALL 1999; BERTRAM *et al.* 2000; CARVALHO AND ZHENG 2003), whereas nuclear localization of *A.*

nidulans PacC and AmyR is regulated by intramolecular masking (MINGOT *et al.* 2001; MAKITA *et al.* 2009).

GATA transcription factors regulate transcription of genes involved in a range of processes, including hematopoiesis and cardiac development in mammals, as well as nitrogen metabolism, iron siderophore metabolism, sexual development and light response in fungi (SCAZZOCCHIO 2000). They have a zinc finger DNA binding domain composed of four cysteine residues and bind to the HGATAR consensus sequence (SCAZZOCCHIO 2000). In *A. nidulans*, the GATA transcription factor AreA is responsible for expression of genes subject to nitrogen metabolite repression (KUDLA *et al.* 1990), reviewed in Todd (2016). When cells are grown under nitrogen limiting conditions, AreA activity is partially derepressed due to increased levels of *areA* transcription and stability of *areA* mRNA compared with nitrogen sufficient conditions (LANGDON *et al.* 1995; PLATT *et al.* 1996b; MOROZOV *et al.* 2000; MOROZOV *et al.* 2001). AreA activity is further increased during nitrogen limitation due to reduced activity of the NmrA corepressor (ANDRIANOPOULOS *et al.* 1998; LAMB *et al.* 2004; WONG 2007; KOTAKA *et al.* 2008; ZHAO *et al.* 2010). An additional level of control is observed during nitrogen starvation. AreA accumulates in the nucleus when cells are nitrogen starved and this is accompanied by elevated AreA-dependent gene expression (TODD *et al.* 2005). Within minutes of addition of a nitrogen nutrient, accumulated AreA is rapidly exported from the nucleus and elevated AreA-dependent gene expression is attenuated (TODD *et al.* 2005). This rapid response identifies nuclear export as the mechanism of regulation of AreA nuclear accumulation. Regulated nuclear localization has now also been shown for the AreA ortholog in *Fusarium fujikuroi* (MICHIELSE *et al.* 2013).

Nuclear import is clearly critical for AreA function. Despite the importance, the mechanism of AreA nuclear import is not known. Herein we identify and characterize the nuclear localization signals in AreA. We show that the AreA protein contains five classical monopartite NLSs, which are conserved in most ascomycete AreA orthologs, and a non-canonical bipartite NLS conserved with the RRX₃₃RXR NLS of mammalian GATA-4 (PHILIPS *et al.* 2007). We determine the effects of mutations affecting these NLSs on AreA function and nuclear localization. When these classical NLS are deleted separately or when point mutations are introduced in place of the four key arginines in the bipartite NLS, nuclear accumulation is not disrupted. However, when all of the NLSs are mutated simultaneously

we found no accumulation of AreA in the nucleus. We also fused the NLSs to GFP and determined that the bipartite NLS is sufficient to direct nuclear localization, and that the classical NLSs together can collaborate to direct nuclear import. The conservation in AreA orthologs of this unusually large number of apparently redundant NLSs suggests they each play a role in directing AreA to the nucleus, possibly via alternative importins.

3.4 Materials and Methods

3.4.1 Strain Construction

Construction of *gpd(p)areA^{HA}* NLS mutants via two-step gene replacement

The recipients for two-step gene replacement, MH11131 (*gpd(p)areA^{HA} pyroA4 ΔnkuA::argB*) or MH11457 (*gpd(p)areA^{HA.Δ60-423} pyroA4 nkuAΔ::Bar*), were constructed by meiotic crossing to introduce the nonhomologous end-joining *nkuAΔ* mutation (NAYAK *et al.* 2006).

Mutation of the bipartite NLS

The *R685A, R686A, R720A, R722A* bipartite NLS mutation (*bip^{ALA}*) construct was made in two inverse PCR steps using pCW7273 (wild type JFareA1-JFareA2 *areA* in pBluescript-SK+) as template. In the first inverse PCR, primers DeltaZnF3 and AreAR720AR722A were used. The PCR product was gel purified, phosphorylated, ligated, and the resultant plasmid (pSL7199) was sequenced to confirm the presence of the R720AR722A mutations. The second inverse PCR used primers newAreAR685AR686A and newAreA688invF to amplify using pSL7199 as template. The 1.2kb *Sall-NotI* fragment from the resulting plasmid was subcloned into pSM6363 digested with *Sall* and *NotI* to generate pRT7309. pRT7309 was transformed into MH11131 and transformants were selected for pyridoxine prototrophy. One transformant was selfed, and the progeny were screened for loss of *AfpyroA* and *areA* loss-of-function on nitrate to identify RT49 (*gpd(p)areA^{HA.R685A,R686A,R720A,R722A} pyroA4*).

NLS mutant combinations

The Δ NLS4,*R685A, R686A, R720A, R722A, ΔNLS5* (NLS4Δ-*bip^{ALA}*-NLS5Δ) construct (pRT145) was made similarly to the bipartite NLS mutation construct in two inverse PCR steps followed by subcloning into the *AfpyroA* vector pSM6363, except using the NLS4ΔNLS5Δ plasmid pCW6609 as the primary template to generate pSL7200, which was used as the template in the second step. pRT145 was transformed into MH11131, and pyridoxine prototrophs were selected, selfed, and the progeny were screened for pyridoxine auxotrophs that had lost the *AfpyroA* selectable marker and were *areA* loss-of-function mutants, i.e., two-step gene replacements. Depending on the position of the crossovers in the

first and second steps, different outcomes are possible in the two-step gene replacement progeny. Sequence analysis of JFareA1-JFareA2 PCR amplicons from genomic DNA of second-step pRT145 gene replacement progeny identified two different gene replacements: NLS4Δbip^{ALA} (RT1: *gpd(p)areA*^{HA.Δ609-615.R685A,R686A,R720A,R722A} *pyroA4*) and NLS4Δbip^{ALANLS5Δ} (RT2: *gpd(p)areA*^{HA.Δ609-615.R685A,R686A,R720A,R722A.Δ811-816} *pyroA4*). For bip^{ALANLS5Δ}: The bip^{ALANLS5Δ} region of pRT145 was separated from NLS4Δ by amplification with areANLS4-InvF and JFareA2, then cloned into the *Sma*I site of pSM6363 to generate pKS138. pKS138 was transformed into MH11131 and transformants were selected for pyridoxine prototrophy, selfed, and the progeny were screened for loss of *AfpyroA* and *areA* loss-of-function on nitrate to identify RT231 (*gpd(p)areA*^{HA.R685A,R686A,R720A,R722A.Δ811-816} *pyroA4*).

NLS mutants that contained Δ60-423 (i.e., ΔNLS1,2,3) were made by two-step gene replacement in a MH11457 (*gpd(p)areA*^{HA.Δ60-423} *pyroA4* Δ*nkuA::Bar*) recipient isolated from a cross of MH10041 × MH11072. In each case, the constructs contained *areA* sequences in the *AfpyroA* vector pSM6363, and transformants were selected for pyridoxine prototrophy, selfed, and progeny screened for loss of pyridoxine prototrophy. The second step of the gene replacement was confirmed by sequence of PCR products amplified with JFareA1 and JFareA2. RT175 (*gpd(p)areA*^{HA.Δ60-423.Δ609-615} *pyroA4*) was made by transformation with the construct pCH225 which carried a JFareA1-JFareA2 PCR product from MH11099 (NLS4Δ) genomic DNA cloned into *Sma*I site of pSM6363. RT168 (*gpd(p)areA*^{HA.Δ60-423.Δ811-816} *pyroA4*) was made by transformation with the construct pKS139, which carried a JFareA1-JFareA2 PCR product from a pSL7191 (NLS5Δ) template cloned into *Sma*I site of pSM6363. RT46 (*gpd(p)areA*^{HA.Δ60-423.Δ609-615.Δ811-816} *pyroA4*) was made by transformation with the construct pKS19, which carried a JFareA1-JFareA2 PCR product from pCW6607 cloned into the *Sma*I site of pSM6363. RT147 (*gpd(p)areA*^{HA.Δ60-423.R685A,R686A,R720A,R722A} *pyroA4*) was made by transformation with the construct pRT7309. RT30 (*gpd(p)areA*^{HA.Δ60-423.Δ609-615.R685A,R686A,R720A,R722A} *pyroA4*) and RT37 (*gpd(p)areA*^{HA.Δ60-423.Δ609-615.R685A,R686A,R720A,R722A.Δ811-816} *pyroA4*) were made by transformation with the construct pRT145. The positions of the crossovers were different in RT30 and RT37, as revealed by sequencing. RT237 (*gpd(p)areA*^{HA.Δ60-423.R685A,R686A,R720A,R722A.Δ811-816} *pyroA4*) was made by transformation with the construct pKS138.

Construction of GFP-NLS fusions

Constructs: We constructed *gfp-NLS* fusions in *wA*-targeting vectors in two steps. First, pDFC6917, which was derived by end-fill of the unique *Bgl*III site in the polylinker of the *gpd(p)gfp* fusion plasmid pALX213 (pAA4362; (SMALL *et al.* 2001)), was used to construct *gfp-nls* fusions expressed from the *gpdA* promoter. The NLSs were amplified with primers containing *Bam*HI or *Hind*III sites, and the amplicons were digested with *Bam*HI and *Hind*III, and ligated into the *Bam*HI and *Hind*III sites of pDFC6917. Second, the *gpd(p)gfpNLS* sequence was PCR-amplified with primers *Not*I T7 and T3, and the *Not*I-*Bam*HI restriction fragment was subcloned into the *Not*I and *Bam*HI sites of the *wA* targeting vector pCW6500, which was constructed by insertion of an internal 2.15 kbp *Eco*ICRI fragment of the *wA* (white) gene, amplified with primers whitecodF and whitecodR, into the *Nru*I site of pSM6363. For the GFP control, *gpd(p)gfp* was PCR-amplified from pDFC6917 and subcloned into pCW6500 to generate pCH183. For GFP-NLS1,2,3, *areA* codons 204-287 were amplified from MH1 genomic DNA using CCHNLS123F1 and CCHNLS123R1 primers, cut with *Bam*HI and *Hind*III and ligated into pDFC6917. The *gpd(p)gfpNLS123* sequence was subcloned into pCW6500 to generate pCH59. For GFP-NLS4, KSNLS4F and KSNLS4R primers were used to amplify *areA* codons 600-630 using the pKS5 (JFareA1-JFareA2 *areA* amplified from MH1 genomic DNA cloned into the *Sma*I site of pBluescriptSK+) template. The *gpd(p)gfpNLS4* sequence was subcloned into pCW6500 to generate pCH212. For GFP-NLS5, KSNLS5F and KSNLS5R primers were used to amplify *areA* codons 801-826 from pKS5 template. The *gpd(p)gfpNLS5* sequence was transferred into pCW6500 to generate pCH62. For GFP-bipNLS, KSareAzfF and KSareAzfR primers were used to amplify *areA* codons 646-764 from pKS5 template. The *gpd(p)gfpbipNLS* sequence was transferred into pCW6500 to generate pCH64. For GFP-bip^{ALA}NLS, KSareAzfF and KSareAzfR primers were used to amplify *areA* codons 646-746 from pRT7309. The *gpd(p)gfpbip^{ALA}NLS* sequence was transferred into pCW6500 to generate pCH65. For GFP-NLS1,2,3,5, the NLS5 encoding codons 801-826 were amplified with primers CCHNLS5BglIIF and KSNLS5R using pKS5 template, digested with *Bgl*III and *Bam*HI and ligated into the *Bam*HI site of pCH59 to generate pCH180. For GFP-NLS1,2,3,4, the NLS4 encoding codons 600-630 were amplified with primers CCHNLS4BglIIF and KSNLS4R using pKS5 as template, digested with *Bgl*III and *Bam*HI and ligated into the *Bam*HI site of pCH59 to generate pCH227. For GFP-NLS4,5 the NLS5 encoding codons 801-

826 were amplified with primers CCHNLS5BglIIF and KSNLS5R using pCH62 template, digested with *Bgl*II and *Bam*HI and ligated into the *Bam*HI site of pCH212 to generate pCH226. For GFP-NLS1,2,3,4,5 the NLS4 and NLS5 encoding codons 600-630 and 801-826 were amplified with primers CCHNLS4BglIIF and KSNLS5R using pCH226 as template, digested with *Bgl*II and *Bam*HI and ligated in to the *Bam*HI site of pCH59 to generate pCH228.

GFP strains

The *gpd(p)-gfp-NLS* plasmids pCH59, pCH212, pCH62, pCH64, pCH65, pCH180, pCH226, pCH227, and pCH228 and the *gpd(p)gfp* control pCH183 were transformed into RT96 (*pyrG89 biA1 gpd(p)areA^{HA} fmdS-lacZ pyroA4 nkuAΔ::Bar crmA^{T525C}::pyrG⁺*). Transformants were selected for pyridoxine prototrophy and transformants with targeted integration at the *wA* gene by the internal *wA* fragment in the vector were visible as white colored colonies). Single copy integration was confirmed by Southern analysis (data not shown).

3.4.2 *Aspergillus nidulans* strains used in Chapter 3

Table 3.2 AreA^{HA} strains and strains used for construction in Chapter 3

Strain	Genotype^a
MH50	<i>yA adE20 su(adE20) areA102 pyroA4 riboB2</i>
MH764	<i>wA3 riboB2 facB101</i>
MH9883	<i>wA3 gpd(p)areA^{HA} riboB2 facB101</i>
MH9922	<i>wA3 areA::riboB(5') riboB2 facB101</i>
MH9949	<i>biA1 gpd(p)areA^{HA} amdS-lacZ</i>
MH10041	<i>wA3 gpd(p)areA^{HA.Δ60-423} pyroA4</i>
MH10266	<i>wA3 gpd(p)areA^{HA::riboB(3')} riboB2 facB101</i>
MH10897	<i>yA1 pabaA1 gpd(p)areA^{HA} fmdS-lacZ</i>
MH11050	<i>yA1 pabaA1 gpd(p)areA^{HA::riboB(3')} fmdS-lacZ</i>
MH11072	<i>yA1 pabaA1 gpd(p)areA^{HA::riboB(3')} fmdS-lacZ pyroA4 nkuAΔ::Bar</i>
MH11099	<i>yA1 pabaA1 gpd(p)areA^{HA.Δ609-615} fmdS-lacZ pyroA4 nkuAΔ::Bar</i>
MH11131	<i>yA1 pabaA1 gpd(p)areA^{HA} pyroA4 nkuAΔ::argB⁺</i>
MH11457	<i>gpd(p)areA^{HA.Δ60-423} pyroA4 nkuAΔ::Bar</i>
MH11668	<i>yA1 pabaA1 gpd(p)areA^{HA.Δ811-816} pyroA4 fmdS-lacZ nkuAΔ::Bar</i>
MH11967	<i>yA1 pabaA1 gpd(p)areA^{HA.Δ609-615.Δ811-816} fmdS-lacZ pyroA4 nkuAΔ::Bar</i>
RT1	<i>yA1 pabaA1 gpd(p)areA^{HA.Δ609-615.R685A,R686A,R720A,R722A} pyroA4 nkuAΔ::argB⁺</i>
RT2	<i>yA1 pabaA1 gpd(p)areA^{HA.Δ609-615.R685A,R686A,R720A,R722A.Δ811-816} pyroA4 nkuAΔ::argB⁺</i>
RT30	<i>gpd(p)areA^{HA.Δ60-423.Δ609-615.R685A,R686A,R720A,R722A} pyroA4 nkuAΔ::Bar</i>
RT37	<i>gpd(p)areA^{HA.Δ60-423.Δ609-615.R685A,R686A,R720A,R722A.Δ811-816} pyroA4 nkuAΔ::Bar</i>
RT46	<i>gpd(p)areA^{HA.Δ60-423.Δ609-615.Δ811-816} pyroA4 nkuAΔ::Bar</i>
RT49	<i>yA1 pabaA1 gpd(p)areA^{HA.R685A,R686A,R720A,R722A} pyroA4 nkuAΔ::argB⁺</i>
RT54	<i>pyrG89 gpd(p)areA^{HA} fmdS-lacZ</i>
RT147	<i>gpd(p)areA^{HA.Δ60-423.R685A,R686A,R720A,R722A} pyroA4 nkuAΔ::Bar</i>
RT168	<i>gpd(p)areA^{HA.Δ60-423.Δ811-816} pyroA4 nkuAΔ::Bar</i>
RT175	<i>gpd(p)areA^{HA.Δ60-423.Δ609-615} pyroA4 nkuAΔ::Bar</i>
RT231	<i>yA1 pabaA1 gpd(p)areA^{HA.R685A,R686A,R720A,R722A.Δ811-816} pyroA4 nkuAΔ::argB⁺</i>
RT237	<i>gpd(p)areA^{HA.Δ60-423.R685A,R686A,R720A,R722A.Δ811-816} pyroA4 nkuAΔ::Bar</i>

^a All strains carry the *veA1* mutation.

Table 3.2 AreA^{HA} strains and strains used for construction in Chapter 3 (continued)

Strain	Genotype^a
NLS-GFP strains	
RT96	<i>pyrG89 biA1 gpd(p)areA^{HA} fmdS-lacZ pyroA4 nkuAΔ::Bar crmA^{T525C}::pyrG⁺</i>
RT184	<i>pyrG89 biA1 wA::gpd(p)-gfp::areANLS123-AfpyroA gpd(p)areA^{HA} fmdS-lacZ pyroA4 nkuAΔ::Bar crmA^{T525C}::pyrG⁺</i>
RT187	<i>pyrG89 biA1 wA::gpd(p)-gfp::areAzf-AfpyroA gpd(p)areA^{HA} fmdS-lacZ pyroA4 nkuAΔ::Bar crmA^{T525C}::pyrG⁺</i>
RT189	<i>pyrG89 biA1 wA::gpd(p)-gfp::areANLS5-AfpyroA gpd(p)areA^{HA} fmdS-lacZ pyroA4 nkuAΔ::Bar crmA^{T525C}::pyrG⁺</i>
RT289	<i>pyrG89 biA1wA:: gpd(p)-gfp-AfpyroA gpd(p)areA^{HA} fmdS-lacZ pyroA4 nkuAΔ::Bar crmA^{T525C}::pyrG⁺</i>
RT294	<i>pyrG89 biA1 wA::gpd(p)-gfp::areANLS123,5-AfpyroA gpd(p)areA^{HA} fmdS-lacZ pyroA4 nkuAΔ::Bar crmA^{T525C}::pyrG⁺</i>
RT295	<i>pyrG89 biA1 wA::gpd(p)-gfp::areAzfbip^{ALA}-AfpyroA gpd(p)areA^{HA} fmdS-lacZ pyroA4 nkuAΔ::Bar crmA^{T525C}::pyrG⁺</i>
RT372	<i>pyrG89 biA1 wA::gpd(p)-gfp::areANLS4-AfpyroA gpd(p)areA^{HA} fmdS-lacZ pyroA4 nkuAΔ::Bar crmA^{T525C}::pyrG⁺</i>
RT393	<i>pyrG89 biA1 wA::gpd(p)-gfp::areANLS4,5-AfpyroA gpd(p)areA^{HA} fmdS-lacZ pyroA4 nkuAΔ::Bar crmA^{T525C}::pyrG⁺</i>
RT396	<i>pyrG89 biA1 wA::gpd(p)-gfp::areANLS123,4-AfpyroA fmdS-lacZ gpd(p)areA^{HA} pyroA4 nkuAΔ::Bar crmA^{T525C}::pyrG⁺</i>
RT397	<i>pyrG89 biA1 wA::gpd(p)-gfp::areANLS123,4,5-AfpyroA gpd(p)areA^{HA} fmdS-lacZ pyroA4 nkuAΔ::Bar crmA^{T525C}::pyrG⁺</i>
Strains for reporter gene assays	
MH10897	<i>yA1 pabaA1 gpd(p)areA^{HA} fmdS-lacZ</i>
MH11432	<i>gpd(p)areA^{HA.Δ60-423} fmdS-lacZ pyroA4 nkuAΔ::Bar</i>
MH10967	<i>yA1 areAΔ::riboB fmdS-lacZ pyroA4 riboB2 facB101</i>
RT121	<i>yA1 pabaA1 gpd(p)areA^{HA.Δ609-615.R685A,R686A,R720A,R722A} fmdS-lacZ pyroA4 nkuAΔ::argB⁺</i>
RT123	<i>yA1 pabaA1 gpd(p)areA^{HA.Δ609-615.R685A,R686A,R720A,R722A.Δ811-816} fmdS-lacZ pyroA4 nkuAΔ::argB⁺</i>

^a All strains carry the *veA1* mutation.

Table 3.2 AreA^{HA} strains and strains used for construction in Chapter 3 (continued)

Strain	Genotype^a
Strains for reporter gene assays (continued)	
RT129	<i>yA1 pabaA1 gpd(p)areA^{HA.Δ60-423.Δ609-615.R685A,R686A,R720A,R722A} fmdS-lacZ pyroA4</i>
RT131	<i>yA1 pabaA1 gpd(p)areA^{HA.Δ60-423.Δ609-615.R685A,R686A,R720A,R722A.Δ811-816} fmdS-lacZ pyroA4</i>
RT132	<i>yA1 pabaA1 gpd(p)areA^{HA.Δ60-423.Δ609-615.Δ811-816} fmdS-lacZ</i>
RT134	<i>yA1 pabaA1 gpd(p)areA^{HA.R685A,R686A,R720A,R722A} fmdS-lacZ pyroA4 nkuAΔ::argB⁺</i>
RT212	<i>gpd(p)areA^{HA.Δ60-423.Δ811-816} fmdS-LacZ</i>
RT214	<i>gpd(p)areA^{HA.Δ60-423.R685A,R686A,R720A,R722A} fmdS-lacZ pyroA4</i>
RT216	<i>gpd(p)areA^{HA.Δ60-423.Δ609-615} fmdS-lacZ</i>
RT248	<i>yA1 gpd(p)areA^{HA.Δ60-423.R685A,R686A,R720A,R722A.Δ811-816} fmdS-lacZ pyroA4</i>
RT273	<i>yA1 pabaA1 gpd(p)areA^{HA.bipΔNLS5} fmdS-lacZ</i>
<i>gpd(p)gfp::areA</i> strains	
RT556	<i>yA1 pabaA1 gpd(p)gfp::areA(A2) fmdS-lacZ pyroA4 nkuAΔ::Bar</i>
RT557	<i>yA1 pabaA1 gpd(p)gfp::areA(A13) fmdS-lacZ pyroA4 nkuAΔ::Bar</i>
RT558	<i>yA1 pabaA1 gpd(p)gfp::areA(A16) fmdS-lacZ pyroA4 nkuAΔ::Bar</i>
RT559	<i>yA1 pabaA1 gpd(p)gfp::areA(A19) fmdS-lacZ pyroA4 nkuAΔ::Bar</i>
RT560	<i>yA1 pabaA1 gpd(p)gfp::areA(A21) fmdS-lacZ pyroA4 nkuAΔ::Bar</i>
RT561	<i>yA1 pabaA1 gpd(p)gfp::areA(A23) fmdS-lacZ pyroA4 nkuAΔ::Bar</i>

^a All strains carry the *veA1* mutation.

3.4.3 Oligonucleotides used in this study

Table 3.3 Oligonucleotides used in this study

Name	Sequence	Coordinates[†]
JFareA1	5'-CGACTCGGATGTTGAAGATG-3'	+1591 - +1610
areANLS4-InvR	5'-GTCTTGATCCCGATTGCGCACCTCGC-3'	+1885 - +1860
RTareANLS5Del	5'-CAGAGGCCTTTTCCAGAGCCACCTGTA-3'	+2525 - +2510, +2491 - +2481
JFareA2	5'-GCGTCACTCGTAACCATCAA-3'	+2881 - +2862
areANLS4-invF	5'-CGCACCTCGTCCACTCCAAACACAGC-3'	+1907 - +1932
DeltaZnF3	5'-AACAGCGCCAATAGCCTTGC-3'	+2006 - +2012, +2235 - +2257
AreAR720AR722A	5'-GGCGTTAGCCTTCTTGATCA -3'	+2227 - +2208
newAreAR685AR686A	5'-GTTAGCCGCCACAGCGG-3'	+2122 - +2105
newAreA688invF	5'-CCTGAAGGTCAGCCGCTGT-3'	+2123 - +2141
NotIT7	5'-TTGCGCCGCTAATACGACTCACTATAGGG-3'	N/A
T3	5'-AATTAACCCTCACTAAAGGG-3'	N/A
CCHNLS123F1	5'-AAAAGCTTCACAACGAAAGCCTCCGAAGCC-3'	+670 - +691
CCHNLS123R1	5'-AAGGATCCGGACACAGGCGGTACGTGAG-3'	+922 - +903
KSNLS4F	5'-AAAAGCTTCAGCGAGGTGCGCAATCGG-3'	+1859 - +1876
KSNLS4R	5'-AAGGATCCGCTCTGGCGTAGTAGTTGG-3'	+1951 - +1933
CCHNLS4BglIIF	5'-AAAGATCTAGCGAGGTGCGCAATCGG-3'	+1859 - +1876
KSNLS5F	5'-AAAAGCTTAAACAACGGTTGTGGTGCGGT-3'	+2461 - +2481
KSNLS5R	5'-AAGGATCCCGCCATATCAACATCAGAG-3'G	+2520 - +2539
CCHNLS5BglIIF	5'-AAAAGATCTAACAACCGGTTGTTGTGCG-3'	+2462 - +2479
KSareAzfF	5'-TTAAGCTTGTGCGGTCTAAACAGCGC-3'	+1996 - +2013
KSareAzfR	5'-TTGGATCCGGATGTCGTATTGCTTTGG-3'	+2353 - +2335
whitecodF	5'-TATGGTGCCAATCCACGG-3'	N/A
whitecodR	5'-TGATGGAAGATCCTGGCC-3'	N/A
T7	5'-TAATACGACTCACTATAGGG-3'	N/A
GFPRLINKR	5'-TTTACTCATTCCTCGTTCGGAACCTCTCAG CCAAGTCACCCTTGACAGCTCGTCCAT-3'	N/A
5'AreANoStarLINKF	5'-TCGGAACACGGGGAATGAGTAAAGGAGAAGA ACTTTTCACTTCTGGGTTGACTCTCGGG-3'	N/A
AreA3'800bpR	5'-GGTAACACAACGTACCTGGAAGTC-3'	N/A

[†] Relative to the A of the *areA* ATG at position +1.

3.5 Results

3.5.1 AreA has multiple conserved Nuclear Localization Signals

The *A. nidulans* AreA sequence was analyzed for nuclear localization signals using the PSORTII program (NAKAI AND HORTON 1999), which identifies sequences with similarity to consensus targeting signals. Five classical NLSs were identified within AreA by their adherence to the PKKKRKV classical SV-40 Large T antigen-type NLS consensus sequence (HICKS AND RAIKHEL 1995): NLS1 (residues 216-222), NLS2 (residues 252-258), NLS3 (residues 271-277), NLS4 (residues 609-615), and NLS5 (residues 811-816) (Figure 3.1)

We aligned the protein sequences of AreA orthologs (Figure 3.2). NLS1, NLS2, NLS3, and NLS5 were strongly conserved in most ascomycete homologs of AreA. NLS4 was conserved in many ascomyetes but showed poor conservation with *F. fujikuroi* AreA, *M. oryzae* NUT1, and *N. crassa* NIT2. None of the classical NLSs were conserved in either Gln3p or Gat1p from *S. cerevisiae*. Gln3p contains two predicted NLSs, only one of which is required for nuclear localization (CARVALHO AND ZHENG 2003). Neither of these sequences corresponds in position with any of the classical NLSs in the AreA orthologs.

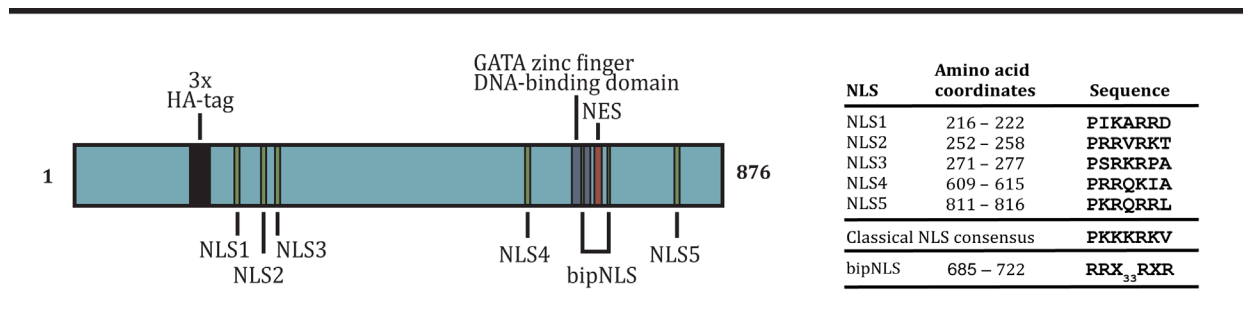


Figure 3.1 Nuclear Localization Signals in AreA

Sequences of the five classical NLSs identified by similarity to the consensus sequence PKKKRKV using PSORTII analysis. The bipartite NLS conforms to the noncanonical bipartite arginine NLS RRX₃₃RXR. Position of the NLSs in the AreA protein. The NLSs are indicated as green bars, the GATA zinc finger DNA-binding domain is a dark blue box, the NES is a red box, and the HA-tag is indicated as a black box.

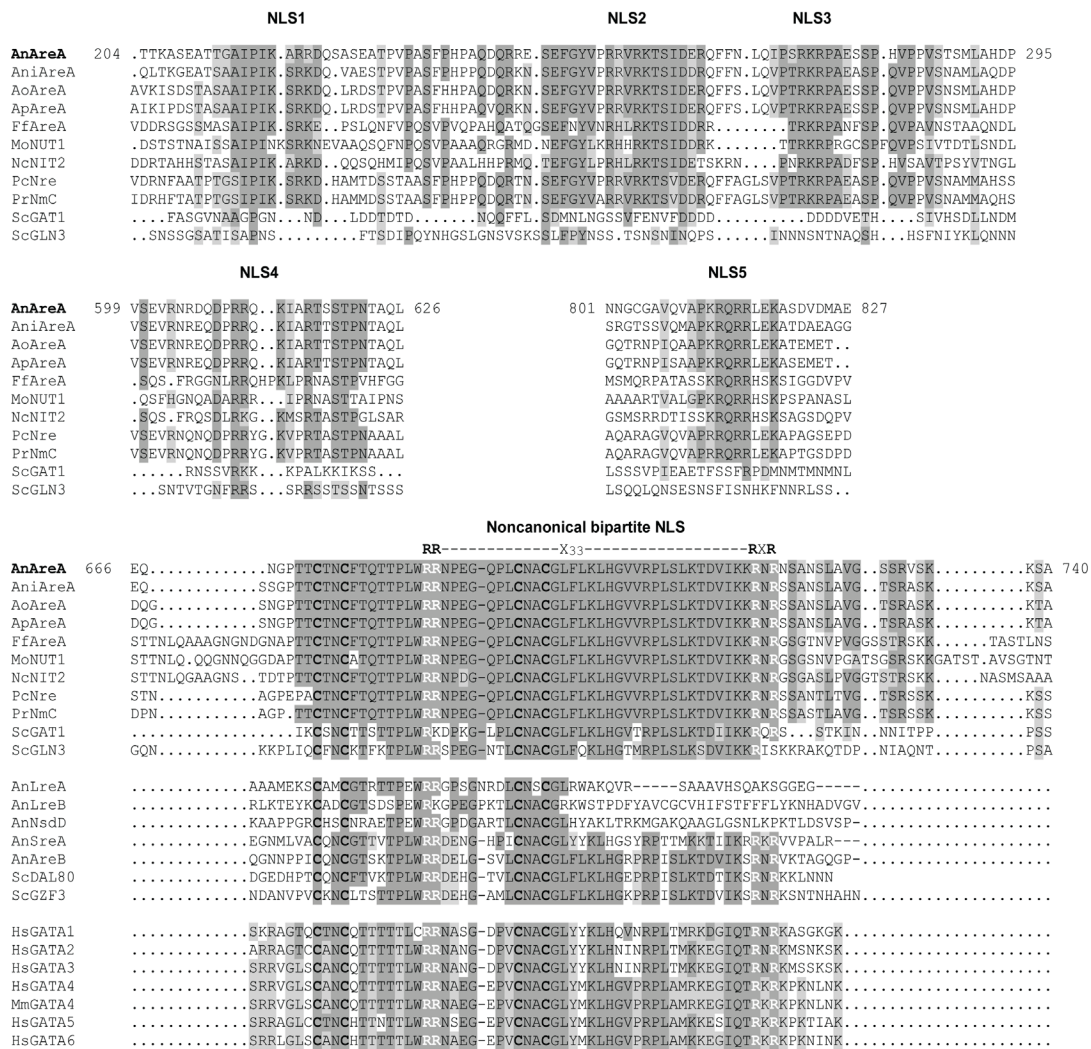


Figure 3.2 AreA NLS protein sequence alignment

Partial protein sequence alignment of AreA homologs showing the conservation of the nuclear localization signals across species. An = *A. nidulans*, Ani = *Aspergillus niger*, Ao = *Aspergillus oryzae*, Ap = *Aspergillus parasiticus*, Ff = *F. fujikuroi*, Mo = *M. oryzae*, Nc = *N. crassa*, Pc = *Penicillium chrysogenum*, Pr = *Penicillium roqueforti*, Sc = *Saccaromyces cerevisiae*, Hs = *Homo sapiens*, Mm = *Mus musculus*. For the fungal NLSs including the non-canonical bipartite NLS dark grey shading represents >60% identity, light grey shading represents >60% similarity. The arginine-based bipartite NLS has the arginine residues bolded in white along with the cysteine residues for the GATA zinc finger binding domain bolded in black. For the human and mouse GATA transcription factors, dark grey shading represents identity with the fungal amino acids, light grey shading represents identity within the mammalian GATA factors but not with the fungal zinc finger binding domain. Coordinates are shown for *A. nidulans* AreA.

3.5.2 Effects of mutation of AreA classical NLSs on AreA activity

We constructed a battery of HA-epitope tagged AreA mutant strains by direct selection or by two-step gene replacement (see Methods) in order to determine the effects of the loss of NLSs on AreA function and localization. The AreA^{HA} variants were expressed from the constitutive *gpdA* promoter (*gpd(p)*) to uncouple any effects of the mutations on autogenous control of *areA* transcript levels (TODD *et al.* 2005). We deleted NLS1, NLS2, and NLS3 together in a single deletion mutation of residues 60-423 (Δ NLS1,2,3). NLS4 (residues 609-615) and NLS5 (residues 811-816) were deleted individually to generate the NLS4 Δ and NLS5 Δ mutations. We also made all of the possible double and triple combinations of the Δ NLS1,2,3, Δ NLS4, and Δ NLS5 mutations. The seven mutants, with wild type and *areA* Δ controls, were tested for growth on a range of sole nitrogen sources including the preferred nitrogen sources ammonium and glutamine, and various alternative nitrogen sources (Figure 3.3). Mutation of the classical NLSs in all combinations including altogether, resulted in growth comparable to the wild type controls for all nitrogen sources tested.

In order to determine the effects of these mutations on AreA-dependent gene expression the *fmdS-lacZ* reporter gene (FRASER *et al.* 2001) was introduced into the NLS mutants by meiotic crossing. We assayed β -galactosidase activity of the *gpd(p)areA*^{HA}-NLS mutant *fmdS-lacZ* progeny grown on ammonium or grown on ammonium and then transferred to either alanine or nitrogen-free media (Figure 3.4). The wild type *gpd(p)areA*^{HA} control showed low levels of gene expression when grown on ammonium, increased AreA-dependent expression on the alternative nitrogen source alanine, and even higher AreA-dependent expression following transfer to media lacking nitrogen, as observed previously (TODD *et al.* 2005). Deletion of the classical NLSs (NLS1,2,3, NLS4, and NLS5) in all combinations had no effect on the expression of FmdS-LacZ.

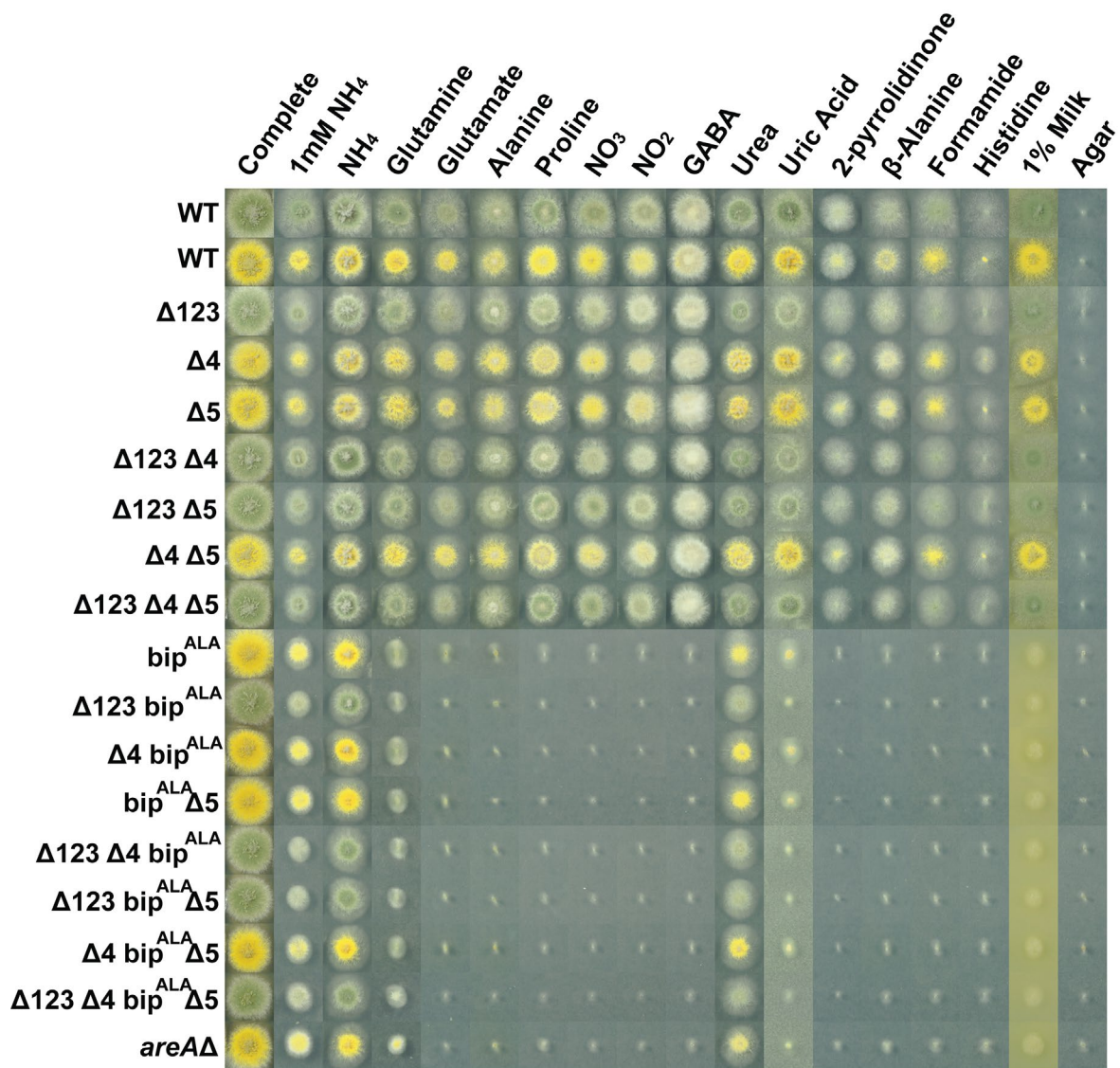


Figure 3.3 Effects of the mutations of AreA NLSs on *A. nidulans* growth

The various nuclear localization signal mutant strains and green and yellow conidial-colored wild type strains were grown on complete media, or supplemented minimal media containing a range of nitrogen sources at 10mM, except where otherwise indicated, for two days at 37°C.

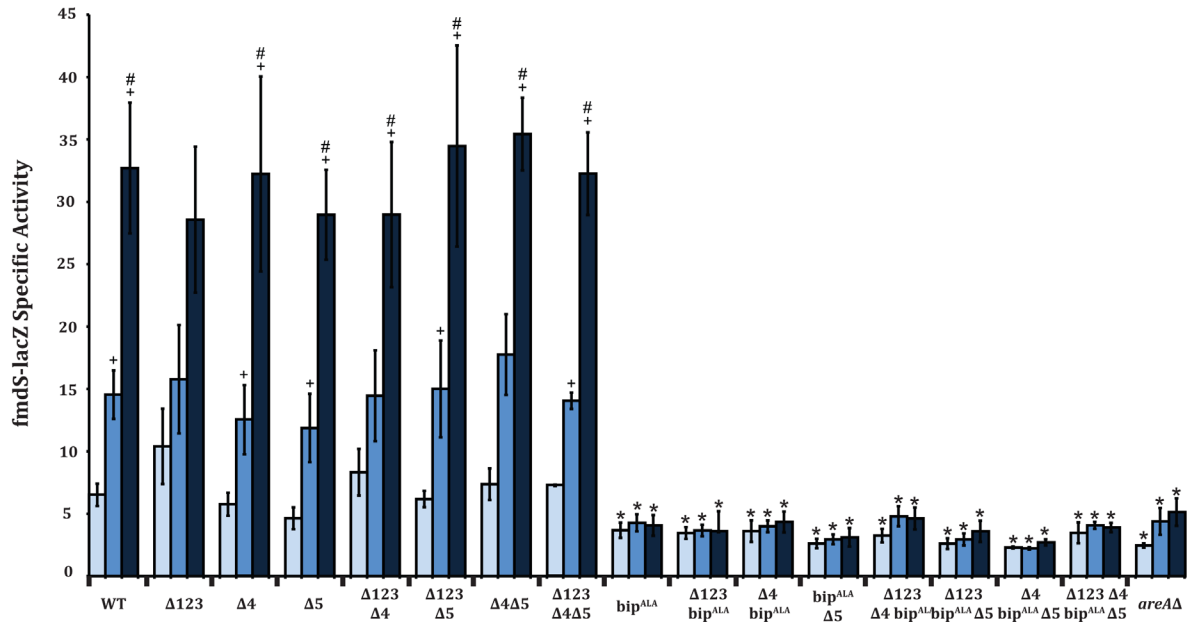


Figure 3.4 Effects of mutation of AreA NLSs on AreA-dependent gene expression

Wild type and *areA* NLS mutation or deletion strains carrying the *fmdS-lacZ* reporter gene were grown in supplemented minimal media for 16h with 10mM ammonium tartrate (NH₄) as a nitrogen source. The mycelia were then harvested or washed with supplemented liquid media without nitrogen and transferred for 4h to 10mM alanine (ALA) or nitrogen-free (-N) minimal media. Soluble protein extracts were prepared from the harvested mycelia and assayed for β-galactosidase specific activity. Error bars depict SEM (n≥3). * represents P-value <0.05 between WT and mutants of the same nitrogen condition. + represents P-value <0.05 between NH₄ and either ALA or -N within a strain. # represents P-value <0.05 between ALA and -N within a strain.

3.5.3 Analysis of the effects of NLS mutations in AreA

3.5.3.a Analysis of AreA classical NLS mutations on nuclear accumulation

The wild type AreA^{HA} protein accumulates in the nucleus after nitrogen starvation but not after growth in nitrogen sufficient or nitrogen limiting conditions (TODD *et al.* 2005). To determine which of the NLSs were necessary for nuclear accumulation of AreA we immunostained the HA-epitope tagged AreA NLS mutant strains (Figure 3.5). Deletion of the five classical NLSs individually (Δ NLS1,2,3, Δ NLS4, or Δ NLS5), in combinations (Δ NLS1,2,3- Δ NLS4, or Δ NLS1,2,3- Δ NLS5, or Δ NLS4- Δ NLS5), or together (Δ NLS1,2,3- Δ NLS4- Δ NLS5) did not abolish nuclear accumulation of AreA, indicating that other non-classical nuclear localization signals are involved in AreA nuclear import.

3.5.3.b A non-canonical bipartite NLS in AreA is conserved with mammalian GATA-4

The mouse transcription factor GATA-4 has a non-canonical arginine-based bipartite NLS RRX₃₃RXR within the GATA zinc finger DNA binding domain (PHILIPS *et al.* 2007). As the PSORTII algorithm does not include this non-canonical bipartite NLS, we identified by manual inspection an RRX₃₃RXR motif within the AreA zinc finger domain at residues 685-722 as a bipartite sixth NLS (bip) (Figure 3.1A, B). The AreA bipartite NLS is highly conserved within the zinc finger across most fungal AreA homologs, with *S. cerevisiae* Gln3p and Gat1p being the notable exceptions showing only partial conservation of this motif (RRX₃₃RXS and RKX₃₃RXR, respectively). The bipartite NLS is also conserved in the *A. nidulans* GATA factors AreB, the C-terminal zinc finger of *A. nidulans* SreA, the *S. cerevisiae* GATA factors Dal80p and Gzf3p, and the C-terminal zinc finger of all six mammalian GATA factors, suggesting this NLS is ancient in origin (Figure 3.2). The bipartite NLS was not conserved in the other *A. nidulans* GATA factors LreA, LreB, or NsdD. An additional RRX₃₃RXR motif separated from the zinc finger is also found in SreA.

As the bipartite NLS spans the GATA zinc finger, we mutated the bipartite NLS by point mutation of the four key arginine residues R685A, R686A, R720A, R722A (bip^{ALA}). We also made all of the possible double, triple, and quadruple combinations of bip^{ALA} with the Δ NLS1,2,3, Δ NLS4, and Δ NLS5 mutations. Deletion of all five classical NLSs in conjunction with the bip^{ALA} bipartite NLS mutation (Δ NLS1,2,3- Δ NLS4-bip^{ALA}- Δ NLS5) prevented nuclear accumulation of AreA during nitrogen starvation (Figure 3.5), implicating the bipartite NLS

as a major nuclear localization sequence. However, the *bip*^{ALA} single mutant strain showed nuclear accumulation (Figure 3.5), indicating that the five classical NLSs together can mediate AreA nuclear import without the bipartite NLS. The *bip*^{ALA} mutant alone or in combination with any of the classical NLSs showed a loss-of-function phenotype with growth comparable to the *areAΔ* strain (Figure 3.3). Furthermore, mutation of the bipartite NLS affected FmdS-LacZ activity as severely as *areAΔ*, indicating that the four arginine residues comprising the bipartite NLS are critical for AreA function, presumably for AreA DNA binding (Figure 3.4). We found that the Δ NLS1,2,3-*bip*^{ALA}- Δ NLS5 mutant AreA protein lacking all NLSs except NLS4 weakly accumulated in the nucleus, showing that NLS4 is able to direct AreA nuclear accumulation by itself. NLS1,2,3 (i.e., in the Δ NLS4-*bip*^{ALA}- Δ NLS5 mutant) and NLS5 (i.e., in the Δ NLS1,2,3- Δ NLS4-*bip*^{ALA} mutant) did not individually confer AreA nuclear accumulation, but in the Δ NLS4-*bip*^{ALA} mutant which has NLS1,2,3 and NLS5 intact, we observed strong nuclear accumulation. Therefore, although NLS1,2,3 and NLS5 are separately insufficient for nuclear accumulation they appear to work together to signal AreA nuclear localization.

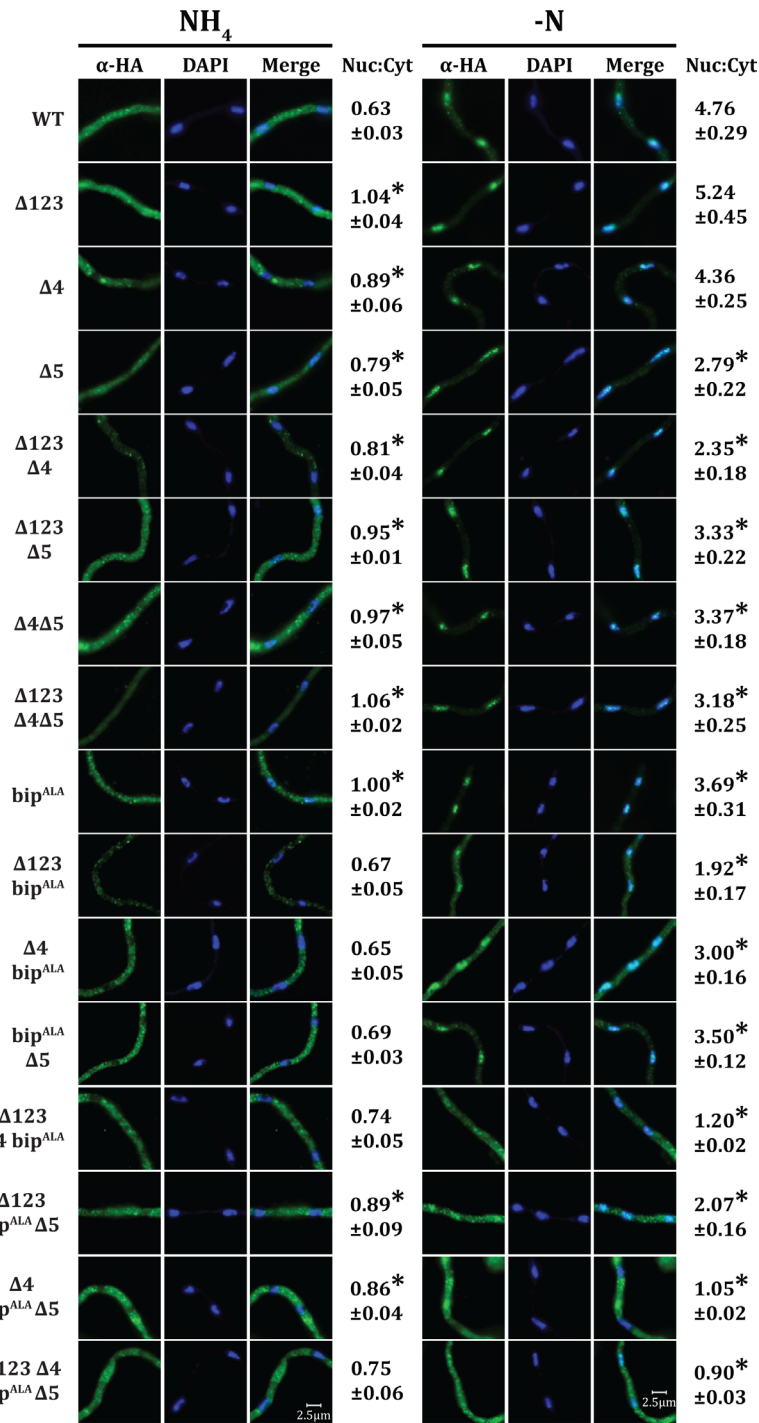


Figure 3.5 The effects of mutating the AreA NLSs on AreA^{HA} nuclear accumulation

The subcellular distribution of AreA^{HA} (α-HA) in gene-replaced *gpd(p)areA^{HA}* variants after 14h growth on 10mM ammonium and 4h transfer to minimal media containing 10mM ammonium (NH₄) or no nitrogen source (-N) was visualized by UV fluorescence microscopy following immunostaining with α-HA (3F10) and goat α-rat alexa-488 antibodies. A representative image of at least 100 nuclei is shown. Nuclei are stained with DAPI. Nuc:Cyt indicates the mean α-HA nuclear fluorescence to cytoplasmic fluorescence ratio with SEM for 25 randomly paired nuclear and cytoplasmic regions. * represents P-value <0.025 comparing WT and mutants grown under the same nitrogen condition.

3.5.4 Identification of AreA NLSs sufficient for nuclear localization

3.5.4.a Construction of the GFP-NLS fusion proteins

The mutational analysis above strongly suggests that all the identified NLSs in AreA are functional and show redundancy. In order to dissect the nuclear import function of the six NLSs, we fused the AreA NLSs to the C-terminus of GFP expressed from the constitutive *gpdA* promoter in a *wA* targeting vector. The *gpd(p)gfp*-NLS constructs and a *gpd(p)gfp* control construct lacking sequences encoding a NLS were targeted in single copy at the *A. nidulans* *wA* gene (see Section 3.4.1 for details concerning specific strain construction).

Here I will present a general overview of how the fusion proteins were constructed. Primers were designed to PCR amplify each region of *areA* containing an NLS and its short flanking sequences. NLS 1, NLS 2, and NLS 3 were included together as a single PCR amplification. A *HindIII* restriction site was included in the 5' primer to allow in-frame fusion with *gfp* in the *gfp* expression vector pDC6917 and a *BamHI* site was included in the 3' primer to allow a similar directional cloning protocol to be used for each construct (Figure 3.6). The PCR product was cloned into the *HindIII* and *BamHI* restriction sites of the pDC6917 vector. The approximate size of the putative clones was determined by gel electrophoresis and the presence of the inserts determined by PCR using the NLS-specific primers. Once confirmed to have inserts, Sanger sequencing was used to confirm accuracy.

To avoid position effects during the transformation into *A. nidulans* the *gpd(p)areA::nls* sequences were transferred to the *wA* targeting vector pCW6500 by PCR amplification with primers Not1T7 and T3. The pCW6500 vector and the Not1T7-*gpd(p)areA::nls*-T7 PCR fragment were double digested with *Not1* and *BamHI* restriction enzymes and then ligated together to form a *wA gpd(p)areA::nls* targeting construct. These constructs were again checked for accuracy by Sanger sequencing the insert.

The constructs were transformed into a green colored (wild type) recipient strain of *A. nidulans* RT96 (*pyrG89 bia1 gpd(p)areA^{HA} fmdS-lacZ pyroA4 nkuAΔ::Bar crmA^{T525C}::pyrG⁺*). The *nkuAΔ* mutation in the recipient strain confers defective non-homologous end-joining and therefore prevents ectopic integration of the fusion construct (NAYAK *et al.* 2006). Cross over at the *wA* gene will cause a disruption in pigment production in the recipient strain causing the transformants to have a white conidia phenotype whereas a cross over event at

any other genomic location (in our case, at the *gpdA* promoter or the AreA NLS itself) will result in a green conidia phenotype (Figure 3.6).

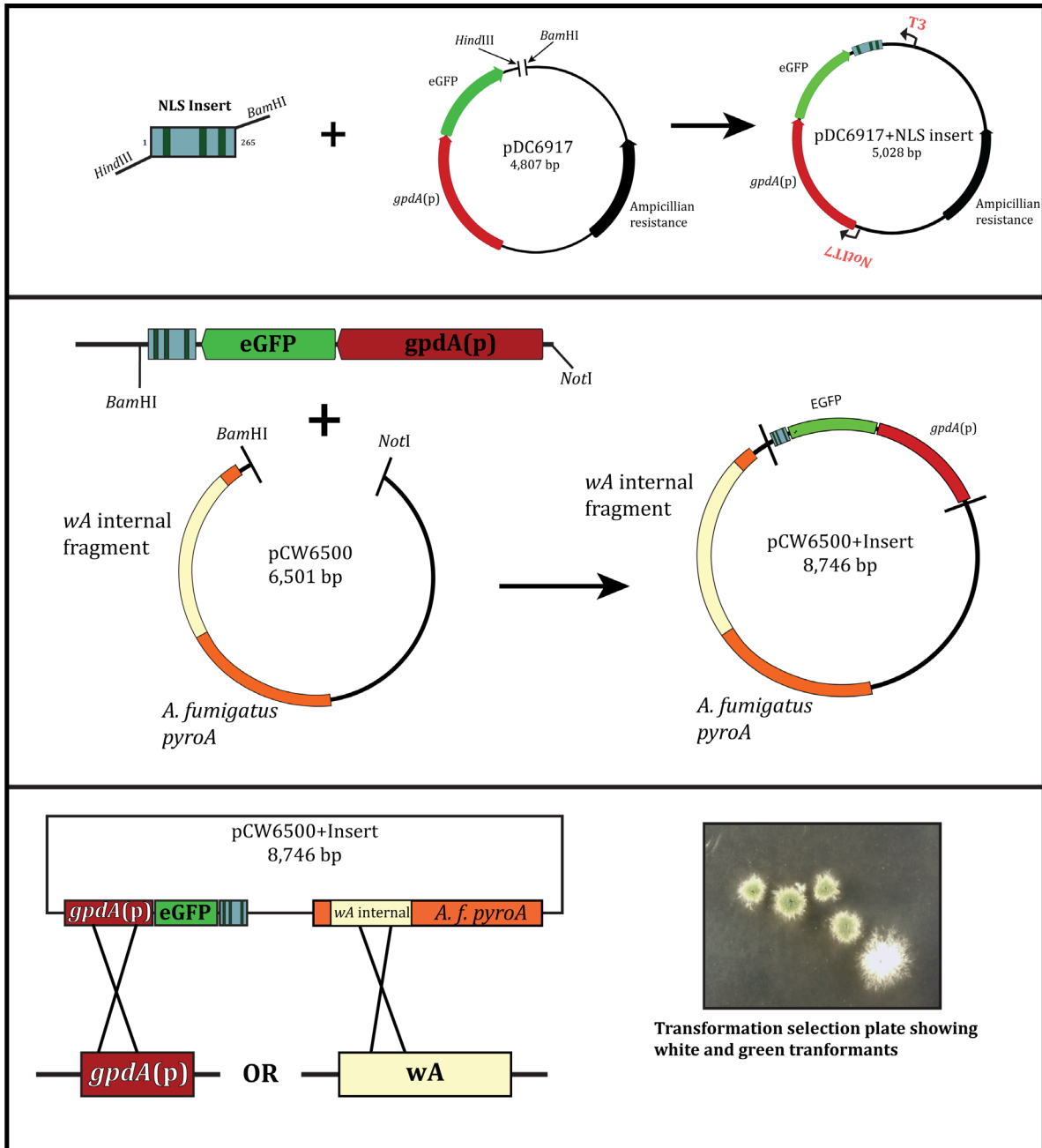


Figure 3.6 *gpd(p)::egfp::areANLS* fusion gene construct

Diagram of *gfp* fusion constructs and integration strategy.

3.5.4.b Analysis of GFP-NLS fusions

Subcellular localization of the GFP-NLS fusion proteins was determined by direct UV fluorescence microscopy. Similar patterns of subcellular distribution were observed for each fusion protein after growth for 14 hours on 10mM ammonium (data not shown) and after 4 hours nitrogen starvation (Figure 3.7). The GFP control was distributed throughout the hyphae and not directed specifically to the nucleus, similar to previous observations for GFP expressed from randomly integrated constructs (SUELMANN *et al.* 1997; SMALL *et al.* 2001; NIKOLAEV *et al.* 2003). The GFP-zinc finger region fusion protein containing the bipartite NLS (GFP-bipNLS) was strongly localized to the nucleus. The GFP-zinc finger bip^{ALA} mutant fusion protein (GFP-bip^{ALA}NLS) showed markedly reduced nuclear accumulation compared to the wild type GFP-zinc finger fusion. Therefore, the bipartite NLS alone acts as a strong nuclear localization signal. Neither GFP fused to NLS1, NLS2, and NLS3 together, nor GFP fused separately to NLS4 or NLS5 accumulated in the nucleus. For NLS1,2,3 and NLS5 this is consistent with the NLS deletions in AreA. However, the lack of nuclear accumulation of GFP-NLS4 coupled with the weak nuclear accumulation we observed for the Δ NLS1,2,3-bip^{ALA}- Δ NLS5 mutant suggests that NLS4 has weak or context-dependent activity. We tested whether the classical NLSs might be separately weak NLSs that could function in combination. GFP was fused to both NLS4 and NLS5, to NLS1, NLS2, NLS3 and either NLS4 or NLS5, and fused to all five classical NLSs. These combinations of NLSs in the context of a single fusion protein conferred nuclear accumulation of GFP. NLS4 and NLS5 together weakly conferred nuclear accumulation whereas NLS1, NLS2, and NLS3 fused to NLS4 and/or NLS5 conferred strong nuclear accumulation. Taken together, these results strongly indicate that the five classical NLSs and the bipartite NLS can cooperatively target AreA to the nucleus (Figure 3.7).

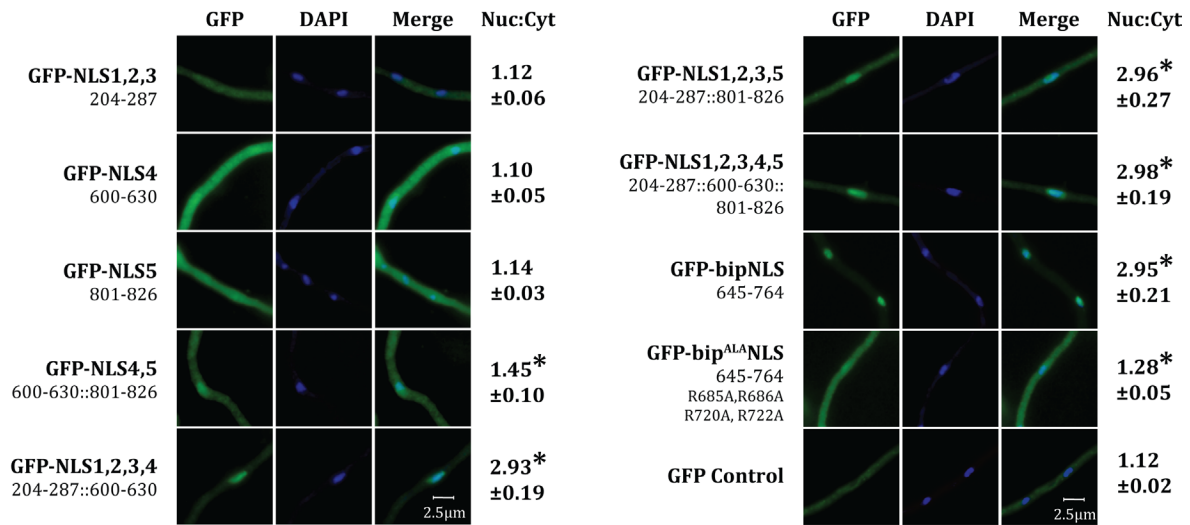


Figure 3.7 Subcellular distribution of GFP-NLS proteins

Direct UV fluorescence GFP microscopy of germlings of *gpdA(p)gfp-NLS* transformants after 14h growth in minimal media containing 10mM ammonium and then a 4h transfer to nitrogen-free (-N) minimal media. A representative image of at least 100 nuclei is shown. Nuclei are stained with DAPI. Nuc:Cyt indicates the mean GFP nuclear fluorescence to cytoplasmic fluorescence ratio with SEM for 25 randomly paired nuclear and cytoplasmic regions. The coordinates of AreA sequences included in the GFP fusion proteins are shown. * represents P-value <0.005 comparing the GFP control and GFP-NLS fusion proteins.

3.5.5 Construction and preliminary analysis of a *gpd(p)gfp::areA* fusion protein

Throughout this chapter and the ones to follow we demonstrate how AreA^{HA} subcellular localization can be affected by nutrient conditions, mutations, temperature, and other substrates. Each time we analyze these changes in different conditions we are taking a snapshot, a still image taken at a moment in time that has been predetermined. This can tell us a lot about what we are trying to understand, but the cell is a dynamic system and transcription factors like AreA move in and out of the nucleus unless they are being sequestered like we see during starvation. A GFP-tagged version of AreA would provide us with a much broader understanding of intracellular dynamics. Previous attempts at constructing a GFP-AreA fusion protein were unsuccessful (TODD Personal Communication). Herein we constructed a GFP-AreA fusion construct with a linker inserted between the GFP and AreA sequences.

First we created four primers. The first and the fourth primers were designed as outside flanking primers. Primer 1 is a forward primer that was within a *gpd(p)gfp* fusion vector which had previously been created and has been discussed already in this chapter. Amplification of *gpd(p)gfp* from pALX 213+4 with Primer1 and Primer2. Primer2 is 60 bp. 18 bp binding to *gfp* 42 bp tail which makes up two-thirds of the Linker sequence. There is a 24 bp overlap between Primer2 and Primer3 for the fusion PCR. The PCR product was 1,876 bp (Figure 3.8A). The second step was the amplification of *areA*^{HA} without the start codon and with an 800 bp 3'UTR from RT52 gDNA with Primer3 and Primer4. As with Primer2, Primer3 is 60 bp. 18 bp binding to *gfp* 42 bp tail which makes up two-thirds of the Linker sequence. There is a 24 bp overlap between Primer2 and Primer3 for the fusion PCR. This second PCR creates a 3,523 bp product (Figure 3.8A). The third step combined both PCR products from the first two reactions and used primers 1 and 4 for amplification. The final product is 5,459 bp in length (Figure 3.8A). This product was then purified and used to transform by direct selection for AreA function on nitrate by double crossover integration into the *yA1 gpd(p)areA*^{HA}::*riboB*(3' Δ) *nkuA* Δ recipient MH11072. A resultant transformant (RT557) was confirmed and chosen for analysis (Figure 3.8B). Growth testing of RT557 showed that the GFP-AreA^{HA} protein conferred similar nitrogen utilization phenotypes in growth tests as the wild type (Figure 3.9A). Direct UV-fluorescence microscopy of RT557 germlings after 14h growth on ammonium and after 4h transfer to nitrogen-free media

showed localization to the cytoplasm or nuclear accumulation, respectively (Figure 3.9B). Therefore, the GFP-AreA^{HA} fusion protein behaved similarly to the AreA^{HA} protein with respect to function and nuclear accumulation.

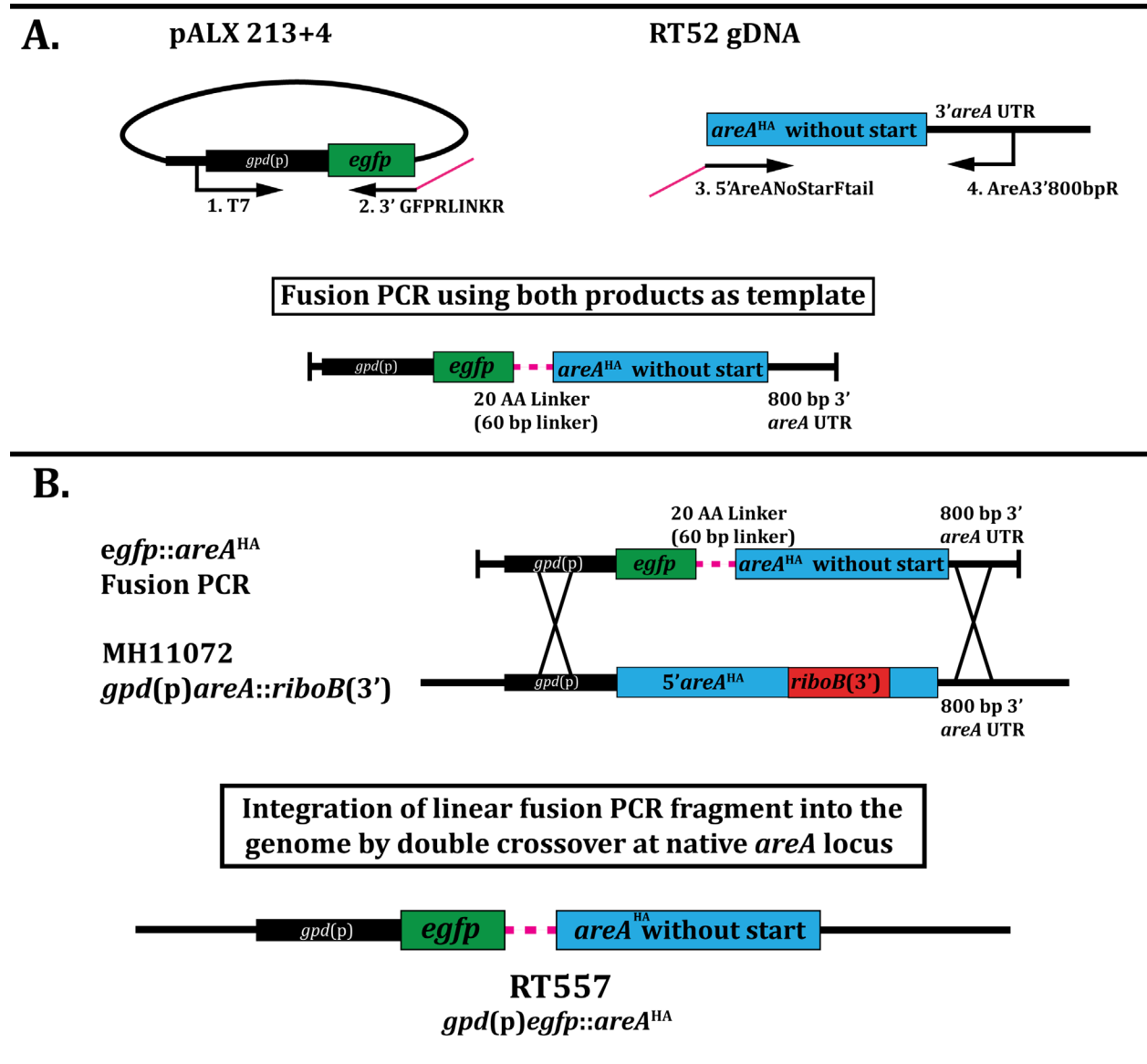


Figure 3.8 Strategy for construction of a *gfp::areA* fusion gene

A. Fusion PCR was used to generate a *gpd(p)areA^{HA}* fusion construct from two initial PCR products, one containing *gpd(p)gfp* and a linker sequence, and the other containing the linker sequence fused to *areA^{HA}* lacking a start codon. Primer 1 and Primer 4 were used to generate the full length *gpd(p)gfp::areA^{HA}* fusion gene with *gfp* and *areA^{HA}* separated by a linker sequence. **B.** Gene-replacement strategy for integration of the *gpd(p)gfp::areA^{HA}* fusion gene at the native *areA* locus by double homologous crossover.

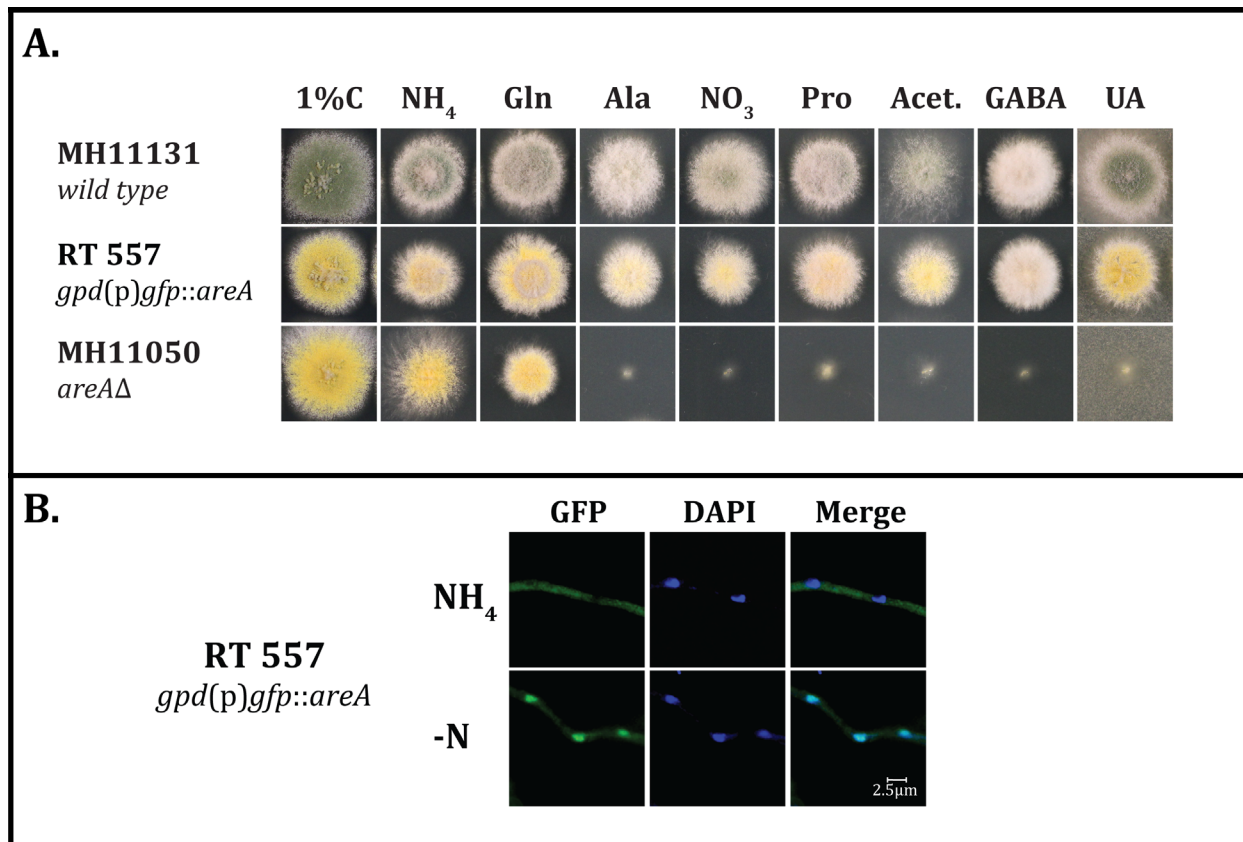


Figure 3.9 Construction of a functional GFP-AreA^{HA} fusion protein

A. Growth tests of MH11131 (*gpd(p)areA^{HA}*), RT557 (*gpd(p)gfp::areA^{HA}*), and MH11050 (*gpd(p)areA^{HA}riboB(3'Δ)*) on complete (1%C) or supplemented minimal media containing a range of nitrogen sources (ammonium tartrate, glutamine, alanine, nitrate, proline, acetamide, gamma-amino butyric acid, and uric acid) at 10mM for two days at 37°C. **B.** Direct UV fluorescence microscopy of RT557 grown for 14h on supplemented minimal media containing 10mM ammonium tartrate or transferred for 4h to supplemented minimal media lacking a nitrogen source (-N) with nuclei stained with DAPI.

3.6 Discussion

The presence of sequences capable of interacting with nuclear transport machinery is a vital component for nuclear entry of most transcription factors. We have now shown that AreA has multiple functional NLSs. The RRX₃₃RXR bipartite NLS is conserved in filamentous fungal AreA orthologs, in the *A. nidulans* GATA factors AreB and SreA, *S. cerevisiae* negative-acting GATA factors Dal80p and Gzf3p and in mammalian GATA factors. Yeast Gat1p has a conservative substitution of one of the bipartite NLS arginines for lysine and it is conceivable that this sequence may act as an NLS. In yeast Gln3p, however, there is a non-conservative substitution in one of the key arginine residues and evidence that this region does not serve as a functional NLS (CARVALHO AND ZHENG 2003). The five classical NLSs found in AreA are conserved across most of the filamentous fungi but not in the *S. cerevisiae* nitrogen GATA factors. These NLSs appear to work together in various combinations to mediate nuclear import, and the bipartite NLS is independently able to localize AreA to the nucleus. The four arginine residues in the bipartite NLS are critical for AreA-dependent gene expression as seen in growth tests on a range of nitrogen nutrients and in *fmdS-lacZ* reporter gene assays. This is likely due to the fact that they are DNA contact residues in the AreA zinc finger, and the arginine to alanine mutations likely disrupt AreA DNA binding (STARICH *et al.* 1998). Mutation of these four arginine residues simultaneously in the GATA-4 bipartite NLS abolish nuclear localization, and mutation of any of the four residues abolishes or severely inhibits DNA binding and transcriptional activation (PHILIPS *et al.* 2007). Although mutation of the bipartite NLS abolishes AreA function, the bipartite NLS mutant AreA protein accumulates in the nucleus during nitrogen starvation. However, when we deleted all five of the classical NLSs and mutated the bipartite NLS simultaneously, AreA was not functional and did not accumulate in the nucleus.

There is a stark mechanistic difference in the localization of *A. nidulans* AreA compared with its *S. cerevisiae* homolog Gln3p. In *S. cerevisiae*, nuclear import is the regulated step, as Gln3p is held in the cytoplasm by a cytoplasmic anchor, Ure2p, during nitrogen sufficient conditions (BECK AND HALL 1999). During nitrogen limitation, dephosphorylation of Gln3p and Ure2p leads to release of Gln3p, and Gln3p is imported into the nucleus (BECK AND HALL 1999; CARVALHO AND ZHENG 2003). Gln3p has only one functional

classical NLS that is inactivated by cytoplasmic anchoring (CARVALHO AND ZHENG 2003). A second potential NLS in Gln3p was found to be dispensable for nuclear import (CARVALHO AND ZHENG 2003). In contrast, AreA nuclear localization is regulated primarily by nuclear export via CrmA, as the export in response to addition of nitrogen nutrients of AreA is rapid (TODD *et al.* 2005). The kinetics of AreA nuclear accumulation, however, are slow and we have found no evidence for differential regulation of AreA nuclear import.

AreA is unusual in the large number of NLSs it contains. Nuclear localization signals in other transcription factors are quite variable in both type and number. For many transcription factors a single NLS mediates nuclear import. For example, *A. nidulans* PrnA, the constitutively nuclear transcriptional activator for proline utilization pathway genes, has a tripartite NLS located in its N-terminal region (POKORSKA *et al.* 2000). A single NLS is also found in other *A. nidulans* transcription factors: AlcR, NirA and AmyR each have a tripartite NLS (NIKOLAEV *et al.* 2003; BERGER *et al.* 2006; MAKITA *et al.* 2009), and VeA and PacC have a classical bipartite NLS (MINGOT *et al.* 2001; FERNÁNDEZ-MARTÍNEZ *et al.* 2003; STINNETT *et al.* 2007). There are many examples of nuclear proteins containing multiple NLSs, however there are usually no more than three (LUO *et al.* 2004; REISENAUER *et al.* 2010). *A. nidulans* HapB has two monopartite NLSs located in the C-terminal domain (STEIDL *et al.* 2004; TUNCHER *et al.* 2005). One of these NLSs is conserved in fungal, yeast, and human HapB orthologs, and is functional in *A. nidulans* HapB, *S. cerevisiae* Hap2p, and human NF-YA proteins expressed in yeast (TUNCHER *et al.* 2005). The other NLS is found only in the aspergilli but is required for nuclear localization of HapB in *A. nidulans* (TUNCHER *et al.* 2005). Both NLSs are functional in *Aspergillus oryzae* HapB (GODA *et al.* 2005). The AreA NLSs show apparent redundancy in their ability to promote localization of AreA and GFP to the nucleus. If these sequences share truly redundant functions, we might expect them to be lost over time in different lineages. However, all of the NLSs are conserved across most fungal species, suggesting that each NLS has an important and unique function. One possibility is that AreA may use alternative importins for nuclear import under different growth conditions due to differential expression of importins. *A. nidulans* has 17 nuclear importins, but the expression of these across different growth conditions has not been determined (MARKINA-INARRAIRAEGUI *et al.* 2011). Alternatively, multiple NLSs could allow for more efficient nuclear import. The cooperativity we observed for the AreA classical NLSs suggests low binding affinities of

individual NLSs to nuclear importin(s). α -importin binds to different NLSs, including classical NLSs, via either of two NLS-binding grooves (KOSUGI *et al.* 2009). Binding of multiple AreA NLSs to different binding grooves of importin(s) may confer stronger binding affinity and more efficient nuclear import. The RRX₃₃RXR bipartite NLS of GATA-4 interacts with β -importin but not α -importin (PHILIPS *et al.* 2007). If the interaction with β -importin is conserved for AreA, the AreA NLSs may mediate interaction with both importins of the α -importin- β -importin complex.

The presence of multiple NLSs has been proposed to allow for multiple regulatory steps for import to mediate a gradation of nuclear protein levels under different conditions compared with having only a single strong NLS, which could function more like an on/off switch (LUO *et al.* 2004). None of our observations suggest that nuclear import of AreA is differentially regulated, or that the six AreA NLSs allow varied levels of nuclear import depending on nitrogen conditions. We have demonstrated a high degree of redundancy of the NLSs in AreA. Either the bipartite NLS alone or the classical NLSs together can strongly promote protein accumulation into the nucleus. What is unclear is why this functional redundancy has not been curtailed by evolution. This hints to the possibility of various importins recognizing AreA to ensure import during constantly changing environmental conditions and nitrogen nutrient availability.

Chapter 4 - Regulation of AreA nuclear accumulation

4.1 Abstract

The primary regulator of nitrogen metabolic genes in fungi is the ortholog of the GATA transcription factor AreA. In *Aspergillus nidulans*, the activity of AreA is regulated by multiple mechanisms including regulated nuclear accumulation. When *A. nidulans* is grown in the presence of a nitrogen source, AreA is found predominantly throughout the cytoplasm, but when transferred from a nitrogen-containing media to an environment depleted of nitrogen AreA accumulates in the nucleus. In the previous chapter we demonstrated that AreA has multiple, conserved, nuclear localization sequences which intrinsically mediate AreA nuclear import. The mechanisms underlying AreA nuclear import and accumulation are largely unknown. We have attempted to elucidate both the causes for and the mechanisms behind AreA nuclear import and accumulation. Using strains with HA-epitope tagged versions of wild type and mutant AreA we have shown that nuclear import of AreA is regulated in multiple ways: (i) the α -importin KapA mediates, at least in part, nuclear import of AreA, (ii) the small ubiquitin-like modifier SumO plays a role in both import and export of AreA and KapA, and (iii) inhibition of the Target of Rapamycin (TOR) kinase by rapamycin or deletion of individual TOR pathway genes prevents AreA nuclear accumulation. Collectively our data reveals complex and multi-tiered regulation of the subcellular localization of the GATA transcription factor AreA.

Do the absolute best you can
today. And that will be enough. <3

4.2 Introduction

Regulation of nuclear accumulation of AreA is a complex process that involves balancing the active transport of AreA into and out of the nucleus by transporter proteins involved in the regulation of nutrient metabolism. To understand how AreA nuclear accumulation is regulated, we must first review the general process involved in the active transport of proteins into the nucleus.

4.2.1 Overview of the nuclear pore and the general mechanisms of nuclear import

The active import of proteins into the nucleus is a complex process which has been studied in a multitude of systems. The nuclear pore complex (NPC) is made up of multiple copies of ~30 different proteins and has a molecular mass dependent on the organism, e.g., 22-44MDa in *S. cerevisiae* and 60 – 125MDa in vertebrates (ROUT AND AITCHISON 2000; CRONSHAW *et al.* 2002; STRAMBIO-DE-CASTILLIA *et al.* 2010; SURESH AND OSMANI 2019). The number of nuclear pores per nucleus varies widely depending upon the cell type, organism, and cell cycle stage; but in *S. cerevisiae* ranges from 65 pores in G1 to 182 pores in late anaphase (WINEY *et al.* 1997). Developments in the understanding of how and when nuclear pore complexes are formed and inherited through mitosis have been recently reviewed by SURESH AND OSMANI (2019), who presented two modes of NPC assembly; during interphase into a preexisting nuclear envelope and during mitotic exit after the nuclear pore complex and nuclear envelope disassemble. Here we will focus on the general mechanisms of NPC function (Figure 4.1). NPCs allow passive transport of proteins which are smaller than 30kDa (GORLICH AND KUTAY 1999).

The majority of proteins that enter and exit the nucleus must be transported actively. The transport of large proteins to the nucleus is achieved by dedicated transporter proteins called karyopherins. Karyopherins that import proteins from the cytoplasm to the nucleus are called importins, whereas those that export proteins to the cytoplasm are referred to as exportins. Importins bind large cargo proteins in the cytoplasm by recognition of specific positively charged amino acid sequences called nuclear localization signals (NLSs). One of the best characterized transport proteins, importin- α , binds to importin- β (an importin associated with the NPC, and is found in the nuclear periphery) to form a ternary complex

which directly interacts with the large number of phenylalanine and glycine repeats (FG-repeats) present in the NPC to mediate import into the nucleus (GOLDFARB *et al.* 2004). Once inside the nucleus, the cargo protein is released from the importin- α/β heterodimer by the binding of Ran-GTP to the complex, promoting a conformational change which releases the cargo (CHOOK AND BLOBEL 2001). The binding of Ran-GTP is performed by a guanine exchange factor called Ran-GEF, which changes the state of Ran-GDP to Ran-GTP by adding a third phosphate group to Ran-GDP. The export of proteins from the nucleus occurs via nuclear exportins to complete the other half of this cycle (Figure 4.1). This cycle is an active process which uses energy to change Ran-GDP to Ran-GTP (STRAMBIO-DE-CASTILLIA *et al.* 2010).

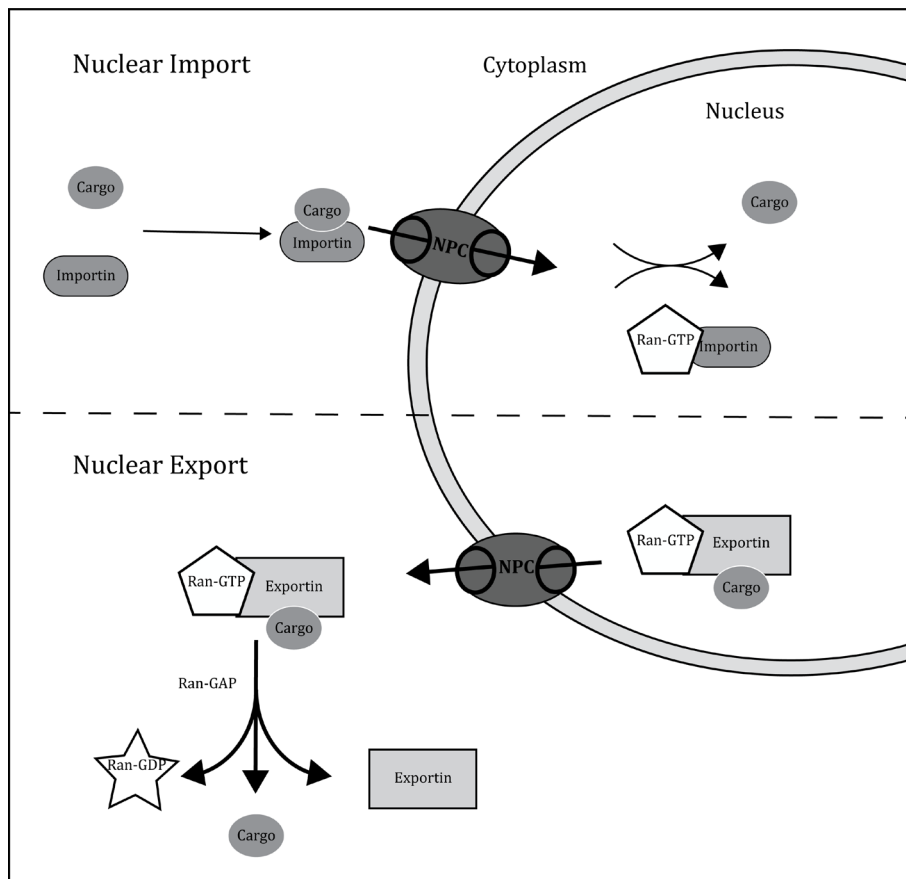


Figure 4.1 General overview of nuclear import and export

During nuclear import cargo binds to an importin, is translocated into the nucleus and then the cargo is released from the importin. During nuclear export cargo binds to an exportin/Ran-GTP complex, translocates across the nuclear membrane into the cytoplasm and then the cargo, exportin, and Ran-GTP are dislodged from each other.

4.2.2 The α -Importin KapA

In *Aspergillus nidulans* there are 14 members of the karyopherin- β superfamily, 4 of which are essential (MARKINA-INARRAIRAEGUI *et al.* 2011). The most well known of the 4 essential importins are the importin- α , KapA, and the importin- β , KapB. KapB resides in the perinuclear space. It interacts directly with the nuclear pore and forms a complex with importin- α to transport cargo through the nuclear pore and into the nucleus. The importin- α /importin- β heterodimer is capable of binding to proteins which contain non-canonical NLSs to directly transport them through the nuclear pore and into the nucleus (CHOOK AND BLOBEL 2001). Kosugi *et al.* (2009) defined six different classes of NLSs capable of binding to importin- α . Among these were the SV40 large T antigen classical monopartite NLS (PKKKRKV) and Nucleoplasmin classical bipartite NLS (KRPAAIKKAGQAKKKK), which were found previously (KALDERON *et al.* 1984; ROBBINS *et al.* 1991; KOSUGI *et al.* 2009). In *S. cerevisiae*, the KapA homologue, Srp1p, is required for transport of the AreA homologue, Gln3p, into the nucleus during nitrogen starvation (CARVALHO *et al.* 2001). As shown in Chapter 3, AreA has five classical monopartite SV40 large T antigen type NLSs and one noncanonical arginine based bipartite NLS (HUNTER *et al.* 2014).

4.2.3 SumO modification and its role in nuclear localization

Small ubiquitin-related modifier (SUMO) proteins are a highly conserved family of proteins in eukaryotes (JOHNSON 2004). SUMO proteins form reversible covalent modifications of proteins similar to ubiquitin, alter their function and are responsible for cell cycle progression, DNA-repair, transcription, nuclear transport, and many other essential cellular functions (JOHNSON 2004). This group of proteins has been extensively studied in vertebrates, which have four different SUMO proteins (SUMO1, SUMO2, SUMO3, and SUMO4). *S. cerevisiae*, *S. pombe*, and *A. nidulans* only have one isoform of the SUMO protein (JOHNSON 2004; WONG *et al.* 2008b). Loss of the SUMO gene, *SMT3*, in *S. cerevisiae* is lethal (JOHNSON *et al.* 1997). Conversely, in *S. pombe* and *A. nidulans* loss of the SUMO gene *pmt3* and *sumO*, respectively, confers significantly reduced growth but is not lethal (TANAKA *et al.* 1999; WONG *et al.* 2008b).

The effects of *sumO* Δ , *sumO* over-expression, and the subcellular localization of SumO along with its conjugated proteins in *A. nidulans* has been previously characterized (WONG *et*

al. 2008b). That study showed that the *sumOΔ* strain formed smaller colonies with non-uniform growth at the colony edges and a nearly 17-fold reduction in conidia compared to the wild type when grown on complete media. The *sumO* over-expression strain had no detectable effect on either growth or metabolism. The *in vivo* localization of GFP-SumO revealed high levels of accumulation into punctate spots in or around the edges of the nucleus (WONG *et al.* 2008b). In addition, a more recent study using a high affinity tag and sensitive mass spectrometry identified 149 SUMOylated proteins in *A. nidulans*, many of which are involved in transcription, transcription regulation, RNA processing and DNA replication or repair (HORIO *et al.* 2019).

4.2.4 The TOR Signaling Pathway

The Target of Rapamycin (TOR) signaling pathway is highly conserved throughout eukaryotes. TOR signaling from growth factors and nutrients regulates cell cycle progression, metabolism, cellular growth, ribosome biogenesis, and autophagy (KAMADA *et al.* 2000; SARBASSOV *et al.* 2005; AZIM *et al.* 2010). In mammalian cells, perturbations in the TOR pathway have been implicated in a range of cancers (XU *et al.* 2014). The immunosuppressant drug rapamycin is a potent inhibitor of TOR and is used by organ transplant recipients and cancer patients as an anti-tumorigen and is in trials for treatment of Tuberous Sclerosis Complex (TSC), a pleiotropic genetic disease caused by deletions in either the TSC1 or TSC2 genes (HUYNH *et al.* 2015). Downstream of the TOR complex, FgSit4 and FgPpg1 phosphatases have been shown to regulate virulence and vegetative development in *F. graminearum* (YU *et al.* 2014).

In *S. cerevisiae* inhibition of the TOR pathway by rapamycin leads to downstream effects, including nuclear localization of the GATA transcription factors Gln3p and Gat1p, which activate nitrogen metabolic genes (BECK AND HALL 1999). The initial work by Beck and Hall (1999) showed that Gln3p was anchored in the cytoplasm by Ure2. Many studies in *S. cerevisiae* have focused on regulation of the AreA homologue Gln3p. Tate *et al.* 2019, demonstrated a more complex version in which Ure2, Sit4 and PP2A each play a role in regulating Gln3p nuclear import. Ure2 functions as a cytoplasmic anchor to sequester Gln3 from the nucleus during nitrogen replete conditions (BECK AND HALL 1999; TATE *et al.* 2019) (Figure 4.2). Dephosphorylation of Gln3p by the phosphatases, Sit4 and PP2A, (acting in

different nutrient conditions) allow Ure2 to bind to Gln3p to maintain cytoplasmic sequestration.

The components of the TOR pathway are conserved between yeast and *Aspergillus nidulans* (FITZGIBBON *et al.* 2005). In contrast to *S. cerevisiae* Gln3p, nuclear accumulation of *A. nidulans* AreA is regulated via nuclear export by the Crm1^{KapK} nuclear exportin in response to nitrogen starvation rather than via nuclear import (TODD *et al.* 2005). Therefore, the TOR pathway may be rewired in *A. nidulans* compared with yeast. The TOR pathway gene *jipA* has little effect on nitrogen utilization (FITZGIBBON *et al.* 2005). Furthermore, due to the rewiring of the signaling pathway and the inactivity of the supposed Ure2p homologue GstA having no effect on nitrogen regulation (FRASER *et al.* 2002), the regulation of AreA via nuclear import has not been studied extensively.

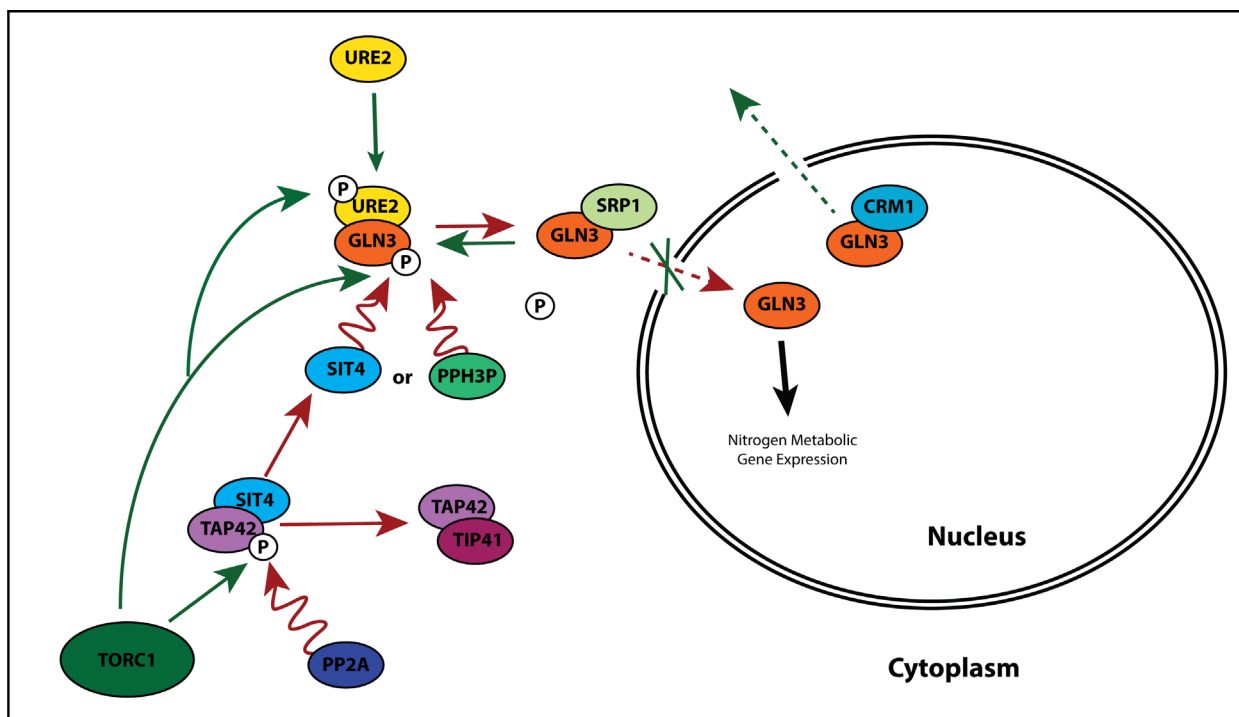


Figure 4.2 Rudimentary TOR signaling pathway in *S. cerevisiae*

Simplified model of the various components of the TOR signaling pathway and their effects on the subcellular localization of Gln3. Green arrows indicate repressing conditions (NH_4 or Glutamine) leading to cytoplasmic anchoring of Gln3 by Ure2. Red arrows indicate derepressing conditions (nitrogen limitation or treatment with rapamycin) leading to nuclear localization of Gln3 and subsequent increase in nitrogen metabolic gene expression.

4.2.5 Autolysis and Autophagy in *A. nidulans*

A. nidulans along with other filamentous fungi respond to environmental nitrogen starvation using two cannibalistic strategies, autophagy, and autolysis, to obtain nutrients. Autophagy is an intracellular process that degrades cytoplasmic proteins and organelles to recycle them into nutrients for the cell. Autolysis is a form of apoptosis which destroys the cells in order to release nutrients into the environment for the rest of the colony to consume. The macroautophagy pathway has been extensively studied in *S. cerevisiae* and *A. nidulans* (XIE AND KLIONSKY 2007; PINAR *et al.* 2013). In *A. nidulans*, the p53-like transcription factor XprG mediates aspects of the carbon starvation response including autolysis (KATZ *et al.* 2013; KATZ *et al.* 2015; KATZ 2018). Two key autophagy genes *atgA* and *atgH* (ATG1 and ATG8 orthologs respectively) play crucial roles in starvation-induced autophagy in *A. nidulans*.

4.2.6 Regulation of AreA nuclear import

In this chapter we attempt to better elucidate the regulation of AreA nuclear import and its subsequent accumulation in the nucleus. To better characterize the role KapA plays in the nuclear import of AreA we analyze the co-localization of AreA^{HA} and KapA::eGFP. We create a point mutant *kapA*^{S111F} to determine if partial loss of KapA function affected AreA nuclear accumulation. We also overexpress *kapA* to determine the effects of overabundance of the nuclear importin. We examine the involvement of the small ubiquitin-like modifier SumO on nuclear accumulation of AreA. We then explore the role nutrient signaling plays on AreA nuclear accumulation by analyzing mutants affected in the TOR signaling pathway as well as mutants with defects in the autophagy and autolysis pathways.

4.3 Materials and Methods

4.3.1 Strain construction

Genotypes of the strains used in this chapter can be found in Table 4.1.

FGSC gene knockout strains

A. nidulans gene knockout constructs (McCLUSKEY *et al.* 2010; DE SOUZA *et al.* 2013) were obtained from the Fungal Genetics Stock Center, Manhattan, KS. Gene replacements were confirmed by PCR.

Table 4.1 *Aspergillus nidulans* strains used in Chapter 4

Strain	Genotype^a
MH9949	<i>biA1 gpd(p)areA^{HA} amdS-lacZ</i>
MH11072	<i>yA1 pabaA1 areAΔ::ribo(3') fmdS-lacZ pyroA4 nkuAΔ::Bar</i>
MH11263	<i>yA1 gpd(p)areA^{HA} fmdS-lacZ sumOΔ::Bar</i>
MH11481	<i>gpd(p)areA^{HA} amdS-lacZ pyroA4 sumOΔ::Bar::xylP(p)sumO</i>
MH12068	<i>yA1 pabaA1 gpd(p)areA^{HA}Δ703-712 pyroA4 nkuAΔ::argB</i>
MH12226	<i>yA1 pabaA1 gpd(p)areA^{HA} pyroA4 nkuAΔ::argB kapA::xylP(p)kapA-AfpyroA</i>
MH12236	<i>yA1 pabaA1 gpd(p)areA^{HA} amdS-lacZ nkuAΔ::argB kapA::xylP(p)kapA-AfpyroA sumOΔ::Bar</i>
MH12318	<i>gpd(p)areA^{HA} amdS-lacZ pyroA4 kapA::kapA::GFP-Afribob</i>
MH12328	<i>pabaA1 gpd(p)areA^{HA} amdS-lacZ kapA::kapA::GFP-Afribob sumOΔ::Bar</i>
RT210	<i>pyrG89 gpd(p)areA^{HA} fmdS-lacZ pyroA4 nkuAΔ::Bar kapA^{S111F}</i>
RT211	<i>pyrG89 gpd(p)areA^{HA} fmdS-lacZ pyroA4 nkuAΔ::Bar kapA^{S111F}</i>
RT235	<i>gpd(p)areA^{HA} fmdS-lacZ pyroA4 nkuAΔ::Bar kapA^{S111F}</i>
RT238	<i>pyrG89 wA::gpd(p)gfp::areANLS4-Afpyro gpd(p)areA^{HA} fmdS-lacZ pyroA4 nkuAΔ::Bar crmA^{T525C}::pyrG⁺</i>
RT334	<i>pyrG89 wA::gpd(p)gfp::areANLS123::AfpyroA gpd(p)areA^{HA} fmdS-lacZ pyroA4 nkuAΔ::Bar kapA^{S111F} crmA^{T525C}::pyrG</i>

^a All strains carry the *veA1* mutation.

Table 4.1 A. *nidulans* strains used in Chapter 4 (continued)

Strain	Genotype^a
RT335	<i>pyrG89 wA::gpd(p)gfp::areAzf::AfpyroA gpd(p)areA^{HA} fmdS-lacZ pyroA4 nkuAΔ::Bar kapA^{S111F} crmA^{T525C}::pyrG⁺</i>
RT336	<i>pyrG89 biA1 wA::gpd(p)gfp::areAzfbip::AfpyroA gpd(p)areA^{HA} fmdS-lacZ pyroA4 nkuAΔ::Bar kapA^{S111F} crmA^{T525C}::pyrG⁺</i>
RT337	<i>pyrG89 biA1 wA::gpd(p)-gfp::areANLS5::AfpyroA gpd(p)areA^{HA} fmdS-lacZ pyroA4 nkuAΔ::Bar kapA^{S111F} crmA^{T525C}::pyrG⁺</i>
RT338	<i>pyrG89 biA1 wA::gpd(p)gfp::AfpyroA gpd(p)areA^{HA} fmdS-lacZ pyroA4 nkuAΔ::Bar kapA^{S111F} crmA^{T525C}::pyrG⁺</i>
RT339	<i>pyrG89 gpd(p)areA^{HA} fmdS-lacZ pyroA4 nkuAΔ::Bar kapA^{S111F} crmA^{T525C}::pyrG⁺</i>
RT401	<i>pyrG89 biA1 wA::gpd(p)-gfp::areANLS123+5::AfpyroA gpd(p)areA^{HA} fmdS-lacZ pyroA4 nkuAΔ::Bar kapA^{S111F} crmA^{T525C}::pyrG⁺</i>
RT402	<i>pyrG89 wA::gpd(p)-gfp::areANLS123+5::AfpyroA gpd(p)areA^{HA} fmdS-lacZ pyroA4 nkuAΔ::Bar kapA^{S111F} crmA^{T525C}::pyrG⁺</i>
RT407	<i>pyrG89 yA1 pabaA1 areA(5'Δ)::riboB fmdS-lacZ pyroA4 AN0504Δ::AfpyrG⁺</i>
RT408	<i>pyrG89 yA1 pabaA1 areA(5'Δ)::riboB fmdS-lacZ AN0504Δ::AfpyrG⁺</i>
RT409	<i>pyrG89 areA(5'Δ)::riboB fmdS-lacZ AN0504Δ::AfpyrG⁺</i>
RT410	<i>pyrG89 areA(5'Δ)::riboB fmdS-lacZ pyroA4 AN0504Δ::AfpyrG⁺</i>
RT433	<i>gpd(p)areA^{HA} fmdS-lacZ AN0504Δ::AfpyrG⁺</i>
RT434	<i>yA1 pabaA1 gpd(p)areA^{HA} fmdS-lacZ pyroA4 AN0504Δ::AfpyrG⁺</i>
RT435	<i>yA1 pabaA1 amdR44 argB::amdS-lacZ areA217 riboB2</i>
RT436	<i>yA1 pabaA1 amdR44 argB::amdS-lacZ areA217 riboB2</i>
RT467	<i>pyrG89 jipAΔ::AfpyrG gpd(p)areA^{HA} fmdS-lacZ pyroA4 nkuAΔ::Bar</i>
RT468	<i>pyrG89 jipAΔ::AfpyrG gpd(p)areA^{HA} fmdS-lacZ pyroA4 nkuAΔ::Bar</i>
RT469	<i>pyrG89 areA(5'Δ)::riboB pyroA4 atmAΔ::AfpyrG⁺</i>
RT470	<i>gpd(p)areA^{HA} pyroA4 nkuAΔ::argB atmAΔ::AfpyrG⁺</i>
RT471	<i>pabaA gpd(p)areA^{HA} pyroA4 nkuAΔ::argB atmAΔ::AfpyrG⁺</i>
RT480	<i>pyrG89 yA1 pabaA1 areA(5'Δ)::riboB fmdS-lacZ pyroA4 AN0103Δ::AfpyrG⁺</i>
RT481	<i>pyrG89 areA(5'Δ)::riboB fmdS-lacZ pyroA4 AN0103Δ::AfpyrG⁺</i>

^a All strains carry the *veA1* mutation.

Table 4.1 *A. nidulans* strains used in Chapter 4 (continued)

Strain	Genotype^a
RT482	<i>pyrG89 yA1 pabaA1 areA(5'Δ)::riboB fmdS-lacZ AN0103Δ::AfpyrG⁺</i>
RT496	<i>pyrG89 gpd(p)areA^{HA} fmdS-lacZ pyroA4 AN0103Δ::AfpyrG⁺</i>
RT497	<i>pyrG89 yA1 gpd(p)areA^{HA} fmdS-lacZ pyroA4 AN0103Δ::AfpyrG⁺</i>
RT580	<i>yA1 pabaA1 gpd(p)areA^{HA.Δ703-712} pyroA4 sumOΔ::Bar</i>
RT581	<i>yA1 pabaA1 gpd(p)areA^{HA.Δ703-712} fmdS-lacZ pyroA4 sumOΔ::Bar</i>
RT582	<i>yA1 pabaA1 gpd(p)areA^{HA.Δ703-712} amdS-lacZ kapA::xylP(p)kapA sumOΔ::Bar</i>
RT583	<i>yA1 pabaA1 gpd(p)areA^{HA.Δ703-712} amdS-lacZ kapA::xylP(p)kapA sumOΔ::Bar</i>
RT602	<i>yA1 gpd(p)areA^{HA} fmdS-lacZ pyroA4 kapA^{S111F} sumOΔ::Bar</i>
RT603	<i>gpd(p)areA^{HA} fmdS-lacZ pyroA4 kapA^{S111F} sumOΔ::Bar</i>
RT604	<i>yA1 gpd(p)areA^{HA} fmdS-lacZ kapA^{S111F} sumOΔ::Bar</i>
RT605	<i>gpd(p)areA^{HA} fmdS-lacZ kapA^{S111F} sumOΔ::Bar</i>
RT606	<i>yA1 gpd(p)areA^{HA.703-712Δ} pyroA4 kapA^{S111F}</i>
RT607	<i>gpd(p)areA^{HA.703-712Δ} pyroA4 kapA^{S111F}</i>
RT620	<i>gpd(p)areA^{HA} amdS-lacZ pyroA4 kapA::kapA::gfp-AfriboB sumO::xylP(p)sumO-Bar</i>
RT621	<i>gpd(p)areA^{HA} amdS-lacZ pyroA4 kapA::kapA::gfp-AfriboB sumO::xylP(p)sumO-Bar</i>
RT622	<i>yA1 pabaA1 gpd(p)areA^{HA.703-712Δ} pyroA4 kapA::xylP(p)kapA-AfpyroA</i>
RT623	<i>yA1 pabaA1 gpd(p)areA^{HA.703-712Δ} pyroA4 kapA::xylP(p)kapA-AfpyroA</i>

^a All strains carry the *veA1* mutation.

4.3.2 Molecular techniques

Standard molecular techniques were as described in SAMBROOK AND RUSSELL (2001) or, for kits or enzymes, according to instructions from the manufacturer. PCR to generate gene replacement constructs used proof-reading enzymes: Pfu (Agilent), PfuTurbo (Stratagene), Phusion (Thermo Scientific) or Ex Taq (TaKaRa). Southern analysis to confirm gene replacements was performed using the DIG-High Prime DNA Labeling and Detection Starter Kit II (Roche).

4.3.3 Immunostaining, immunofluorescence, and direct fluorescence microscopy

Immunostaining was conducted as described previously (HUNTER *et al.* 2014). Indirect UV immunofluorescence microscopy was performed using an Olympus BX51 upright biological reflected fluorescence microscope equipped with Nomarski Differential Interference Contrast (DIC), an EXFO X-Cite 120 Q fluorescence illumination system and a UPlanFLN Plan Semi Apochromat (Field Number FN26.5) Fluorite 100x oil objective with a numerical aperture of 1.30. Alexa-488 immunofluorescence was detected using a BrightLine Fluorescein Isothiocyanate (FITC) filter set (excitation wavelength band pass, 482/35 nm; dichroic mirror, 506 nm; emission 536/40 nm ZPIXEL). 4', 6-diamidino-2-phenylindole) DAPI fluorescence was detected using a BrightLine DAPI Hi Contrast filter set (excitation wavelength band pass, 387/11 nm; dichroic mirror, 409 nm; ZPIXEL). At least 30 nuclei from each of two independent experiments were analyzed for each growth condition. Photomicrographs were captured using an Olympus DP72 12.8 Megapixel digital color camera and DP2-BSW digital camera software. Images were manipulated similarly within and between experiments using Adobe Photoshop CC 2015. Images were cropped, and the tonal range was increased by adjusting highlights and shadows without altering the color balance.

4.4 Results

4.4.1 The α -importin KapA aids in AreA nuclear localization

4.4.1.a Subcellular co-localization of KapA::GFP and AreA^{HA}

The wild-type AreA^{HA} protein accumulates in the nuclei of hyphae strongly after four hours of nitrogen starvation but not during nitrogen sufficient or nitrogen limiting conditions (TODD *et al.* 2005; HUNTER *et al.* 2014). To better understand how the intracellular dynamics of the α -importin KapA affect AreA^{HA} subcellular distribution we used immunofluorescence microscopy to determine the simultaneous subcellular localization of both AreA^{HA} and KapA::GFP during nitrogen sufficiency and nitrogen starvation. In these experiments, AreA^{HA} was expressed from the constitutive *gpd*(p) promoter to prevent effects of autoregulation (TODD *et al.* 2005).

When hyphae were grown in nitrogen sufficient conditions (NH₄), AreA^{HA} was dispersed throughout the cytoplasm and excluded from the nucleus (Figure 4.3A). KapA::GFP was similarly dispersed throughout the cytoplasm, and also appeared in a few concentrated punctate spots of potential aggregation around the nucleus (Figure 4.3A). AreA^{HA} and KapA::GFP did not appear to be co-localized, because the overlaid images reveal that they are spatially separated and intertwined within the cytoplasm.

When hyphae were grown in nitrogen sufficient conditions (NH₄), and then transferred for 4h to nitrogen starvation conditions (-N), AreA^{HA} accumulated in the nucleus, and was almost non-existent in the cytoplasm (Figure 4.3B). KapA::GFP accumulated in the nucleus but was also localized in small aggregations around the nucleus and in the cytoplasm. AreA^{HA} and KapA::GFP were co-localized within the nucleus (Figure 4.3B). The co-localization of AreA^{HA} and KapA::GFP is consistent with AreA nuclear import occurring via the KapA α -importin.

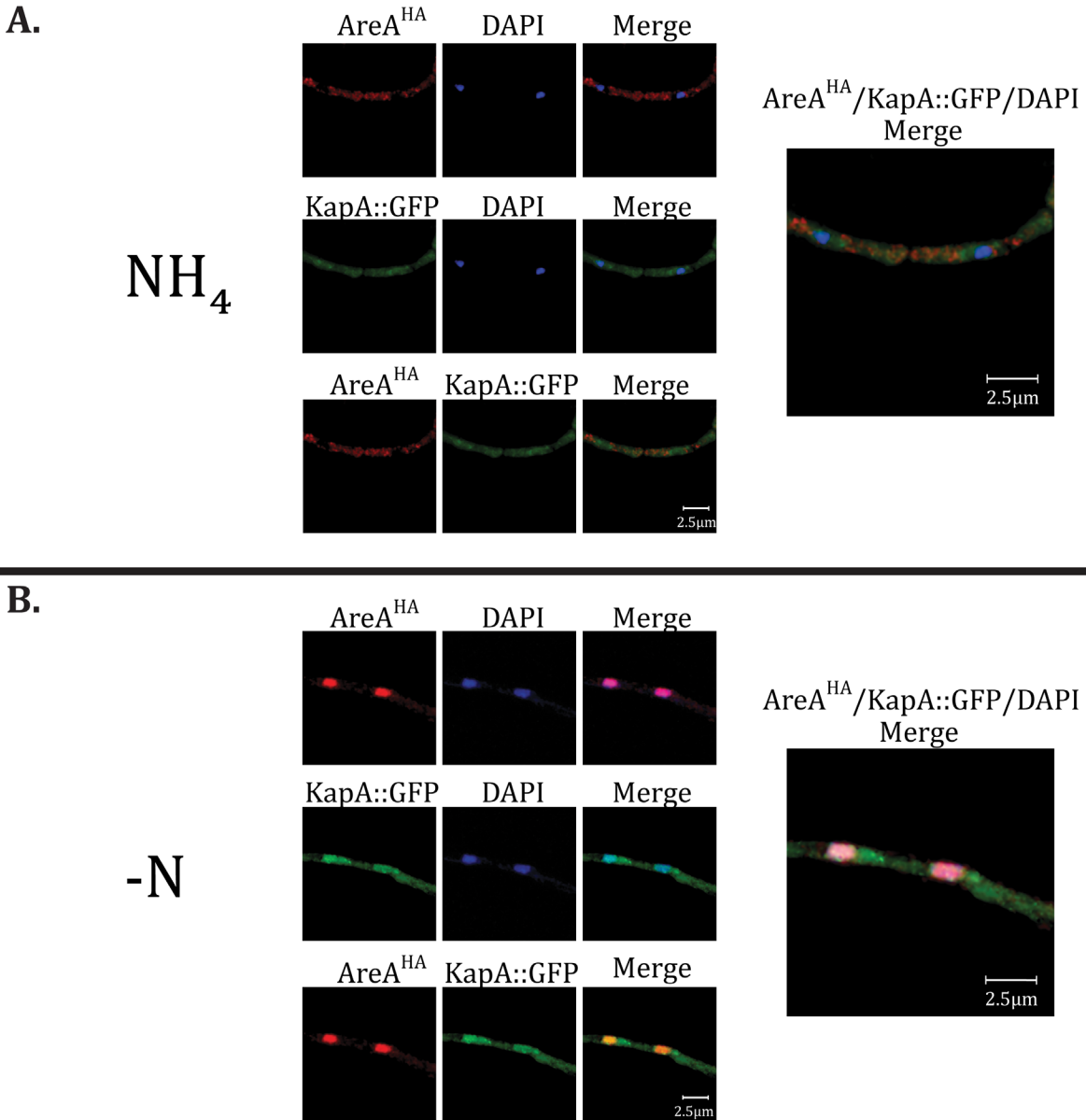


Figure 4.3 Co-localization of AreA^{HA} and KapA::eGFP

The subcellular distribution of AreA^{HA} (α -HA) and KapA::GFP in a gene-replaced *gpd(p)areA^{HA}* strain after 14h growth on supplemented 10mM ammonium-minimal media and 4h transfer to supplemented minimal medium containing 10mM ammonium (NH_4) or no nitrogen source (-N) was visualized by UV fluorescence microscopy following immunostaining with α -HA (3F10) and Alexa Fluor 594-conjugated goat anti-rat antibodies. A representative image of at least 100 nuclei is shown. Nuclei are stained with DAPI. Strain shown is MH12318: *gpd(p)areA^{HA} kapA::gfp*.

4.4.1.b Construction of the *kapA*^{S111F} point mutant

Deletion of the *A. nidulans kapA* gene is lethal (ARAUJO-BAZAN *et al.* 2009). However, a point mutant allele *kapA*^{S111F}, which substitutes a conserved serine residue for phenylalanine, confers temperature sensitive nuclear import, as is also observed for the equivalent mutation in the *S. cerevisiae kapA* ortholog *SRP1* (TABB *et al.* 2000; ARAUJO-BAZAN *et al.* 2009). We constructed a *kapA*^{S111F} point mutant using two-step gene replacement to determine if AreA^{HA} is transported into the nucleus using the KapA α -importin pathway (Figure 4.4).

We constructed the *kapA* mutant DNA fragment in a vector containing the *AfpyrG* selectable marker. A 5' 560 bp portion of the *kapA* coding sequence lacking the start codon was amplified with primers KapAF1 and KapAR2, and the 3' 1.8 kb portion of *kapA* was amplified with KapAF2 and KapAR1, using MH1 (*kapA*⁺) genomic DNA as template. KapAR2 and KapAF2 are complementary and contained a TCC to TTC transition mutation in codon 111 leading to the S111F substitution. The two overlapping PCR products were annealed and used as template for amplification with the flanking primers KapAF1 and KapAR1 and the 2.3 kbp amplification product was gel-purified and cloned into pGEM-Teasy. The 2.3 kbp PCR product was excised with *NotI* and subcloned into the *NotI* site in the polylinker of pKS6 (which contains the *AfpyrG SpeI-EcoI*CRI fragment from the *AfpyrG* clone pSM6364 inserted into the blunted *SspI* site in the pBluescript-SK+ backbone) to generate the mutant *kapA* plasmid kapA12a. The insert was sequenced to confirm the presence of the *kapA*^{S111F} mutation. We used a two-step gene replacement strategy to replace the wild type genomic copy of *kapA* (Figure 4.4). The growth phenotypes of the parent (RT52), first-step integrant (RT206), intermediate (RT210) and final (RT235) two-step gene replacement are shown in Figure 4.5. For the first step, the pKS28 plasmid was transformed into RT52 (*gpd(p)areA*^{HA} *nkuA* Δ ::*Bar pyrG89*) and PyrG prototrophs were selected at 30°C (as the *kapA*^{S111F} mutant was known to have a temperature sensitive phenotype (ARAUJO-BAZAN *et al.* 2009). Due to the *nkuA* Δ non-homologous end-joining mutation in the recipient, only homologous integration of the construct could occur by single-crossover and the transformants were expected to have a wild type phenotype if the integration occurred by a cross-over to the right of the mutation in the plasmid or a mutant phenotype if the cross-over was to the left of the mutation. The PyrG⁺ prototrophs displayed a wild type morphology and did not show

temperature sensitivity at 42°C. One PyrG⁺ prototroph (RT206) was chosen for the second step, which evicted the selectable marker plasmid by vegetative selection on glucose-ammonium minimal media supplemented with uracil and uridine and containing 1 mg/ml 5-fluoro-orotic acid (5-FOA). Eviction of the plasmid removes the selectable marker and plasmid sequences; but depending on the site of the crossover in the second step, either the original wild type sequence or the *kapA*^{S111F} mutation is resolved. 5-FOA-resistant sectors were picked to supplemented minimal medium. 26 PyrG⁻ auxotrophic “pop-out” strains were isolated and one of these (RT210) showed poor conidiation at 30°C and temperature sensitivity at 42°C suggesting that this strain carried the *kapA*^{S111F} mutation (Figure 4.5). The 2.3 kbp *kapAF1*-*kapAR1* fragment was PCR-amplified from genomic DNA from this strain and sequenced with the *KapAF1* primer to confirm the presence of the *kapA*^{S111F} mutation. RT210 (*gpd(p)areA^{HA} pyrG89 nkuAΔ::Bar kapA^{S111F}*) was crossed to MH11072 (*yA1 areAΔ::riboB(3') nkuAΔ::Bar*) to remove the *pyrG89* marker, which is associated with cold sensitivity (KAFFER AND MAY 1988) and RT235 (*gpd(p)areA^{HA} kapA^{S111F} nkuAΔ::Bar*) was isolated and used for phenotypic analysis. The *kapA*^{S111F} mutant (RT235) shows poor conidiation and poor growth (Figure 4.5). Furthermore, relative growth of the mutant compared to WT is reduced at 42°C and 37°C compared with 30°C.

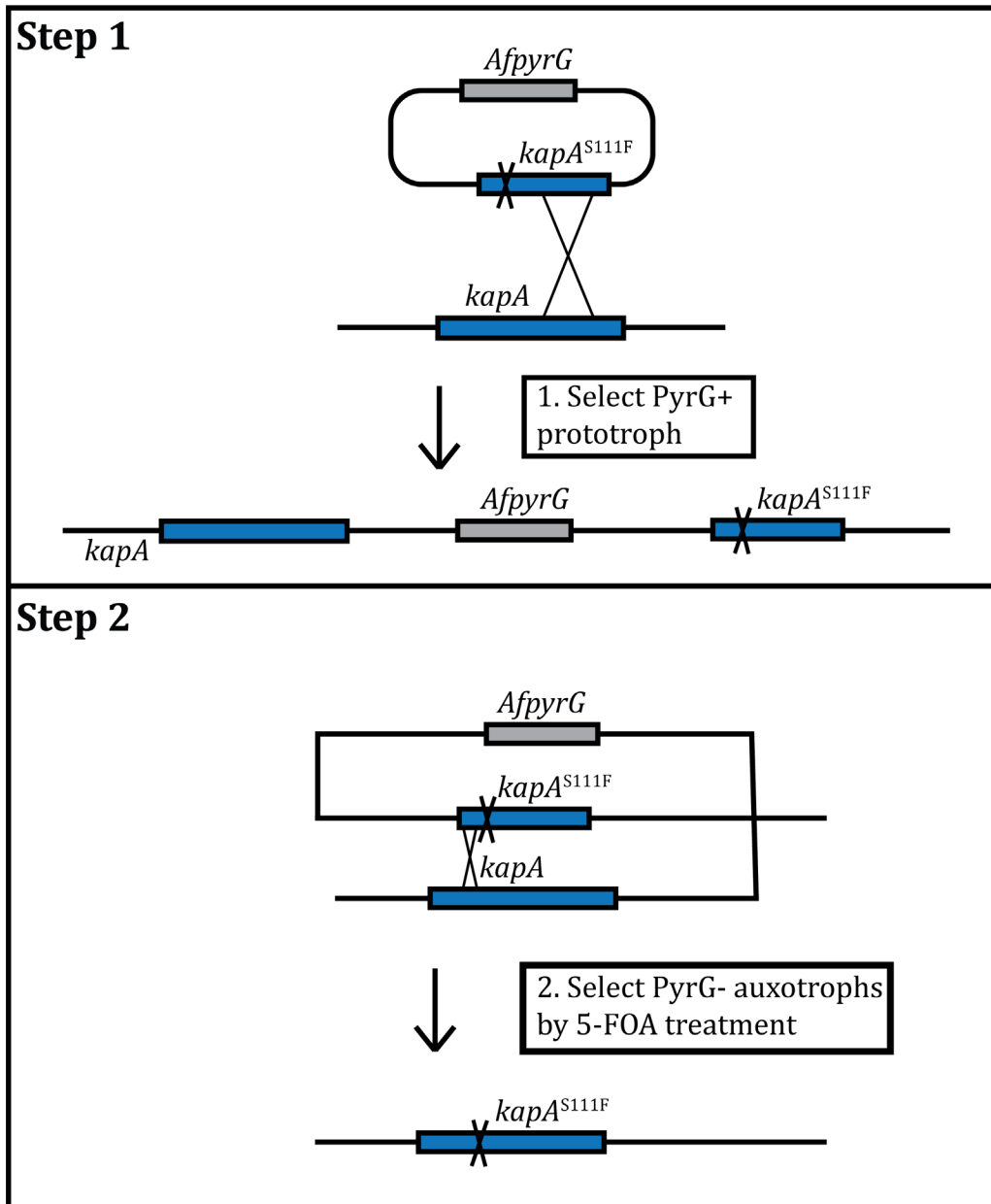


Figure 4.4 *kapA^{S111F}* two-step gene replacement strategy

A model for the two-step gene replacement strategy used to replace the wild type *kapA* gene with the *kapA^{S111F}* point mutation. **Step 1:** Integration of the *kapA^{S111F}-AfpyrG* plasmid by single-crossover. The *AfpyrG* marker allows selection of transformants by PyrG+ prototrophy. **Step 2:** Using 5-FOA the plasmid is evicted by vegetative selection resulting in a single copy *kapA^{S111F}*, PyrG- auxotroph.

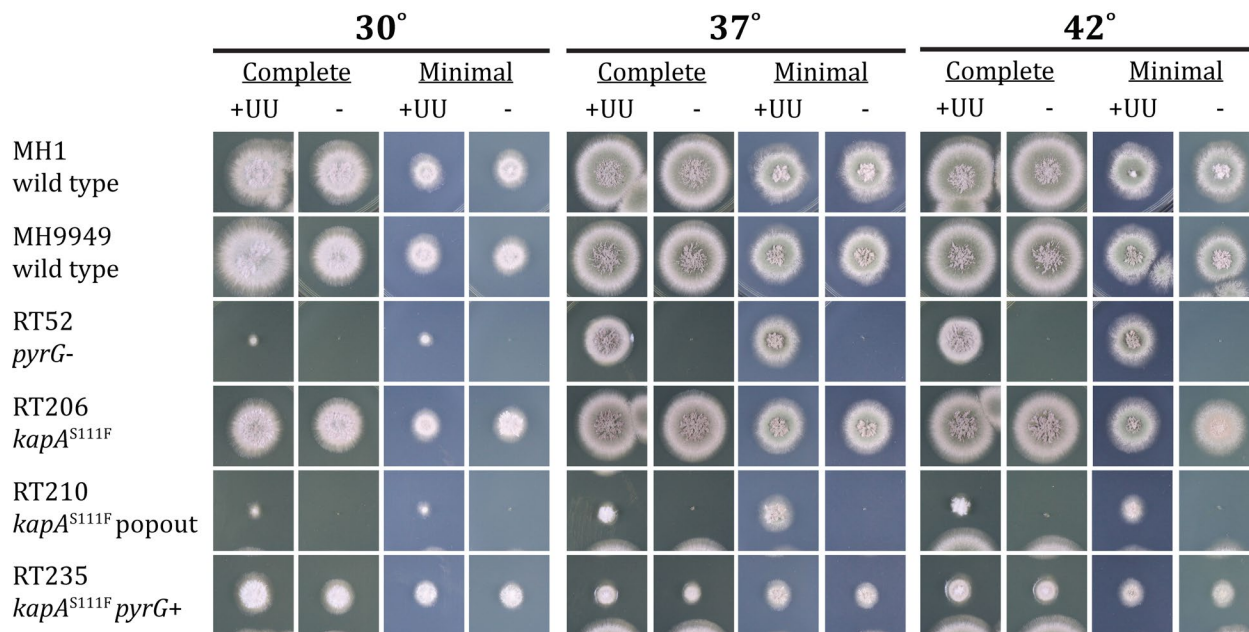


Figure 4.5 *kapA*^{S111F} growth phenotype

Growth of *kapA*^{S111F} mutants, construction intermediates, the recipient RT52, and wild type controls MH1 and MH9949 at 30°C, 37°C, and 42°C. Minimal is supplemented ANM (*Aspergillus* Nitrogen-free medium) with 10mM ammonium tartrate. +UU stands for 5mM Uridine and 5mM Uracil.

4.4.1.c Effects of *kapA*^{S111F} on AreA subcellular localization

KapA::GFP was primarily distributed throughout the cytoplasm during nitrogen sufficiency and accumulated in and around the nucleus during nitrogen starvation (see section 4.4.1.a). This mimics the AreA^{HA} subcellular localization pattern observed under the same conditions. If KapA is the major importin responsible for transporting AreA into the nucleus, an observable reduction (if not complete loss) of AreA^{HA} in the nucleus during nitrogen starvation should occur in the *kapA*^{S111F} mutant. The *kapA*^{S111F} point-mutant shows little to no AreA^{HA} accumulation in the nucleus compared to the wild type and a much stronger presence of AreA^{HA} in the cytoplasm during nitrogen starvation at 25°C (Figure 4.6). At 42°C there was less AreA^{HA} in the cytoplasm for the *kapA*^{S111F} strain on 10mM NH₄. We observed slight nuclear accumulation of AreA^{HA} in the *kapA*^{S111F} strain at 42°C during starvation, but the hyphae seem to be under more stress than the wild type. The hyphae are thinner, less robust, and there appears to be less density of AreA^{HA} in the hyphae compared to the wild type.

AreA^{HA} nuclear import appears to be dependent on the KapA importin- α for nuclear accumulation. On nitrogen sufficient conditions, where AreA^{HA} is cytoplasmic in a wild-type background, we did not see any significant differences in AreA^{HA} subcellular distribution between the *kapA*⁺ control and the *kapA*^{S111F} mutant, the two minor differences were that there appeared to be a slightly more nuclear exclusion (clear voids where the nucleus is) and the density of the fluorescence in the mutant appears slightly lower.

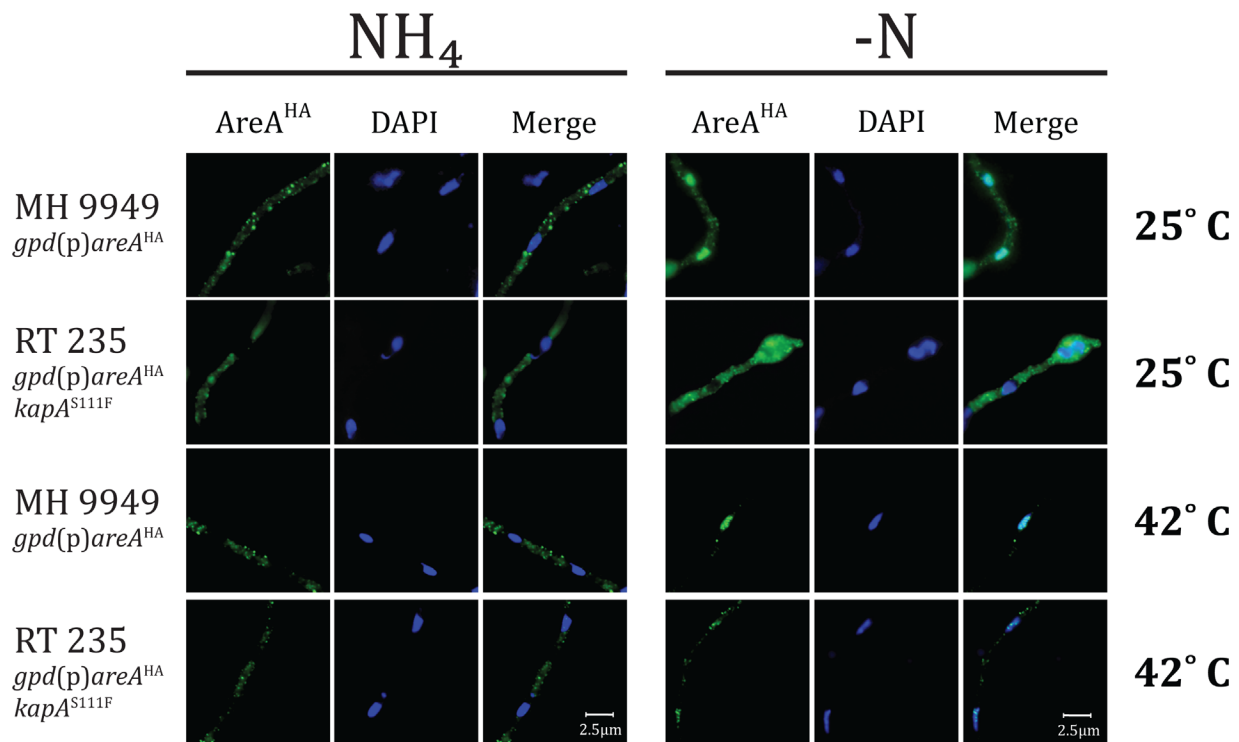


Figure 4.6 Localization of AreA^{HA} in a *kapA^{S111F}* mutant

The subcellular distribution of AreA^{HA} (α-HA) in gene-replaced *gpd(p)areA^{HA}* variants after 14h growth on minimal media supplemented with 10mM ammonium (NH₄) then transferred for 4h to supplemented minimal medium containing 10mM NH₄ or no nitrogen source (-N). Visualized by UV fluorescence microscopy following immunostaining with anti-HA (3F10) and Alexa Fluor 488-conjugated goat anti-rat antibodies. A representative image of at least 100 nuclei is shown. Nuclei are stained with DAPI.

4.4.1.d Effects of *kapA*^{S111F} on AreA NLSs::eGFP

Knowing that KapA^{S111F} significantly reduces nuclear accumulation of AreA^{HA} during nitrogen starvation we attempted to determine if this affected the classical SV40 Large T Antigen-type NLSs on AreA as well as the noncanonical bipartite NLS. To do this we crossed the GFP fusion strains (Chapter 3) with the *kapA*^{S111F} mutant. The GFP-NLS fusion *kapA*^{S111F} progeny were chosen by white spore color (as the GFP constructs were integrated at the *wA* (*white conidia*) gene) and the *kapA*^{S111F} temperature sensitive growth phenotype. The distribution of the GFP-NLS fusion proteins within *kapA*^{S111F} hyphae was determined using direct UV-fluorescence microscopy (Figure 4.7). There appears to be a reduction of nuclear accumulation of GFP::NLS 4 in a KapA^{S111F} strain at both 25°C and 42°C compared to KapA^{WT}, consistent with nuclear import via NLS4 at least partially occurring via KapA. In contrast to the full-length wild type AreA^{HA} protein containing all six redundant NLSs, the α -importin mutant does not appear to have any significant effect at 25°C or 42°C when multiple classical NLSs together or the non-canonical bipartite NLS are fused to GFP.

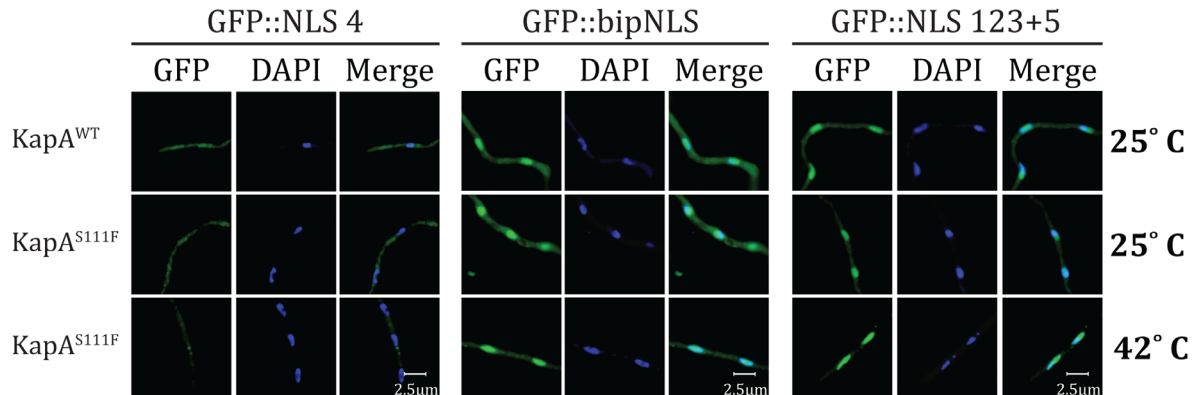


Figure 4.7 Localization of GFP::NLSs in a KapA^{S111F} mutant strain

The subcellular distribution of GFP-NLS proteins. Direct UV fluorescence GFP microscopy of germlings of *gpd(p)gfp-NLS* transformants in a *kapA* wild type or *kapA*^{S111F} strain after 14h growth in minimal media containing 10mM ammonium and then a 4h transfer to nitrogen-free (-N) minimal media. A representative image of at least 100 nuclei is shown. Nuclei are stained with DAPI.

4.4.1.e KapA overexpression leads to loss of AreA^{HA} nuclear accumulation

To determine the effect of KapA overexpression on AreA^{HA} nuclear accumulation *kapA* was expressed from the xylose-inducible *xylP* promoter (ZADRA *et al.* 2000), K.H. Wong, M.A. Davis and R.B. Todd, unpublished). KapA overexpression conferred inhibited growth (Figure 4.8A). Nuclear accumulation of AreA^{HA} was not observed during nitrogen starvation or on ammonium in the KapA over expression strain on both 1% glucose and 1% xylose (Figure 4.8B). Therefore, overexpression of KapA did not lead to increased nuclear accumulation of AreA^{HA}.

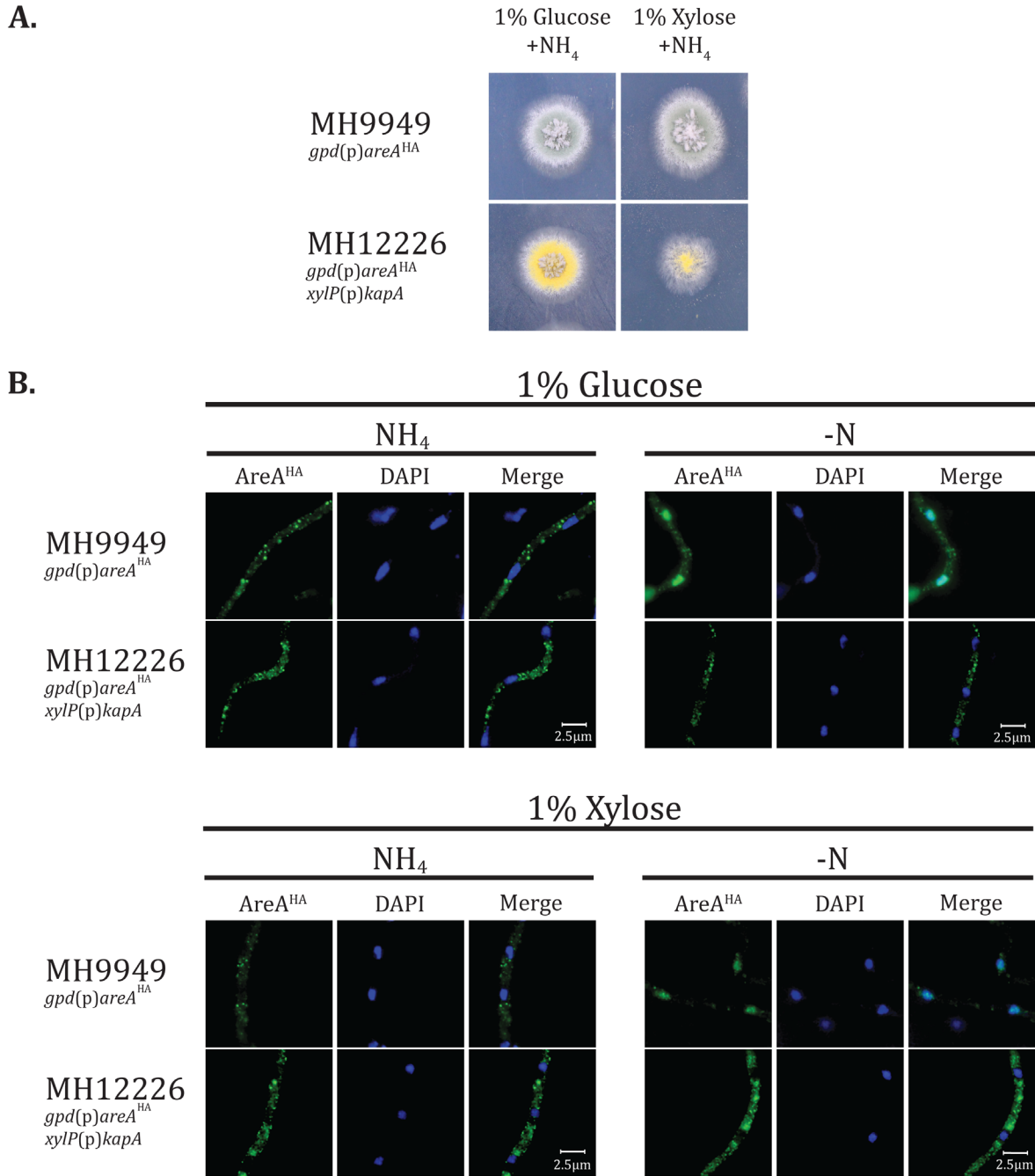


Figure 4.8 Loss of AreA^{HA} nuclear accumulation in a *kapA* overexpression strain

A. Colonial growth of *gpd(p)areA^{HA}* (wt) and *xylP(p)kapA* (*kapA*OE) strains on supplemented minimal media with 10mM ammonium (NH₄) containing 1% glucose and on carbon-free media 10mM NH₄ + 1% xylose.

B. The subcellular distribution of AreA^{HA} after 14h growth on minimal media supplemented with 10mM NH₄ and 4h transfer to minimal media containing 10mM NH₄ or no nitrogen source (-N). 1% xylose was added to supplemented carbon-free minimal media as indicated during the 4h transfer. Visualized by UV fluorescence microscopy following immunostaining with α -HA (3F10) and Alexa Fluor 488-conjugated goat anti-rat antibodies. A representative image of at least 100 nuclei is shown. Nuclei are stained with DAPI.

4.4.2 The Relationship between SumO, AreA, and KapA

4.4.2.a Effects of *sumO* Δ and SumO overexpression on *A. nidulans* growth and AreA^{HA} subcellular localization

The *sumO* gene in *A. nidulans* was previously characterized (WONG *et al.* 2008b). Preliminary experiments suggested that the *sumO* Δ mutation affects AreA^{HA} subcellular localization (TODD Unpublished data; WONG 2007). Herein, I have further examined the mechanism underlying the effects of SumO on nuclear accumulation of AreA^{HA}. This section confirms previous findings and uses an AreA^{HA} nuclear export mutant to determine if the *sumO* Δ mutation completely inhibits AreA^{HA} nuclear import.

The *sumO* Δ mutant has a substantially reduced morphological phenotype on all conditions tested compared to wildtype except on complete media, which promotes an abundance of asexual spore development and partially rescues the *sumO* Δ growth phenotype (Figure 4.9). Deletion of the *sumO* gene results in the loss of AreA^{HA} accumulation in the nucleus on nitrogen starvation (Figure 4.10). The lack of AreA^{HA} nuclear accumulation could conceivably be due to a block in AreA^{HA} nuclear import or promotion of AreA^{HA} nuclear export in the *sumO* Δ mutant, or a combination of these two potential mechanisms. To determine if the loss of *sumO* completely prevents nuclear import of AreA^{HA}, we crossed a *sumO* Δ strain and a *gpd(p)areA^{HA.NES} Δ* strain, which carries an in-frame deletion of the AreA nuclear export signal at residues 703-712, to construct a *gpd(p)areA^{HA.NES} Δ sumO* Δ strain. In a wild-type background, the Δ 703-712 mutation confers AreA nuclear accumulation (TODD Unpublished data). On both NH₄ and during nitrogen starvation AreA^{HA.NES} Δ accumulated in the nucleus of *sumO* Δ hyphae (Figure 4.10). This indicates that deletion of *sumO* does not prevent AreA nuclear import. We then analyzed the effects of xylose-inducible overexpression of SumO on the subcellular localization of AreA^{HA} using a *xyLP(p)sumO^{FLAG}* strain. The *xyLP* promoter is adjustable due to repression by glucose and induction by xylose (ZADRA *et al.* 2000). When hyphae were grown on ammonium with either 1% glucose or 1% xylose as a carbon source AreA^{HA} was distributed throughout the cytoplasm. During nitrogen starvation AreA^{HA} accumulated in the nucleus on both 1% glucose and 1% xylose. AreA^{HA} nuclear accumulation was slightly weaker when *sumO* was overexpressed on 1% xylose compared with 1% glucose, suggesting that SumO may promote AreA nuclear export.

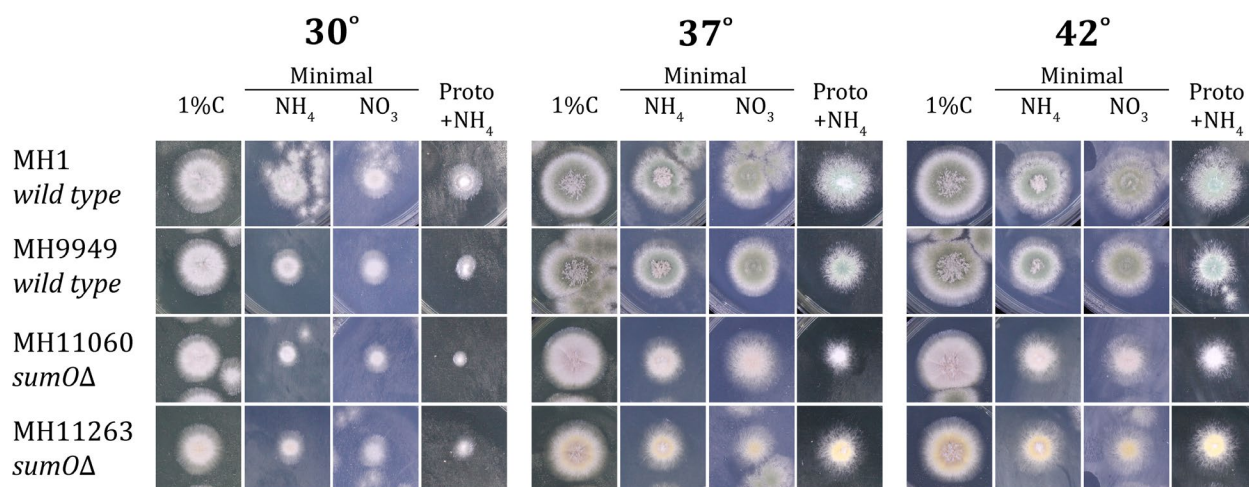


Figure 4.9 Colonial growth of *sumOΔ* strains

Colonial growth of wild type and the *sumOΔ* mutant at 30°C, 37°C, and 42°C grown for 2 days. The nitrogen concentration is 10mM unless otherwise noted. 1%C is complete media. Minimal is supplemented ANM minimal media with 10mM ammonium tartrate or 10mM sodium nitrate. Proto+NH₄ is supplemented protoplast medium (containing 1.0M sucrose with PABA, pyridoxine, biotin) and 10mM ammonium tartrate.

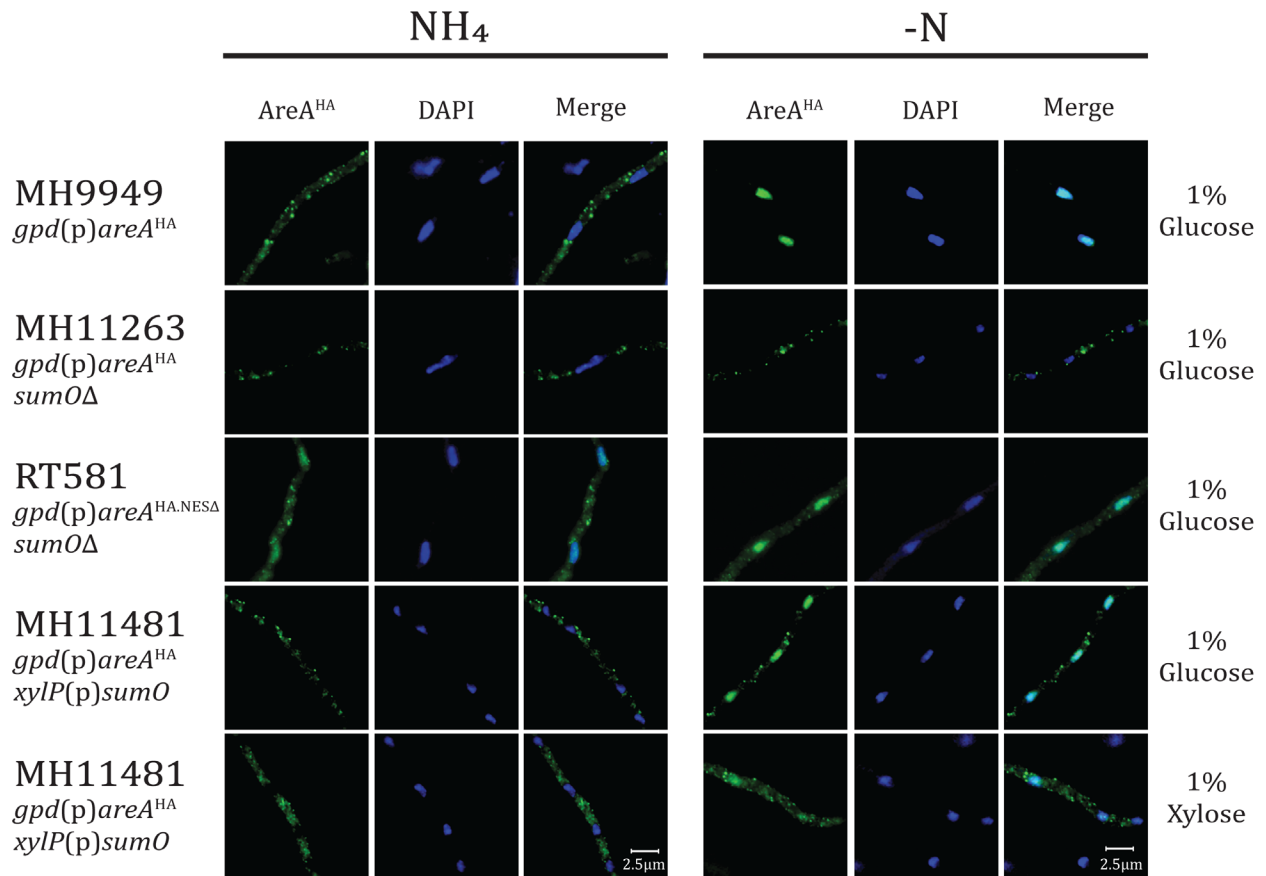


Figure 4.10 AreA^{HA} subcellular localization in *sumOΔ* and overexpression strains

The subcellular distribution of AreA^{HA} (α -HA) in gene-replaced *gpd(p)areA^{HA}* variants after 14h growth on minimal media supplemented with 10mM ammonium (NH₄) and 4h transfer to minimal medium containing 10mM NH₄ or no nitrogen source (-N). 1% Xylose was added to select treatments during the 4h transfer. Visualized by UV fluorescence microscopy following immunostaining with α -HA (3F10) and Alexa Fluor 488-conjugated goat anti-rat antibodies. A representative image of at least 100 nuclei is shown. Nuclei are stained with DAPI.

4.4.2.b Effects of *sumOΔ* on KapA::GFP subcellular localization

To determine if SumO plays any role in the KapA α -importin-dependent AreA^{HA} nuclear import pathway we compared the subcellular localization of KapA-GFP in an *areA* wild-type background and a *kapA::gfp gpd(p)areA^{HA} sumOΔ* strain (MH12328) using immunofluorescence microscopy. When hyphae were grown in nitrogen sufficient conditions (NH₄), we observed similar subcellular localization of both KapA::GFP and AreA^{HA} in a *sumOΔ* mutant as we did in the *sumO* wild-type strain (Figure 4.3, Figure 4.11). There does appear to be an increase in bright punctate aggregations of KapA::GFP in the *sumOΔ* mutant. These punctate spots appear to be commonly associated with the perinuclear region. Similar to what is seen in the *sumO* wild-type strain, in the *sumOΔ* mutant, AreA^{HA} and KapA::GFP distribution seldom overlapped during nitrogen sufficient conditions (Figure 4.11).

There are stark differences when comparing the effects of the *sumOΔ* mutant (Figure 4.11) on the subcellular localization of both KapA::GFP and AreA^{HA} to the *sumO* wild-type control during nitrogen starvation (-N) (Figure 4.3). Neither AreA^{HA} nor KapA::GFP accumulated in the nucleus during nitrogen starvation in the *sumOΔ* mutant. We observed distinct red and green color profiles in the merged image with little to no overlap of the two colors, indicating that there is minimal opportunity for physical interaction between KapA and AreA^{HA} in a *sumOΔ* mutant (Figure 4.11).

MH 12328 - *gpd(p)areA^{HA} sum0Δ, kapA::gfp*

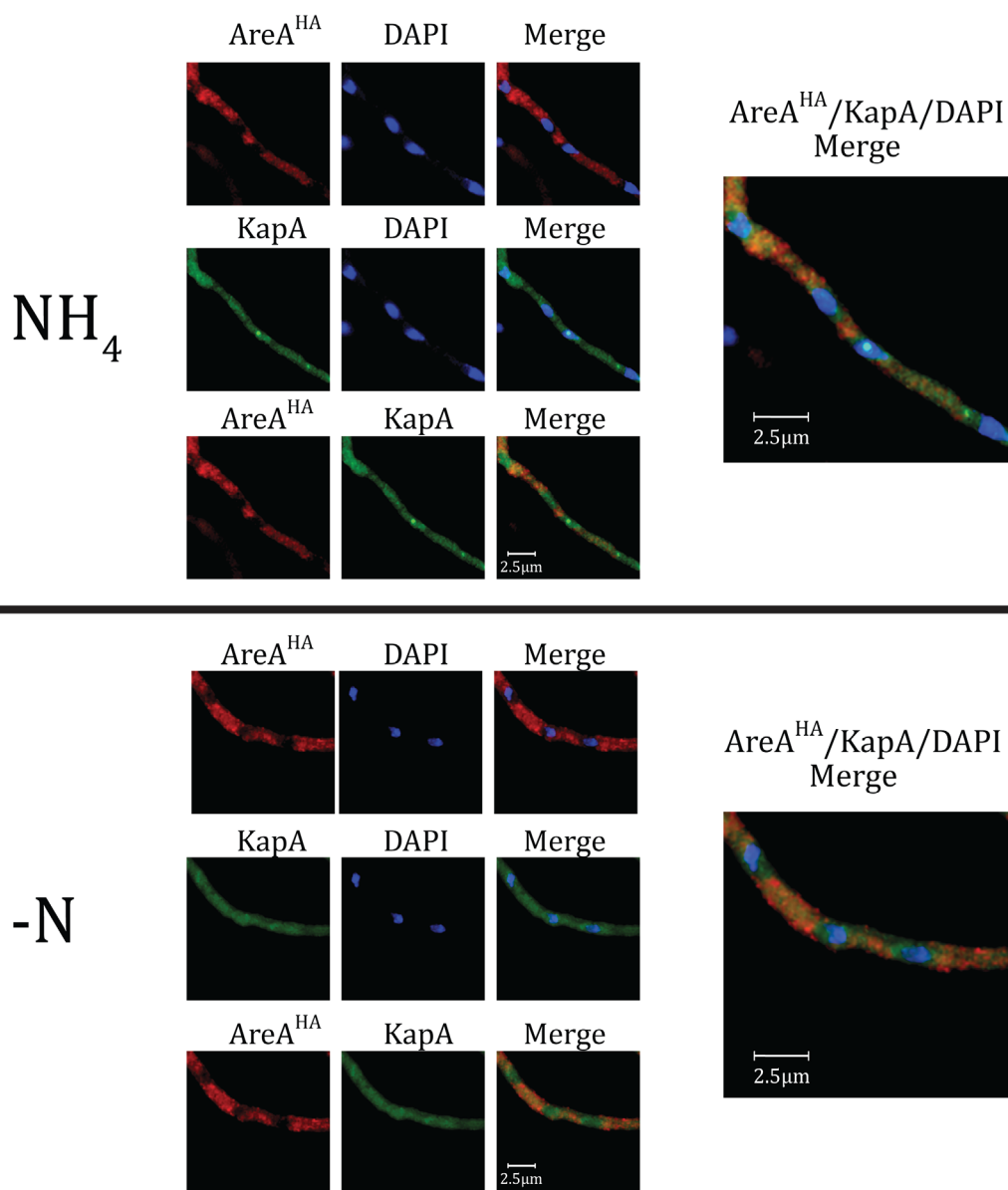


Figure 4.11 Co-localization of *AreA^{HA}* and *KapA::eGFP* in a *sum0Δ* background

The subcellular distribution of *AreA^{HA}* (α -HA) in gene-replaced *gpd(p)areA^{HA}* variants after 14h growth on minimal media supplemented with 10mM ammonium (NH_4) and 4h transfer to supplemented minimal medium containing 10mM NH_4 or no nitrogen source (-N) was visualized by UV fluorescence microscopy following immunostaining with α -HA (3F10) and Alexa Fluor 594-conjugated goat anti-rat antibodies. A representative image of at least 100 nuclei is shown. Nuclei are stained with DAPI.

4.4.2.c Effects of *sumO* overexpression on KapA::GFP subcellular localization

The loss of *sumO* prevents KapA::GFP accumulation in and around the nucleus during nitrogen starvation (Figure 4.11). To further understand the extent that KapA::GFP and SumO genetically interact, we crossed a *gpd(p)areA^{HA} kapA::gfp* strain (MH12318) with a *sumO* overexpression strain (MH11481). A progeny strain carrying all three genetic markers was then analyzed using immunofluorescence microscopy.

Overexpression of SumO did not have any apparent effect on the nuclear accumulation of AreA^{HA} (Figure 4.12). During nitrogen sufficiency, on both 1% glucose (where *xyIP(p)sumO* is repressed) and when transferred to 1% xylose (where *xyIP(p)sumO* is overexpressed), AreA^{HA} did not accumulate in the nucleus. During nitrogen starvation on 1% glucose or when transferred to 1% xylose media, AreA^{HA} accumulated in the nucleus. There does appear to be an increase in AreA^{HA} crowding leading up to the nucleus when SumO is over-expressed on both NH₄ and -N.

When *sumO* was overexpressed, KapA::GFP accumulated in and around the nucleus irrespective of the nitrogen condition. This effect appears to be more severe during nitrogen starvation than during nitrogen sufficiency, though in nitrogen starved cells the effect on KapA::GFP was no more severe than in the *sumO* wild-type strain (Figure 4.13). The subcellular localization of SumO in Wong et al. 2008 (WONG *et al.* 2008b), showed a similar perinuclear localization pattern as both KapA::GFP and over-expressed *sumO*^{FLAG}.

RT 620 - *gpd(p)areA^{HA} kapA::gfp xylP(p)::sumO*

1% Glucose

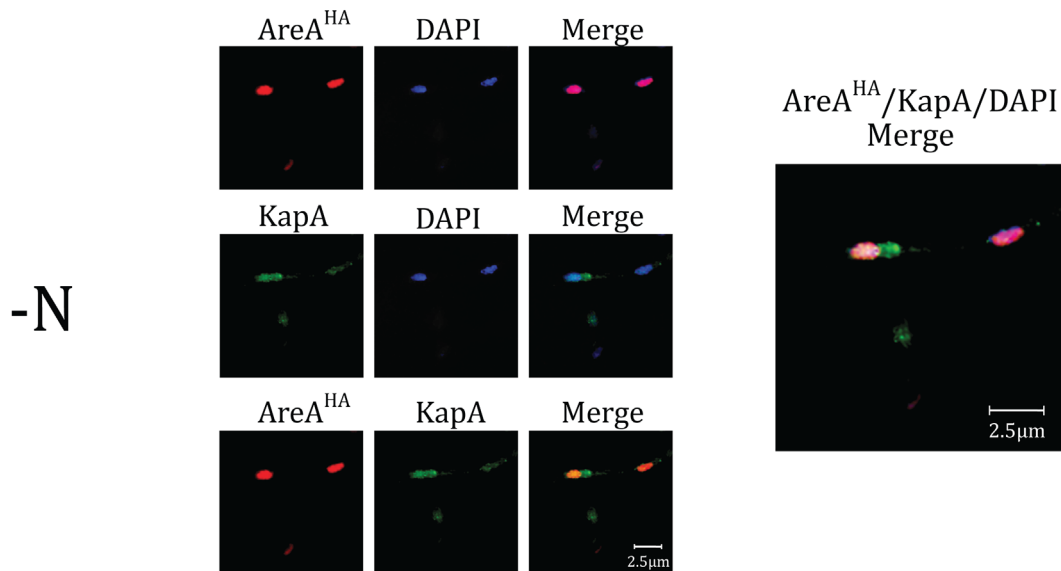
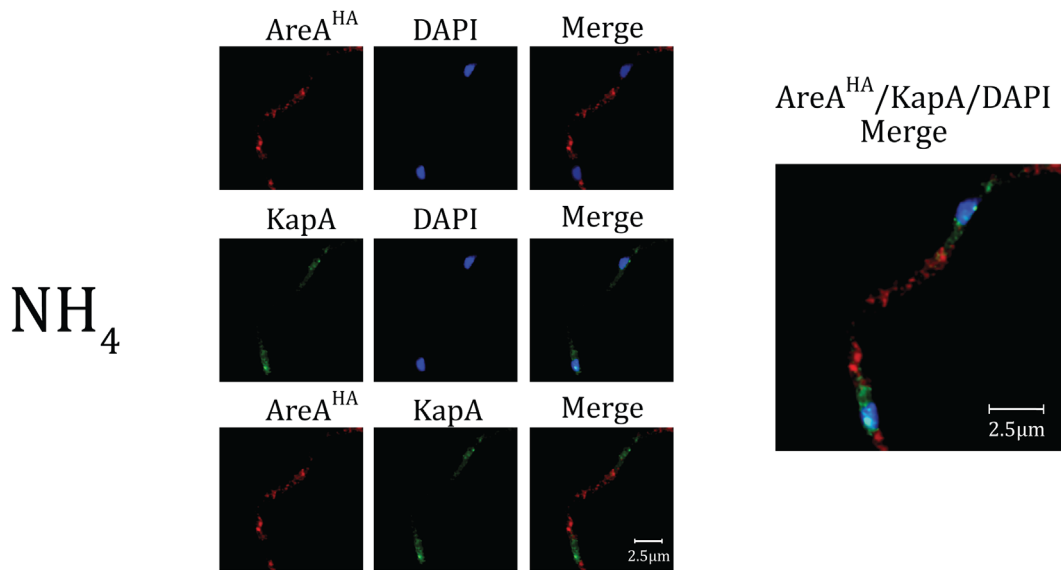


Figure 4.12 Subcellular localization of AreA^{HA} and KapA::eGFP in a *sumO* overexpression strain on 1% glucose

The subcellular distribution of AreA^{HA} (α -HA) in gene-replaced *gpd(p)areA^{HA}* variants after 14h growth on minimal media supplemented with 10mM ammonium (NH_4) and 4h transfer to supplemented minimal medium containing 10mM NH_4 or no nitrogen source (-N). The 1% xylose was added to select treatments during the 4h transfer. Visualized by UV fluorescence microscopy following immunostaining with α -HA (3F10) and Alexa Fluor 594-conjugated goat anti-rat antibodies. A representative image of at least 100 nuclei is shown. Nuclei are stained with DAPI.

RT 620 - *gpd(p)areA^{HA} kapA::gfp xylP(p)::sumO*

1% Xylose

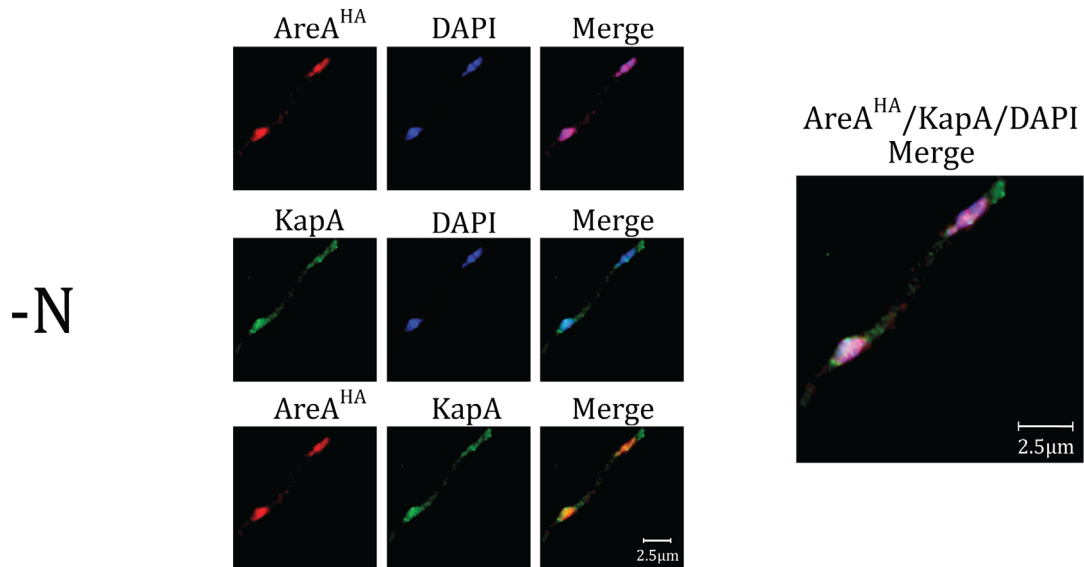
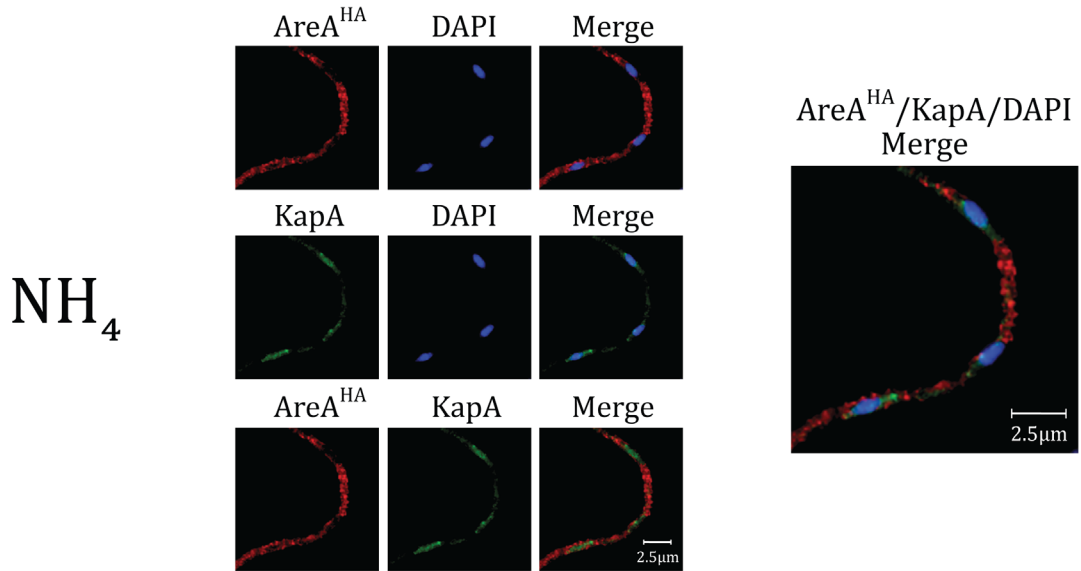


Figure 4.13 Subcellular localization of AreA^{HA} and KapA::eGFP during *sumO* overexpression on 1% xylose

The subcellular distribution of AreA^{HA} (α -HA) and KapA::eGFP in gene-replaced *gpd(p)areA^{HA}* variants after 14h growth on minimal media supplemented with 10mM ammonium (NH_4) and 4h transfer to supplemented minimal medium containing 10mM NH_4 or no nitrogen source (-N). The 1% xylose was added to select treatments during the 4h transfer. Visualized by UV fluorescence microscopy following immunostaining with α -HA (3F10) and Alexa Fluor 594-conjugated goat anti-rat antibodies. A representative image of at least 100 nuclei is shown. Nuclei are stained with DAPI.

4.4.2.d Effects of *kapA* overexpression on AreA^{HA} subcellular localization in a *sumOΔ* mutant

KapA and SumO both work to promote AreA^{HA} nuclear import. In section 3.3 we showed that during nitrogen starvation nuclear accumulation of AreA^{HA} can be prevented by the temperature-sensitive point mutation *kapA*^{S111F} (Figure 4.6) or by deletion of the *sumO* gene (Figure 4.11). The previous three subsections have shown that *sumO* is necessary for the transition from the primarily diffused throughout the cytoplasm distribution to the accumulation in and around the nucleus localization patterns that we observe for both KapA::GFP and AreA^{HA}. Overexpression of the *sumO* gene did not alter the localization pattern of AreA^{HA} but leads to KapA::GFP accumulation in and around the nucleus (Figure 4.13). These results suggest that *sumOΔ* may affect AreA^{HA} sub-cellular localization by inhibiting nuclear import via KapA α -importin. To test this, we overexpressed *kapA* in a *sumOΔ* background (MH12236) to determine if *sumO* was essential for KapA mediated nuclear import of AreA^{HA}.

Overexpression of *kapA* in a *sumOΔ* background did not affect the subcellular localization of AreA^{HA} during nitrogen sufficiency as it was primarily sequestered in the cytoplasm on both 1% glucose and 1% xylose (Figure 4.14). When transferred to nitrogen starvation conditions for four hours, AreA^{HA} accumulated in the nucleus in the *xyIP(p)kapA sumOΔ* strain under both low-level expression on 1% glucose and during high-level overexpression on 1% xylose. This is the same AreA^{HA} accumulation pattern as the AreA^{HA} wild type control strain MH9949, indicating that overexpression of *kapA* can overcome the inhibition of AreA^{HA} nuclear accumulation in a *sumOΔ* background. Therefore, KapA acts downstream of SumO, and SumO is not required for KapA-dependent nuclear import.

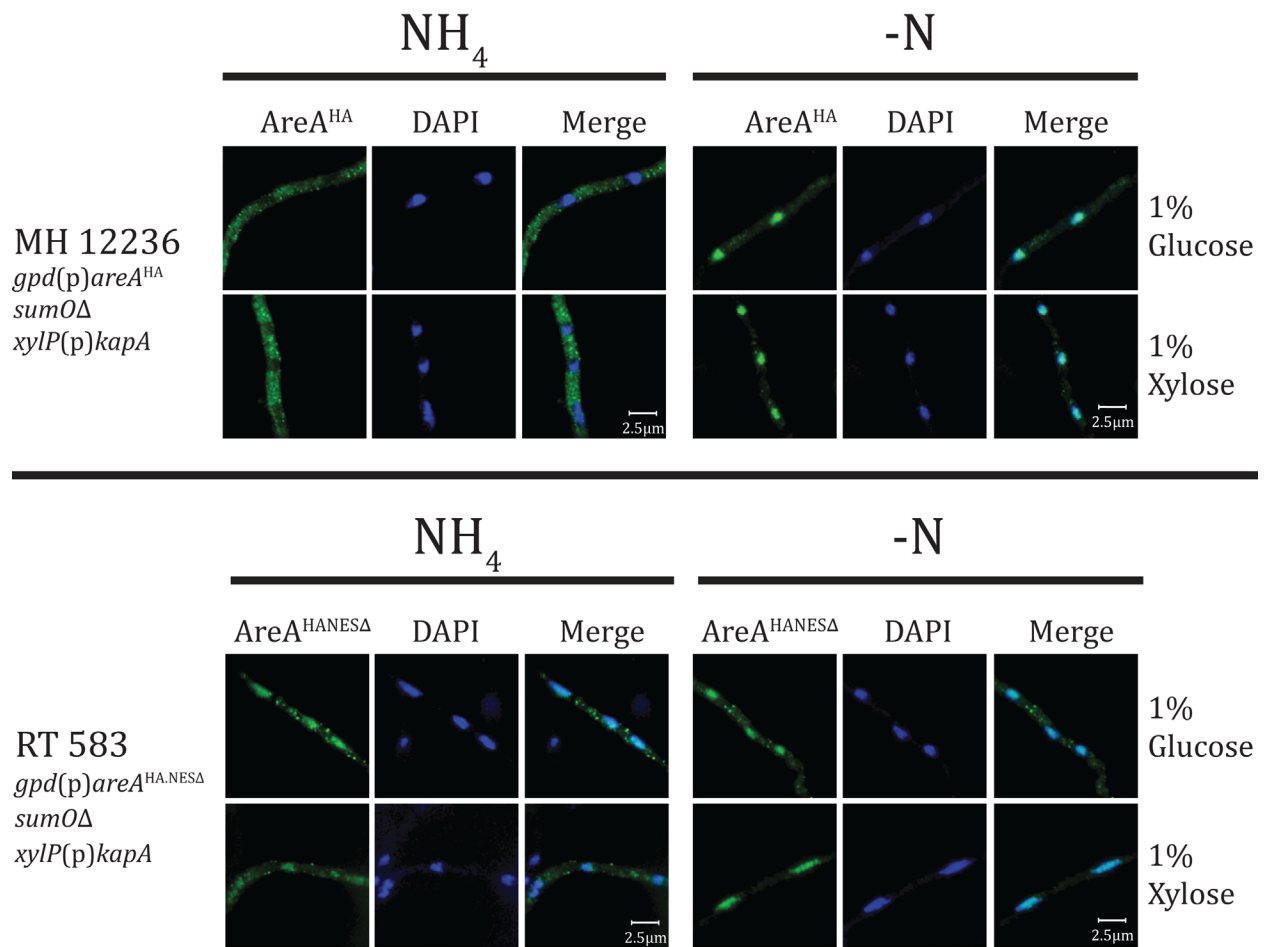


Figure 4.14 *kapA* overexpression in a *sum0Δ* mutant

The subcellular distribution of AreA^{HA} (α-HA) in gene-replaced *gpd(p)areA^{HA}* variants after 14h growth on minimal media supplemented with 10mM ammonium (NH₄) and 4h transfer to supplemented minimal medium containing 10mM NH₄ or no nitrogen source (-N). The 1% xylose was added to select treatments during the 4h transfer. Visualized by UV fluorescence microscopy following immunostaining with α-HA (3F10) and Alexa Fluor 488-conjugated goat anti-rat antibodies. A representative image of at least 100 nuclei is shown. Nuclei are stained with DAPI.

4.4.3 TOR signaling pathway components regulate AreA nuclear accumulation

4.4.3.a Rapamycin Inhibits AreA nuclear accumulation

In *A. nidulans*, the antifungal compound rapamycin reduces colonial growth and potentially plays a role in nitrogen signaling via the Target of Rapamycin (TOR) pathway (FITZGIBBON *et al.* 2005; KATZ *et al.* 2015). The components of the TOR pathway are conserved in *A. nidulans* (Table 4.2). Analysis of AreA^{HA} subcellular localization in the presence of rapamycin reveals that during nitrogen sufficiency (10mM NH₄) AreA^{HA} is localized to the cytoplasm, as observed in media lacking rapamycin (Figure 4.15). This similarity to wildtype does not extend to nitrogen starvation, where AreA^{HA} is excluded from the nucleus when transferred to nitrogen starvation in the presence of rapamycin (Figure 4.15). Furthermore, addition of rapamycin to nitrogen-starved cells containing nuclear accumulated AreA^{HA} does not trigger AreA^{HA} nuclear export (TODD Personal communication). Therefore, the inhibition of the TOR complex, and subsequently the components of the TOR pathway play a role in the regulation of AreA nuclear import. Notably, prevention of AreA nuclear accumulation by rapamycin contrasts with the rapamycin triggered translocation from the cytoplasm to the nucleus of the AreA homologue Gln3p in *S. cerevisiae* (BECK AND HALL 1999). Therefore, the TOR signaling pathway has been rewired in *A. nidulans* compared with yeast. Nevertheless, the effect of rapamycin on AreA nuclear accumulation has provided us rudimentary guidelines for understanding what other genes could be involved in nuclear import of AreA.

Table 4.2 Identification of the TOR pathway genes

Gene Locus	Gene Name	Function	<i>S. cerevisiae</i> Homologue
AN8667	<i>areA</i>	Nitrogen Regulation GATA Transcription Factor	Gln3
AN4905	<i>gstA</i>	Glutathione S-Transferase	Ure2 Homologue
AN2142	<i>kapA</i>	Karyopherin Alpha	Srp1
AN3255	undefined (<i>ure2</i>)	Predicted Glutathione Peroxidase	Ure2 Homologue
AN0504	<i>sitA</i>	Protein Phosphatase	Sit4
AN0103	undefined (<i>pph3</i>)	Protein Phosphatase	Pph3 Homologue
AN5814	<i>jipA</i>	Putative TapA Inhibitor Protein	Tip41
AN5982	<i>torA</i>	Phosphatidylinositol 3-Kinase	Tor2
AN1414	<i>xprG</i>	p53-like Transcription Factor	Ndt80 Binding Domain
AN10756	undefined (<i>tscA</i>)	TOR Kinase Inhibition	TSC11
AN6590	undefined (<i>tscB</i>)	Tor Kinase Inhibition	none defined

MH 9949 - *gpd(p)areA^{HA}*

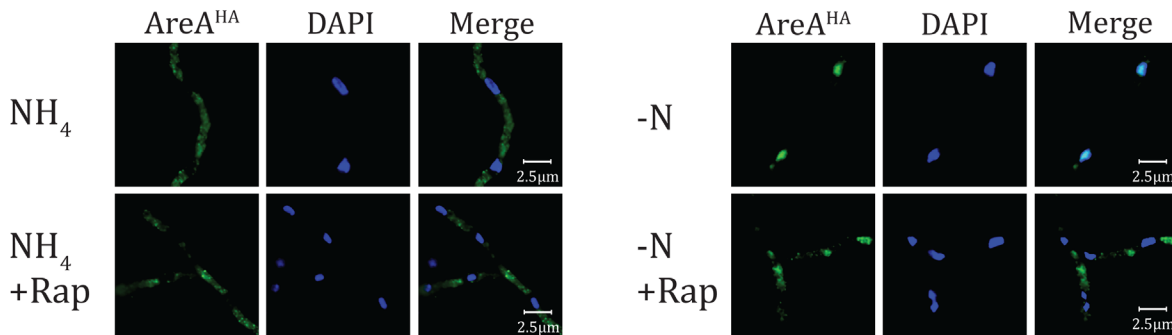


Figure 4.15 Localization of AreA^{HA} in the presence of rapamycin

The subcellular distribution of AreA^{HA} (α -HA) in gene-replaced *gpd(p)areA^{HA}* variants after 14h growth on minimal media supplemented with 10mM ammonium (NH₄) and 4h transfer to supplemented minimal media containing 10mM NH₄ or no nitrogen source (-N) with or without the addition of rapamycin (Rap) was visualized by UV fluorescence microscopy following immunostaining with α -HA (3F10) and Alexa Fluor 488-conjugated goat anti-rat antibodies. A representative image of at least 100 nuclei is shown. Nuclei are stained with DAPI.

4.4.3.b Identifying a functional homologue for Ure2p: the Gln3p cytoplasmic anchor

4.4.3.b.i *gstA* does not inhibit AreA nuclear accumulation

In *S. cerevisiae*, the unique glutathione-S-transferase (GST) Ure2p acts as a negative regulator of Gln3p, inhibiting transcription activity in the presence of a primary nitrogen source (BLINDER *et al.* 1996). Ure2p is phosphorylated during nutrient sufficiency by the TOR signaling pathway which leads to Gln3p cytoplasmic sequestration (BECK AND HALL 1999; CARDENAS *et al.* 1999). Fraser and colleagues (2002) subsequently characterized a putative Ure2p homologue in *A. nidulans*, *gstA*, which contributes to heavy metal and xenobiotic resistance but did not appear to be involved in nitrogen metabolite repression. They performed both plate growth tests and gene expression assays on *gstAΔ* strains and concluded that *gstA* does not play a role in nitrogen metabolite repression. To determine whether *gstA* plays a role in regulating AreA nuclear accumulation by cytoplasmic sequestration during nitrogen sufficient conditions, as Ure2p does to Gln3p (BECK AND HALL 1999), we used immunofluorescence microscopy to observe the subcellular localization of AreA^{HA} in a *gstAΔ* strain (MH11374) and a *gstA* over-expression strain (MH12263) using the inducible *xyLP*(p) promoter. (Figure 4.16) There was no difference between AreA^{HA} subcellular localization from wild type for either *gstAΔ* or *gstA* over-expression during nitrogen sufficient or nitrogen starvation conditions (Figure 4.16). This indicates that *gstA* does not play a role in the cytoplasmic sequestration of AreA as URE2p does for Gln3p.

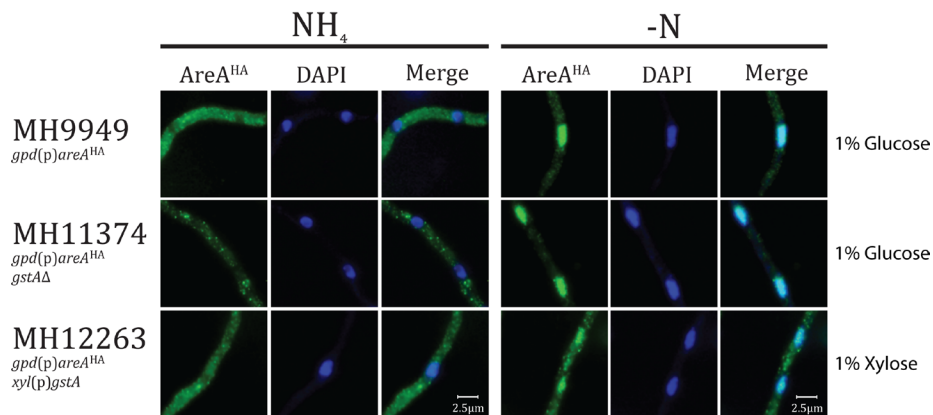


Figure 4.16 Localization of AreA^{HA} in a *gstAΔ* and a *gstA* overexpression strain

The subcellular distribution of AreA^{HA} after 14h growth on supplemented 10mM NH₄-minimal media and 4h transfer to supplemented minimal media containing 10mM NH₄ or no nitrogen source (-N). Visualized by UV fluorescence microscopy following immunostaining with α-HA (3F10) and Alexa Fluor 488-conjugated goat anti-rat antibodies. A representative image of at least 100 nuclei is shown. Nuclei are stained with DAPI.

4.4.3.b.ii AN3255Δ URE2

To determine if there was a Ure2p ortholog in *A. nidulans* a BLASTp search was conducted using the AspGD Multi-Genome search tool analyzing only the *A. nidulans* genome with the URE2p protein sequence as the query to identify similar protein sequences in *A. nidulans*. The uncharacterized protein AN3255 was the most similar protein identified (36% identity, 50.6% similarity over 243 amino acids, $2e^{-34}$), with Gsta being the second hit (31.1% identity, 49.2% similarity over 238 amino acids, $5e^{-28}$). Sequence alignment of the three proteins confirmed the greater identity between URE2 and AN3255 (Figure 4.17).

```

AN4905 - gsta 1 -----MCGVTPAARLLK.....GCFSQSS.....NSNRIPLKHSQ
URE2      1 MMNNGNOVENLSNLRQVNIIGNRNSNTTDDQSNINSESTGVNNSNNNSSSNNNVQNNNSGRNGSQNDNENNINKTLEQHRQQQA
AN3255    1 -----MCGVTPAARLLK.....GCFSQSS.....NSNRIPLKHSQ

AN4905 - gsta 34 LNSASRPFNRLFSTTSPVMSRPDITLYTAQTENGIKLSHAEELGIPKVEKIDISKNVQKPEWLELNFNCRIPALTDFTTQOKIRL
URE2      91 FSDMSHVEYSRITKFFQEQPLEGYLLESHRSAPNGEKVATVLSLGFHNTITFLDENLGEHRAPPEVSVNPNARVPALIDHGMD..NLSI
AN3255    1 -----MTKPLVWVLTTPPCENPKVITVINELELGVVYNIHS..LKFDDVKRPPETININPNCRVPAIVDENT...DWTI

AN4905 - gsta 124 FESCSHLYTAEQMDKQYKIS..YPRGTREYYETISWLFQNAEVCPLMCOQANHEERYAPERIEYGVNRYVNEVRRVYGVLDKHLANS..
URE2      179 WESGATLLEHVNKYKGTGNPLTSSDDADQSQINAWLFFQTSCHAPMIGQALHRYFHSCKTASAVERYTDEVRRVYGVVEMALAEERRE
AN3255    67 WESGATLQYLEDVYDTK...LTYTSLKEKHLINQWLFQMSQCFYFGQAGWENVLAEKLPSEERYENEVHRLVGNVTALE...

AN4905 - gsta 210 .....KSGYLVGDHITITADISHWGVAAGWAEVD.....IDFPHLKAWEERLAAREGVKGRHV
URE2      269 ALVMELDTENAAAYSAGTFPMSQSRFFDYVWLVGDKLTIADLAFVFNWVDRIC.....INIKLEFPEVYKWKHMRRPVAIKALRG
AN3255    150 .....GRNVLVGDKCFADLAFVFNWVDRIC.....INIKLEFPEVYKWKHMRRPVAIKALRG

AN4905 - gsta 266 PSPH.....TIKDLLKDKKAEIEAAQGRAWVQEGMKNDAAK*
URE2      354 E*-----
AN3255    212 RDRLMDEQGLMPNGMPKGVSNMKEYEELMSR.QAKERECK*-----

```

Figure 4.17 Clustal-Ω sequence alignment of Gsta and AN3255 to *S. cerevisiae* URE2p
 Black shading = identity; Grey shading = Similar functional side group.

Using the AN3255 knockout construct obtained from the Fungal Genetics Stock Center (FGSC) (DE SOUZA *et al.* 2013). The AN3255 gene was replaced with the *AfpyrG⁺* gene by transformation of the construct into *A. nidulans* recipient strain RT52, which lacks a functional native *pyrG* gene. Using immunofluorescence microscopy, we found no difference in AreA^{HA} nuclear accumulation in the AN3255Δ strain compared with wild type when grown in nitrogen sufficient or nitrogen starvation conditions (Figure 4.18). This is not completely unexpected, since nuclear export of AreA is not blocked during nitrogen sufficiency in *A. nidulans*. It is likely that if AN3255 does function as a cytoplasmic anchor for AreA, we would not be able to detect an increase in nuclear import if the rate of export is capable of matching the increase in import. One observation of note in the AN3255Δ strain, when grown in nitrogen sufficiency, there was a high proclivity for a phenomenon of fluorescence gradient

where there was strong fluorescence of AreA^{HA} in the cytoplasm towards the hyphal tip, which faded to near loss of fluorescence farther away from the tip (Figure 4.18).

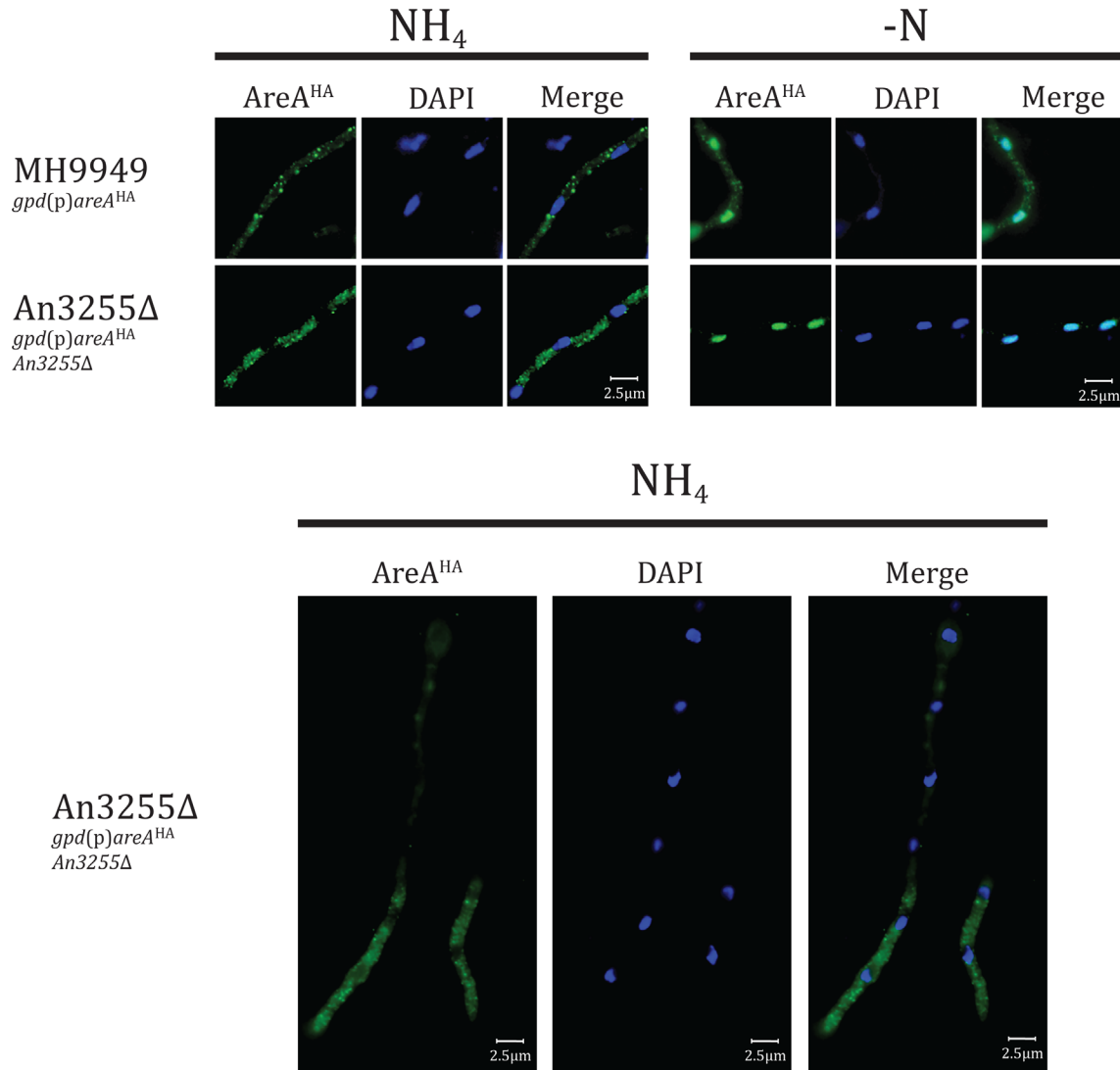


Figure 4.18 Subcellular distribution of AreA^{HA} in an AN3255Δ strain

The subcellular distribution of AreA^{HA} (α -HA) in gene-replaced *gpd(p)areA^{HA}* variants after 14h growth on minimal media supplemented with 10mM ammonium (NH₄) and 4h transfer to supplemented minimal media containing 10mM NH₄ or no nitrogen source (-N). Visualized by UV fluorescence microscopy following immunostaining with α -HA (3F10) and Alexa Fluor 488-conjugated goat anti-rat antibodies. A representative image of at least 100 nuclei is shown. Nuclei are stained with DAPI.

4.4.3.c Analysis of TOR pathway deletions on AreA^{HA} nuclear localization

The Target of Rapamycin (TOR) signaling pathway is highly conserved throughout eukaryotes and has been shown to regulate cell cycle progression, metabolism, cellular growth, ribosome biogenesis, and autophagy (KAMADA *et al.* 2000; SARBASSOV *et al.* 2005). We have shown the TOR pathway inhibitor, Rapamycin, is capable of preventing nuclear accumulation of AreA^{HA} if it is supplemented during nitrogen starvation. Four genes were independently deleted that are part of the TOR pathway: two downstream intermediates, a protein phosphatase, SitA, and a putative phosphatase inhibitor, JipA, as well as two upstream genes AN10756 and AN6590 that function to as TOR kinase inhibitors (orthologs of Tsc1 and Tsc2, which we named *tscA* and *tscB*, respectively). Deletion of the two downstream intermediate genes *sitA* and *jipA* confers a reduction in AreA^{HA} nuclear accumulation during nitrogen starvation in comparison to wild type (Figure 4.19). In addition, the *jipA*Δ mutant shows an apparent reduction in overall levels of AreA^{HA} in the hyphae. We also observed a similar hyphal tip gradient bias like in AN3255Δ, in the *sitA*Δ strain, as well as a bias towards the hyphal wall in the *jipA*Δ strain. Preliminary analysis of the two putative upstream TOR kinase inhibitor deletion strains (AN10756Δ and AN6590Δ) showed no significant change in AreA^{HA} nuclear accumulation from the wild type strain when deleted (Figure 4.19). Unfortunately, the AN10756Δ and AN6590Δ strains used in the experiment in Figure 4.19 were lost. New AN10756Δ and AN6590Δ mutants were constructed, but to date the microscopy has not been repeated with these new strains.

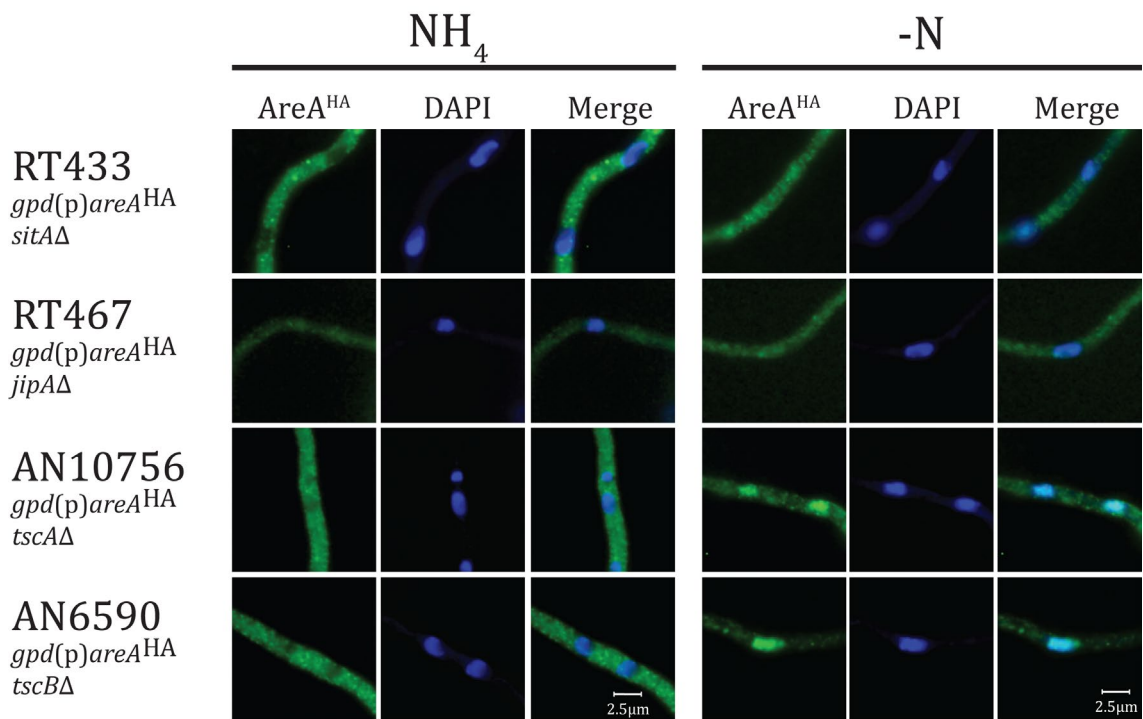


Figure 4.19 Localization of AreA^{HA} in TOR pathway deletion mutants

The subcellular distribution of AreA^{HA} (α-HA) in gene-replaced *gpd(p)areA^{HA}* variants after 14h growth on minimal media supplemented with 10mM ammonium (NH₄) and 4h transfer to supplemented minimal media containing 10mM NH₄ or no nitrogen source (-N). Visualized by UV fluorescence microscopy following immunostaining with α-HA (3F10) and Alexa Fluor 488-conjugated goat anti-rat antibodies. A representative image of at least 100 nuclei is shown. Nuclei are stained with DAPI.

4.4.3.d XprG links Autolysis and regulation to AreA

Contribution statement: The experiments described in this section have been published as part of: Katz, M.E., Buckland, R., Hunter, C.C., and Todd, R.B. (2015) Distinct roles for the p53-like transcription factor XprG and autophagy genes in the response to starvation. *Fungal Genetics and Biology*. **83**: 10-18. doi: <http://dx.doi.org/10.1016/j.fgb.2015.08.006> [KAES contribution: 15-091-J]. MK624, MK627, and MK647 were provided by Prof. M.E. Katz. The experiments presented in Figure 4.20 were performed by C.C. Hunter.

The transcription factor, AreA, activates transcription of genes that are subject to nitrogen metabolite repression that are activated in response to nitrogen limitation and nitrogen starvation (ARST JR AND COVE 1973; HYNES 1975b; TODD *et al.* 2005). During nitrogen starvation AreA accumulates in the nucleus and this accumulation parallels the activation of nitrogen-starvation responsive genes (TODD *et al.* 2005). During nitrogen starvation two cannibalistic nutrient acquisition pathways operate in *A. nidulans*, autophagy and autolysis. The transcription factor XprG mediates aspects of the starvation response by activating extracellular protease genes, N-acetylglucosamine metabolism genes and regulating autolysis (KATZ *et al.* 2006; KATZ *et al.* 2015; KATZ *et al.* 2016; KATZ 2018). We examined whether nuclear accumulation of AreA^{HA} occurred more rapidly in the absence of an intact autophagy pathway by deleting a key autophagy gene, *atgH*, the ATG8 ortholog. To understand the effects of autolysis on AreA^{HA} nuclear accumulation we used the loss of function *xprG2* mutant. The results showed that in both the *atgH*Δ mutant and a wild-type strain, low levels of AreA^{HA} were detected in the nucleus 1h after transfer to nitrogen-free medium and much higher levels after 4h (Figure 4.20A). Therefore, AreA nuclear accumulation is not affected by the loss of autophagy. In contrast, AreA^{HA} did not accumulate in the nucleus after 4h nitrogen starvation in the *xprG2* loss-of-function mutant or *xprG*Δ mutant (Figure 4.20B), suggesting that an intact autolysis pathway via a functional *xprG* transcription factor is required for AreA nuclear accumulation in response to nitrogen starvation.

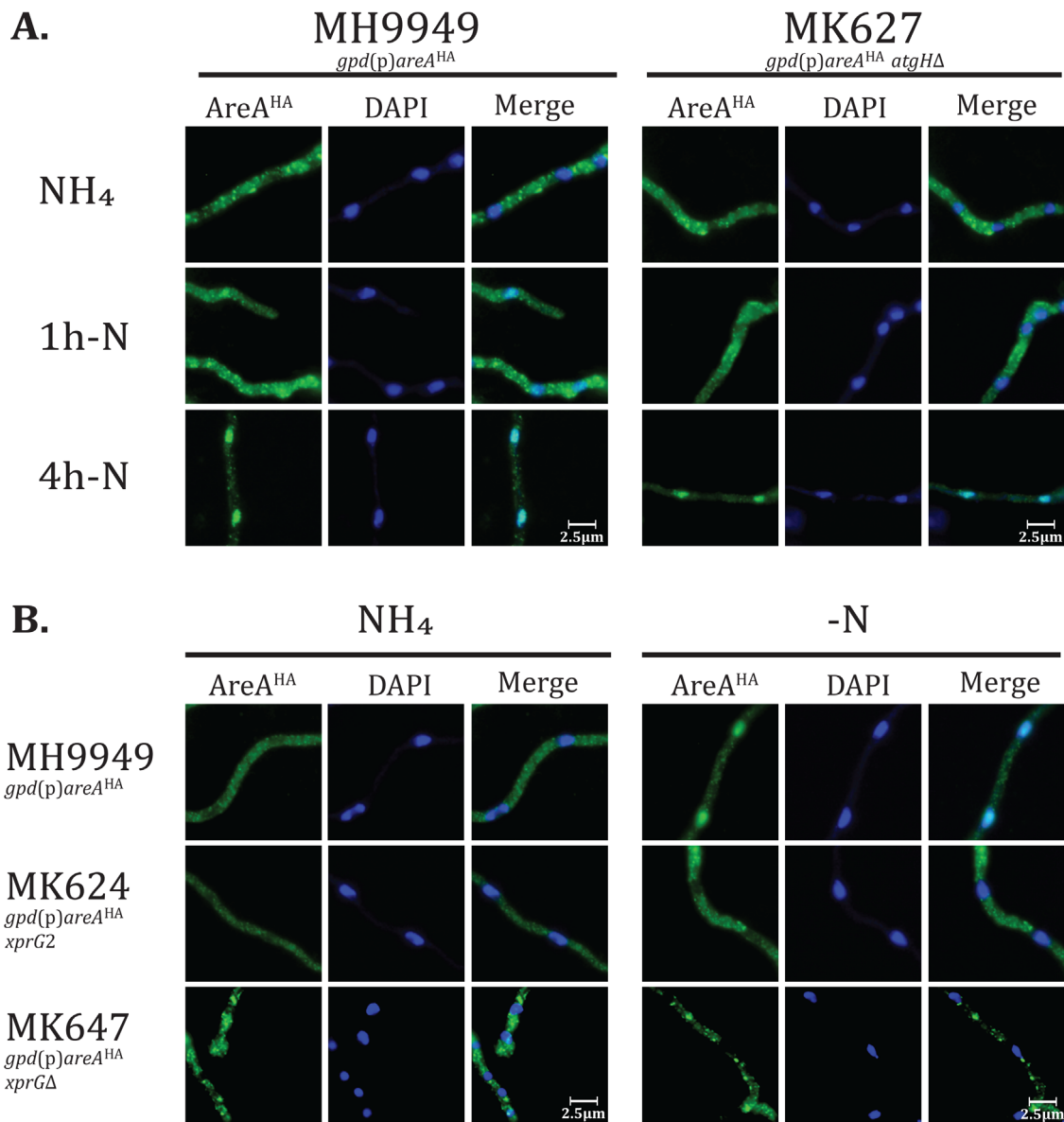


Figure 4.20 Effects of the *atgHΔ*, *xprG2*, and *xprGΔ* mutations on AreA^{HA} nuclear accumulation

The subcellular distribution of AreA^{HA} (α -HA) in (A) *atgHΔ gpd(p)areA^{HA}* and (B) *xprG2 gpd(p)areA^{HA}* and *xprGΔ gpd(p)areA^{HA}* strains compared with wild type *gpd(p)areA^{HA}* (WT) is shown. For both (A.) and (B.), hyphae were grown for 14h on supplemented minimal media containing 10mM ammonium (NH₄) then transferred for 4h to supplemented minimal media containing 10mM NH₄ or no nitrogen source for either 1h or 4h (1h -N and 4h -N). AreA^{HA} was visualized by UV fluorescence microscopy following immunostaining with α -HA (3F10) and goat α -rat alexa-488 antibodies. A representative image of at least 100 nuclei is shown. Nuclei are stained with DAPI.

4.5 Discussion

The role of KapA and SUMO in AreA nuclear accumulation

AreA nuclear import is governed by six NLSs (HUNTER *et al.* 2014). Nuclear import of protein cargo in *A. nidulans* occurs via the α -importin KapA (ARAUJO-BAZAN *et al.* 2008; ARAUJO-BAZAN *et al.* 2009). In *A. nidulans*, KapA is distributed throughout the cytoplasm during nitrogen sufficient conditions. During nitrogen starvation KapA remains in the cytoplasm but also is found accumulated in the nucleus, and in the perinuclear space. There is a close overlap of both KapA and AreA in the nucleus which suggests that interactions between these two proteins leads to nuclear accumulation. We further analyzed the role of KapA in AreA^{HA} nuclear import by perturbing the function of KapA by construction of a temperature-sensitive loss-of-function point mutation *kapA*^{S111F} and by overexpression of KapA through the inducible *xylP* promoter. Both the loss of KapA activity and the overexpression of KapA led to the loss of AreA nuclear accumulation. Additionally, KapA^{S111F} reduces the nuclear accumulation of GFP::NLS4, suggesting that KapA α -importin is a key mediator of AreA nuclear import. It is important to note that KapA is not likely to be the only means of nuclear import for AreA as GFP fused to the noncanonical bipartite NLS and GFP fused to multiple classical NLSs accumulated in the nucleus in the *kapA*^{S111F} mutant. This could be due to the ncbipNLS binding directly to KapB, an importin associated with the nuclear pore and the multiple classical NLSs interacting with KapB or other karyopherins. The ncbipNLS of AreA is conserved with the noncanonical bipartite NLS of mammalian GATA-4, which interacts with importin β (PHILIPS *et al.* 2007). The overexpression of KapA leading to a loss of AreA nuclear accumulation is an unexpected result, but we saw a reduction in colony size when KapA is overexpressed. This points towards indirect effects that confer the loss of AreA accumulation which are not yet understood.

We assessed the role of SumO in AreA nuclear accumulation and found that *sumO* Δ leads to the loss of AreA nuclear accumulation, but it does not prevent AreA nuclear import because when the nuclear export sequence of AreA was deleted in a *sumO* Δ strain, AreA accumulated in the nucleus during both nitrogen sufficiency and starvation conditions. When we overexpressed SumO from the *xylP* inducible promoter, AreA nuclear accumulation occurred during nitrogen starvation during both repressing and inducing conditions. When

induced on 1% xylose there was a slight reduction in AreA nuclear accumulation. The slight reduction in AreA^{HA} nuclear accumulation could indicate that sumoylation plays a role in reducing nuclear retention. Alternatively, it is possible that when SumO is overexpressed, the machinery involved in AreA^{HA} nuclear import are loaded with the nuclear import of other proteins, leading to a molecular traffic jam of sorts near the nucleus. This is consistent with the aggregation of AreA^{HA} just outside of the nucleus that can be seen during SumO overexpression (Figure 4.10). SumO does play a role in the subcellular distribution of KapA::GFP. In a *sumOΔ* mutant, KapA::GFP no longer accumulated in the nucleus or the perinuclear space but was distributed throughout the cytoplasm. Overexpression of SumO led to nuclear accumulation of KapA::GFP during both nitrogen sufficiency and nitrogen starvation. Overexpression of KapA in a *sumOΔ* strain conferred the the reestablishment of AreA nuclear accumulation during nitrogen starvation. Together these experiments establish that SumO plays a role in the subcellular distribution of KapA::GFP and AreA^{HA}. When SumO is deleted, KapA is sequestered to the cytoplasm and perinuclear space. When SumO is overexpressed KapA is localized to the nucleus and the perinuclear space. When SumO is present, KapA OE prevents AreA from accumulating in the nucleus. This could be caused by a molecular traffic jam of sorts. Blockage of the nuclear pore by KapA due to occupancy occlusion (keeping AreA from interacting with KapB or some alternative mode of nuclear import directly) could lead to a significant reduction in nuclear AreA. This functionally increases the time it would take for AreA to accumulate on starvation and slows down the efficiency of the fungus, causing all global interactions with the environment to be on a delay. The slow growth phenotype and increased AreA^{HA} accumulation around the nucleus support this hypothesis.

A putative sumoylation site at residues 712-715 (LKTD) in AreA conforms to the sumoylation consensus ψ KXD/E (where ψ is a large hydrophobic residue) and overlaps the nuclear export signal (residues 703-712) and bipartite RRR₃₃RXR NLS (see Chapter 3). The K713R substitution mutation, which would prevent sumoylation via the lysine residue, does not affect AreA nuclear accumulation (TODD Personal communication). Biochemical analyses using SumO^{FLAG} successfully detected sumoylated proteins (WONG *et al.* 2008b). However, experiments assessing whether AreA is sumoylated did not provide any evidence that AreA

is directly sumoylated, suggesting that the effects of *sumOΔ* on AreA nuclear accumulation are indirect (WONG *et al.* 2007). Furthermore, proteomic experiments to determine the *A. nidulans* SUMO-ome also did not find any evidence for sumoylation of AreA (HORIO *et al.* 2019). However, the SUMO-ome was examined only in extracts made from mycelia grown on complete media, not during different nitrogen conditions or starvation. The work presented in this chapter showed that overexpression of KapA suppressed the loss of AreA nuclear accumulation observed in the *sumOΔ* mutant and suggests that the effect of SumO on AreA nuclear accumulation is at the level of AreA nuclear import. However, the effects of *sumO* on AreA localization are unlikely due to direct effects of SumO on KapA-dependent AreA nuclear import. The *A. nidulans* SUMO-ome study did reveal that multiple proteins in the nuclear transport network are sumoylated (HORIO *et al.* 2019). These included AN6591 (KapE) the ortholog of *S. cerevisiae* Cse1p, a nuclear envelope protein that mediates nuclear export for recycling of alpha-importin Srp1p (HOOD AND SILVER 1998), two Ran Binding Proteins (AN0084 and AN5482), and possibly AN2164 (karyopherin KapG). AN0906 (KapB beta-importin) was identified as a possible SumO binding protein. Although, the effects of sumoylation or SumO interaction for these proteins is unknown, it is possible that SumO plays multiple roles in the nuclear transport network that may indirectly affect AreA nuclear localization.

In *S. cerevisiae*, SUMO indirectly affects nuclear import of the AreA homolog Gln3p. Gln3p is imported into the nucleus by the α -importin Srp1p (CARVALHO *et al.* 2001). Srp1p binds the SUMO peptide Smt3p (ITO *et al.* 2010). SMT3 inactivation leads to Srp1p nuclear accumulation (STADE *et al.* 2002). Thus, Smt3p (SUMO) is required for Srp1p nuclear export and recycling. Cse1p is the exportin responsible for export of Srp1p into the cytoplasm and is likely sumoylated (HOOD AND SILVER 1998; HORIO *et al.* 2019). The loss of sumoylation likely inhibits its function leading to Srp1p accumulation. Therefore, SMT3 inactivation indirectly leads to impaired Srp1p-dependent nuclear import, as only de novo synthesized Srp1p is available to transport cargo to the nucleus. The molecular pathways seem to be largely conserved between *A. nidulans* and *S. cerevisiae*, though there has clearly been a rewiring of the mechanisms for nuclear import and export between them.

The role of the TOR pathway in AreA nuclear accumulation

We have used an epitope tagged version of AreA to investigate the effects of rapamycin and the TOR pathway on AreA subcellular localization. In *S. cerevisiae* the TOR inhibitor, rapamycin, triggers the nuclear import and accumulation of Gln3p and Gat1p. We found that in *A. nidulans* rapamycin prevented AreA nuclear accumulation in response to nitrogen starvation, similar to what was seen in a *sum0Δ* strain. Addition of rapamycin to nitrogen-starved cells did not trigger rapid AreA nuclear export as is expected for nitrogen nutrients or carbon starvation, this suggests that the TOR pathway can control AreA nuclear import. In response to this result, we investigated the effects of the other components in the TOR pathway SitA, JipA, and GstA on AreA nuclear localization. Deletion of *jipA* (TapA inhibitor) and of *sitA* (type 2A-related phosphatase) significantly reduce AreA^{HA} accumulation during nitrogen starvation, just like rapamycin. This suggests they function in a similar manner to their orthologues in yeast. Deletion of the cytoplasmic anchor Ure2p confers Gln3p nuclear localization (BECK AND HALL 1999). In contrast, deletion of the Ure2p ortholog AN3255 or homolog GstA had no effect on AreA nuclear accumulation during nitrogen starvation or growth on ammonium. However, a gradient of AreA distribution biased towards the hyphal tip was observed in the AN3255Δ mutant in ammonium-grown hyphae suggesting a genetic interaction between AreA and AN3255 in the cytoplasm. Hyphal tip to nucleus communication was observed for the upstream developmental pathway transcription factor FlbB, which controls conidiation in response to developmental signals (ETXEESTE *et al.* 2009; PEREZ-DE-NANCLARES-ARREGI AND ETXEESTE 2014; OIARTZABAL-ARANO *et al.* 2016). Collectively our data suggests rewiring of the TOR pathway for controlling AreA nuclear import in *A. nidulans* (Figure 4.21).

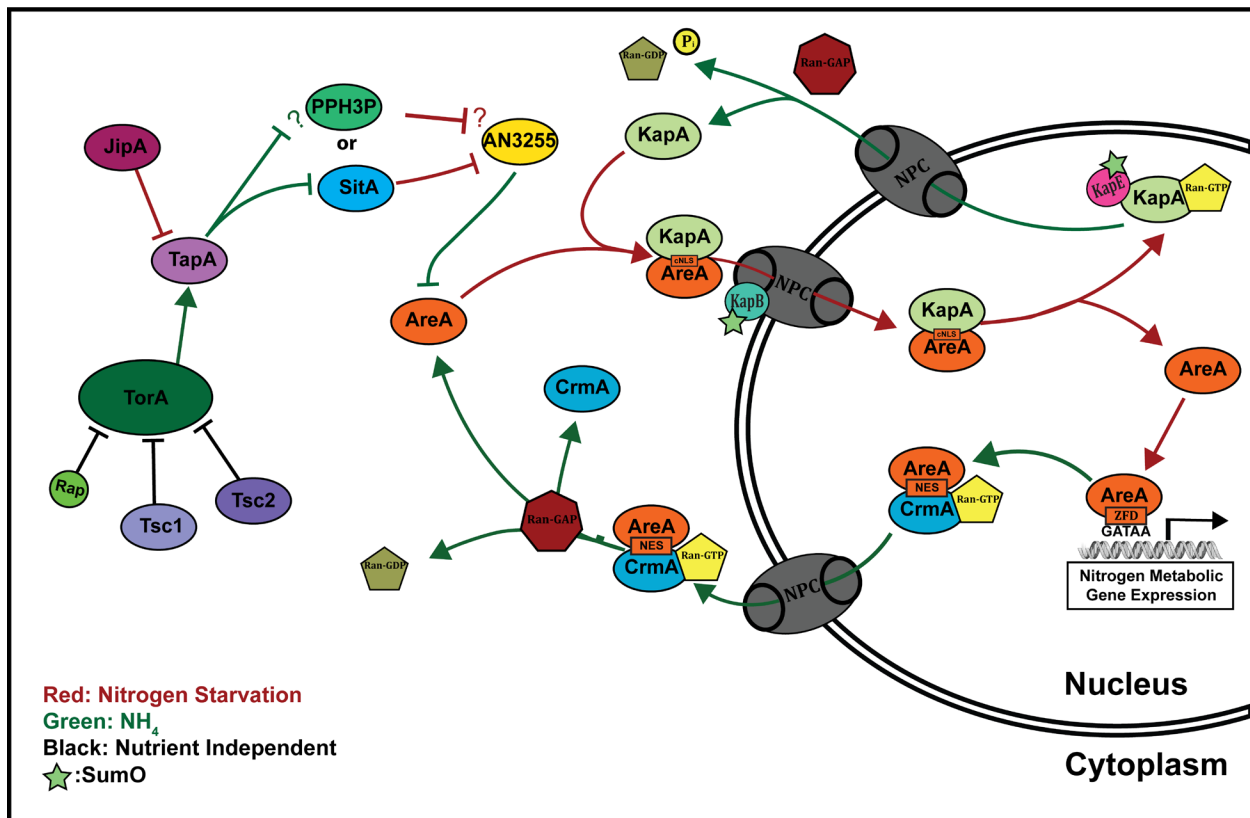


Figure 4.21 Working model of TOR pathway control of AreA nuclear import

Model of the various components of the TOR signaling pathway and rapamycin (Rap) and their effects on the subcellular localization of AreA and KapA. Green arrows indicate repressing conditions (NH_4) leading to possible cytoplasmic sequestration of AreA by AN3255. Red arrows indicate derepressing conditions (nitrogen starvation) leading to nuclear localization of AreA and subsequent increase in nitrogen metabolic gene expression.

In *A. nidulans*, two cannibalistic nutrient starvation pathways exist: autophagy, which recycles nutrients internally, and autolysis, which recovers extracellular nutrients. We assessed whether AreA nuclear accumulation was affected by either of these pathways using mutants that block each pathway. While AreA nuclear accumulation was unaltered when autophagy was blocked in the *atgHΔ* mutant, AreA did not accumulate in the nucleus in loss of function mutants affecting the carbon starvation and autolysis transcription factor XprG. Therefore, function of the autolysis transcription factor XprG appears to be essential for AreA nuclear accumulation pointing to a link between autolysis and regulation of AreA. The molecular mechanism(s) of XprG regulation of AreA nuclear accumulation are unknown.

The world is indeed full of peril and in it there are many dark places. But still there is much that is fair. And though in all lands, love is now mingled with grief, it still grows, perhaps, the greater."

Chapter 5 - Nitrogen sensing and AreA nuclear accumulation in *Aspergillus nidulans*

5.1 Abstract

To determine whether AreA DNA binding affects the subcellular localization of AreA we HA-epitope-tagged two classical DNA binding mutant proteins; the AreA102 altered DNA binding specificity mutant protein, and the AreA217 non-DNA binding mutant protein. The AreA102^{HA} mutant protein showed a similar subcellular localization pattern to wild-type AreA^{HA} except when transferred to uric acid, a nitrogen source the *areA102* mutant cannot utilize due to loss of AreA-dependent expression of uric acid utilization genes. On uric acid AreA102^{HA} accumulated in the nucleus as observed during nitrogen starvation. The AreA217^{HA} non-DNA binding mutant protein accumulated in the nuclei of nitrogen-starved cells, demonstrating that DNA binding is not required for AreA nuclear accumulation. In contrast to wild type, AreA217^{HA} accumulated in the nucleus when nitrogen sources were available. We assessed the effects on nuclear accumulation for two other AreA putative non-DNA binding mutant proteins, AreA^{HA}ZF Δ 631-702, which lacks the entire zinc finger, and AreA^{HA}bip^{ALA}, which carries disruptive amino acid substitutions in DNA contact residues. AreA^{HA}ZF Δ 631-702 accumulated in the nucleus under all conditions tested, whereas AreA^{HA}bip^{ALA} accumulated in the nucleus in nitrogen-starved cells and on most alternative nitrogen sources. These findings demonstrate that nuclear accumulation of AreA is independent of DNA binding and is consistent with AreA DNA binding to metabolic gene promoters being required for signaling nitrogen availability to prevent its nuclear accumulation. We also consider the alternative explanation that an intrinsic property of the AreA^{HA} mutant proteins may affect their subcellular localization, and we begin to assess this by complementation of the signaling phenotypes with an ectopic wild type *areA* gene. We also show that nitrogen metabolism mutants blocking metabolic signaling of nitrogen availability confer AreA nuclear accumulation. We propose that AreA nuclear accumulation, a measure for the transition between nitrogen sufficiency and nitrogen starvation, is signaled by the levels of intracellular glutamine.

5.2 Introduction

Fungal models have been used by researchers as an efficient way to study the various networks and mechanisms involved in environmental sensing of cues such as: nutrients, pheromones, light, gas, and various stresses (BAHN *et al.* 2007; CONRAD *et al.* 2014; BRAUNSDORF *et al.* 2016; RAMOS *et al.* 2016). Nutrient sensing in fungi has been broadly researched in both *Saccharomyces cerevisiae* and *Aspergillus nidulans*. Studying nutrient pathways more specifically will lead to greater clarity in our understanding of the mechanisms involved in cell proliferation and growth. This would be beneficial in medical, industrial, and agricultural fields. Elucidation of the underlying mechanisms for sensing and metabolizing nutrients allows targeting of specific pathways which have been altered in cancer cells or are specific to plant pathogens. This chapter provides a broad summary of what is known about nitrogen sensing in fungi and adds clarity to the understanding of the role Nitrogen Metabolite Repression (NMR) plays in the overall picture of nitrogen sensing in fungi.

To understand how nitrogen sensing occurs in fungi we must first review nutrient acquisition, how nutrients are transported from the environment to the intracellular lumen. In fungi, this is primarily achieved by a class of proteins called fungal amino acid transporters (fAATs). Both broad-specificity and single amino acid specific fAATs have been classified and shown to localize to various cellular membranes (JAUNIAUX AND GRENSON 1990; TAVOULARIS *et al.* 2003; GOURNAS *et al.* 2016). PrnB, the proline specific transporter in *A. nidulans*, is used as a model for understanding how amino acid permeases bind with specificity to their substrate (GOURNAS *et al.* 2015). Other fAAT-like transmembrane proteins like the SPS complex in *S. cerevisiae*, which consists of Ssy1p, Ptr3p and Ssy5p, function together as extracellular amino acid sensors. This complex has lost its ability to transport amino acids, but instead senses the presence of extracellular amino acids and signals upregulation of specific amino acid permease genes and amino acid metabolic genes (FORSBERG *et al.* 2001). During nitrogen starvation, expression of these specific amino acid permeases decreases and expression of the general amino acid permease Gap1 increases (DIDION *et al.* 1998; FORSBERG *et al.* 2001; WU *et al.* 2006; LJUNGDAHL AND DAIGNAN-FORNIER 2012). Additionally, in *S. cerevisiae*, Gap1 and the ammonium permease, Mep2, can act as transceptors, membrane transporters capable of

switching conformation to activate other signaling proteins such as protein kinase A (PKA) (DONATON *et al.* 2003; VAN NULAND *et al.* 2006; VAN DEN BERG *et al.* 2016).

In *A. nidulans*, four ammonium permeases have been characterized MeaA, MepA, MepB, and MepC. MeaA functions as the primary ammonium transporter and is necessary for optimal growth of *A. nidulans* when ammonium is the sole nitrogen source (MONAHAN *et al.* 2002b). *mepA* and *mepB* are similar in terms of role in ammonium transport except *mepA* is expressed during both nitrogen limiting and nitrogen starvation growth conditions and *mepB* is expressed solely during nitrogen starvation, but both seem to act as ammonium scavengers (MONAHAN *et al.* 2002a; MONAHAN *et al.* 2006). *mepC* is expressed at a low level during all ammonium conditions but does not appear to significantly contribute to ammonium uptake (MONAHAN *et al.* 2006). There has been no evidence that these ammonium transporters play a role in signaling nitrogen availability (MONAHAN *et al.* 2002a; MONAHAN *et al.* 2006). As they have been shown to be regulated by AreA under nitrogen sufficient, nitrogen limiting, and starvation conditions, there is likely a different component involved in signaling nitrogen availability to the cell. Studies of mutants affected in the nitrogen assimilation pathway have shown that glutamine synthesis is key for signaling nitrogen metabolite repression (MARGELIS *et al.* 2001). Additional evidence from measuring free intracellular amino acids concentrations also indicates that glutamine levels, which are low during nitrogen starvation and high when nitrogen nutrients are available, is important for nitrogen signaling (BERGER *et al.* 2008; SCHINKO *et al.* 2010).

In this chapter we wanted to understand the interplay between nitrogen sensing and the signaling of the transition between nitrogen sufficiency and nitrogen starvation. We have used growth assays and immunofluorescence microscopy assays of HA-epitope tagged versions of AreA as a metric for the transition from nitrogen sufficiency to nitrogen starvation. This chapter furthers the understanding of what signals that transition and where that signal originates. Our first approach was to determine what concentration of ammonium tartrate is needed for growth and signaling in wild type *A. nidulans*. Next, we observed four different mutants containing different mutations in or around the zinc finger DNA-binding domain of AreA. By assessing the subcellular localization of different AreA DNA-binding mutants we aim to understand if binding to promoters to activate gene expression effects

the nuclear accumulation of AreA. We then analyze nitrogen metabolic mutants to determine if a nitrogen source must be metabolized to signal nitrogen sufficiency.

5.3 Materials and Methods

5.3.1 Strain Construction

Genotype of the strains used in this chapter can be found in Table 5.1.

Table 5.1 *Aspergillus nidulans* strains used in Chapter 5

Strain	Genotype^a
MH1	<i>biA1</i>
MH50	<i>yA1 adE20 su(adE20) areA102 pyroA4 riboB2</i>
MH54	<i>biA1 niiA4</i>
MH5699	<i>yA1 adE20 su(adE20) areAΔ::riboB⁺ pyroA4 riboB2</i>
MH8767	<i>yA1 pabaA1 amdR44 argB::amdS-lacZ areA217 riboB2</i>
MH9883	<i>wA3 gpd(p)areA^{HA} riboB2 facB101</i>
MH9949	<i>biA1 gpd(p)areA^{HA} amdS-lacZ</i>
MH9962	<i>yA1 glnAΔ::riboB⁺ amdS-lacZ areA102 pyroA4</i>
MH10244	<i>yA1 wA1 riboB2</i>
MH10266	<i>wA3 gpd(p)areA^{HA}::riboB(3') riboB2</i>
MH10267	<i>wA3 gpd(p)areA102^{HA} riboB2</i>
MH10504	<i>yA2 pabaA2 acuE201</i>
MH10609	<i>biA1 wA3 gpd(p)areA102^{HA}</i>
MH10653	<i>yA1 pabaA1 amdR44 argB::amdS-lacZ areA217 niiA4 riboB2 [amdR-tamA ectopic]</i>
MH10665	<i>yA1 gpd(p)areA^{HA} pyroA4 prn-309</i>
MH10696	<i>yA1 pabaA1 amdR44 argB::amdS-lacZ areA217::riboB⁺(5') niiA4 riboB2 [amdR-tamA ectopic]</i>
MH10798	<i>yA1 pabaA1 gpd(p)areA217^{HA} amdR44 argB::amdS-lacZ niiA4 riboB2 [amdR-tamA ectopic]</i>
MH10827	<i>yA1 pabaA1 gpd(p)areA217^{HA} pyroA4</i>
MH11052	<i>yA1 pabaA1 gpd(p)areA^{HA} fmdS-lacZ niiA4</i>
MH11186	<i>yA1 pabaA1 gdhAΔ::riboB gpd(p)areA^{HA} fmdS-lacZ pyroA4</i>
RT49	<i>yA1 pabaA1 gpd(p)areA^{HA}-bip pyroA4 nkuAΔ::argB⁺</i>

^a All strains carry the *veA1* mutation.

Table 5.1 A. *nidulans* strains used in Chapter 5 (continued)

Strain	Genotype^a
RT52	<i>pyrG89 gpd(p)areA^{HA} fmdS-lacZ pyroA4 nkuAΔ::Bar</i>
RT268	<i>yA1 pabaA1 gpd(p)areA^{HA-H704A} pyroA4 nkuAΔ::argB⁺</i>
RT269	<i>yA1 pabaA1 gpd(p)areA^{HA-H704A} pyroA4 nkuAΔ::argB⁺</i>
RT270	<i>yA1 pabaA1 gpd(p)areA^{HA-H704A} pyroA4 nkuAΔ::argB⁺</i>
RT271	<i>yA1 pabaA1 gpd(p)areA^{HA-H704A} pyroA4 nkuAΔ::argB⁺</i>
RT289	<i>pyrG89 biA1 wA::gpd(p)gpf::AfpyroA gpd(p)areA^{HA} fmdS-lacZ pyroA4 nkuAΔ::Bar crmA^{T525C}::pyrG⁺</i>
RT290	<i>pyrG89 biA1 wA::gpd(p)gpf::AfpyroA gpd(p)areA^{HA} fmdS-lacZ pyroA4 nkuAΔ::Bar crmA^{T525C}::pyrG⁺</i>
RT291	<i>pyrG89 biA1 wA::gpd(p)gpf::areA^{102zf}::AfpyroA gpd(p)areA^{HA} fmdS-lacZ pyroA4 nkuAΔ::Bar crmA^{T525C}::pyrG⁺</i>
RT292	<i>pyrG89 biA1 wA::gpd(p)gpf::areA^{102zf}::AfpyroA gpd(p)areA^{HA} fmdS-lacZ pyroA4 nkuAΔ::Bar crmA^{T525C}::pyrG⁺</i>
RT293	<i>pyrG89 biA1 wA::gpd(p)gpf::areA^{102zf}::AfpyroA gpd(p)areA^{HA} fmdS-lacZ pyroA4 nkuAΔ::Bar crmA^{T525C}::pyrG⁺</i>
RT331	<i>wA::gpd(p)gpf::areA^{NLS102zf}::AfpyroA areAΔ::riboB⁺ pyroA4</i>
RT332	<i>wA::gpd(p)gpf::AfpyroA areA::riboB⁺ pyroA4</i>
RT373	<i>pyrG89 biA1 wA::gpd(p)gpf::areA^{NLS217zf} AfpyroA gpd(p)areA^{HA} fmdS-lacZ pyroA4 nkuAΔ::Bar crmA^{T525C}::pyrG⁺</i>
RT435	<i>yA1 pabaA1 amdR44 argB::amdS-lacZ areA217 riboB2</i>
RT490	<i>pyrG89 gpd(p)areA^{HA} fmdS-lacZ pyroA4 nkuAΔ::Bar AN1923Δ::AfpyrG</i>
RT491	<i>pyrG89 gpd(p)areA^{HA} fmdS-lacZ pyroA4 nkuAΔ::Bar AN1923Δ::AfpyrG</i>
RT492	<i>pyrG89 gpd(p)areA^{HA} fmdS-lacZ pyroA4 nkuAΔ::Bar AN1923Δ::AfpyrG</i>
RT493	<i>pyrG89 gpd(p)areA^{HA} fmdS-lacZ pyroA4 nkuAΔ::Bar AN1923Δ::AfpyrG</i>
RT509	<i>pyrG89 pyroA4 nkuAΔ::Bar AN6026Δ1::AfpyrG⁺</i>
RT510	<i>pyrG89 AN6026Δ2::AfpyrG⁺ pyroA4 nkuAΔ::Bar</i>
RT511	<i>pyrG89 AN6027Δ2::AfpyrG⁺ pyroA4 nkuAΔ::Bar</i>

^a All strains carry the *veA1* mutation.

Table 5.1 A. *nidulans* strains used in Chapter 5 (continued)

Strain	Genotype^a
RT512	<i>pyrG89 AN6027Δ8::AfpYrG⁺ pyroA4 nkuAΔ::Bar</i>
RT513	<i>pyrG89 AN6028Δ1::AfpYrG⁺ pyroA4 nkuAΔ::Bar</i>
RT514	<i>pyrG89 AN6028Δ3::AfpYrG⁺ pyroA4 nkuAΔ::Bar</i>
RT515	<i>pyrG89 AN6029Δ2::AfpYrG⁺ pyroA4 nkuAΔ::Bar</i>
RT516	<i>pyrG89 AN6029Δ3::AfpYrG⁺ pyroA4 nkuAΔ::Bar</i>
RT517	<i>pyrG89 AN6029Δ4::AfpYrG⁺ pyroA4 nkuAΔ::Bar</i>
RT518	<i>pyrG89 AN11221Δ1::AfpYrG⁺pyroA4 nkuAΔ::Bar</i>
RT519	<i>pyrG89 AN11221Δ6::AfpYrG⁺ pyroA4 nkuAΔ::Bar</i>
RT553	<i>yA1 gpd(p)areA^{HA} fmdS-lacZ prn309</i>
RT554	<i>yA1 pabaA1 gpd(p)areA^{HA} fmdS-lacZ pyroA4 prn-309</i>
RT555	<i>yA1 glnAΔ::riboB⁺ gpd(p)areA^{HA} fmdS-lacZ pyroA4</i>
RT564	<i>pyrG89 AN3846Δ2::AfpYrG⁺ pyroA4 nkuAΔ::Bar</i>
RT565	<i>pyrG89 AN3846Δ3::AfpYrG⁺ pyroA4 nkuAΔ::Bar</i>
RT575	<i>biA1 wA3 gpd(p)areA102 niaD15</i>
RT576	<i>biA1 gpd(p)areA102 niaD15</i>
RT588	<i>pyrG89 pyroA4 nkuAΔ::Bar AN1730Δ2::AfpYrG⁺</i>
RT589	<i>pyrG89 pyroA4 nkuAΔ::Bar AN1810Δ4::AfpYrG⁺</i>
RT590	<i>pyrG89 pyroA4 nkuAΔ::Bar AN0454Δ6::AfpYrG⁺</i>
RT590	<i>pyrG89 pyroA4 nkuAΔ::Bar AN0454Δ6::AfpYrG⁺</i>
RT591	<i>pyrG89 pyroA4 nkuAΔ::Bar AN0454Δ7::AfpYrG⁺</i>
RT592	<i>pyrG89 pyroA4 nkuAΔ::Bar AN1731Δ4::AfpYrG⁺</i>
RT593	<i>pyrG89 AN6048Δ10::AfpYrG⁺ pyroA4 nkuAΔ::Bar</i>
RT594	<i>pyrG89 AN6048Δ11::AfpYrG⁺ pyroA4 nkuAΔ::Bar</i>
RT595	<i>pyrG89 AN6048Δ12::AfpYrG⁺ pyroA4 nkuAΔ::Bar</i>
RT596	<i>pyrG89 pyroA4 nkuAΔ::Bar AN1730Δ2::AfpYrG⁺ AN1810Δ5::AfpYrG⁺</i>
RT597	<i>biA1 wA1 gpd(p)areA^{HA} fmdS-lacZ niaD15</i>
RT598	<i>gpd(p)areA^{HA} fmdS-lacZ niaD15</i>

^a All strains carry the *veA1* mutation.

Table 5.1 *A. nidulans* strains used in Chapter 5 (continued)

Strain	Genotype^a
RT624	<i>pyrG89 pyroA4 nkuAΔ::Bar AN1406Δ::Afp_{pyrG}⁺</i>
RT625	<i>pyrG89 pyroA4 nkuAΔ::Bar AN1406Δ::Afp_{pyrG}⁺</i>
RT626	<i>pyrG89 pyroA4 nkuAΔ::Bar AN1418Δ::Afp_{pyrG}⁺</i>
RT627	<i>pyrG89 pyroA4 nkuAΔ::Bar AN1418Δ::Afp_{pyrG}⁺</i>
RT628	<i>pyrG89 pyroA4 nkuAΔ::Bar AN1420Δ::Afp_{pyrG}⁺</i>
RT629	<i>pyrG89 pyroA4 nkuAΔ::Bar AN1420Δ::Afp_{pyrG}⁺</i>
RT673	<i>yA1 pabaA1 wA::areA⁺ gpd(p)areA217^{HA} pyroA4</i>

^a All strains carry the *veA1* mutation.

5.3.2 Molecular techniques

Standard molecular techniques were as described in SAMBROOK AND RUSSELL (2001) or, for kits or enzymes, according to instructions from the manufacturer. PCR to generate gene replacement constructs used proof-reading enzymes: Pfu (Agilent), PfuTurbo (Stratagene), Phusion (Thermo Scientific) or Ex Taq (TaKaRa). Southern analysis to confirm gene replacements was performed using the DIG-High Prime DNA Labeling and Detection Starter Kit II (Roche).

5.3.3 Construction of *gpd(p)areA102^{HA}*

This fusion gene was constructed by Dr. James Fraser

JFareA1-JFareA2 PCR product (+1591 to +2881) containing the *areA102* mutation was generated using MH50 (*areA102*) genomic DNA template and cloned into pGEM-Teasy to generate pJAF5458. *gpd(p)areA102^{HA}* was constructed by two successive gene replacements. First, a strain MH10266 (*wA3 gpd(p)areA^{HA}::riboB(3') riboB2 facB101*) in which 3' *areA* sequences of the *gpd(p)areA^{HA}* fusion gene were replaced with *riboB* was made by gene replacement of the 3' *areA* sequences in MH9883 (*wA3 gpd(p)areA^{HA} riboB2 facB101*) (TODD *et al.* 2005) with a JFareA1-JFareA2 PCR-amplified *areA::riboB(3')* gene replacement cassette. The *areA::riboB(3')* construct was made from pJAF5458 by digestion with *SphI* (Klenow-blunted) and *StuI*, and the 0.6kb *SphI-StuI* mutation-containing fragment (+1951 to +2520) was replaced by the 2.6 kb *XbaI* (partial, end-filled)-*SmaI riboB* selectable marker fragment of pPL3 (OAKLEY *et al.* 1987). Second, the JFareA1-JFareA2 *areA102* mutant PCR product, amplified from pJAF5458, was transformed into MH10266 and transformants were directly selected on 10 mM nitrate. Integration by homologous gene replacement was accompanied by loss of riboflavin prototrophy and confirmed by Southern blot. One transformant MH10267 was outcrossed to MH1 (*biA1*) to generate MH10609 (*biA1 wA3 gpd(p)areA102^{HA}*).

5.3.4 Construction of *gpd(p)areA217^{HA}*

This fusion gene was constructed by Dr. Richard Todd

The *gpd(p)areA217^{HA}* mutant was generated in three steps. First, an *areA217* strain containing *amdR-tamA* was generated by transformation of pAS5140 (*amdR-tamA*) (SMALL *et al.* 1999) into MH8767 (*yA1 pabaA1 amdR44 argB::amdS-lacZ areA217 riboB2*) and direct selection on 10mM acetamide as a sole nitrogen source. A single copy *amdR-tamA* transformant (MH10653: *yA1 pabaA1 amdR44 argB::amdS-lacZ areA217 riboB2 [amdR-tamA]*), which grew more strongly than the MH8767 parent on acetamide or GABA as a sole nitrogen source, was identified by Southern blot (data not shown). Second, the 5' portion of *areA217* (-18 to +811) was gene replaced, leaving intact the *areA217* mutation, in MH10653 with the *riboB* gene using the *ApaI*-linearised *areA*(5') deletion construct pJAF5224 (TODD *et al.* 2005). *RiboB* prototrophs were selected. Southern blot analysis confirmed the correct gene replacement in the transformant MH10696 (*yA1 pabaA1 amdR44 argB::amdS-lacZ areA217::riboB(5') niiA4 riboB2 [amdR-tamA]*). Third, *ApaI*-linearized pJAF5200 (TODD *et al.* 2005) containing 5' flanking *areA* sequences -895 to -575 and *gpd(p)areA^{HA}* truncated within *areA* at +1475 was introduced by transformation into MH10696 and transformants were selected for *AreA217* activity on 10mM GABA as a sole nitrogen source. One transformant (MH10798), which grew stronger than the parent on acetamide or GABA as a sole nitrogen source and was a riboflavin auxotroph was further analyzed. Southern analysis revealed gene replacement of the *riboB* cassette with *gpdA* promoter and 5' coding *areA^{HA}* sequences, generating a full-length *gpd(p)areA217^{HA}*. The ectopic *amdR-tamA* fusion gene was removed by outcrossing. The resultant strain (MH10827) was used for analysis of *gpd(p)areA217^{HA}*.

5.3.5 Immunostaining, and Immunofluorescence Microscopy

Immunostaining was conducted as described previously (HUNTER *et al.* 2014). Indirect UV immunofluorescence microscopy was performed using an Olympus BX51 upright biological reflected fluorescence microscope equipped with Nomarski Differential Interference Contrast (DIC), an EXFO X-Cite 120 Q fluorescence illumination system and a UPlanFLN Plan Semi Apochromat (Field Number FN26.5) Fluorite 100x oil objective with a numerical aperture of 1.30. Alexa-488 immunofluorescence was detected using a BrightLine

Fluorescein Isothiocyanate (FITC) filter set (excitation wavelength band pass, 482/35 nm; dichroic mirror, 506 nm; emission 536/40 nm ZPIXEL). 4', 6-diamidino-2-phenylindole) DAPI fluorescence was detected using a BrightLine DAPI Hi Contrast filter set (excitation wavelength band pass, 387/11 nm; dichroic mirror, 409 nm; ZPIXEL). At least 30 nuclei from each of two independent experiments were analyzed for each growth condition. Photomicrographs were captured using an Olympus DP72 12.8 Megapixel digital color camera and DP2-BSW digital camera software. Images were manipulated similarly within and between experiments using Adobe Photoshop CC 2015. Images were cropped, and the tonal range was increased by adjusting highlights and shadows without altering the color balance.

5.4 Results

5.4.1 The effects of ammonium concentration on AreA nuclear accumulation

We use 10mM ammonium tartrate ((NH₄)₂T) as our standard preferred nitrogen source because it leads to strong growth and promotes repression of nitrogen metabolic genes (HYNES 1974; DAVIS AND HYNES 1987; DAVIS *et al.* 1988; ANDRIANOPOULOS *et al.* 1998). We tested the colonial growth of *A. nidulans* on a range of ammonium concentrations starting at 10mM and decreasing in 10-fold increments down to 0.01mM ammonium and starvation (0mM) (Figure 5.1). The colonial growth at 10mM NH₄ was strong and substantial sporulation was visible as green coloration. At a concentration of 1mM, the hyphal extension of the colony was similar to 10mM but there was a clearly decreased green area where spores were produced. At 0.1mM, spore production was nearly eliminated but hyphal extension was still similar to that observed at higher concentrations though not quite as dense. At both 0.01mM and 0mM we observed complete elimination of spore production evident as lack of green coloration and, although hyphal extension, measured as colony diameter, was similar to the 10mM concentration, the reduction in the density of hyphae being produced is clear (Figure 5.1).

Next, the subcellular localization of AreA^{HA} was assessed on the same range of ammonium concentrations (Figure 5.1). AreA^{HA} did not accumulate in the nucleus after 4h transfer to 10mM, 1mM, or 0.1mM NH₄. At each of these concentrations AreA^{HA} was excluded from the nucleus and sequestered in the cytoplasm. As the NH₄ concentration reduced from 10mM to 1mM and from 1mM to 0.1mM we observed slight increases in the concentration of AreA^{HA} within the cytoplasm. At a concentration of 0.01mM NH₄ AreA^{HA} accumulated in the nucleus and was also observed in the cytoplasm. It was only after 4 hours of nitrogen starvation that wild-type AreA^{HA} protein was completely accumulated within the nucleus (Figure 5.1). This suggests that at 0.01mM NH₄ there is a transition state due to nitrogen availability in which AreA^{HA} is both nuclear and cytoplasmic, similar to that observed during the gradual nuclear accumulation of AreA^{HA} over 4 hours during nitrogen starvation (TODD *et al.* 2005).

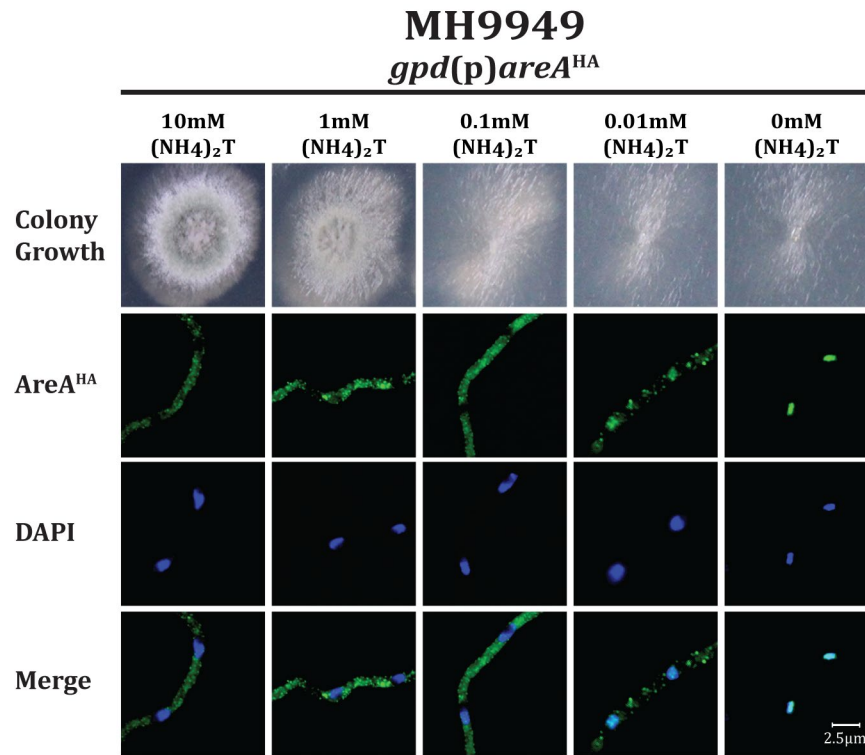


Figure 5.1 Wild type *A. nidulans* colony growth and AreA^{HA} subcellular localization on decreasing ammonium concentrations

The wild-type *A. nidulans* colonies were grown on supplemented ANM media with the indicated concentration of (NH₄)₂T for 2 days. The subcellular distribution of AreA^{HA} (α-HA) in the gene-replaced *gpd(p)areA^{HA}* strain after 14h growth on 10mM ammonium ((NH₄)₂T) and 4h transfer to minimal medium containing 10mM (NH₄)₂T, 1mM (NH₄)₂T, 0.1mM (NH₄)₂T, 0.01mM (NH₄)₂T, or 0mM (NH₄)₂T (-N). Visualized by UV fluorescence microscopy following immunostaining with α-HA (3F10) and Alexa Fluor 488-conjugated goat anti-rat antibodies. A representative image of at least 100 nuclei is shown. Nuclei are stained with DAPI.

5.4.2 The effects of DNA-binding domain mutants on nitrogen sensing in *A. nidulans*

5.4.2.a The classical *areA* zinc finger DNA-binding domain mutants alter colonial growth of *A. nidulans* on alternative nitrogen sources

The classical DNA-binding mutants *areA102* and *areA217* been extensively studied (ARST JR AND COVE 1973; HYNES 1973a; HYNES 1973b; HYNES 1974; ARST AND MACDONALD 1975; POLKINGHORNE AND HYNES 1975; ARST 1977; KATZ AND HYNES 1989; KUDLA *et al.* 1990). The *areA102* mutant arose as a single point mutation causing substitution of Leucine 683 to Valine in the AreA protein (KUDLA *et al.* 1990). It was selected for increased growth on acetamide as a nitrogen source and shows increased growth on histidine but reduced growth on uric acid as nitrogen sources (Figure 5.2) (HYNES 1972). The *areA102* mutation confers altered DNA-binding specificity from HGATAR to TGATAR (H = A, C, or T; R = purine) (RAVAGNANI *et al.* 1997). The *areA217* mutant has a loss-of-function mutation that was selected for by lack of growth on 10mM histidine in an *areA102* background and because of the loss-of-function phenotype is unable to utilize alternative nitrogen sources (HYNES 1975a). The *areA217* mutant has two point-mutations. The first is the same L683V point mutation that is in *areA102*, and the second point mutation is 15 amino acids away and substitutes the glycine at 698 for an aspartic acid (Figure 5.5) (KUDLA *et al.* 1990). The additional point mutation in *areA217* abolishes AreA DNA-binding (PLATT *et al.* 1996b).

An HA-epitope tagged version of *areA102* expressed from the constitutive *gpdA* promoter, *gpd(p)areA102^{HA}*, was constructed through two successive gene replacements (as detailed in section 5.3.3). The *gpdA* promoter was used to avoid any effects of autoregulation (TODD *et al.* 2005). The *gpd(p)areA102^{HA}* mutant has the same nitrogen utilization growth phenotypes as the original *areA102* mutant (Figure 5.2). Note that different unrelated background mutations affect other growth phenotypes, such as when MH50 was compared to MH10609, where in the HA-tagged version the *riboB2* mutation is absent but a mutation is present in the *wA* gene, which led to the white conidia phenotype. As with the *areA102* mutant, an HA-epitope tag and the constitutive *gpd* promoter were added to the *areA217* mutant through a series of gene replacements (Figure 5.3). The *gpd(p)areA217^{HA}* strain is unable to grow on alternative nitrogen sources (alanine, acetamide) like the original *areA217* mutant (Figure 5.3).

The colonial growth of both of the classical DNA-binding mutants and their epitope-tagged variants was also tested on a decreasing range of ammonium concentrations starting at 10mM and decreasing in 10-fold increments down to 0.01mM and nitrogen starvation as done for wild type in Section 5.4.1 (Figure 5.4). The colonial growth of the *areA102* mutant strain (in which the mutant *areA* gene is expressed from its native promoter) and a strain expressing the *areA102* mutant gene from the constitutive *gpd*(p) promoter both showed similar growth to wild type on all NH₄ concentrations. The colonial growth of the *areA217* mutant strain expressing *areA217* from its native promoter and a strain expressing *areA217* from the constitutive *gpd* promoter had weak growth compared to wild type on all ammonium concentrations tested. The growth was slightly stronger than the *areAΔ* control.

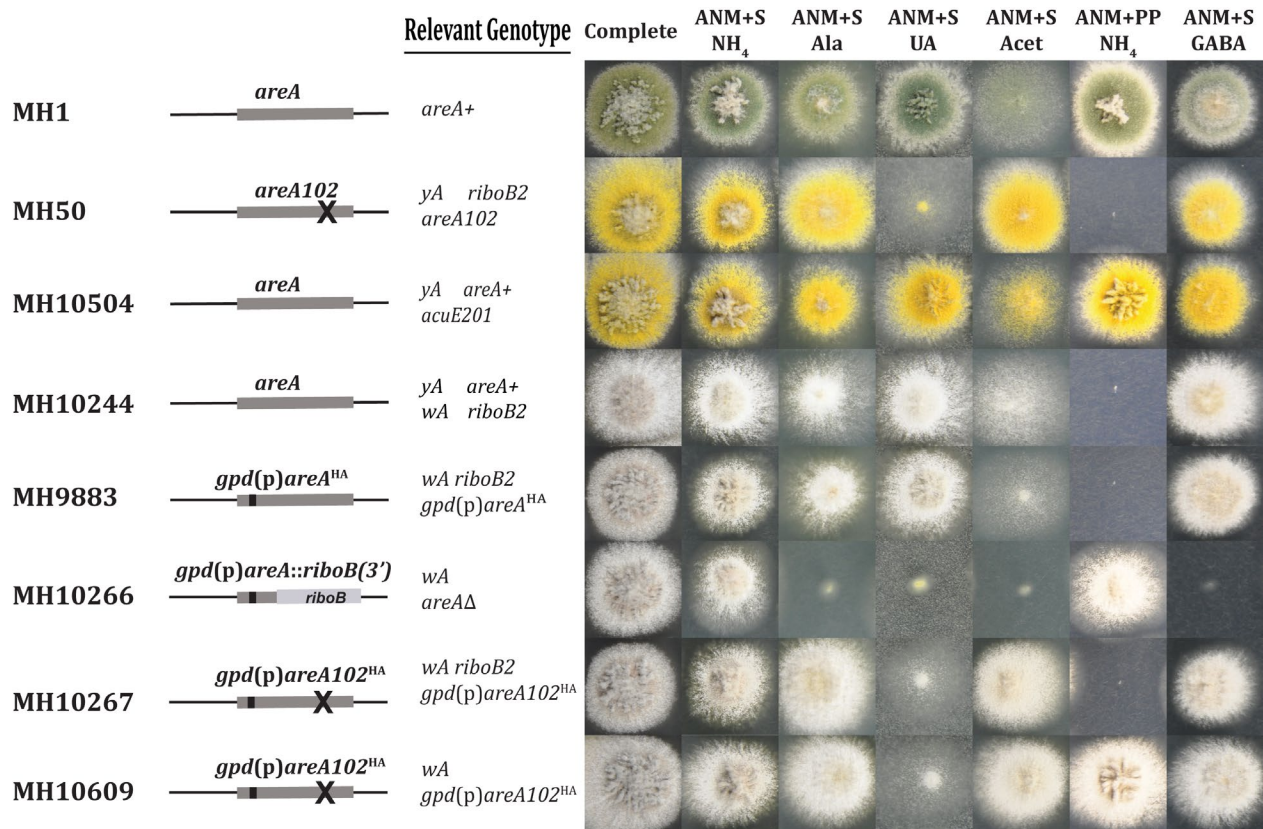


Figure 5.2 Construction and growth phenotypes of *gpd(p)areA102*^{HA}

Effects of the *areA102* mutation on colony growth on various nitrogen sources and a diagram of the changes at the *areA* gene locus. The various *areA102* mutants have green, yellow, and white conidial pigment mutations in the background genotype. Strains were grown on complete media, or supplemented minimal media (ANM+S) containing a range of nitrogen sources (NH₄, ammonium tartrate; Ala, alanine; UA, uric acid; Acet, acetamide; GABA, gamma-amino butyric acid) at 10mM, for two days at 37°C. ANM+PP, minimal media supplemented with only p-amino benzoic acid and pyridoxine.

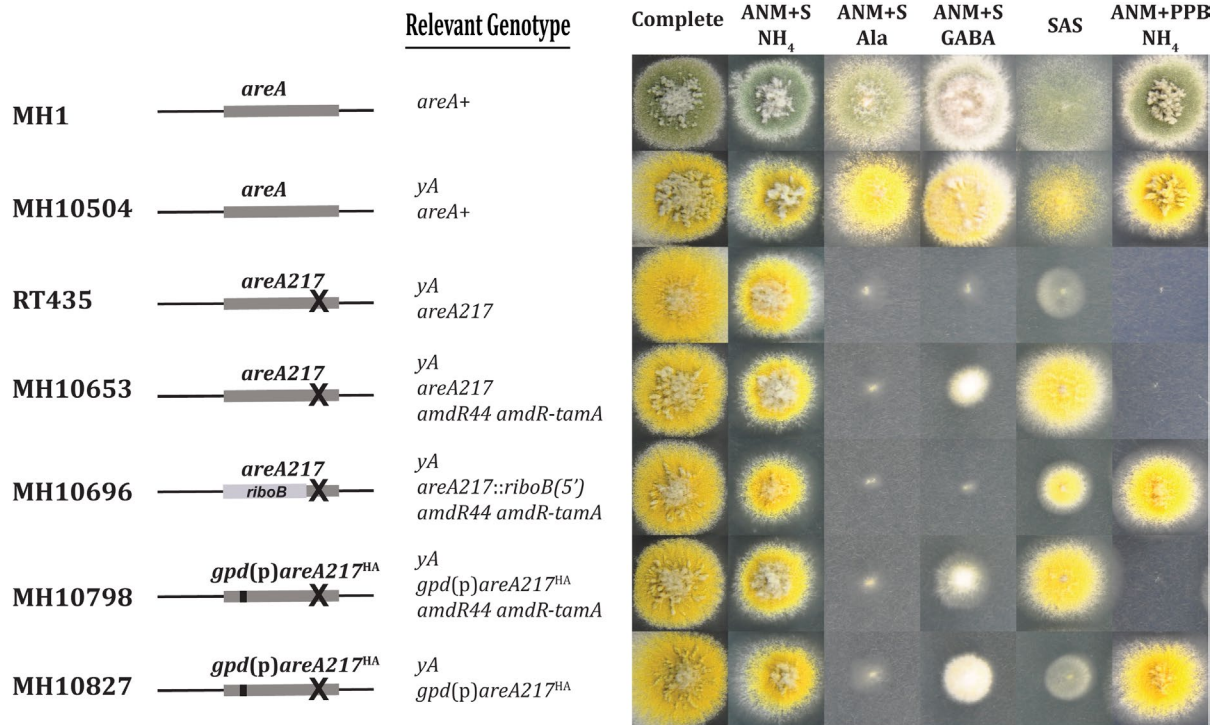


Figure 5.3 Construction and growth phenotypes of *gpd(p)areA217^{HA}* mutants

Effects of the *areA217* mutation on colony growth on various nitrogen sources and a diagram of the changes at the *areA* gene locus. The various *areA217* mutants have green, yellow, and white conidial pigment mutations in the background genotype. Strains were grown on complete media or supplemented minimal media (ANM+S) containing a range of nitrogen sources (NH₄, ammonium tartrate; Ala, alanine; GABA, gamma-amino butyric acid; SAS, acetamide) at 10mM, for two days at 37°C. SAS, supplemented ANM minimal media with 1% glucose replaced with 1% sucrose, ANM+PPB, minimal media supplemented with only p-amino benzoic acid, pyridoxine and biotin.

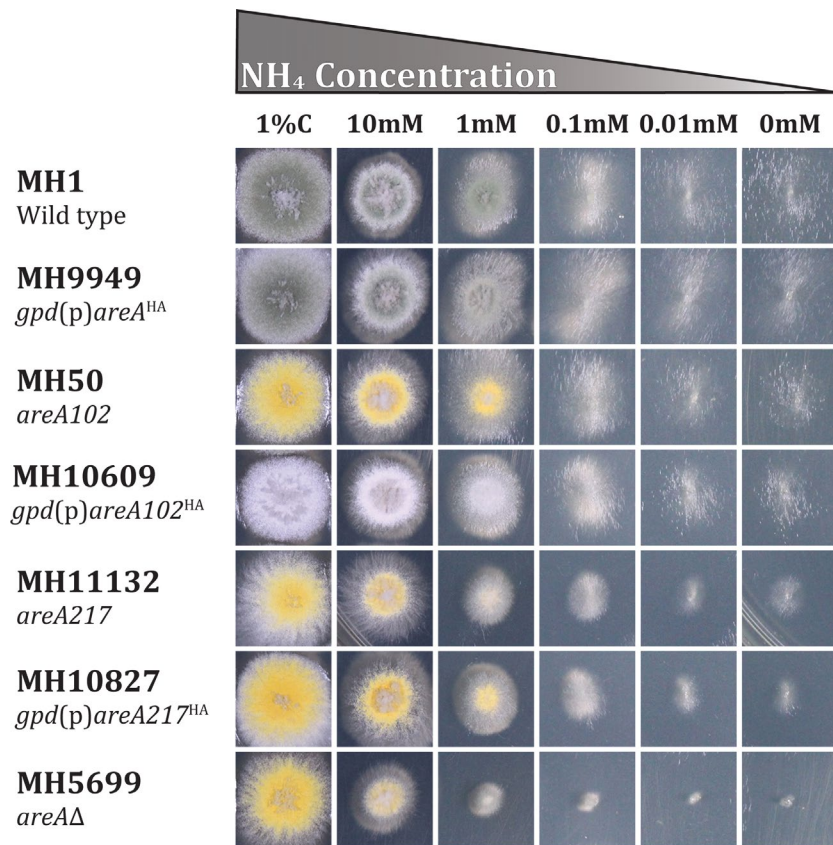


Figure 5.4 Growth of DNA-binding mutants on decreasing ammonium concentrations

The *Aspergillus nidulans* classical DNA-binding mutants and their epitope-tagged variants expressed from the *gpd* promoter were grown on complete media (1%C) or supplemented minimal media containing the indicated concentration of ammonium tartrate ((NH₄)₂T) for 2 days at 37°C. The *areAΔ* mutant MH5699 was included as a control.

5.4.2.b Analysis of DNA-binding mutants on the nuclear accumulation of AreA^{HA}

To test the role DNA binding has in AreA nuclear accumulation we analyzed the two classical DNA-binding mutant strains *gpd(p)areA102^{HA}* and *gpd(p)areA217^{HA}* using immunofluorescence microscopy. Two additional *gpd(p)areA^{HA}* mutant strains were also studied. We further analyzed the *gpd(p)areA^{HA}bip^{ALA}* mutant (RT49) studied in Chapter 3 (HUNTER *et al.* 2014), which is defective in only one NLS but was unable to activate gene expression likely due to the mutations affecting DNA contact residues (Figure 5.5), and a zinc-finger deletion mutant, *gpd(p)areA^{HA}ZF^Δ631-702* (MH12080), containing a 71-codon deletion of the zinc finger DNA-binding domain (residues 631-702), removing from 42 codons N-terminal of the first cysteine residue of the zinc finger to 4 codons C-terminal to the zinc finger, up to Lysine-702 located just before the NES. Both mutants are loss-of-function mutants, do not grow on alternative nitrogen sources, and phenotypically present the same as the *areAΔ* mutant.

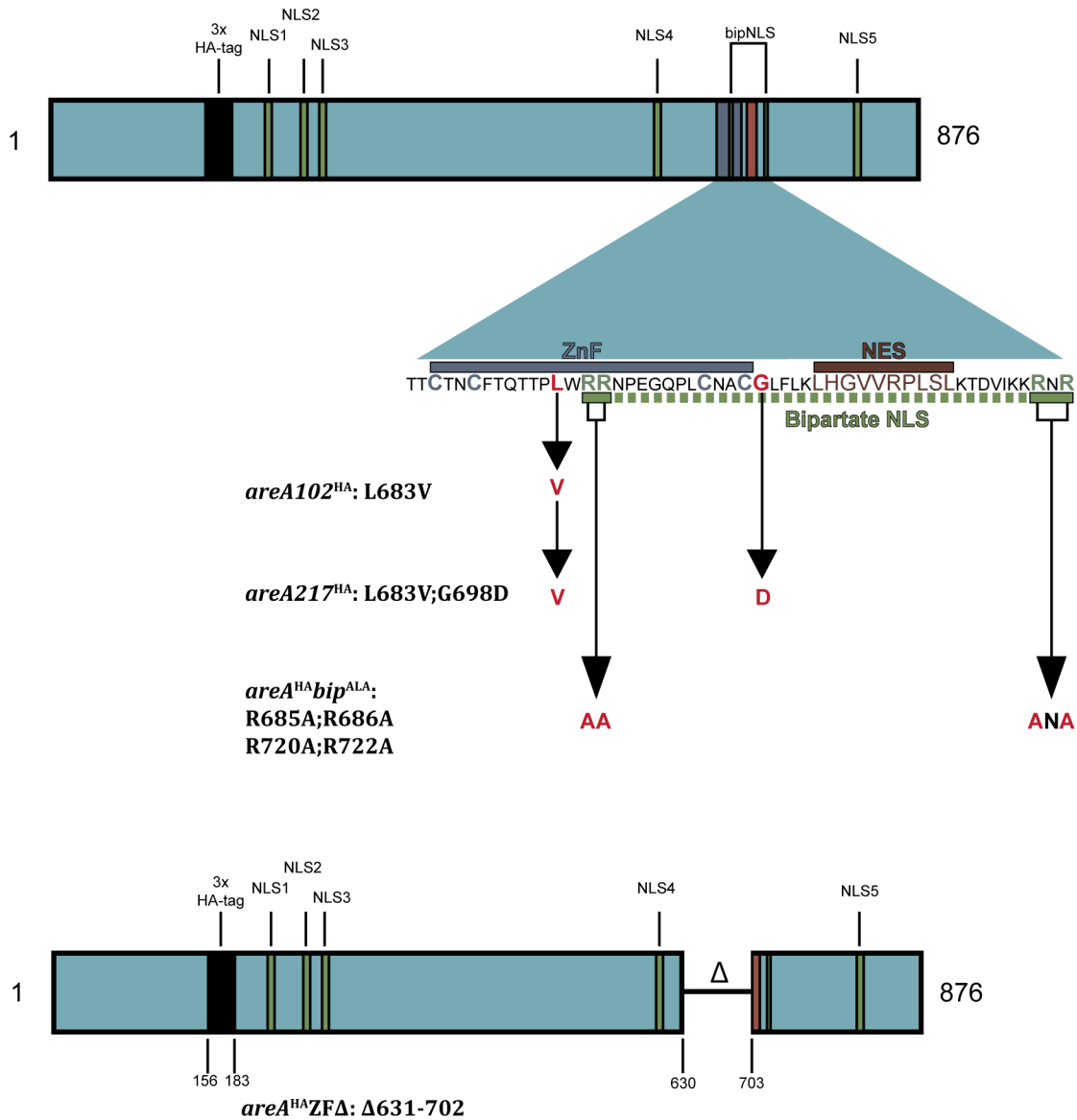


Figure 5.5 Mutations in the *areA* DNA-binding mutants

The *areA102* point mutation causes a conservative substitution of leucine 683 to valine. The *areA217* mutant has the same conservative substitution L683V as *areA102* and in addition there is a second nonconservative point mutation 15 amino acids apart, just outside of the zinc finger DNA-binding domain which substitutes glycine698 for an aspartic acid residue and abolishes AreA DNA-binding. The *areA*^{HA}*bip*^{ALA} mutant has 4 arginine to alanine substitutions. Two are located within the zinc finger DNA-binding domain and the second two are located 8 and 10 amino acids C-terminal of the nuclear export sequence. The *areA*^{HA}*ZF*Δ mutant has a 71 amino acid deletion which begins 15 amino acids downstream of NLS4 and ends at leucine702 in the NES.

The TGATAR DNA-binding specificity mutant protein AreA102^{HA} had a similar nuclear accumulation pattern to wild type AreA^{HA} on the range of nitrogen sources tested with the one exception being uric acid (Figure 5.6). When hyphae were transferred from 10mM ammonium tartrate to 10mM uric acid for four hours, AreA102^{HA} accumulated in the nucleus, as was observed for the AreA102^{HA} and wild type AreA^{HA} proteins after 4 h of nitrogen starvation. Therefore, on uric acid, which the *areA102* mutant is unable utilize (KUDLA *et al.* 1990; PLATT *et al.* 1996b), but not on other nitrogen sources, AreA102 mimics nitrogen starvation. This suggests that uptake or metabolism of uric acid, rather than the presence of uric acid, is required to signal nitrogen availability for regulation of AreA nuclear accumulation.

The non-DNA binding mutant protein AreA217^{HA}, like wild-type AreA^{HA}, was cytoplasmic on 10mM ammonium and accumulated in the nucleus during nitrogen starvation (Figure 5.6). This demonstrates that AreA DNA binding is dispensable for AreA nuclear accumulation. However, unlike wild type, AreA217^{HA} showed nuclear accumulation on all alternative nitrogen sources tested. This is consistent with DNA binding by AreA for activation of its target genes being required for signaling of nitrogen availability to prevent AreA nuclear accumulation.

The nuclear accumulation phenotype of AreA^{HA}ZF Δ ⁶³¹⁻⁷⁰² was more severe than AreA217^{HA}. AreA Δ ^{HA}ZF Δ ⁶³¹⁻⁷⁰² accumulated in the nucleus during nitrogen starvation as well as on all nitrogen sources tested, including 10mM ammonium tartrate (Figure 5.7). The AreA^{HA}bip^{ALA} mutant protein accumulated in the nucleus during nitrogen starvation and did not accumulate in the presence of 10mM ammonium tartrate, similar to the wild-type AreA^{HA} distribution pattern and consistent with previous observations (HUNTER *et al.* 2014). When the range of nitrogen sources is expanded, unlike wild type, AreA^{HA}-bip^{ALA} accumulated in the nucleus after a four-hour transfer to each of the alternative nitrogen sources tested except for 10mM proline (Figure 5.7). Therefore, except for on proline, the AreA^{HA}bip^{ALA} mutant protein, like AreA217^{HA}, shows nuclear accumulation on nutrients it cannot utilize. On 10mM glutamine, AreA217^{HA} and AreA^{HA}ZnF Δ showed nuclear accumulation whereas AreA^{HA}bip^{ALA}, like wild-type AreA^{HA}, did not accumulate in the nucleus.

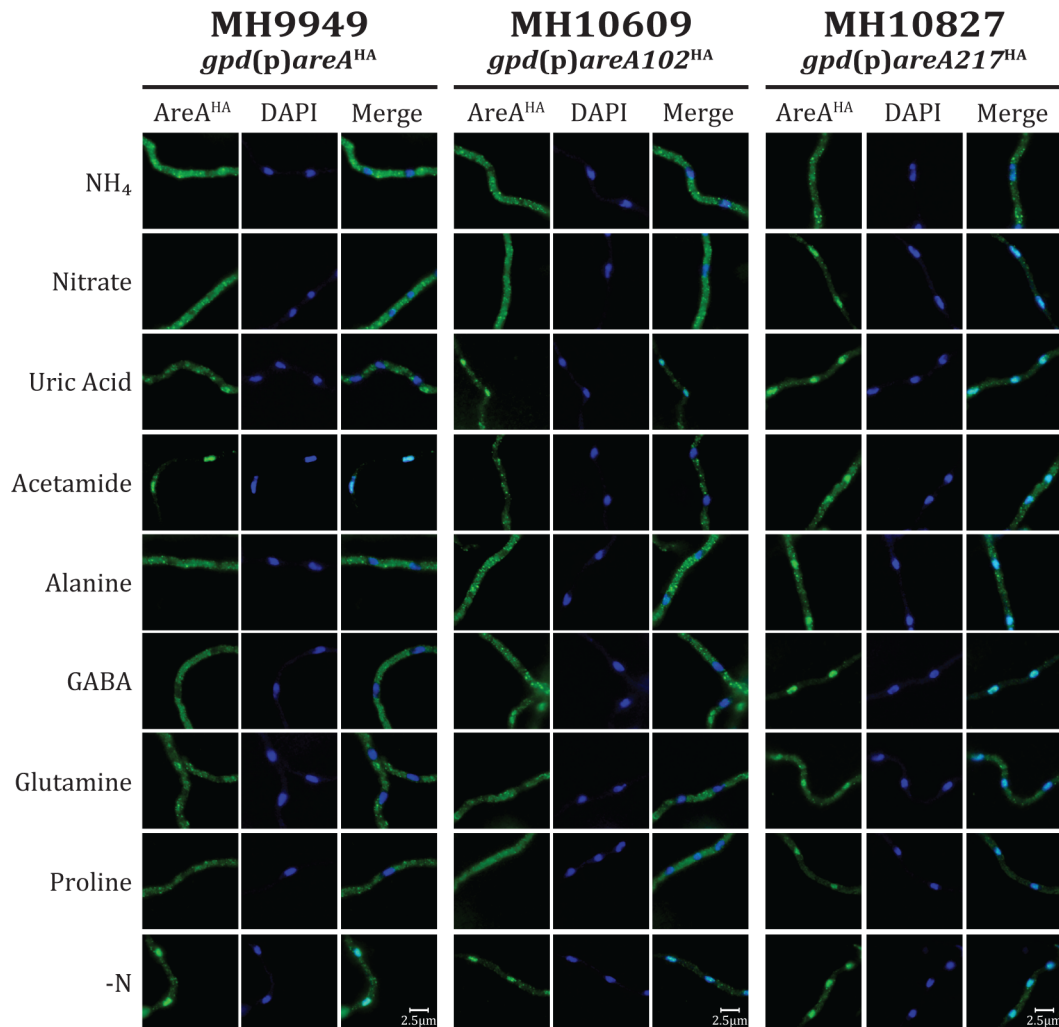


Figure 5.6 Nuclear localization of the classical AreA^{HA} DNA-binding mutants on a range of nitrogen sources

The subcellular distribution of AreA^{HA}, AreA102^{HA}, and AreA217^{HA} epitope-tagged classical mutant proteins expressed from the constitutive *gpd* promoter after 14h growth on 10mM ammonium-containing supplemented minimal media and 4h transfer to supplemented minimal media containing 10mM of the specified nitrogen source or nitrogen starvation (-N) was visualized by UV fluorescence microscopy following immunostaining with α -HA (3F10) and goat α -rat alexa-488 antibodies. A representative image of at least 100 nuclei is shown. Nuclei are stained with DAPI.

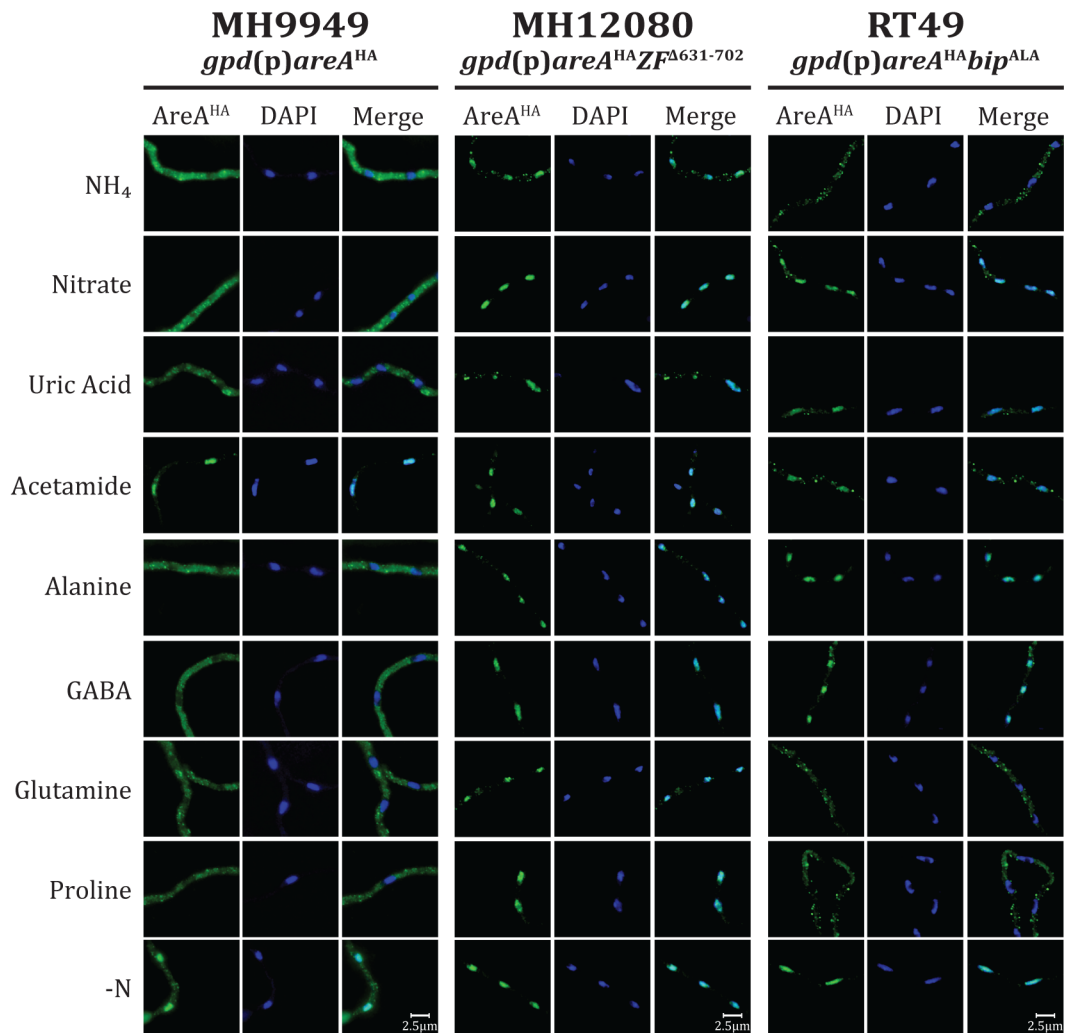


Figure 5.7 Nuclear localization of the AreA^{HA} DNA-binding mutants on a range of nitrogen sources

The subcellular distribution of AreA^{HA}, AreA^{HA}ZF^Δ, and AreA^{HA}bip^{ALA} mutant proteins expressed from the constitutive *gpd* promoter after 14h growth on 10mM ammonium-containing supplemented minimal media and 4h transfer to minimal media containing 10mM of the specified nitrogen source or nitrogen starvation (-N) was visualized by UV fluorescence microscopy following immunostaining with α -HA (3F10) and goat α -rat alexa-488 antibodies. A representative image of at least 100 nuclei is shown. Nuclei are stained with DAPI.

5.4.2.c Construction of a strain with wild-type *areA* at *wA* and *gpd(p)areA217^{HA}* at the native *areA* locus

The nuclear accumulation of mutant variants of the AreA^{HA} protein on nitrogen sources that cannot be utilized by the corresponding mutant observed in the previous section suggests that AreA-dependent activation of the metabolic genes for uptake and metabolism of the nitrogen source may be important for signaling nitrogen availability to prevent AreA nuclear accumulation. This seems highly likely for AreA102, where localization of the mutant protein is affected only on the nitrogen source this mutant cannot utilize and not on other nitrogen sources. However, we considered that for some of these DNA-binding mutants an alternative explanation may account for the observations, where an intrinsic property of the mutant protein may alter its nuclear accumulation pattern directly rather than via an indirect mechanism associated with the loss of AreA DNA binding and expression of metabolic signaling genes. To begin to distinguish these possibilities we devised a strategy to examine the subcellular distribution of the mutant proteins in a background where an ectopic untagged wild-type *areA* complements the signaling and metabolic defects of the mutants while the epitope-tagged mutant protein can be detected.

To construct a strain containing both *gpd(p)areA217^{HA}* at the native *areA* locus and wild-type *areA* with its native promoter inserted at the *wA* gene locus we used Fusion PCR to create a wild type *areA* PCR fragment flanked by a 5'*wA* UTR fragment and a 3'*wA* UTR fragment and then transformed the PCR fusion fragment into MH10827 (*yA1 gpd(p)areA217^{HA}*) protoplasts. The 787 bp 5'*wA* UTR region was amplified using the 20bp 5'*wA*Forward primer and the 40 bp 5'*wA*Reverse primer. The 4,459 bp *areA* fragment was amplified using the 40 bp 5'*areA*UTRFwd primer and the 40 bp 3'*areA*UTRRev primer. The 742 bp 3'*wA* UTR region was amplified using the 40 bp 3'*wA*Forward primer and the 20 bp 3'*wA*Reverse primer. The three PCR amplified fragments were PCR Cleaned and then diluted to 100ng/μl to be used as the templates for a three template PCR Fusion. Each of the 40 bp primers from the previous amplifications were designed to bind to 20 bp of their target gene and have a 20 bp tail which binds to a corresponding 20 bp region of another primer (Figure 5.8). The three PCR templates were amplified using 20 bp 5'*wA*Forward primer and the 20 bp 3'*wA* Reverse primer to make a 5,988 bp fusion PCR product. This product was PCR cleaned and gel purified before it was transformed into MH10827 and integrated at the *wA*

gene by homologous double crossover. Transformants were selected for growth on nitrate as sole nitrogen source, i.e., complementation of the *gpd(p)areA217^{HA}* phenotype. The transformation yielded primarily yellow transformants caused by integration of the PCR product somewhere other than the *wA* gene locus. Five white transformants were selected. Two of these transformants RT672 and RT673 were outcrossed to MH54 (*biA1, niiA4*) and it was determined that the progeny of both crosses segregated as expected for a single integration of the fusion construct at *wA* and *gpd(p)areA217^{HA}* at the native locus. Two new primers, 5'*wA*outsideF and 3'*wA*outsideR, which bind to regions flanking the insert at *wA* were used to verify that the amplified region was consistent with integration of *areA* at *wA* by homologous double crossover and loss of the native *wA* locus (7,618 bp) compared to if the native *wA* locus was present (10 kb).

A.

Name	Sequence	Sequence Length
Primer 1. 5' <i>wA</i> Forward	5' -CTACGCTGAATAGTGCTGAC-3'	20
Primer 2. 5' <i>wA</i> Reverse	5' -CATTACTGGACTCCGATTCCAGGAGAAGGAGAGTCAAGT-3'	40
Primer 3. 5' <i>areA</i> UTR Fwd	5' -ACTTGACTCTCCTTCTCCTGGAATCCGGAGTCCAGTAATG-3'	40
Primer 4. 3' <i>areA</i> UTR Rev	5' -GTGGCTGAACACTTAGATGCCATAGATGGGTAACACAACG-3'	40
Primer 5. 3' <i>wA</i> Forward	5' -CGTTGTGTACCCATCTATGCGATCTAAGTGTTCAGCCAC-3'	40
Primer 6. 3' <i>wA</i> Reverse	5' -GAATCTCTGCTGTCAGTACG-3'	20

B.

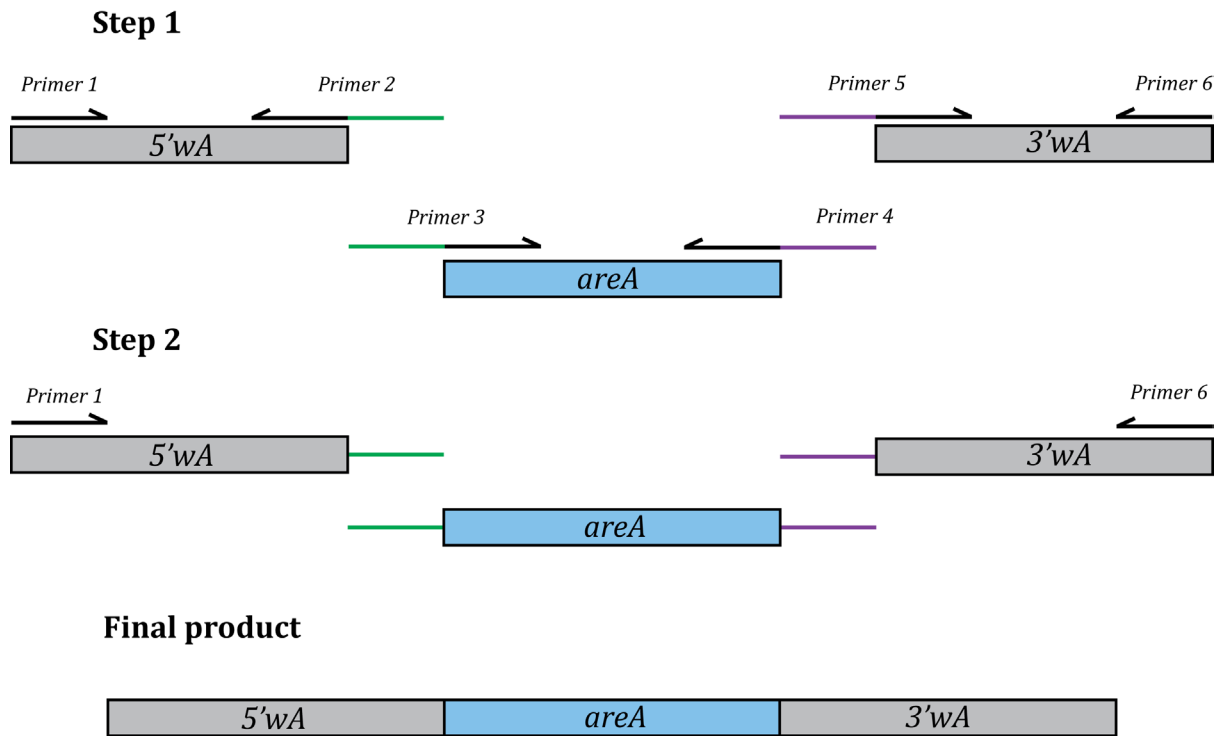


Figure 5.8 Two-step PCR fusion strategy

The two-step PCR fusion strategy used to replace the wild type *wA* gene with the wild type *areA*.

A. Table of the primer sequences and length.

B. Step 1: PCR amplification of the three separate fragments and their respective primer pairs. Step 2: Fusion of the three PCR products produced in Step 1 by amplification using the outside primer pair Primer 1 and Primer 6.

5.4.2.d Analysis of wild-type *areA* targeted to *wA* in a *gpd(p)areA217^{HA}* strain

To assess whether the effects on localization of the AreA217^{HA} protein were intrinsic to the mutant protein or are related to its loss of function we complemented the *gpd(p)areA217^{HA}* mutation with an ectopic copy of wild-type *areA* (Section 5.4.2.c). Integration of wild type *areA* at the *wA* gene (*wA::areA⁺*) in a *gpd(p)areA217^{HA}* background restored *A. nidulans* growth on alternative nitrogen sources (Figure 5.9A). The one notable exception was the reduced growth of *wA::areA⁺ gpd(p)areA217^{HA}* on alanine, which was accompanied by the production of a secondary metabolite pigment which darkened the agar on the plates and released a strongly aromatic compound. Further research on this phenomenon was beyond the scope of this project. The subcellular localization of the AreA217^{HA} protein by immunofluorescence in a phenotypically wild type strain demonstrated that on any nitrogen limiting or nitrogen starvation conditions AreA217^{HA} strongly accumulated in the nucleus (Figure 5.9B), as was observed in the AreA217^{HA} strain lacking a wild-type *areA* gene (Figure 5.6). When supplemented with 10mM ammonium, AreA217^{HA} did not show nuclear accumulation in the presence of a wild-type *areA* gene (Figure 5.9B), similar to the observation in wild-type AreA^{HA} strains and for AreA217^{HA} in the absence of a wild-type *areA* gene. However, on 10mM glutamine AreA217^{HA} accumulated in the nucleus only in the absence of the ectopic wild-type *areA* gene (compare Figure 5.6 and 5.9). This difference on glutamine could be due to repression of the wild-type ectopic *areA* gene expressed from the *areA* promoter, compared with constitutive expression of AreA217^{HA}. Therefore, these data suggest that an intrinsic property of the AreA217 protein likely confers its nuclear accumulation on alternative nitrogen sources.

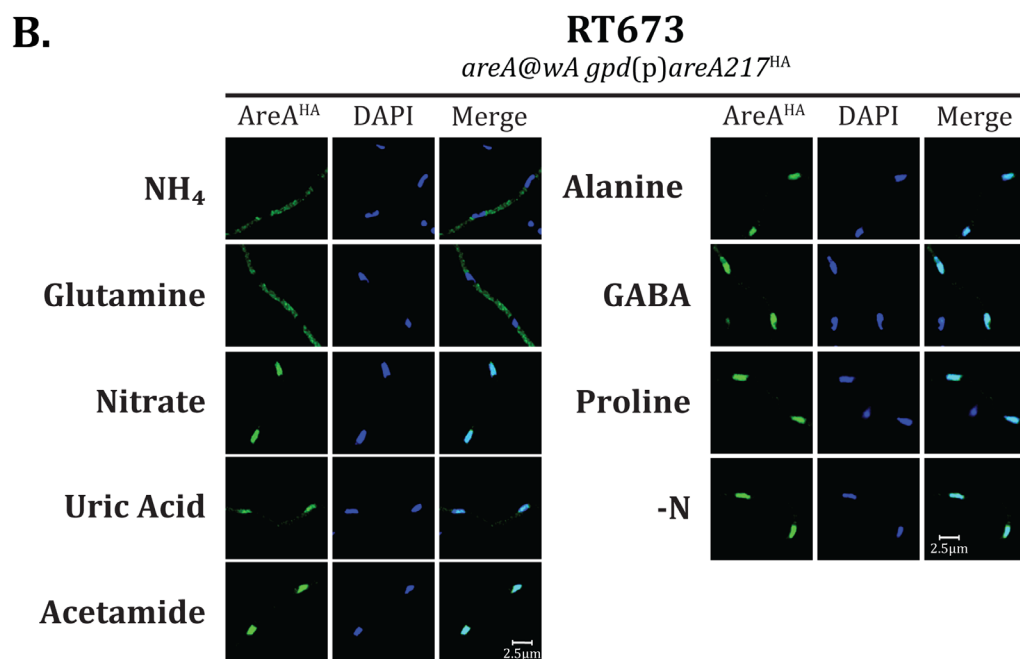
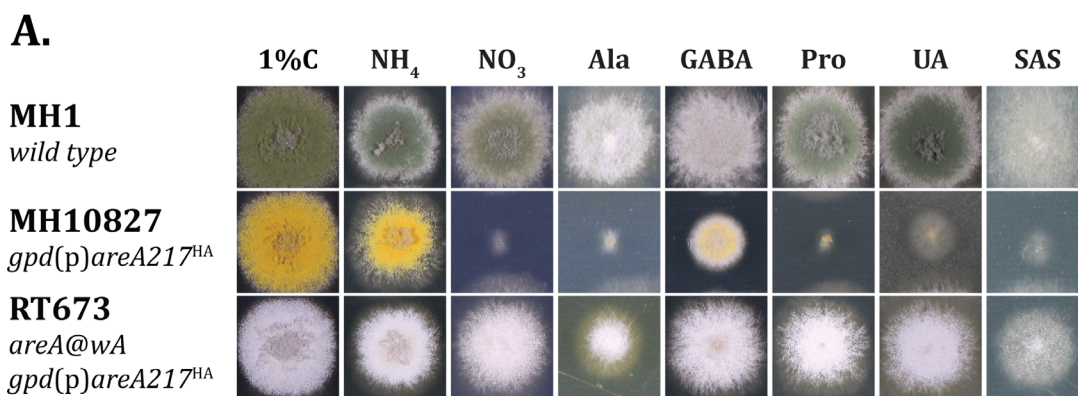


Figure 5.9 Colonial growth and nuclear localization of AreA217^{HA} in a *gpd(p)areA217^{HA}* mutant expressing wild type *areA* at the *wA* locus

A. Effects of inserting the wild-type *areA* gene at the *wA* locus in a *gpd(p)areA217^{HA}* mutant on colonial growth compared to wild type and the *gpd(p)areA217^{HA}* mutant strains. Colonies were grown on complete media or supplemented minimal media containing a range of nitrogen sources (NH₄, ammonium tartrate; NO₃, nitrate; Ala, alanine; GABA, gamma-amino butyric acid; Pro, proline; UA, uric acid; SAS, acetamide) at 10mM for two days at 37°C. SAS, supplemented ANM minimal media with 1% glucose replaced with 1% sucrose. **B.** The subcellular distribution of AreA217^{HA} mutant in the presence of wild-type *areA* (integrated at *wA*) after 14h growth on 10mM ammonium and 4h transfer to supplemented minimal media containing 10mM of the specified nitrogen source or nitrogen starvation (-N) was visualized by UV fluorescence microscopy following immunostaining with α-HA (3F10) and goat α-rat alexa-488 antibodies. A representative image of at least 100 nuclei is shown. Nuclei are stained with DAPI.

5.4.3 The role of nitrogen metabolic mutants on nitrogen sensing via AreA^{HA} nuclear accumulation

To understand the role AreA-dependent metabolism plays in cellular nitrogen signaling we analyzed five metabolic mutants using AreA^{HA} nuclear accumulation as our metric for nitrogen sensing. The five metabolic mutants we assessed were: (i) *niiA4*, which affects the nitrite reductase gene required for nitrate/nitrite utilization (TOMSETT AND COVE 1979), (ii) *amdS-lacZ* an in-frame fusion gene that replaced the native copy of the *amdS* gene and has interrupted the function of the acetamidase enzyme that hydrolyses acetamide (DAVIS *et al.* 1988), (iii) *prn-309*, which is a large deletion within the proline utilization gene cluster affecting both uptake and utilization of proline (DURRENS *et al.* 1986), (iv) *gdhAΔ*, which affects the NADP-dependent glutamate dehydrogenase gene important for nitrogen assimilation (ARST JR AND MACDONALD 1973; KINGHORN AND PATEMAN 1973) and (v) *glnAΔ*, which affects the glutamine synthetase nitrogen assimilation gene (MARGELIS *et al.* 2001). (Figure 5.10)

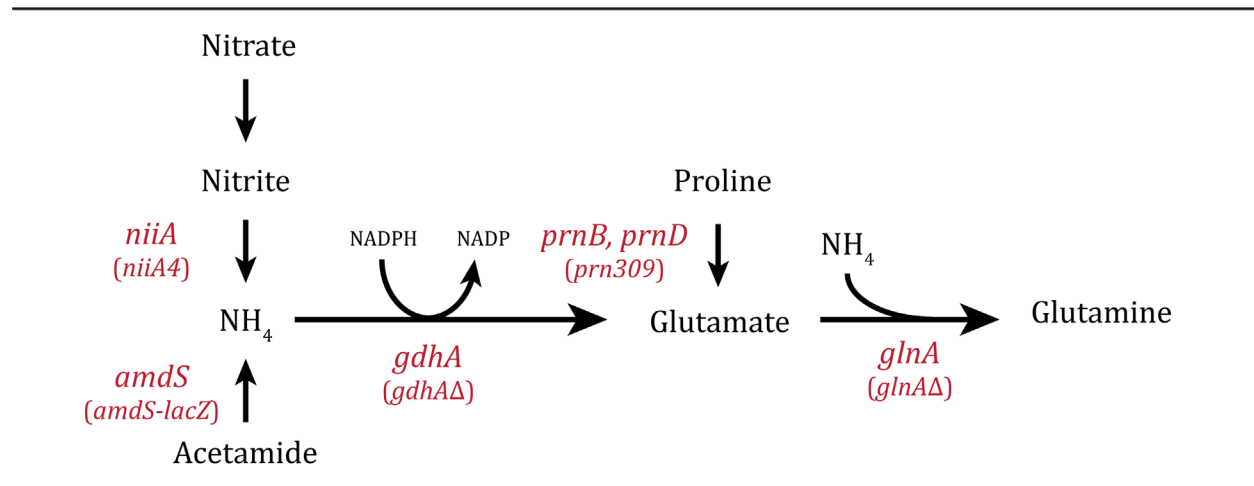


Figure 5.10 Nitrogen assimilation in *A. nidulans*

Diagram of metabolic steps of relevant nitrogen sources and its corresponding metabolic mutant.

The *niiA4*, *amdS-lacZ*, and *prn-309* strains could not sense nitrate, acetamide, or proline respectively, which led to AreA^{HA} nuclear accumulation mimicking nitrogen starvation. The *gdhAΔ* mutation had no effect on AreA^{HA} nuclear accumulation on the conditions tested (Figure 5.11).

A. nidulans has one gene that is primarily responsible for glutamine synthesis, *glnA* (Figure 5.10, Figure 5.12A). This gene has been previously shown to be an effector of nitrogen metabolite repression (MARGELIS *et al.* 2001). To understand the role that this gene plays on nitrogen sensing the *glnA* deletion strain (MH9962) was crossed with a *gpd(p)areA^{HA}* strain (RT52) to construct a *glnAΔ, gpd(p)areA^{HA}* strain (RT555). This strain is a tight glutamine auxotroph that shows weak growth even when supplemented with 10mM glutamine on complete media (MARGELIS *et al.* 2001). Supplementation with 50mM glutamine on complete media allows the strain to grow more comparably to wild type (Figure 5.12B). On minimal media even when supplemented with 50mM Glutamine we saw negligible growth in the *glnAΔ* strain (Figure 5.12B).

AreA^{HA} did not accumulate in the nucleus in the *glnAΔ* mutant when it was supplemented with 50mM glutamine and 10mM ammonium tartrate for 14 hours and then transferred for 4 hours to any nitrogen condition including nitrogen free media (Figure 5.12C). This could either mean that during pre-growth on high glutamine, enough nitrogen had been stored in the cells before the transfer that the nitrogen starvation signal has yet to be sensed after 4 hours of nitrogen starvation, or that GlnA plays a role in the signaling for nuclear accumulation of AreA^{HA} during nitrogen starvation.

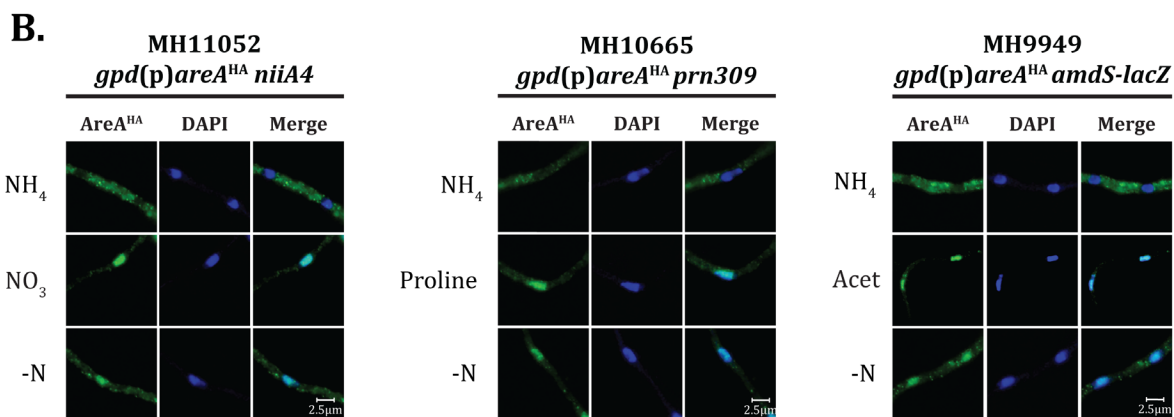
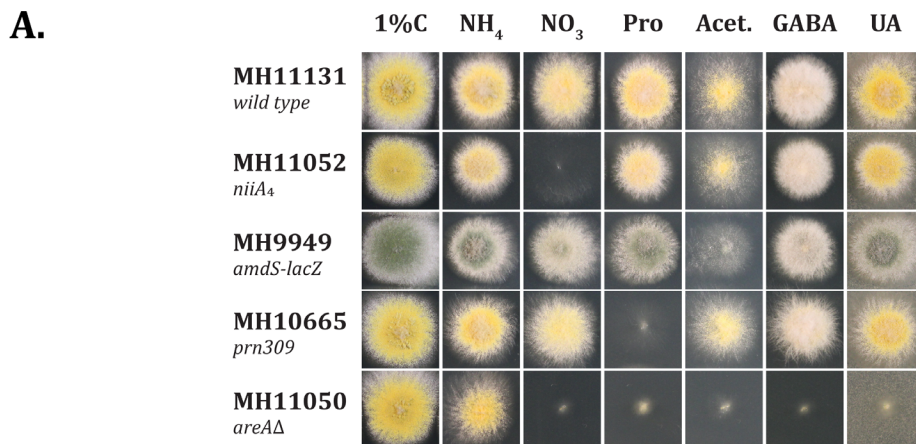


Figure 5.11 Colonial growth and AreA^{HA} localization in nitrogen metabolic mutants

A. Strains were grown on complete media, or supplemented minimal media (ANM+S) containing a range of nitrogen sources (NH₄, ammonium tartrate; NO₃, nitrate; Pro, proline; UA, uric acid; Acet, acetamide, GABA, gamma-amino butyric acid) at 10mM, for two days at 37°C. **B.** The subcellular distribution of AreA^{HA} after 14h growth on 10mM ammonium and 4h transfer to minimal media containing 10mM of the specified nitrogen source or nitrogen starvation (-N) was visualized by UV fluorescence microscopy following immunostaining with α-HA (3F10) and goat α-rat alexa-488 antibodies. A representative image of at least 100 nuclei is shown. Nuclei are stained with DAPI.

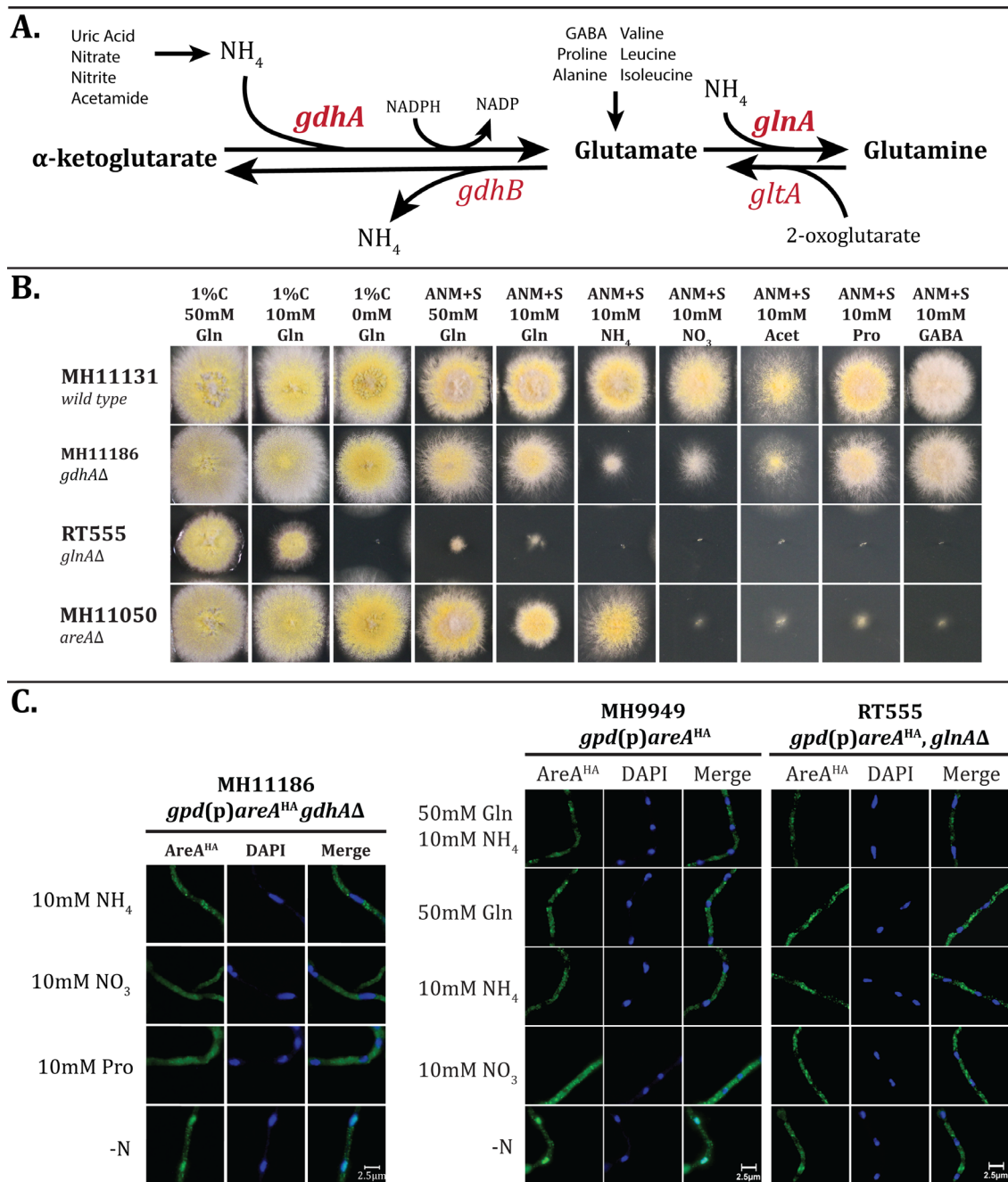


Figure 5.12 Colonial growth of the *glnΔ* mutant in comparison to wild-type *areA^{HA}* and *areAΔ* strains on various nitrogen sources and concentrations

A. Nitrogen assimilation pathway with emphasis on key metabolic mutants. **B.** Growth of the tight glutamine auxotroph on various nitrogen sources (Gln, glutamine; NH₄, ammonium tartrate; NO₃, nitrate; Pro, proline; Acet, acetamide; GABA, gamma-amino butyric acid) and concentrations in comparison with *gpd(p)areA^{HA}* and *areAΔ* strains. **C.** The subcellular distribution of AreA^{HA} for *gdhΔ*: after 14h growth on 10mM ammonium and 4h transfer to minimal media containing 10mM of the specified nitrogen source or nitrogen starvation (-N) for *glnΔ*: after 18h growth on supplemented minimal media containing 50mM glutamine, 10mM ammonium and 4h transfer to supplemented minimal media containing the specified nitrogen source or nitrogen starvation (-N) was visualized by UV fluorescence microscopy following immunostaining with α-HA (3F10) and goat α-rat alexa-488 antibodies. A representative image of at least 100 nuclei is shown. Nuclei are stained with DAPI.

5.5 Discussion

5.5.1 The effects of ammonium concentration on colonial growth and AreA^{HA} nuclear accumulation

Fungi respond to changes in nitrogen nutrient availability by altering their metabolism through transcriptional control. *A. nidulans* can sense different nitrogen nutrient sources as well as nitrogen abundance and adjust gene expression accordingly. An additional response of nuclear accumulation of the nitrogen utilization transcription factor AreA occurs during complete nitrogen starvation (TODD *et al.* 2005; HUNTER *et al.* 2014). A key question was at what nitrogen levels does *A. nidulans* sense nitrogen starvation. To address this question, we used AreA^{HA} nuclear accumulation as the metric for starvation. As the concentration of ammonium decreased from 10mM to 1mM to 0.1mM there was an increase in cytoplasmic concentration of AreA^{HA}, which corresponded with a decrease in conidia formation indicating a shift from an emphasis on reproduction to survival as nutrient availability decreases. Preliminary research indicates that this is also accompanied by a stepwise upregulation of AreA-dependent gene expression as the ammonium concentration decreases (CLARKE *et al.* Unpublished data). We found at 0.01mM ammonium was where the transition to starvation was readily seen. At 0.01mM ammonium the intracellular localization of AreA^{HA} was found to accumulate in the nucleus but was also clearly still in the cytoplasm, though the amount was visibly reduced compared to the higher concentrations of ammonium. This points towards *A. nidulans* being in a transition state between nitrogen sufficiency and starvation. This state is also supported by evidence in the colonial growth test. At the higher concentrations of ammonium, the production of spores was observed, indicating that asexual reproduction is occurring, even though there is a clear reduction as the concentration decreases. At 0.01mM ammonium concentration AreA^{HA} nuclear accumulation begins, spores were not produced (indicating a loss in asexual reproduction), but hyphal extension in the growth media still occurs. This may be a scavenging behavior by the colony to search for new sources of nutrients. The transition into the starvation response at very low levels of nitrogen likely sets off a cascade of AreA-dependent responses. The sequestration of AreA into the nucleus by the inhibition of nuclear export leads to the elevation of AreA-dependent gene expression due to the inability of AreA to leave the

nucleus, which would lead to increased promoter occupancy contributing to the 6-fold increase in expression observed from 10mM ammonium, and the 2.5-fold increase seen on alanine, when AreA is able to cycle in and out of the nucleus (Figure 3.4).

5.5.2 The role of DNA-binding mutants on nitrogen sensing and AreA nuclear accumulation

We have analyzed the subcellular localization of four different AreA^{HA} DNA-binding mutant proteins and in doing so have found varied patterns of nuclear accumulation depending on the mutant analyzed. These experiments were initially focused on the two classical DNA-binding mutants *areA102* and *areA217*. Colonial growth tests confirmed that adding an HA epitope-tag to the mutant proteins did not have any effect on growth phenotype when compared to the original mutants.

The AreA102^{HA} mutant protein showed nuclear accumulation when the cells were nitrogen starved either due to the absence of a nitrogen source or, in the case of uric acid, due to the inability to utilize the uric acid as a nitrogen source in the *areA102* mutant. It is unlikely that this specific effect on uric acid would be associated with an intrinsic property of the AreA102 mutant protein affecting nuclear accumulation only observed when uric acid is the nitrogen source. It is more likely a result of reduced promoter binding and the subsequent loss of expression of uric acid uptake and metabolism genes by the altered DNA binding specificity of the AreA102 protein. We could also be seeing the effects of inducer exclusion. In RAVAGNANI *et al.* (1997) they show that in the AreA102 mutant there is poor activation of the CGATAR and the AGATAR sites upstream of the *uapA* permease but strong binding to TGATAR sites (leading to the increased colonial growth on acetamide compared to wild type). This paper also shows that both *uapA* and *uapC* permeases have near null expression in the *areA102* mutant. This indicates that the primary reason for poor uric acid utilization in this mutant is due to the lack of uric acid uptake into the cell.

An *E. coli* expressed AreA217 protein was shown to be defective in DNA binding (PLATT *et al.* 1996b). Therefore, our subcellular localization experiments with the AreA217^{HA} mutant protein demonstrated that DNA binding is not required for AreA nuclear accumulation. This indicates that either AreA DNA-binding is needed for signaling nuclear export when alternative nitrogen sources are present or the AreA217^{HA} mutant protein may

itself be defective in nuclear export. Complementation with ectopic wild type *areA*, revealed that the AreA217^{HA} protein has an intrinsic property that affects its subcellular localization resulting in its nuclear accumulation on alternative nitrogen sources. The G698D point mutation in *areA217* adds a charged residue within 5 amino acids of the NES in AreA. This could directly affect the interaction with CrmA (*A. nidulans* nuclear exportin) or it could alter the protein structure of AreA leading to NES occlusion.

We analyzed two other mutants of the AreA DNA-binding domain, the *gpd(p)areA^{HA}ZF^Δ631-702* (AreAZF Δ) mutant and the *areA^{HA}bip^{ALA}* mutant. The AreAZF Δ mutant was a 71-codon deletion of the AreA^{HA} zinc finger region which extends up to the first codon before the NES and half of the non-canonical bipartite NLS (Figure 5.5). The five classical NLSs are still intact in this mutant and are capable of promoting AreA nuclear import without the ncbipartite NLS (Figure 3.5). The AreAZF Δ accumulated in the nucleus under all nitrogen conditions tested. This suggests that nuclear export of the AreAZF Δ protein is inhibited as nuclear accumulation was observed on both 10mM NH₄ and 10mM GLN.

We have not yet distinguished for the AreA^{HA}bip^{ALA} mutant if the nuclear accumulation on alternative nitrogen sources is due to signaling or an intrinsic property of the mutant protein. However, nuclear accumulation of the AreA^{HA}bip^{ALA} mutant protein was not observed in all conditions, leaving open the possibility that this mutant affects signaling indirectly via uptake or metabolism. Specifically, in cells grown on ammonium, glutamine, proline, and acetamide, AreA^{HA}bip^{ALA} nuclear accumulation was not observed, leaving open the possibility that this mutant affects signaling indirectly via uptake or metabolism. The *gpd(p)areA^{HA}bip^{ALA}* mutant growth phenotype demonstrated in Chapter 3 indicates that there is a loss of activation, a loss that is likely due to DNA binding as the mutated residues include DNA contact points. This suggests that the bip^{ALA} mutant is affecting the signaling pathway. The lack of nuclear accumulation of AreA^{HA}bip^{ALA} on proline and acetamide but not on other alternative nitrogen sources appears counterintuitive. However, the genes for acetamide and proline metabolism are under AreA-dependent and AreA-independent controls (HYNES *et al.* 1988; GONZALEZ *et al.* 1997; TAZEBAY *et al.* 1997), and AreA-independent controls would not be disrupted in the AreA^{HA}bip^{ALA} mutant.

In order to elucidate our findings more clearly, we constructed a strain containing both *gpd(p)areA217^{HA}* at the native *areA* locus with wild type *areA* inserted at the *wA* gene.

This should be done with the other three mutant strains in the future, but we examined the effects of the wild-type *areA* gene integrated at *wA* in *gpd(p)areA217^{HA}* as a starting point. We found that the new strain grew similarly to a wild type strain except for an odd result on alanine, which led to a slight reduction in growth and an aromatic secondary metabolite. We also no longer observed accumulation of AreA217^{HA} when 10mM NH₄ or 10mM Gln were present in the media. One possible explanation for this result is that in the presence of NH₄ or Gln when wild-type AreA is present, AreA217 is being broken down and recycled more efficiently in an AreA-dependent manner.

5.5.3 The role of metabolism in nitrogen sensing

The *Aspergillus nidulans* GATA transcription factor AreA activates expression of genes for uptake and metabolism of nitrogen nutrients and is required for growth on alternative nitrogen sources (TODD 2016). In the presence of alternative nitrogen sources AreA is actively transported into the nucleus via nuclear importins but does not accumulate in the nucleus because nuclear export is functional. The nuclear accumulation of AreA is regulated via nuclear export by the Crm1^{KapK} nuclear exportin in response to nitrogen starvation, during which export of AreA from the nucleus is inhibited (TODD *et al.* 2005). The signaling for AreA nuclear accumulation is not fully understood.

One possibility is that the presence of an extracellular nitrogen source causes a signal to be sent which indicates nutrient availability to the cell, reopening nuclear export, and leading to the loss of AreA nuclear accumulation. This is plausible as it has been previously shown that AreA^{HA} nuclear accumulation during starvation is a slow process and takes up to 4 hours, whereas loss of AreA^{HA} nuclear accumulation after 4 hours of starvation when a nitrogen source is reintroduced is rapid and can take less than a minute depending on the nitrogen source, but for all nitrogen sources tested took less than 15 minutes (TODD *et al.* 2005). This signal could come from a plasma membrane sensor like the SPS sensor (see ZHANG *et al.* (2018) for a great review) or it could be signaled as the nitrogen source passes through one of the amino acid or ammonium permeases in the plasma membrane. Many of these permeases in *A. nidulans* are regulated by AreA. This was demonstrated previously in this chapter by the *areA102* mutant's poor activation of the CGATAR and AGATAR promoter sites upstream of *uapA* and *uapC* permeases (RAVAGNANI *et al.* 1997), leading to AreA102^{HA}

nuclear accumulation on uric acid (Figure 5.6). This shows that the loss of amino acid specific permease function, leads to the inability for the cell to recognize extracellular nutrient availability. This indicates that the signaling of nitrogen availability leading to loss of AreA nuclear accumulation and the decrease of AreA dependent gene expression is unlikely to be an independent signaling pathway like the SPS sensor system.

The sensing and signaling of nitrogen availability could be regulated by intracellular nitrogen metabolism. If this is the case, the breakdown of a sufficient amount nitrogen by the cell to signal relief from nitrogen starvation is extremely rapid and leads to the question, what nitrogen metabolite or metabolic protein signals nitrogen availability and subsequently leads to the loss of accumulation of AreA^{HA} from the nucleus? We analyzed metabolic mutants using AreA^{HA} nuclear accumulation as our metric for nitrogen sensing. The *prn-309* mutant impairs the function of both *prnB* (the proline transferase) and *prnD* (the proline dehydrogenase) and it could not sense when proline was available; this is a similar result to what we found in the *areA102* mutant. The loss of nitrogen uptake by the inactivity of a permease leads to the inability to sense that specific nitrogen source. The *amdS-lacZ* fusion strain is unable to metabolize acetamide and subsequently cannot sense acetamide as a nitrogen source. The *niiA4* mutant is a bit more interesting because in the *niiA4* mutant nitrate is metabolized to nitrite by NiaD (nitrate reductase) but is unable to further break down nitrite. This demonstrates that sensing of alternative nitrogen sources requires a metabolic signal but that the signal is not metabolism itself but something that is further downstream.

The final two metabolic mutants that we analyzed, *gdhAΔ* and *glnAΔ*, are more complicated. The *gdhA* gene encodes for the NADP-glutamate dehydrogenase which catalyzes α -ketoglutarate (an important intermediate in the TCA cycle) and ammonium into glutamate. The *glnA* gene encodes for glutamine synthetase which converts glutamate and ammonium into glutamine. In addition, glutamate can also be reconverted back from glutamine by the glutamate synthetase *gltA* (MACHEDA *et al.* 1999) (Figure 5.12A). Margelis *et al.*, 2001, thoroughly detail the interplay between *glnA* and *gdhA* and the effects of their mutations on nitrogen metabolite repression (MARGELIS *et al.* 2001). The *gdhA10* loss-of-function mutant shows increased AreA-dependent gene expression on ammonium, the *glnAΔ* mutant showed low levels of expression and the *gdhA10 glnAΔ* double mutant showed

elevated levels of expression (HYNES 1974; MARGELIS *et al.* 2001). The *gdhAΔ* mutant showed reduced colonial growth on all nitrogen sources which are metabolized to ammonium, but AreA^{HA} only accumulated in the nucleus during nitrogen starvation (Figure 5.12B,C). The *glnAΔ* mutant was able to grow comparably to wild type only when supplemented with 50mM of glutamine on complete media. We found in the *glnAΔ* mutant AreA^{HA} did not accumulate in the nucleus on any condition tested including after 4 hours of nitrogen starvation (Figure 5.12B,C). These data suggest that *glnA* is essential for signaling nitrogen starvation leading to AreA^{HA} accumulation. The loss of GlnA leads to the inability to convert glutamate to glutamine and leads to increased levels of intracellular glutamate. It has been suggested that the excessive levels of glutamate could lead to toxic effects on the cell (MARGELIS *et al.* 2001). This could also account for the loss of AreA^{HA} nuclear accumulation we observed. The loss of GlnA leads to an increase in intracellular glutamate levels, AreA does not accumulate because the levels are too high, even during nitrogen starvation, to signal inhibition of nuclear export. Increase in intracellular glutamate levels could also account for the loss of AreA nuclear accumulation during carbon starvation (and treatment with rapamycin) if glutamate production is upregulated (via *gltA*) in order to increase the supply of α -ketoglutarate for the TCA cycle. Conversely, in the metabolism and uptake mutants, intracellular glutamate levels would be expected to be low provided the mutant is affected in an *areA*-dependent gene.

Chapter 6 - Discussion and Future Directions

The title of this dissertation is “Nitrogen signaling and nuclear localization of the *Aspergillus nidulans* GATA transcription factor AreA.” Though that is an accurate title of the work that has been presented, when reflected upon, it is this author’s opinion that it is disingenuous to the work it truly represents. If Nature or Science was publishing this work it would be titled something flashy like, “Nucleocytoplasmic transport, a spotlight on fungal GATA”. This chapter will attempt to give an overarching view of what has been done and discuss what could be done in the future. To present what the data as a whole could be indicating, and to suggest further areas of inquiry into what potentially could be part of a map to help someone traverse the pathways of NMR on their quest to find the mechanisms behind regulation of nuclear accumulation of a fungal nitrogen metabolism regulating GATA transcription factor, or what some would call, “the Holy Grail”, (to paraphrase LJUNGDAHL AND DAIGNAN-FORNIER (2012) (and Monty Python)). The scope of this work can be generally encompassed by three questions:

- (i) What within AreA allows it to be delivered from the cytoplasm to the nucleus?
- (ii) What mechanisms regulate its delivery?
- (iii) What signals nitrogen availability and subsequently the delivery, retention, and release of AreA to and from nucleus?

We addressed the first question in chapter three. We discovered that AreA has an unusually high number of NLSs with six, five cNLSs and one noncanonical arginine-based bipartite NLS (RRX₃₃RXR). This was done by mutating the predicted NLSs individually and in tandem. We found that the NLSs of AreA show redundancy and work in tandem in order to promote nuclear import of both AreA and when fused to GFP. Without all of the NLSs AreA cannot localize in the nucleus. This work represents one of the most detailed studies of multiple NLSs within a single transcription factor in any system. Most of the NLSs are conserved in AreA orthologs, suggesting that the redundancy observed in *A. nidulans* may occur throughout Ascomycetes and the presence of multiple NLSs in AreA orthologs likely provide a selective advantage. We also demonstrated that when AreA is incapable of

regulating gene expression (as we see with the bipartite mutant) it can still be imported into the nucleus and its export is still blocked during nitrogen starvation (though the starvation conditions changed to include any non-preferred nitrogen source, as expression of the genes for the metabolism of non-preferred nitrogen source is AreA-dependent).

The second question zooms out a bit further to analyze what mechanisms regulate AreA nuclear import. *A. nidulans* has eighteen predicted nuclear transporters. Fourteen of those fall into the karyopherin- β superfamily (MARKINA-INARRAIRAEGUI *et al.* 2011) The mechanisms of α -importin and β -importin nuclear import has been thoroughly detailed in other systems. One of the key features is that α -importin interacts specifically with cNLSs. In *A. nidulans*, KapA is the α -importin homologue. We used a temperature sensitive point mutant *kapA*^{S111F} and a *gfp*-tagged *kapA* strain to elucidate the potential interplay between AreA and KapA. We found that in the *kapA* point mutant AreA did not accumulate in the nucleus which indicates that it is likely the main importin mediating AreA nuclear import. With this in mind we then assessed the interactions the small ubiquitin-like modifier, SumO, had on the localization of AreA and KapA. The loss of SumO led to loss of AreA and KapA accumulation in the nucleus. AreA and KapA do not seem to be interacting in the cytoplasm though there might be slight overlap next to the nucleus hinting at the potential for interaction. Overexpression of SumO led to constitutive nuclear accumulation of KapA and reversion of AreA to wild type subcellular localization patterns. We then showed that overexpression of KapA was able to overcome the loss of nuclear accumulation in a strain lacking SumO.

The last part of chapter 4 examined the TOR signaling pathway and how components of that pathway might affect accumulation. We showed that addition of the TOR inhibitor, rapamycin, prevents AreA nuclear accumulation when added before the transition to nitrogen starvation signaling. The loss of the JipA inhibitor or the SitA phosphatase led to significantly reduced nuclear accumulation during starvation. We also showed that loss of the regulation of autolysis by deleting the transcription factor *xprG* prevents AreA nuclear accumulation.

Chapter 5 analyzed the last question and explored what signals nitrogen availability and subsequently the delivery, retention, release of AreA to and from nucleus. Through analysis of AreA DNA binding mutants and nitrogen metabolic mutants we were able to

conclude that the signal is a product of nitrogen metabolism. That product most likely is the intracellular levels of either glutamine or glutamate (or a ratio of both).

As often is the case when the end of a project arrives, there are more questions to be answered now than were clear at the beginning. I would like to circle back and discuss some of those questions and potentially how they could be investigated. I have found that my thoughts have consistently landed on cellular kinetics and the role the rate of nuclear import/export is having on AreA accumulation, and subsequently the upregulation of AreA-dependent gene expression. It is known that α -importin and β -importin interact by α -importin binding to cargo, then interacting with β -importin to be imported into the nucleus. There is evidence to suggest that arginine based ncNLS are capable of directly interacting with β -importin to be imported into the nucleus (TRUONG *et al.* 2012). In addition, KapB (*A. nidulans* β -importin homologue) has been shown to be a SumO binding partner (HORIO *et al.* 2019), which indicates that it interacts with a protein bound to SumO. Furthermore, in *A. nidulans* the putative Ran homologue has been identified as a sumoylated protein. It would be logical to assume that these two proteins (KapB and Ran) would interact with each other, and it is hypothesized that the interaction between karyopherins and Ran-GTP increases the rate in which cargo is released (ROTHENBUSCH *et al.* 2012). Towards the end of this research, I constructed a functional GFP-AreA fusion protein, which behaves similarly to the HA-epitope-tagged AreA protein. This GFP-AreA fusion will allow live imaging and analysis of AreA transport dynamics in real time in future experiments. This fusion protein could be used to test if our observations in a *sumO* Δ mutant are due to a severe reduction in nuclear import or a deregulation of nuclear export. Additionally, tagging *kapA* and *kapA*^{S111F} with a different colored fluorescent tag would provide the ability to assess the kinetics of each together to better understand the dynamics. Is what we are seeing not complete loss of import but, rather, the ratio/timing of nuclear import to export is messed up? Are we seeing reduced import? Are we seeing that the loss of cargo release by potentially KapA and KapB leads to lack of nuclear import because of the loss of recycling of these two importins back to the cytoplasm. Our *sumO* Δ , KapA overexpression data suggests that this might be the case. We could also use the GFP-AreA fusion to further assess in real time the addition of nitrogen sources to nitrogen-starved cells and better understand the rate at which AreA nuclear export is triggered.

A few additional topics of exploration that would be of interest include other possible ways that KapA/AreA would get into/out of the nucleus in a SumO-independent manner. Does β -importin-independent nuclear localization via the AreA ncNLS occur? Does KapA associate with NtfA (another importin which potentially is SumO-independent). Does the redundancy in NLSs match the redundancy in the use of karyopherins as vehicles for transport and are different karyopherins used for AreA nucleocytoplasmic transport during different stress conditions?

It appears that much of this research going forward is potentially dependent on the SumO pathway. There are even potential ties to SumO in chapter 5 because LeuR (a transcription regulator which is sumoylated), which along with the leucine biosynthesis pathway transcription factor LeuB, has been shown to regulate *gdhA* and *gltA* promoters, both of which promote intracellular glutamate production (DOWNES *et al.* 2013; HORIO *et al.* 2019; STEYER *et al.* 2021). Hinting that SumO affects the ability to potentially signal intercellular nitrogen starvation and/or relief of starvation.

In conclusion, this research has established a strong basis for study of the intracellular dynamics of the GATA transcription factor AreA. It has provided answers to many questions that we began with, answers to many questions we weren't expecting, and has left us with more questions than we started with. The completionist in me finds this a trifle upsetting, yet the researcher is able to smile and understand that the work is never completed, even though the journey might be over, such is how quests to find "The Holy Grail" often end.

References

- Andrianopoulos, A., S. Kourambas, J. A. Sharp, M. A. Davis and M. J. Hynes, 1998 Characterization of the *Aspergillus nidulans nmrA* gene involved in nitrogen metabolite repression. *Journal of Bacteriology* 180: 1973-1977.
- Araujo-Bazan, L., S. Dhingra, J. Chu, J. Fernandez-Martinez, A. M. Calvo and E. A. Espeso, 2009 Importin alpha is an essential nuclear import carrier adaptor required for proper sexual and asexual development and secondary metabolism in *Aspergillus nidulans*. *Fungal Genetics and Biology* 46: 506-515.
- Araujo-Bazan, L., J. Fernandez-Martinez, V. M. Rios, O. Etxebeste, J. P. Albar, M. A. Penalva and E. A. Espeso, 2008 NapA and NapB are the *Aspergillus nidulans* Nap/SET family members and NapB is a nuclear protein specifically interacting with importin alpha. *Fungal Genetics and Biology* 45: 278-291.
- Arceci, R. J., A. A. King, M. C. Simon, S. H. Orkin and D. B. Wilson, 1993 Mouse GATA-4: a retinoic acid-inducible GATA-binding transcription factor expressed in endodermally derived tissues and heart. *Molecular and Cellular Biology* 13: 2235-2246.
- Arnaud, M. B., G. C. Cerqueira, D. O. Inglis, M. S. Skrzypek, J. Binkley, M. C. Chibucos, J. Crabtree, C. Howarth, J. Orvis, P. Shah, F. Wymore, G. Binkley, S. R. Miyasato, M. Simison, G. Sherlock and J. R. Wortman, 2012 The *Aspergillus* Genome Database (AspGD): recent developments in comprehensive multispecies curation, comparative genomics and community resources. *Nucleic Acids Research* 40: D653-659.
- Arst, H. N., 1977 Some genetical aspects of ornithine metabolism in *Aspergillus nidulans*. *Molecular and General Genetics* MGG 151: 105-110.
- Arst, H. N., and D. W. MacDonald, 1975 A gene cluster in *Aspergillus nidulans* with an internally located cis-acting regulatory region. *Nature* 254: 26-31.
- Arst Jr, H. N., and D. J. Cove, 1973 Nitrogen metabolite repression in *Aspergillus nidulans*. *Molecular and General Genetics* MGG 126: 111-141.
- Arst Jr, H. N., and D. W. MacDonald, 1973 A mutant of *Aspergillus nidulans* lacking NADP-linked glutamate dehydrogenase. *Molecular and General Genetics* MGG 122: 261-265.
- Azim, H., H. A. Azim, Jr. and B. Escudier, 2010 Targeting mTOR in cancer: renal cell is just a beginning. *Targeted Oncology* 5: 269-280.
- Bahn, Y. S., C. Xue, A. Idnurm, J. C. Rutherford, J. Heitman and M. E. Cardenas, 2007 Sensing the environment: lessons from fungi. *Nature Reviews Microbiology* 5: 57-69.

- Bauer, N. C., P. W. Doetsch and A. H. Corbett, 2015 Mechanisms regulating protein localization. *Traffic* 16: 1039-1061.
- Beck, T., and M. N. Hall, 1999 The TOR signalling pathway controls nuclear localization of nutrient-regulated transcription factors. *Nature* 402: 689-692.
- Berger, H., A. Basheer, S. Böck, Y. Reyes-Dominguez, T. Dalik, F. Altmann and J. Strauss, 2008 Dissecting individual steps of nitrogen transcription factor cooperation in the *Aspergillus nidulans* nitrate cluster. *Molecular Microbiology* 69: 1385-1398.
- Berger, H., R. Pachlinger, I. Morozov, S. Goller, F. Narendja, M. Caddick and J. Strauss, 2006 The GATA factor AreA regulates localization and in vivo binding site occupancy of the nitrate activator NirA. *Molecular Microbiology* 59: 433-446.
- Bertram, P. G., J. H. Choi, J. Carvalho, W. Ai, C. Zeng, T. F. Chan and X. F. Zheng, 2000 Tripartite regulation of Gln3p by TOR, Ure2p, and phosphatases. *Journal of Biological Chemistry* 275: 35727-35733.
- Blinder, D., P. W. Coschigano and B. Magasanik, 1996 Interaction of the GATA factor Gln3p with the nitrogen regulator Ure2p in *Saccharomyces cerevisiae*. *Journal of Bacteriology* 178: 4734-4736.
- Bradford, M. M., 1976 A rapid and sensitive method for the quantitation of microgram quantities of protein utilizing the principle of protein-dye binding. *Analytical Biochemistry* 72: 248-254.
- Braunsdorf, C., D. Mailander-Sanchez and M. Schaller, 2016 Fungal sensing of host environment. *Cellular Microbiology* 18: 1188-1200.
- Burich, R., and M. Lei, 2003 Two bipartite NLSs mediate constitutive nuclear localization of Mcm10. *Current Genetics* 44: 195-201.
- Caddick, M. X., H. N. Arst, Jr., L. H. Taylor, R. I. Johnson and A. G. Brownlee, 1986 Cloning of the regulatory gene *areA* mediating nitrogen metabolite repression in *Aspergillus nidulans*. *The EMBO Journal* 5: 1087-1090.
- Cardenas, M. E., N. S. Cutler, M. C. Lorenz, C. J. Di Como and J. Heitman, 1999 The TOR signaling cascade regulates gene expression in response to nutrients. *Genes & Development* 13: 3271-3279.
- Carvalho, J., P. G. Bertram, S. R. Wentz and X. F. Zheng, 2001 Phosphorylation regulates the interaction between Gln3p and the nuclear import factor Srp1p. *Journal of Biological Chemistry* 276: 25359-25365.

- Carvalho, J., and X. F. Zheng, 2003 Domains of Gln3p interacting with karyopherins, Ure2p, and the target of rapamycin protein. *Journal of Biological Chemistry* 278: 16878-16886.
- Chang, C. C., and K. C. Hsia, 2020 More than a zip code: global modulation of cellular function by nuclear localization signals. *The FEBS Journal*.
- Chang, P. K., J. Yu, D. Bhatnagar and T. E. Cleveland, 2000 Characterization of the *Aspergillus parasiticus* major nitrogen regulatory gene, *areA*. *Biochimica et Biophysica Acta* 1491: 263-266.
- Chen, C. F., S. Li, Y. Chen, P. L. Chen, Z. D. Sharp and W. H. Lee, 1996 The nuclear localization sequences of the BRCA1 protein interact with the importin-alpha subunit of the nuclear transport signal receptor. *Journal of Biological Chemistry* 271: 32863-32868.
- Chook, Y. M., and G. Blobel, 2001 Karyopherins and nuclear import. *Current Opinion in Structural Biology* 11: 703-715.
- Christensen, T., M. J. Hynes and M. A. Davis, 1998 Role of the regulatory gene *areA* of *Aspergillus oryzae* in nitrogen metabolism. *Applied and Environmental Microbiology* 64: 3232-3237.
- Clarke, D. F., M. A. Davis and R. B. Todd, Unpublished data.
- Clutterbuck, A. J., 1973 Gene symbols in *Aspergillus nidulans*. *Genetics Research* 21: 291-296.
- Clutterbuck, A. J., 1974 *Aspergillus nidulans*, pp. 447-510 in *Bacteria, Bacteriophages, and Fungi*. Springer.
- Coffman, J. A., R. Rai, T. Cunningham, V. Svetlov and T. G. Cooper, 1996 Gat1p, a GATA family protein whose production is sensitive to nitrogen catabolite repression, participates in transcriptional activation of nitrogen-catabolic genes in *Saccharomyces cerevisiae*. *Molecular and Cellular Biology* 16: 847-858.
- Cohen, B. L., 1972 Ammonium repression of extracellular protease in *Aspergillus nidulans*. *Journal of General Microbiology* 71: 293-299.
- Conlon, H., I. Zadra, H. Haas, H. N. Arst, Jr., M. G. Jones and M. X. Caddick, 2001 The *Aspergillus nidulans* GATA transcription factor gene *areB* encodes at least three proteins and features three classes of mutation. *Molecular Microbiology* 40: 361-375.
- Conrad, M., J. Schothorst, H. N. Kankipati, G. Van Zeebroeck, M. Rubio-Teixeira and J. M. Thevelein, 2014 Nutrient sensing and signaling in the yeast *Saccharomyces cerevisiae*. *FEMS Microbiology Reviews* 38: 254-299.

- Cove, D. J., 1966 The induction and repression of nitrate reductase in the fungus *Aspergillus nidulans*. *Biochimica et Biophysica Acta* 113: 51-56.
- Cronshaw, J. M., A. N. Krutchinsky, W. Zhang, B. T. Chait and M. J. Matunis, 2002 Proteomic analysis of the mammalian nuclear pore complex. *Journal of Cell Biology* 158: 915-927.
- Cunningham, T. S., and T. G. Cooper, 1991 Expression of the *DAL80* gene, whose product is homologous to the GATA factors and is a negative regulator of multiple nitrogen catabolic genes in *Saccharomyces cerevisiae*, is sensitive to nitrogen catabolite repression. *Molecular and Cellular Biology* 11: 6205-6215.
- Davis, M. A., C. S. Cobbett and M. J. Hynes, 1988 An *amdS-lacZ* fusion for studying gene regulation in *Aspergillus*. *Gene* 63: 199-212.
- Davis, M. A., and M. J. Hynes, 1987 Complementation of *areA*⁻ regulatory gene mutations of *Aspergillus nidulans* by the heterologous regulatory gene *nit-2* of *Neurospora crassa*. *Proceedings of the National Academy of Sciences of the United States of America* 84: 3753-3757.
- Davis, M. A., A. J. Small, S. Kourambas and M. J. Hynes, 1996 The *tamA* gene of *Aspergillus nidulans* contains a putative zinc cluster motif which is not required for gene function. *Journal of Bacteriology* 178: 3406-3409.
- De Souza, C. P., S. B. Hashmi, A. H. Osmani, P. Andrews, C. S. Ringelberg, J. C. Dunlap and S. A. Osmani, 2013 Functional analysis of the *Aspergillus nidulans* kinome. *PLoS One* 8: e58008.
- De Souza, C. P., S. B. Hashmi, A. H. Osmani and S. A. Osmani, 2014 Application of a new dual localization-affinity purification tag reveals novel aspects of protein kinase biology in *Aspergillus nidulans*. *PLoS One* 9: e90911.
- De Souza, C. P., K. P. Horn, K. Masker and S. A. Osmani, 2003 The SONB(NUP98) nucleoporin interacts with the NIMA kinase in *Aspergillus nidulans*. *Genetics* 165: 1071-1081.
- De Souza, C. P., A. H. Osmani, S. B. Hashmi and S. A. Osmani, 2004 Partial nuclear pore complex disassembly during closed mitosis in *Aspergillus nidulans*. *Current Biology* 14: 1973-1984.
- De Vit, M. J., J. A. Waddle and M. Johnston, 1997 Regulated nuclear translocation of the Mig1 glucose repressor. *Molecular Biology of the Cell* 8: 1603-1618.
- De Vries, R. P., R. Riley, A. Wiebenga, G. Aguilar-Osorio, S. Amillis, C. A. Uchima, G. Anderluh, M. Asadollahi, M. Askin, K. Barry, E. Battaglia, Ö. Bayram, T. Benocci, S. A. Braus-Stromeyer, C. Caldana, D. Cánovas, G. C. Cerqueira, F. Chen, W. Chen, C. Choi, A. Clum, R. A. C. Dos Santos, A. R. D. L. Damásio, G. Diallinas, T. Emri, E. Fekete, M. Flipphi, S.

- Freyberg, A. Gallo, C. Gournas, R. Habgood, M. Hainaut, M. L. Harispe, B. Henrissat, K. S. Hildén, R. Hope, A. Hossain, E. Karabika, L. Karaffa, Z. Karányi, N. Kraševac, A. Kuo, H. Kusch, K. Labutti, E. L. Lagendijk, A. Lapidus, A. Levasseur, E. Lindquist, A. Lipzen, A. F. Logrieco, A. Maccabe, M. R. Mäkelä, I. Malavazi, P. Melin, V. Meyer, N. Mielnichuk, M. Miskei, Á. P. Molnár, G. Mulé, C. Y. Ngan, M. Orejas, E. Orosz, J. P. Ouedraogo, K. M. Overkamp, H.-S. Park, G. Perrone, F. Piumi, P. J. Punt, A. F. J. Ram, A. Ramón, S. Rauscher, E. Record, D. M. Riaño-Pachón, V. Robert, J. Röhrig, R. Ruller, A. Salamov, N. S. Salih, R. A. Samson, E. Sándor, M. Sanguinetti, T. Schütze, K. Sepčić, E. Shelest, G. Sherlock, V. Sophianopoulou, F. M. Squina, H. Sun, A. Susca, R. B. Todd, A. Tsang, S. E. Unkles, N. Van De Wiele, D. Van Rossen-Uffink, J. V. D. C. Oliveira, T. C. Vesth, J. Visser, J.-H. Yu, M. Zhou, M. R. Andersen, D. B. Archer, S. E. Baker, I. Benoit, A. A. Brakhage, G. H. Braus, R. Fischer, J. C. Frisvad, G. H. Goldman, J. Houbroken, B. Oakley, I. Pócsi, C. Scazzocchio, B. Seiboth, P. A. Vankuyk, J. Wortman, P. S. Dyer, and I. V. Grigoriev, 2017 Comparative genomics reveals high biological diversity and specific adaptations in the industrially and medically important fungal genus *Aspergillus*. *Genome Biology* 18.
- Didion, T., B. Regenber, M. U. Jorgensen, M. C. Kielland-Brandt and H. A. Andersen, 1998 The permease homologue Ssy1p controls the expression of amino acid and peptide transporter genes in *Saccharomyces cerevisiae*. *Molecular Microbiology* 27: 643-650.
- Dingwall, C., S. V. Sharnick and R. A. Laskey, 1982 A polypeptide domain that specifies migration of nucleoplasmin into the nucleus. *Cell* 30: 449-458.
- Donaton, M. C., I. Holsbeeks, O. Lagatie, G. Van Zeebroeck, M. Crauwels, J. Winderickx and J. M. Thevelein, 2003 The Gap1 general amino acid permease acts as an amino acid sensor for activation of protein kinase A targets in the yeast *Saccharomyces cerevisiae*. *Molecular Microbiology* 50: 911-929.
- Dorfman, D. M., D. B. Wilson, G. A. Bruns and S. H. Orkin, 1992 Human transcription factor GATA-2. Evidence for regulation of preproendothelin-1 gene expression in endothelial cells. *Journal of Biological Chemistry* 267: 1279-1285.
- Downes, D. J., M. A. Davis, S. D. Kreutzberger, B. L. Taig and R. B. Todd, 2013 Regulation of the NADP-glutamate dehydrogenase gene *gdhA* in *Aspergillus nidulans* by the Zn(II)2Cys6 transcription factor LeuB. *Microbiology* 159: 2467-2480.
- Downes, D. J., M. A. Davis, K. H. Wong, S. D. Kreutzberger, M. J. Hynes and R. B. Todd, 2014 Dual DNA binding and coactivator functions of *Aspergillus nidulans* TamA, a Zn(II)2Cys6 transcription factor. *Molecular Microbiology* 92: 1198-1211.
- Durrens, P., P. M. Green, H. N. Arst Jr and C. Scazzocchio, 1986 Heterologous insertion of transforming DNA and generation of new deletions associated with transformation in *Aspergillus nidulans*. *Molecular and General Genetics* MGG 203: 544-549.

- El Alami, M., A. Feller, A. Piérard and E. Dubois, 2000 Characterisation of a tripartite nuclear localisation sequence in the regulatory protein Lys14 of *Saccharomyces cerevisiae*. *Current Genetics* 38: 78-86.
- Etxebeste, O., E. Herrero-García, L. Araújo-Bazán, A. B. Rodríguez-Urra, A. Garzia, U. Ugalde and E. A. Espeso, 2009 The bZIP-type transcription factor FlbB regulates distinct morphogenetic stages of colony formation in *Aspergillus nidulans*. *Molecular Microbiology* 73: 775-789.
- Feldherr, C. M., E. Kallenbach and N. Schultz, 1984 Movement of a karyophilic protein through the nuclear pores of oocytes. *Journal of Cell Biology* 99: 2216-2222.
- Fernández-Martínez, J., C. V. Brown, E. Díez, J. Tilburn, H. N. Arst Jr, M. Á. Peñalva and E. A. Espeso, 2003 Overlap of nuclear localisation signal and specific DNA-binding residues within the zinc finger domain of PacC. *Journal of Molecular Biology* 334: 667-684.
- Fitzgibbon, G. J., I. Y. Morozov, M. G. Jones and M. X. Caddick, 2005 Genetic analysis of the TOR pathway in *Aspergillus nidulans*. *Eukaryotic Cell* 4: 1595-1598.
- Forsberg, H., M. Hammar, C. Andreasson, A. Moliner and P. O. Ljungdahl, 2001 Suppressors of *ssy1* and *ptr3* null mutations define novel amino acid sensor-independent genes in *Saccharomyces cerevisiae*. *Genetics* 158: 973-988.
- Fraser, J. A., M. A. Davis and M. J. Hynes, 2001 The formamidase gene of *Aspergillus nidulans*: regulation by nitrogen metabolite repression and transcriptional interference by an overlapping upstream gene. *Genetics* 157: 119-131.
- Fraser, J. A., M. A. Davis and M. J. Hynes, 2002 A gene from *Aspergillus nidulans* with similarity to URE2 of *Saccharomyces cerevisiae* encodes a glutathione S-transferase which contributes to heavy metal and xenobiotic resistance. *Applied and Environmental Microbiology* 68: 2802-2808.
- Froeliger, E. H., and B. E. Carpenter, 1996 *NUT1*, a major nitrogen regulatory gene in *Magnaporthe grisea*, is dispensable for pathogenicity. *Molecular and General Genetics* MGG 251: 647-656.
- Fu, Y. H., and G. A. Marzluf, 1990 nit-2, the major positive-acting nitrogen regulatory gene of *Neurospora crassa*, encodes a sequence-specific DNA-binding protein. *Proceedings of the National Academy of Sciences of the United States of America* 87: 5331-5335.
- Galagan, J. E., S. E. Calvo, C. Cuomo, L. J. Ma, J. R. Wortman, S. Batzoglou, S. I. Lee, M. Basturkmen, C. C. Spevak, J. Clutterbuck, V. Kapitonov, J. Jurka, C. Scacciocchio, M. Farman, J. Butler, S. Purcell, S. Harris, G. H. Braus, O. Draht, S. Busch, C. D'Enfert, C. Bouchier, G. H. Goldman, D. Bell-Pedersen, S. Griffiths-Jones, J. H. Doonan, J. Yu, K. Vienken, A. Pain, M. Freitag, E. U. Selker, D. B. Archer, M. A. Penalva, B. R. Oakley, M. Momany, T. Tanaka, T. Kumagai, K. Asai, M. Machida, W. C. Nierman, D. W. Denning,

- M. Caddick, M. Hynes, M. Paoletti, R. Fischer, B. Miller, P. Dyer, M. S. Sachs, S. A. Osmani and B. W. Birren, 2005 Sequencing of *Aspergillus nidulans* and comparative analysis with *A. fumigatus* and *A. oryzae*. *Nature* 438: 1105-1115.
- Gao, X., T. Sedgwick, Y. B. Shi and T. Evans, 1998 Distinct functions are implicated for the GATA-4, -5, and -6 transcription factors in the regulation of intestine epithelial cell differentiation. *Molecular and Cellular Biology* 18: 2901-2911.
- Gente, S., N. Poussereau and M. Fevre, 1999 Isolation and expression of a nitrogen regulatory gene, *nmc*, of *Penicillium roqueforti*. *FEMS Microbiology Letters* 175: 291-297.
- Goda, H., T. Nagase, S. Tanoue, J. Sugiyama, S. Steidl, A. Tüncher, T. Kobayashi, N. Tsukagoshi, A. A. Brakhage and M. Kato, 2005 Nuclear translocation of the heterotrimeric CCAAT binding factor of *Aspergillus oryzae* is dependent on two redundant localising signals in a single subunit. *Archives of Microbiology* 184: 93-100.
- Goldfarb, D. S., A. H. Corbett, D. A. Mason, M. T. Harreman and S. A. Adam, 2004 Importin alpha: a multipurpose nuclear-transport receptor. *Trends in Cell Biology* 14: 505-514.
- Gonzalez, R., V. Gavrias, D. Gomez, C. Scazzocchio and B. Cubero, 1997 The integration of nitrogen and carbon catabolite repression in *Aspergillus nidulans* requires the GATA factor AreA and an additional positive-acting element, ADA. *The EMBO Journal* 16: 2937-2944.
- Gorlich, D., and U. Kutay, 1999 Transport between the cell nucleus and the cytoplasm. *Annual Review of Cell and Developmental Biology* 15: 607-660.
- Gough, J. A., N. E. Murray and S. Brenner, 1983 Sequence diversity among related genes for recognition of specific targets in DNA molecules. *Journal of Molecular Biology* 166: 1-19.
- Gournas, C., T. Evangelidis, A. Athanasopoulos, E. Mikros and V. Sophianopoulou, 2015 The *Aspergillus nidulans* proline permease as a model for understanding the factors determining substrate binding and specificity of fungal amino acid transporters. *Journal of Biological Chemistry* 290: 6141-6155.
- Gournas, C., M. Prévost, E.-M. Krammer and B. André, 2016 Function and regulation of fungal amino acid transporters: insights from predicted structure. *Advances in Experimental Medicine and Biology* 892: 69-106.
- Haas, H., B. Bauer, B. Redl, G. Stoffler and G. A. Marzluf, 1995 Molecular cloning and analysis of *nre*, the major nitrogen regulatory gene of *Penicillium chrysogenum*. *Current Genetics* 27: 150-158.

- Haas, H., I. Zadra, G. Stoffler and K. Angermayr, 1999 The *Aspergillus nidulans* GATA factor SREA is involved in regulation of siderophore biosynthesis and control of iron uptake. *Journal of Biological Chemistry* 274: 4613-4619.
- Han, K. H., K. Y. Han, J. H. Yu, K. S. Chae, K. Y. Jahng and D. M. Han, 2001 The *nsdD* gene encodes a putative GATA-type transcription factor necessary for sexual development of *Aspergillus nidulans*. *Molecular Microbiology* 41: 299-309.
- Hicks, G. R., and N. V. Raikhel, 1995 Nuclear localization signal binding proteins in higher plant nuclei. *Proceedings of the National Academy of Sciences of the United States of America* 92: 734-738.
- Ho, I. C., P. Vorhees, N. Marin, B. K. Oakley, S. F. Tsai, S. H. Orkin and J. M. Leiden, 1991 Human GATA-3: a lineage-restricted transcription factor that regulates the expression of the T cell receptor alpha gene. *The EMBO Journal* 10: 1187-1192.
- Hood, J. K., and P. A. Silver, 1998 Cse1p is required for export of Srp1p/importin-alpha from the nucleus in *Saccharomyces cerevisiae*. *Journal of Biological Chemistry* 273: 35142-35146.
- Horio, T., E. Szewczyk, C. E. Oakley, A. H. Osmani, S. A. Osmani and B. R. Oakley, 2019 SUMOlock reveals a more complete *Aspergillus nidulans* SUMOylome. *Fungal Genetics and Biology* 127: 50-59.
- Huang, W. Y., E. Cukerman and C. C. Liew, 1995 Identification of a GATA motif in the cardiac alpha-myosin heavy-chain-encoding gene and isolation of a human GATA-4 cDNA. *Gene* 155: 219-223.
- Hunter, C. C., K. S. Siebert, D. J. Downes, K. H. Wong, S. D. Kreutzberger, J. A. Fraser, D. F. Clarke, M. J. Hynes, M. A. Davis and R. B. Todd, 2014 Multiple nuclear localization signals mediate nuclear localization of the GATA transcription factor AreA. *Eukaryotic Cell* 13: 527-538.
- Huynh, H., H.-X. Hao, S. L. Chan, D. Chen, R. Ong, K. C. Soo, P. Pochanard, D. Yang, D. Ruddy and M. Liu, 2015 Loss of Tuberous Sclerosis Complex 2 (TSC2) is frequent in hepatocellular carcinoma and predicts response to mTORC1 inhibitor everolimus. *Molecular Cancer Therapeutics* 14: 1224-1235.
- Hynes, M. J., 1972 Mutants with altered glucose repression of amidase enzymes in *Aspergillus nidulans*. *Journal of Bacteriology* 111: 717-722.
- Hynes, M. J., 1973a Alterations in the control of glutamate uptake in mutants of *Aspergillus nidulans*. *Biochemical and Biophysical Research Communications* 54: 685-689.
- Hynes, M. J., 1973b The effect of lack of a carbon source on nitrate-reductase activity in *Aspergillus nidulans*. *Journal of General Microbiology* 79: 155-157.

- Hynes, M. J., 1974 Effects of ammonium, L-glutamate, and L-glutamine on nitrogen catabolism in *Aspergillus nidulans*. *Journal of Bacteriology* 120: 1116-1123.
- Hynes, M. J., 1975a A cis-dominant regulatory mutation affecting enzyme induction in the eukaryote *Aspergillus nidulans*. *Nature* 253: 210-212.
- Hynes, M. J., 1975b Studies on the role of the *areA* gene in the regulation of nitrogen catabolism in *Aspergillus nidulans*. *Australian Journal of Biological Sciences* 28: 301-313.
- Hynes, M. J., C. M. Corrick, J. M. Kelly and T. G. Littlejohn, 1988 Identification of the sites of action for regulatory genes controlling the *amdS* gene of *Aspergillus nidulans*. *Molecular and Cellular Biology* 8: 2589-2596.
- Ito, T., H. Kitamura, C. Uwatoko, M. Azumano, K. Itoh and J. Kuwahara, 2010 Interaction of Sp1 zinc finger with transport factor in the nuclear localization of transcription factor Sp1. *Biochemical and Biophysical Research Communications* 403: 161-166.
- Jans, D. A., C.-Y. Xiao and M. H. C. Lam, 2000 Nuclear targeting signal recognition: a key control point in nuclear transport? *BioEssays* 22: 532-544.
- Jauniaux, J. C., and M. Grenson, 1990 GAP1, the general amino acid permease gene of *Saccharomyces cerevisiae*: nucleotide sequence, protein similarity with the other bakers yeast amino acid permeases, and nitrogen catabolite repression. *European Journal of Biochemistry* 190: 39-44.
- Johnson, E. S., 2004 Protein modification by SUMO. *Annual Review of Biochemistry* 73: 355-382.
- Johnson, E. S., I. Schwienhorst, R. J. Dohmen and G. Blobel, 1997 The ubiquitin-like protein Smt3p is activated for conjugation to other proteins by an Aos1p/Uba2p heterodimer. *The EMBO Journal* 16: 5509-5519.
- Kafer, E., and G. May, 1988 *pyrG* of *Aspergillus nidulans* meiotic mapping, marker interactions and growth response. *Fungal Genetics Newsletter* 35: 13-15.
- Kalderon, D., B. L. Roberts, W. D. Richardson and A. E. Smith, 1984 A short amino acid sequence able to specify nuclear location. *Cell* 39: 499-509.
- Kamada, Y., T. Funakoshi, T. Shintani, K. Nagano, M. Ohsumi and Y. Ohsumi, 2000 Tor-mediated induction of autophagy via an Apg1 protein kinase complex. *Journal of Cell Biology* 150: 1507-1513.
- Katz, M. E., 2018 Nutrient sensing-the key to fungal p53-like transcription factors? *Fungal Genetics and Biology*.

- Katz, M. E., K. Braunberger, G. Yi, S. Cooper, H. M. Nonhebel and C. Gondro, 2013 A p53-like transcription factor similar to Ndt80 controls the response to nutrient stress in the filamentous fungus, *Aspergillus nidulans*. *F1000Research* 2: 72.
- Katz, M. E., K. S. Braunberger and J. M. Kelly, 2016 Role of HxkC, a mitochondrial hexokinase-like protein, in fungal programmed cell death. *Fungal Genetics and Biology* 97: 36-45.
- Katz, M. E., R. Buckland, C. C. Hunter and R. B. Todd, 2015 Distinct roles for the p53-like transcription factor XprG and autophagy genes in the response to starvation. *Fungal Genetics and Biology* 83: 10-18.
- Katz, M. E., K. A. Gray and B. F. Cheetham, 2006 The *Aspergillus nidulans* *xprG* (*phoG*) gene encodes a putative transcriptional activator involved in the response to nutrient limitation. *Fungal Genetics and Biology* 43: 190-199.
- Katz, M. E., and M. J. Hynes, 1989 Isolation and analysis of the acetate regulatory gene, *facB*, from *Aspergillus nidulans*. *Molecular and Cellular Biology* 9: 5696-5701.
- Kinghorn, J., and J. Pateman, 1973 NAD and NADP L-glutamate dehydrogenase activity and ammonium regulation in *Aspergillus nidulans*. *Microbiology* 78: 39-46.
- Kjærboelling, I., T. Vesth, J. C. Frisvad, J. L. Nybo, S. Theobald, S. Kildgaard, T. I. Petersen, A. Kuo, A. Sato and E. K. Lyhne, 2020 A comparative genomics study of 23 *Aspergillus* species from section *Flavi*. *Nature Communications* 11: 1-12.
- Ko, L. J., M. Yamamoto, M. W. Leonard, K. M. George, P. Ting and J. D. Engel, 1991 Murine and human T-lymphocyte GATA-3 factors mediate transcription through a cis-regulatory element within the human T-cell receptor delta gene enhancer. *Molecular and Cellular Biology* 11: 2778-2784.
- Kosugi, S., M. Hasebe, N. Matsumura, H. Takashima, E. Miyamoto-Sato, M. Tomita and H. Yanagawa, 2009 Six classes of nuclear localization signals specific to different binding grooves of importin alpha. *Journal of Biological Chemistry* 284: 478-485.
- Kotaka, M., C. Johnson, H. K. Lamb, A. R. Hawkins, J. Ren and D. K. Stammers, 2008 Structural analysis of the recognition of the negative regulator NmrA and DNA by the zinc finger from the GATA-type transcription factor AreA. *Journal of Molecular Biology* 381: 373-382.
- Kudla, B., M. X. Caddick, T. Langdon, N. M. Martinez-Rossi, C. F. Bennett, S. Sibley, R. W. Davies and H. N. Arst, Jr., 1990 The regulatory gene *areA* mediating nitrogen metabolite repression in *Aspergillus nidulans*. Mutations affecting specificity of gene activation alter a loop residue of a putative zinc finger. *The EMBO Journal* 9: 1355-1364.

- Lamb, H. K., J. Ren, A. Park, C. Johnson, K. Leslie, S. Cocklin, P. Thompson, C. Mee, A. Cooper, D. K. Stammers and A. R. Hawkins, 2004 Modulation of the ligand binding properties of the transcription repressor NmrA by GATA-containing DNA and site-directed mutagenesis. *Protein Science* 13: 3127-3138.
- Langdon, T., A. Sheerins, A. Ravagnani, M. Gielkens, M. X. Caddik and H. N. Arst Jr, 1995 Mutational analysis reveals dispensability of the N-terminal region of the *Aspergillus* transcription factor mediating nitrogen metabolite repression. *Molecular Microbiology* 17: 877-888.
- Latchman, D. S., 1997 Transcription factors: An overview. *The International Journal of Biochemistry & Cell Biology* 29: 1305-1312.
- Lee, M. E., D. H. Temizer, J. A. Clifford and T. Quertermous, 1991 Cloning of the GATA-binding protein that regulates endothelin-1 gene expression in endothelial cells. *Journal of Biological Chemistry* 266: 16188-16192.
- Lee, S. B., and J. W. Taylor, 1990 Isolation of DNA from fungal mycelia and single spores, pp. 282-287 in *PCR Protocols, a guide to methods and applications*, edited by M. A. Innis, D. H. Gelfand, J. S. Sninsky and T. J. White. Academic Press, San Diego, CA.
- Li, A., C. Parsania, K. Tan, R. B. Todd and K. H. Wong, 2021 Co-option of an extracellular protease for transcriptional control of nutrient degradation in the fungus *Aspergillus nidulans*. *Communications Biology* 4: 1409.
- Li, S. J., Y. Qi, J. J. Zhao, Y. Li, X. Y. Liu, X. H. Chen and P. Xu, 2013 Characterization of nuclear localization signals (NLSs) and function of NLSs and phosphorylation of serine residues in subcellular and subnuclear localization of transformer-2 β (Tra2 β). *Journal of Biological Chemistry* 288: 8898-8909.
- Ljungdahl, P. O., and B. Daignan-Fornier, 2012 Regulation of amino acid, nucleotide, and phosphate metabolism in *Saccharomyces cerevisiae*. *Genetics* 190: 885-929.
- Luo, M., C. W. Pang, A. E. Gerken and T. G. Brock, 2004 Multiple nuclear localization sequences allow modulation of 5-lipoxygenase nuclear import. *Traffic* 5: 847-854.
- MacCabe, A. P., S. Vanhanen, M. D. Sollewign Gelpke, P. J. van de Vondervoort, H. N. Arst, Jr. and J. Visser, 1998 Identification, cloning and sequence of the *Aspergillus niger areA* wide domain regulatory gene controlling nitrogen utilisation. *Biochimica et Biophysica Acta* 1396: 163-168.
- Macheda, M. L., M. J. Hynes and M. A. Davis, 1999 The *Aspergillus nidulans gltA* gene encoding glutamate synthase is required for ammonium assimilation in the absence of NADP-glutamate dehydrogenase. *Current Genetics* 34: 467-471.

- Makita, T., Y. Katsuyama, S. Tani, H. Suzuki, N. Kato, R. B. Todd, M. J. Hynes, N. Tsukagoshi, M. Kato and T. Kobayashi, 2009 Inducer-dependent nuclear localization of a Zn(II)(2)Cys(6) transcriptional activator, AmyR, in *Aspergillus nidulans*. *Bioscience, Biotechnology, and Biochemistry* 73: 391-399.
- Margelis, S., C. D'Souza, A. J. Small, M. J. Hynes, T. H. Adams and M. A. Davis, 2001 Role of glutamine synthetase in nitrogen metabolite repression in *Aspergillus nidulans*. *Journal of Bacteriology* 183: 5826-5833.
- Markina-Inarrairaegui, A., O. Etxebeste, E. Herrero-Garcia, L. Araujo-Bazan, J. Fernandez-Martinez, J. A. Flores, S. A. Osmani and E. A. Espeso, 2011 Nuclear transporters in a multinucleated organism: functional and localization analyses in *Aspergillus nidulans*. *Molecular Biology of the Cell* 22: 3874-3886.
- Marzluf, G. A., 1997 Genetic regulation of nitrogen metabolism in the fungi. *Microbiology and Molecular Biology Reviews* 61: 17-32.
- Mattaj, I. W., and L. Englmeier, 1998 Nucleocytoplasmic transport: the soluble phase. *Annual Review of Biochemistry* 67: 265-306.
- McCluskey, K., A. Wiest and M. Plamann, 2010 The Fungal Genetics Stock Center: a repository for 50 years of fungal genetics research. *Journal of Biosciences* 35: 119-126.
- Michielse, C. B., A. Pfannmuller, M. Macios, P. Rengers, A. Dzikowska and B. Tudzynski, 2013 The interplay between the GATA transcription factors AreA, the global nitrogen regulator and AreB in *Fusarium fujikuroi*. *Molecular Microbiology*.
- Minehart, P. L., and B. Magasanik, 1991 Sequence and expression of *GLN3*, a positive nitrogen regulatory gene of *Saccharomyces cerevisiae* encoding a protein with a putative zinc finger DNA-binding domain. *Molecular and Cellular Biology* 11: 6216-6228.
- Mingot, J. M., E. A. Espeso, E. Diez and M. A. Penalva, 2001 Ambient pH signaling regulates nuclear localization of the *Aspergillus nidulans* PacC transcription factor. *Molecular and Cellular Biology* 21: 1688-1699.
- Monahan, B. J., M. C. Askin, M. J. Hynes and M. A. Davis, 2006 Differential expression of *Aspergillus nidulans* ammonium permease genes is regulated by GATA transcription factor AreA. *Eukaryotic Cell* 5: 226-237.
- Monahan, B. J., J. A. Fraser, M. J. Hynes and M. A. Davis, 2002a Isolation and characterization of two ammonium permease genes, *meaA* and *mepA*, from *Aspergillus nidulans*. *Eukaryotic Cell* 1: 85-94.
- Monahan, B. J., S. E. Unkles, I. T. Tsing, J. R. Kinghorn, M. J. Hynes and M. A. Davis, 2002b Mutation and functional analysis of the *Aspergillus nidulans* ammonium permease

- MeaA and evidence for interaction with itself and MepA. *Fungal Genetics and Biology* 36: 35-46.
- Morozov, I. Y., M. Galbis-Martinez, M. G. Jones and M. X. Caddick, 2001 Characterization of nitrogen metabolite signalling in *Aspergillus* via the regulated degradation of *areA* mRNA. *Molecular Microbiology* 42: 269-277.
- Morozov, I. Y., M. G. Jones, A. A. Razak, D. J. Rigden and M. X. Caddick, 2010 CUCU modification of mRNA promotes decapping and transcript degradation in *Aspergillus nidulans*. *Molecular and Cellular Biology* 30: 460-469.
- Morozov, I. Y., M. G. Martinez, M. G. Jones and M. X. Caddick, 2000 A defined sequence within the 3' UTR of the *areA* transcript is sufficient to mediate nitrogen metabolite signalling via accelerated deadenylation. *Molecular Microbiology* 37: 1248-1257.
- Nakai, K., and P. Horton, 1999 PSORT: a program for detecting sorting signals in proteins and predicting their subcellular localization. *Trends Biochem Sci* 24: 34-36.
- Nayak, T., E. Szewczyk, C. E. Oakley, A. Osmani, L. Ukil, S. L. Murray, M. J. Hynes, S. A. Osmani and B. R. Oakley, 2006 A versatile and efficient gene-targeting system for *Aspergillus nidulans*. *Genetics* 172: 1557-1566.
- Nikolaev, I., M.-F. Cochet and B. Felenbok, 2003 Nuclear import of zinc binuclear cluster proteins proceeds through multiple, overlapping transport pathways. *Eukaryotic Cell* 2: 209-221.
- Oakley, C. E., C. F. Weil, P. L. Kretz and B. R. Oakley, 1987 Cloning of the *riboB* locus of *Aspergillus nidulans*. *Gene* 53: 293-298.
- Oiartzabal-Arano, E., E. Perez-de-Nanclares-Arregi, E. A. Espeso and O. Etxebeste, 2016 Apical control of conidiation in *Aspergillus nidulans*. *Current Genetics* 62: 371-377.
- Osmani, A. H., J. Davies, H. L. Liu, A. Nile and S. A. Osmani, 2006 Systematic deletion and mitotic localization of the nuclear pore complex proteins of *Aspergillus nidulans*. *Molecular Biology of the Cell* 17: 4946-4961.
- Peleg, Y., R. Addison, R. Aramayo and R. L. Metzenberg, 1996 Translocation of *Neurospora crassa* transcription factor NUC-1 into the nucleus is induced by phosphorus limitation. *Fungal Genetics and Biology* 20: 185-191.
- Perez-de-Nanclares-Arregi, E., and O. Etxebeste, 2014 Photo-convertible tagging for localization and dynamic analyses of low-expression proteins in filamentous fungi. *Fungal Genetics and Biology* 70: 33-41.
- Philips, A. S., J. C. Kwok and B. H. Chong, 2007 Analysis of the signals and mechanisms mediating nuclear trafficking of GATA-4. Loss of DNA binding is associated with

- localization in intranuclear speckles. *Journal of Biological Chemistry* 282: 24915-24927.
- Pinar, M., A. Pantazopoulou and M. A. Penalva, 2013 Live-cell imaging of *Aspergillus nidulans* autophagy: RAB1 dependence, Golgi independence and ER involvement. *Autophagy* 9: 1024-1043.
- Platt, A., T. Langdon, H. N. Arst, Jr., D. Kirk, D. Tollervey, J. M. Sanchez and M. X. Caddick, 1996a Nitrogen metabolite signalling involves the C-terminus and the GATA domain of the *Aspergillus* transcription factor AREA and the 3' untranslated region of its mRNA. *The EMBO Journal* 15: 2791-2801.
- Platt, A., A. Ravagnani, H. Arst, Jr., D. Kirk, T. Langdon and M. X. Caddick, 1996b Mutational analysis of the C-terminal region of AREA, the transcription factor mediating nitrogen metabolite repression in *Aspergillus nidulans*. *Molecular and General Genetics MGG* 250: 106-114.
- Pokorska, A., C. Drevet and C. Scazzocchio, 2000 The analysis of the transcriptional activator PrnA reveals a tripartite nuclear localisation sequence. *Journal of Molecular Biology* 298: 585-596.
- Polkinghorne, M., and M. Hynes, 1975 Mutants affecting histidine utilization in *Aspergillus nidulans*. *Genetics Research* 25: 119-135.
- Pontecorvo, G., J. A. Roper, L. M. Chemmons, K. D. Macdonald and A. W. J. Bufton, 1953 *The Genetics of Aspergillus nidulans*, pp. 141-238.
- Poon, I. K., and D. A. Jans, 2005 Regulation of nuclear transport: central role in development and transformation? *Traffic* 6: 173-186.
- Purschwitz, J., S. Muller, C. Kastner, M. Schoser, H. Haas, E. A. Espeso, A. Atoui, A. M. Calvo and R. Fischer, 2008 Functional and physical interaction of blue- and red-light sensors in *Aspergillus nidulans*. *Current Biology* 18: 255-259.
- Ramos, J., H. Sychrova and M. Kschischo, 2016 *Yeast Membrane Transport*. Springer.
- Ravagnani, A., L. Gorfinkiel, T. Langdon, G. Diallinas, E. Adjadj, S. Demais, D. Gorton, H. N. Arst, Jr. and C. Scazzocchio, 1997 Subtle hydrophobic interactions between the seventh residue of the zinc finger loop and the first base of an HGATAR sequence determine promoter-specific recognition by the *Aspergillus nidulans* GATA factor AreA. *The EMBO Journal* 16: 3974-3986.
- Reisenauer, M. R., S. W. Wang, Y. Xia and W. Zhang, 2010 Dot1a contains three nuclear localization signals and regulates the epithelial Na⁺ channel (ENaC) at multiple levels. *The American Journal of Physiology - Renal Physiology* 299: F63-76.

- Robbins, J., S. M. Dilworth, R. A. Laskey and C. Dingwall, 1991 Two interdependent basic domains in nucleoplasmin nuclear targeting sequence: identification of a class of bipartite nuclear targeting sequence. *Cell* 64: 615-623.
- Rothenbusch, U., M. Sawatzki, Y. Chang, S. Caesar and G. Schlenstedt, 2012 Sumoylation regulates Kap114-mediated nuclear transport. *The EMBO Journal* 31: 2461-2472.
- Rout, M. P., and J. D. Aitchison, 2000 Pore relation: nuclear pore complexes and nucleocytoplasmic exchange. *Essays in Biochemistry* 36: 75-88.
- Sambrook, J., E. F. Fritsch and T. Maniatis, 1989 *Molecular cloning: a laboratory manual*. Cold Spring Harbor Laboratory Press, Cold Spring Harbor, N.Y.
- Sambrook, J., and D. W. Russell, 2001 *Molecular cloning: a laboratory manual*. Cold Spring Harbor Laboratory Press, Cold Spring Harbor, N.Y.
- Sarbassov, D. D., S. M. Ali and D. M. Sabatini, 2005 Growing roles for the mTOR pathway. *Current Opinion in Cell Biology* 17: 596-603.
- Scazzocchio, C., 2000 The fungal GATA factors. *Current Opinion in Microbiology* 3: 126-131.
- Schinko, T., H. Berger, W. Lee, A. Gallmetzer, K. Pirker, R. Pachlinger, I. Buchner, T. Reichenauer, U. Guldener and J. Strauss, 2010 Transcriptome analysis of nitrate assimilation in *Aspergillus nidulans* reveals connections to nitric oxide metabolism. *Molecular Microbiology* 78: 720-738.
- Small, A. J., M. J. Hynes and M. A. Davis, 1999 The TamA protein fused to a DNA-binding domain can recruit AreA, the major nitrogen regulatory protein, to activate gene expression in *Aspergillus nidulans*. *Genetics* 153: 95-105.
- Small, A. J., R. B. Todd, M. C. Zanker, S. Delimitrou, M. J. Hynes and M. A. Davis, 2001 Functional analysis of TamA, a coactivator of nitrogen-regulated gene expression in *Aspergillus nidulans*. *Molecular Genetics and Genomics* 265: 636-646.
- Soussi-Boudekou, S., S. Vissers, A. Urrestarazu, J. C. Jauniaux and B. Andre, 1997 Gzf3p, a fourth GATA factor involved in nitrogen-regulated transcription in *Saccharomyces cerevisiae*. *Molecular Microbiology* 23: 1157-1168.
- Stade, K., F. Vogel, I. Schwienhorst, B. Meusser, C. Volkwein, B. Nentwig, R. J. Dohmen and T. Sommer, 2002 A lack of SUMO conjugation affects cNLS-dependent nuclear protein import in yeast. *Journal of Biological Chemistry* 277: 49554-49561.
- Starich, M. R., M. Wikstrom, H. N. Arst, Jr., G. M. Clore and A. M. Gronenborn, 1998 The solution structure of a fungal AREA protein-DNA complex: an alternative binding mode for the basic carboxyl tail of GATA factors. *Journal of Molecular Biology* 277: 605-620.

- Steidl, S., A. Tuncher, H. Goda, C. Guder, N. Papadopoulou, T. Kobayashi, N. Tsukagoshi, M. Kato and A. A. Brakhage, 2004 A single subunit of a heterotrimeric CCAAT-binding complex carries a nuclear localization signal: piggy back transport of the pre-assembled complex to the nucleus. *Journal of Molecular Biology* 342: 515-524.
- Steyer, J. T., D. J. Downes, C. C. Hunter, P. A. Migeon and R. B. Todd, 2021 Duplication and functional divergence of branched-chain amino acid biosynthesis genes in *Aspergillus nidulans*. *mBio* 12: e0076821.
- Stinnett, S. M., E. A. Espeso, L. Cobeno, L. Araujo-Bazan and A. M. Calvo, 2007 *Aspergillus nidulans* VeA subcellular localization is dependent on the importin alpha carrier and on light. *Molecular Microbiology* 63: 242-255.
- Strambio-De-Castillia, C., M. Niepel and M. P. Rout, 2010 The nuclear pore complex: bridging nuclear transport and gene regulation. *Nature Reviews Molecular Cell Biology* 11: 490-501.
- Suelmann, R., N. Sievers and R. Fischer, 1997 Nuclear traffic in fungal hyphae: in vivo study of nuclear migration and positioning in *Aspergillus nidulans*. *Molecular Microbiology* 25: 757-769.
- Suresh, S., and S. A. Osmani, 2019 Poring over chromosomes: mitotic nuclear pore complex segregation. *Current Opinion in Cell Biology* 58: 42-49.
- Suzuki, E., T. Evans, J. Lowry, L. Truong, D. W. Bell, J. R. Testa and K. Walsh, 1996 The human GATA-6 gene: structure, chromosomal location, and regulation of expression by tissue-specific and mitogen-responsive signals. *Genomics* 38: 283-290.
- Tabb, M. M., P. Tongaonkar, L. Vu and M. Nomura, 2000 Evidence for separable functions of Srp1p, the yeast homolog of importin α (Karyopherin α): role for Srp1p and Sts1p in protein degradation. *Molecular and cellular biology* 20: 6062-6073.
- Tanaka, K., J. Nishide, K. Okazaki, H. Kato, O. Niwa, T. Nakagawa, H. Matsuda, M. Kawamukai and Y. Murakami, 1999 Characterization of a fission yeast SUMO-1 homologue, pmt3p, required for multiple nuclear events, including the control of telomere length and chromosome segregation. *Molecular and Cellular Biology* 19: 8660-8672.
- Tate, J. J., E. A. Tolley and T. G. Cooper, 2019 Sit4 and PP2A dephosphorylate nitrogen catabolite repression-sensitive Gln3 when TorC1 is up- as well as downregulated. *Genetics* 212: 1205-1225.
- Tavoularis, S. N., U. H. Tazebay, G. Diallinas, M. Sideridou, A. Rosa, C. Scazzocchio and V. Sophianopoulou, 2003 Mutational analysis of the major proline transporter (PrnB) of *Aspergillus nidulans*. *Molecular Membrane Biology* 20: 285-297.

- Tazebay, U. H., V. Sophianopoulou, C. Scazzocchio and G. Diallinas, 1997 The gene encoding the major proline transporter of *Aspergillus nidulans* is upregulated during conidiospore germination and in response to proline induction and amino acid starvation. *Molecular Microbiology* 24: 105-117.
- Thompson, J. D., T. J. Gibson and D. G. Higgins, 2002 Multiple sequence alignment using ClustalW and ClustalX. *Current Protocols in Bioinformatics* 00: 2.3.1–2.3.22.
- Todd, R. B., Personal Communication.
- Todd, R. B., Unpublished data.
- Todd, R. B., 2016 Regulation of fungal nitrogen metabolism, pp. 281-303 in *The Mycota III: Biochemistry and Molecular Biology*, edited by D. Hoffmeister. Springer International Publishing, Switzerland
- Todd, R. B., M. A. Davis and M. J. Hynes, 2007a Genetic manipulation of *Aspergillus nidulans*: heterokaryons and diploids for dominance, complementation and haploidization analyses. *Nature Protocols* 2: 822-830.
- Todd, R. B., M. A. Davis and M. J. Hynes, 2007b Genetic manipulation of *Aspergillus nidulans*: meiotic progeny for genetic analysis and strain construction. *Nature Protocols* 2: 811-821.
- Todd, R. B., J. A. Fraser, K. H. Wong, M. A. Davis and M. J. Hynes, 2005 Nuclear accumulation of the GATA factor AreA in response to complete nitrogen starvation by regulation of nuclear export. *Eukaryotic Cell* 4: 1646-1653.
- Todd, R. B., M. Zhou, R. A. Ohm, H. A. Leeggangers, L. Visser and R. P. de Vries, 2014 Prevalence of transcription factors in ascomycete and basidiomycete fungi. *BMC Genomics* 15: 214.
- Tomsett, A. B., and D. J. Cove, 1979 Deletion mapping of the *niiA niaD* gene region of *Aspergillus nidulans*. *Genetics Research* 34: 19-32.
- Trainor, C. D., T. Evans, G. Felsenfeld and M. S. Boguski, 1990 Structure and evolution of a human erythroid transcription factor. *Nature* 343: 92-96.
- Tran, E. J., T. A. Bolger and S. R. Wentz, 2007 SnapShot: nuclear transport. *Cell* 131: 420.
- Truong, K., T. D. Lee, B. Li and Y. Chen, 2012 Sumoylation of SAE2 C terminus regulates SAE nuclear localization. *Journal of Biological Chemistry* 287: 42611-42619.
- Tudzynski, B., 2014 Nitrogen regulation of fungal secondary metabolism in fungi. *Frontiers in Microbiology* 5: 656.

- Tudzynski, B., V. Homann, B. Feng and G. A. Marzluf, 1999 Isolation, characterization and disruption of the *areA* nitrogen regulatory gene of *Gibberella fujikuroi*. *Molecular & general genetics* : MGG 261: 106-114.
- Tuncher, A., P. Sprote, A. Gehrke and A. A. Brakhage, 2005 The CCAAT-binding complex of eukaryotes: evolution of a second NLS in the HapB subunit of the filamentous fungus *Aspergillus nidulans* despite functional conservation at the molecular level between yeast, *A. nidulans* and human. *Journal of Molecular Biology* 352: 517-533.
- van den Berg, B., A. Chembath, D. Jefferies, A. Basle, S. Khalid and J. C. Rutherford, 2016 Structural basis for Mep2 ammonium transceptor activation by phosphorylation. *Nature Communications* 7: 11337.
- Van Nuland, A., P. Vandormael, M. Donaton, M. Alenquer, A. Lourenco, E. Quintino, M. Versele and J. M. Thevelein, 2006 Ammonium permease-based sensing mechanism for rapid ammonium activation of the protein kinase A pathway in yeast. *Molecular Microbiology* 59: 1485-1505.
- Weirauch, M. T., and T. R. Hughes, 2011 A catalogue of eukaryotic transcription factor types, their evolutionary origin, and species distribution, pp. 25-73 in *Subcellular Biochemistry: A Handbook of Transcription Factors*, edited by T. R. Hughes. Springer Science+Business Media B.V. 2011.
- Wilson, R. A., and H. N. Arst, Jr., 1998 Mutational analysis of AREA, a transcriptional activator mediating nitrogen metabolite repression in *Aspergillus nidulans* and a member of the "streetwise" GATA family of transcription factors. *Microbiology and Molecular Biology Reviews* 62: 586-596.
- Winey, M., D. Yarar, T. Giddings and D. Mastronarde, 1997 Nuclear pore complex number and distribution throughout the *Saccharomyces cerevisiae* cell cycle by three-dimensional reconstruction from electron micrographs of nuclear envelopes. *Molecular Biology of the Cell* 8: 2119-2132.
- Wong, K. H., 2007 Regulation of nitrogen metabolite repression in *Aspergillus nidulans* Transcriptional and post-translational controls of *areA* and *nmrA*, pp. 250 in *Department of Genetics*. University of Melbourne.
- Wong, K. H., M. J. Hynes and M. A. Davis, 2008a Recent advances in nitrogen regulation: a comparison between *Saccharomyces cerevisiae* and filamentous fungi. *Eukaryotic Cell* 7: 917-925.
- Wong, K. H., M. J. Hynes, R. B. Todd and M. A. Davis, 2007 Transcriptional control of *nmrA* by the bZIP transcription factor MeaB reveals a new level of nitrogen regulation in *Aspergillus nidulans*. *Molecular Microbiology* 66: 534-551.

- Wong, K. H., R. B. Todd, B. R. Oakley, C. E. Oakley, M. J. Hynes and M. A. Davis, 2008b Sumoylation in *Aspergillus nidulans*: *sumO* inactivation, overexpression and live-cell imaging. *Fungal Genetics and Biology* 45: 728-737.
- Wu, B., K. Ottow, P. Poulsen, R. F. Gaber, E. Albers and M. C. Kielland-Brandt, 2006 Competitive intra-and extracellular nutrient sensing by the transporter homologue Ssy1p. *Journal of Cell Biology* 173: 327-331.
- Xiao, S. J., L. Y. Wang, M. Kimura, H. Kojima, H. Kunimoto, F. Nishiumi, N. Yamamoto, K. Nishio, S. Fujimoto, T. Kato, S. Kitagawa, H. Yamane, K. Nakajima and A. Inoue, 2013 S1-1/RBM10: multiplicity and cooperativity of nuclear localisation domains. *Biology of the Cell* 105: 162-174.
- Xie, Z., and D. J. Klionsky, 2007 Autophagosome formation: core machinery and adaptations. *Nature Cell Biology* 9: 1102-1109.
- Xu, S., Y. Cai and Y. Wei, 2014 mTOR signaling from cellular senescence to organismal aging. *Aging and Disease* 5: 263.
- Yano, K., K. Morotomi, H. Saito, M. Kato, F. Matsuo and Y. Miki, 2000 Nuclear localization signals of the BRCA2 protein. *Biochemical and Biophysical Research Communications* 270: 171-175.
- Yu, F., Q. Gu, Y. Yun, Y. Yin, J. R. Xu, W. B. Shim and Z. Ma, 2014 The TOR signaling pathway regulates vegetative development and virulence in *Fusarium graminearum*. *New Phytologist* 203: 219-232.
- Zadra, I., B. Abt, W. Parson and H. Haas, 2000 *xylP* promoter-based expression system and its use for antisense downregulation of the *Penicillium chrysogenum* nitrogen regulator NRE. *Applied and Environmental Microbiology* 66: 4810-4816.
- Zhang, W., G. Du, J. Zhou and J. Chen, 2018 Regulation of sensing, transportation, and catabolism of nitrogen sources in *Saccharomyces cerevisiae*. *Microbiology and Molecular Biology Reviews* 82.
- Zhao, X., S. L. Hume, C. Johnson, P. Thompson, J. Huang, J. Gray, H. K. Lamb and A. R. Hawkins, 2010 The transcription repressor NmrA is subject to proteolysis by three *Aspergillus nidulans* proteases. *Protein Science* 19: 1405-1419.
- Zon, L. I., S. F. Tsai, S. Burgess, P. Matsudaira, G. A. Bruns and S. H. Orkin, 1990 The major human erythroid DNA-binding protein (GF-1): primary sequence and localization of the gene to the X chromosome. *Proceedings of the National Academy of Sciences of the United States of America* 87: 668-672.

Appendix A - Hunter *et al.*, 2014

Research conducted as part of this dissertation from Chapter 3 “Nuclear Localization of the GATA transcription factor AreA” has been published in Hunter, C. C., K. S. Siebert, D. J. Downes, K. H. Wong, S. D. Kreutzberger, J. A. Fraser, D. F. Clarke, M. J. Hynes, M. A. Davis and R. B. Todd, 2014 Multiple nuclear localization signals mediate nuclear localization of the GATA transcription factor AreA. *Eukaryotic Cell* 13: 527-538. The full article is included in this appendix.

**Multiple Nuclear Localization Signals
Mediate Nuclear Localization of the GATA
Transcription Factor AreA**

Cameron C. Hunter, Kendra S. Siebert, Damien J. Downes,
Koon Ho Wong, Sara D. Kreutzberger, James A. Fraser,
David F. Clarke, Michael J. Hynes, Meryl A. Davis and
Richard B. Todd

Eukaryotic Cell 2014, 13(4):527. DOI: 10.1128/EC.00040-14.
Published Ahead of Print 21 February 2014.

Updated information and services can be found at:
<http://ec.asm.org/content/13/4/527>

These include:

REFERENCES

This article cites 92 articles, 33 of which can be accessed free
at: <http://ec.asm.org/content/13/4/527#ref-list-1>

CONTENT ALERTS

Receive: RSS Feeds, eTOCs, free email alerts (when new
articles cite this article), [more»](#)

Information about commercial reprint orders: <http://journals.asm.org/site/misc/reprints.xhtml>
To subscribe to to another ASM Journal go to: <http://journals.asm.org/site/subscriptions/>

Multiple Nuclear Localization Signals Mediate Nuclear Localization of the GATA Transcription Factor AreA

Cameron C. Hunter,^a Kendra S. Siebert,^a Damien J. Downes,^a Koon Ho Wong,^{b*} Sara D. Kreutzberger,^{b*} James A. Fraser,^{b*} David F. Clarke,^{b*} Michael J. Hynes,^b Meryl A. Davis,^b Richard B. Todd^{a,b}

Department of Plant Pathology, Kansas State University, Manhattan, Kansas, USA^a; Department of Genetics, The University of Melbourne, Parkville, VIC, Australia^b

The *Aspergillus nidulans* GATA transcription factor AreA activates transcription of nitrogen metabolic genes in response to nitrogen limitation and is known to accumulate in the nucleus during nitrogen starvation. Sequence analysis of AreA revealed multiple nuclear localization signals (NLSs), five putative classical NLSs conserved in fungal AreA orthologs but not in the *Saccharomyces cerevisiae* functional orthologs Gln3p and Gat1p, and one putative noncanonical RRX₃₃RXR bipartite NLS within the DNA-binding domain. In order to identify the functional NLSs in AreA, we constructed *areA* mutants with mutations in individual putative NLSs or combinations of putative NLSs and strains expressing green fluorescent protein (GFP)-AreA NLS fusion genes. Deletion of all five classical NLSs individually or collectively did not affect utilization of nitrogen sources or AreA-dependent gene expression and did not prevent AreA nuclear localization. Mutation of the bipartite NLS conferred the inability to utilize alternative nitrogen sources and abolished AreA-dependent gene expression likely due to effects on DNA binding but did not prevent AreA nuclear localization. Mutation of all six NLSs simultaneously prevented AreA nuclear accumulation. The bipartite NLS alone strongly directed GFP to the nucleus, whereas the classical NLSs collaborated to direct GFP to the nucleus. Therefore, AreA contains multiple conserved NLSs, which show redundancy and together function to mediate nuclear import. The noncanonical bipartite NLS is conserved in GATA factors from *Aspergillus*, yeast, and mammals, indicating an ancient origin.

Eukaryotic transcription factors are synthesized in the cytoplasm but function in the nucleus to regulate gene expression. This provides a logistical problem for these proteins, as they must be imported into the nucleus for function. Proteins enter the nucleus through the nuclear pore complex (NPC) (1). Depending on the size of the protein, they can either passively diffuse through the pore (<30 kDa), or they must be actively transported through the NPC (>30 kDa) (2, 3). The NPC has been thoroughly studied in *Aspergillus nidulans* and is a dynamic structure of essential and nonessential proteins (4–6). Transport of large proteins through the NPC is facilitated by nuclear importins (karyopherins), which recognize short stretches of positively charged sequences on the cargo proteins that serve as nuclear localization signals (NLSs) (7–10). *A. nidulans* has 17 karyopherins to actively transport proteins between the cytoplasm and the nucleus (11, 12). There are two main types of classical NLSs found in eukaryotes, monopartite NLSs and bipartite NLSs. The monopartite NLSs conform to the classical simian virus 40 (SV40) large T-antigen NLS and are the most commonly found NLS type (9). The classical bipartite NLSs comprise two distinct lysine-rich parts generally separated by 10 to 12 amino acids (13). Other NLS types are known, including tripartite NLSs associated with the zinc binuclear clusters of *Saccharomyces cerevisiae* Lys14p, *A. nidulans* PrnA, AlcR, and NirA (14–17), and a noncanonical arginine-based bipartite NLS (RRX₃₃RXR) discovered in mammalian GATA-4 (10).

Although most nuclear proteins contain a single NLS, some nuclear proteins lacking a NLS are thought to enter the nucleus by piggybacking as a preassembled complex with a protein containing a NLS, as proposed for *A. nidulans* HapC and HapE, which associate with the NLS-containing protein HapB for nuclear import (18). In other cases, two or more NLSs occur within a single protein. Two NLSs were found in *A. nidulans* HapB, *S. cerevisiae* Gln3p, *S. cerevisiae* Mcm10p, human BRCA1, and human BRCA2

(19–23), whereas three NLSs were found in mammalian 5-lipoxygenase, human S1-1/RBM10, human Dot1a, and human Tra2β (24–27). As far as we know, there is no reported example of a nuclear protein with more than three NLSs.

While localization to the proper subcellular compartment constitutes a logistical problem, it also provides a platform for regulating protein function. A number of examples of regulated nuclear localization of transcription factors are known, e.g., *S. cerevisiae* Gln3p, Msn2p, and Mig1p (28, 29), *Neurospora crassa* NUC1 (30), and *A. nidulans* AmyR, PacC, and NirA (17, 31, 32). Regulated localization of nuclear proteins can be achieved by altering the balance of nuclear import and nuclear export using multiple mechanisms including direct covalent modification of targeting sequences to prevent or promote transport, cytoplasmic or nucleoplasmic anchoring, and by intramolecular or intermolecular masking of the NLS or nuclear export signal (NES) (33). Covalent modification by phosphorylation and cytoplasmic anchoring both regulate nuclear import of *S. cerevisiae* Gln3p (20,

Received 11 February 2014 Accepted 19 February 2014

Published ahead of print 21 February 2014

Address correspondence to Richard B. Todd, rbtodd@k-state.edu.

* Present address: Koon Ho Wong, Faculty of Health Sciences, University of Macau, Macau SAR, China; Sara D. Kreutzberger, Rand Farm Supplies, Rand, NSW, Australia; James A. Fraser, Australian Infectious Diseases Research Centre, School of Chemistry and Molecular Biosciences, The University of Queensland, Brisbane, QLD, Australia; David F. Clarke, CSIRO Ecosystem Sciences, Acton, ACT, Australia.

This article is contribution 14-064-J from the Kansas Agricultural Experiment Station.

Copyright © 2014, American Society for Microbiology. All Rights Reserved.

doi:10.1128/EC.00040-14

28, 34), whereas nuclear localization of *A. nidulans* PacC and AmyR is regulated by intramolecular masking (31, 32).

GATA transcription factors regulate transcription of genes involved in a range of processes, including hematopoiesis and cardiac development in mammals, as well as nitrogen metabolism, iron siderophore metabolism, sexual development, and light response in fungi (35). They have a zinc finger DNA-binding domain composed of four cysteine residues and bind to the HGATAR consensus sequence (35). In *A. nidulans*, the GATA transcription factor AreA is responsible for expression of genes subject to nitrogen metabolite repression (36). When cells are grown under nitrogen limiting conditions, AreA activity is partially derepressed due to increased levels of *areA* transcription and stability of *areA* mRNA compared with nitrogen-sufficient conditions (37–40). AreA activity is further increased during nitrogen limitation due to reduced activity of the NmrA corepressor (41–45). An additional level of control is observed during nitrogen starvation. AreA accumulates in the nucleus when cells are nitrogen starved, and this is accompanied by elevated AreA-dependent gene expression (46). Within minutes of addition of a nitrogen nutrient, accumulated AreA is rapidly exported from the nucleus, and elevated AreA-dependent gene expression is attenuated (46). This rapid response identifies nuclear export as the mechanism of regulation of AreA nuclear accumulation. Regulated nuclear localization has now also been shown for the AreA ortholog in *Fusarium fujikuroi* (47).

Nuclear import is clearly critical for AreA function. Despite the importance, the mechanism of AreA nuclear import is not known. Herein we identify and characterize the nuclear localization signals in AreA. We show that the AreA protein contains five classical monopartite NLSs, which are conserved in most ascomycete AreA orthologs, and a noncanonical bipartite NLS conserved with the RRX₃₃RXR NLS of mammalian GATA-4 (10). We determine the effects of mutations affecting these NLSs on AreA function and nuclear localization. When these classical NLSs are deleted separately or when point mutations are introduced in place of the four key arginines in the bipartite NLS, nuclear accumulation is not disrupted. However, when all of the NLSs are mutated simultaneously, we found no accumulation of AreA in the nucleus. We also fused the NLSs to green fluorescent protein (GFP) and determined that the bipartite NLS is sufficient to direct nuclear localization and that the classical NLSs together can collaborate to direct nuclear import. The conservation in AreA orthologs of this unusually large number of apparently redundant NLSs suggests that they each play a role in directing AreA to the nucleus, possibly via alternative importins.

MATERIALS AND METHODS

***A. nidulans* genetic manipulations and growth tests.** *A. nidulans* crosses and genetic analysis were performed as described previously (48). *A. nidulans* transformations were conducted as described previously (49). Growth tests were performed as described in reference 48 at 37°C using *Aspergillus* nitrogen-free minimal medium (ANM) with nitrogen sources added at 10 mM (50). The *A. nidulans* strains used in this study are shown in Table 1.

Sequence analysis. Sanger DNA sequencing to confirm constructs and gene replacements was performed at the Kansas State University DNA Sequencing and Genotyping Facility. DNA sequence analysis was performed using Geneious Pro 5.3.4 (A. J. Drummond, B. Ashton, S. Buxton, M. Cheung, A. Cooper, C. Duran, M. Field, J. Heled, M. Kearse, S. Markowitz, R. Moir, S. Stones-Havas, S. Sturrock, T. Thierer, A. Wilson,

2011) (Biomatters Ltd. Auckland, New Zealand). The AreA protein sequence was examined for NLSs using PSORTII (51) and was examined manually to identify the noncanonical bipartite NLS conserved with GATA-4 (10). Protein sequence alignments were done using ClustalW (52), and protein sequences were obtained from AspGD (<http://aspergillusgenome.org/>) (53), SGD (www.yeastgenome.org/), or the GenBank database (<http://www.ncbi.nlm.nih.gov/GenBank/>): *Aspergillus niger* AreA (CAA57524) (54), *Aspergillus oryzae* AreA (CAA05776) (55), *Aspergillus parasiticus* AreA (AAD37409) (56), *A. nidulans* AreA (CAA36731) (37), *F. fujikuroi* AreA (CAA71897) (57), *Magnaporthe oryzae* NUT1 (AAB03415) (58), *N. crassa* NIT2 (P19212) (59), *Penicillium chrysogenum* Nre (AAA83400) (60), *Penicillium roqueforti* NmC (CAA04815) (61), *S. cerevisiae* Gat1p (P43574) (62), *S. cerevisiae* Gln3p (P18494) (63), *S. cerevisiae* Dal80p (SGD no. YKR034W) (64), *S. cerevisiae* Gzf3p (SGD no. YJL110C) (65), *A. nidulans* AreB beta (AspGD no. AN6221) (66), *A. nidulans* LreA (AspGD no. AN3435) and LreB (AspGD no. AN3607) (67), *A. nidulans* SreA (AspGD no. AN0176) (68), and *A. nidulans* NsdD (AspGD no. AN3152) (69), *Homo sapiens* GATA-1 (P15976) (70, 71), *H. sapiens* GATA-2 (P23769) (72, 73), *H. sapiens* GATA-3 (P23771) (74, 75), *H. sapiens* GATA-4 (P43694) (76), *H. sapiens* GATA-5 (NP_536721) (77), *H. sapiens* GATA-6 (Q92908) (78), and mouse GATA-4 (Q08369) (79).

Molecular techniques. Standard molecular techniques were performed as described in reference 80 or according to instructions from the manufacturer. PCR to generate gene replacement constructs used proof-reading enzymes: *Pfu* (Agilent), *PfuTurbo* (Stratagene), *Phusion* (Thermo Scientific), or *Ex Taq* (TaKaRa). Southern blot analysis to confirm gene replacements was performed using the DIG (digoxigenin) High Prime DNA Labeling and Detection Starter kit II (Roche). Oligonucleotide primers used in this study are shown in Table 2.

Construction of *gpd(p)areA^{HA}* NLS gene replacement mutants via direct selection. (i) Deletion of NLS1, NLS2, and NLS3 in combination. To delete in-frame *areA* codons 60 to 423, which contain NLS1, NLS2, and NLS3, a *gpd(p)areA^{HA,Δ60-423}* (HA stands for hemagglutinin) construct (pJAF5203), in which expression is driven by the constitutive *gpdA* promoter [*gpd(p)*], was generated by digestion of the *gpd(p)areA^{HA}* (truncated at position +1475) plasmid pJAF5200 (46) with *XhoI* (complete)/*SalI* (partial) and religation, deleting a 1.15-kb internal *areA* fragment. This construct was linearized with *Apal* and used to transform *A. nidulans* MH9922 [*areA::riboB(5')* *riboB2*] (46), directly selecting for growth on 10 mM nitrate as the sole nitrogen source. A transformant with the correct gene replacement generating *gpd(p)areA^{HA,Δ60-423}*, as confirmed by Southern blotting (data not shown) and restored riboflavin auxotrophy, was outcrossed to generate *A. nidulans* MH10041.

(ii) Deletion of NLS4 and NLS5 separately and in combination. First, *A. nidulans* MH10266 [*gpd(p)areA^{HA::riboB(3')}* *riboB2*] in which 3' *areA* sequences of the *gpd(p)areA^{HA}* fusion gene were replaced with *riboB* was made by gene replacement of the 3' *areA* sequences in strain MH9883 [*gpd(p)areA^{HA} riboB2*] (46) with a JFareA1-JFareA2 PCR-amplified *areA::riboB(3')* gene replacement cassette. The *areA::riboB(3')* construct was made from pJAF5458 by digestion with *SphI* (Klenow-blunted) and *StuI*, and the 0.6-kbp *SphI*-*StuI* mutation-containing fragment (+1951 to +2520) was replaced by the 2.6-kb *XbaI*(partial, end-filled)-*SmaI* *riboB* selectable marker fragment from pPL3 (81). The *gpd(p)areA^{HA::riboB(3')}* strain MH1072, carrying the nonhomologous end-joining mutation *ΔnkuA::Bar* (82), was generated by meiotic crossing of a MH10266 derivative. Strain MH1072 was used as the recipient for direct selection of *areA* NLS mutations in the 3' portion of *areA*. For NLS4Δ, the NLS4Δ construct pCW6606 was generated from pCW6589 [a wild-type *areA* JFareA1-JFareA2 PCR product (positions +1591 to +2881) cloned into *SmaI* of pBluescript SK(+)] by inverse PCR amplification with NLS4 deletion primers (areANLS4-InvF and areANLS4-InvR), and circularization to delete codons 609 to 615. The NLS4Δ mutant {MH11099 [*gpd(p)areA^{HA,Δ609-615}*] was generated by transformation of the JFareA1-JFareA2 *areA* NLS4Δ fragment from pCW6606 into strain

TABLE 1 A. *nidulans* strains used in this study

Strain	Relevant genotype	Source or reference
AreA ^{HA} strains and strains used for construction		
MH50	<i>ya adE20 su(adE20) areA102 pyroA4 riboB2</i>	M. J. Hynes
MH764	<i>wA3 riboB2 facB101</i>	M. J. Hynes
MH9883	<i>wA3 gpd(p)areA^{HA} riboB2 facB101</i>	This study
MH9922	<i>wA3 areA::riboB(5') riboB2 facB101</i>	This study
MH9949	<i>biA1 gpd(p)areA^{HA} amdS-lacZ</i>	Todd et al. (46)
MH10041	<i>wA3 gpd(p)areA^{HA,Δ60-423} pyroA4</i>	This study
MH10266	<i>wA3 gpd(p)areA^{HA,Δ60-423} riboB(3') riboB2 facB101</i>	This study
MH10897	<i>ya1 pabaA1 gpd(p)areA^{HA} fmdS-lacZ</i>	This study
MH11050	<i>ya1 pabaA1 gpd(p)areA^{HA,Δ811-816} fmdS-lacZ</i>	This study
MH11072	<i>ya1 pabaA1 gpd(p)areA^{HA,Δ609-615,Δ811-816} fmdS-lacZ pyroA4 nkuA::Bar</i>	This study
MH11099	<i>ya1 pabaA1 gpd(p)areA^{HA,Δ609-615} pyroA4 nkuA::Bar fmdS-lacZ</i>	This study
MH11131	<i>ya1 pabaA1 gpd(p)areA^{HA} pyroA4 nkuA::argB⁺</i>	This study
MH11457	<i>gpd(p)areA^{HA,Δ60-423} pyroA4 nkuA::Bar</i>	This study
MH11668	<i>ya1 pabaA1 gpd(p)areA^{HA,Δ811-816} pyroA4 fmdS-lacZ nkuA::Bar</i>	This study
MH11967	<i>ya1 pabaA1 gpd(p)areA^{HA,Δ609-615,Δ811-816} fmdS-lacZ pyroA4 nkuA::Bar</i>	This study
RT1	<i>ya1 pabaA1 gpd(p)areA^{HA,Δ609-615,R685A,R686A,R720A,R722A} pyroA4 nkuA::argB⁺</i>	This study
RT2	<i>ya1 pabaA1 gpd(p)areA^{HA,Δ609-615,R685A,R686A,R720A,R722A,Δ811-816} pyroA4 nkuA::argB⁺</i>	This study
RT30	<i>gpd(p)areA^{HA,Δ60-423,Δ609-615,R685A,R686A,R720A,R722A} pyroA4 nkuA::Bar</i>	This study
RT37	<i>gpd(p)areA^{HA,Δ60-423,Δ609-615,R685A,R686A,R720A,R722A,Δ811-816} pyroA4 nkuA::Bar</i>	This study
RT46	<i>gpd(p)areA^{HA,Δ60-423,Δ609-615,Δ811-816} pyroA4 nkuA::Bar</i>	This study
RT49	<i>ya1 pabaA1 gpd(p)areA^{HA,R685A,R686A,R720A,R722A} pyroA4 nkuA::argB⁺</i>	This study
RT54	<i>gpd(p)areA^{HA} fmdS-lacZ pyrG89</i>	This study
RT147	<i>gpd(p)areA^{HA,Δ60-423,R685A,R686A,R720A,R722A} pyroA4 nkuA::Bar</i>	This study
RT168	<i>gpd(p)areA^{HA,Δ60-423,Δ811-816} pyroA4 nkuA::Bar</i>	This study
RT175	<i>gpd(p)areA^{HA,Δ60-423,Δ609-615} pyroA4 nkuA::Bar</i>	This study
RT231	<i>ya1 pabaA1 gpd(p)areA^{HA,R685A,R686A,R720A,R722A,Δ811-816} pyroA4 nkuA::argB⁺</i>	This study
RT237	<i>gpd(p)areA^{HA,Δ60-423,R685A,R686A,R720A,R722A,Δ811-816} pyroA4 nkuA::Bar</i>	This study
NLS-GFP strains		
RT96	<i>biA1 gpd(p)areA^{HA} pyroA4 fmdS-lacZ crmA^{T525C}::pyrG⁺ pyrG89 nkuA::Bar</i>	This study
RT184	<i>wA::gpd(p)-gfp::areANLS123-Afp_{pyro} biA1 gpd(p)areA^{HA} pyroA4 fmdS-lacZ crmA^{T525C}::pyrG⁺ pyrG89 nkuA::Bar</i>	This study
RT187	<i>wA::gpd(p)-gfp::areAzf-Afp_{pyro} biA1 gpd(p)areA^{HA} pyroA4 fmdS-lacZ crmA^{T525C}::pyrG⁺ pyrG89 nkuA::Bar</i>	This study
RT189	<i>wA::gpd(p)-gfp::areANLS5-Afp_{pyro} biA1 gpd(p)areA^{HA} pyroA4 fmdS-lacZ crmA^{T525C}::pyrG⁺ pyrG89 nkuA::Bar</i>	This study
RT289	<i>wA::gpd(p)-gfp-Afp_{pyro} biA1 gpd(p)areA^{HA} pyroA4 fmdS-lacZ crmA^{T525C}::pyrG⁺ pyrG89 nkuA::Bar</i>	This study
RT294	<i>wA::gpd(p)-gfp::areANLS123,5-Afp_{pyro} biA1 gpd(p)areA^{HA} pyroA4 fmdS-lacZ crmA^{T525C}::pyrG⁺ pyrG89 nkuA::Bar</i>	This study
RT295	<i>wA::gpd(p)-gfp::areAzf^{bip}ALA-Afp_{pyro} biA1 gpd(p)areA^{HA} pyroA4 fmdS-lacZ crmA^{T525C}::pyrG⁺ pyrG89 nkuA::Bar</i>	This study
RT372	<i>wA::gpd(p)-gfp::areANLS4-Afp_{pyro} biA1 gpd(p)areA^{HA} pyroA4 fmdS-lacZ crmA^{T525C}::pyrG⁺ pyrG89 nkuA::Bar</i>	This study
RT393	<i>wA::gpd(p)-gfp::areANLS4,5-Afp_{pyro} biA1 gpd(p)areA^{HA} pyroA4 fmdS-lacZ crmA^{T525C}::pyrG⁺ pyrG89 nkuA::Bar</i>	This study
RT396	<i>wA::gpd(p)-gfp::areANLS123,4-Afp_{pyro} biA1 gpd(p)areA^{HA} pyroA4 fmdS-lacZ crmA^{T525C}::pyrG⁺ pyrG89 nkuA::Bar</i>	This study
RT397	<i>wA::gpd(p)-gfp::areANLS123,4,5-Afp_{pyro} biA1 gpd(p)areA^{HA} pyroA4 fmdS-lacZ crmA^{T525C}::pyrG⁺ pyrG89 nkuA::Bar</i>	This study
Strains for reporter gene assays		
MH10897	<i>ya1 pabaA1 gpd(p)areA^{HA} fmdS-lacZ</i>	This study
MH11432	<i>gpd(p)areA^{HA,Δ60-423} fmdS-lacZ pyroA4 nkuA::Bar</i>	This study
MH10967	<i>ya1 areA::riboB2 riboB2 pyroA4 facB101 fmdS-lacZ</i>	This study
RT121	<i>ya1 fmdS-lacZ gpd(p)areA^{HA,Δ609-615,R685A,R686A,R720A,R722A} nkuA::argB⁺ pabaA1 pyroA4</i>	This study
RT123	<i>ya1 fmdS-lacZ gpd(p)areA^{HA,Δ609-615,R685A,R686A,R720A,R722A,Δ811-816} nkuA::argB⁺ pyroA4 pabaA1</i>	This study
RT129	<i>ya1 fmdS-lacZ gpd(p)areA^{HA,Δ60-423,Δ609-615,R685A,R686A,R720A,R722A} pyroA4 pabaA1</i>	This study
RT131	<i>ya1 fmdS-lacZ gpd(p)areA^{HA,Δ60-423,Δ609-615,R685A,R686A,R720A,R722A,Δ811-816} pyroA4 pabaA1</i>	This study
RT132	<i>ya1 fmdS-lacZ gpd(p)areA^{HA,Δ60-423,Δ609-615,Δ811-816} pabaA1</i>	This study
RT134	<i>ya1 fmdS-lacZ gpd(p)areA^{HA,R685A,R686A,R720A,R722A} nkuA::argB⁺ pabaA1 pyroA4</i>	This study
RT212	<i>gpd(p)areA^{HA,Δ60-423,Δ811-816} fmdS-lacZ</i>	This study
RT214	<i>gpd(p)areA^{HA,Δ60-423,R685A,R686A,R720A,R722A} pyroA4 fmdS-lacZ</i>	This study
RT216	<i>gpd(p)areA^{HA,Δ60-423,Δ609-615} fmdS-lacZ</i>	This study
RT248	<i>ya1 gpd(p)areA^{HA,Δ60-423,R685A,R686A,R720A,R722A,Δ811-816} pyroA4 fmdS-lacZ</i>	This study
RT273	<i>ya1 gpd(p)areA^{HA,R685A,R686A,R720A,R722A,Δ811-816} pabaA1 fmdS-lacZ</i>	This study

MH11072 and direct selection of transformants on nitrate. For NLS5Δ, the PCR product (+1591 to +2526) was generated using the oligonucleotides JFareA1 and RTareANLS5Del with wild-type *areA* pJAF4689 (46) as the template; the PCR product was cloned into pBluescript SK(+) (pSL7190). The AvrII-StuI fragment from pSL7190 was subcloned into the AvrII and StuI sites of pJAF5458, which contains JFareA1-JFareA2 PCR product (+1591 to +2881) from strain MH50 genomic DNA template in pGem-T Easy, to generate pSL7191. The NLS5Δ mutant {MH11668 [*gpd(p)areA^{HA,Δ811-816}*]} was generated by transformation of strain MH11072 with JFareA1-JFareA2 *areA* NLS5Δ PCR product, amplified from pSL7191 as the template, and direct selection on nitrate. For NLS4ΔNLS5Δ, PCR product containing both NLS4Δ and NLS5Δ, made with JFareA1 and RTareANLS5Del primers and pCW6606 (NLS4Δ) as the template was cut with AvrII and StuI and cloned into the AvrII and StuI sites of pCW6606 to generate pCW6607, containing both NLS4Δ and NLS5Δ. The AvrII-StuI fragment of pCW6607 was cloned into pCW6590, which contains

the SnaBI-EcoRV *areA* fragment of pJAF4689 (46) inserted into the SmaI site of the *Aspergillus fumigatus pyroA* (*Afp_{pyro}*) selectable marker plasmid pSM6363 [*Afp_{pyro}* PstI-HindIII(blunted) in SspI of pBluescript SK(+)], to generate pCW6609. The NLS4ΔNLS5Δ mutant {MH11967 [*gpd(p)areA^{HA,Δ609-615,Δ811-816}*]} was generated by transformation of a JFareA1-JFareA2 PCR product amplified from pCW6609 into strain MH11072 and direct selection on nitrate.

Construction of *gpd(p)areA^{HA}* NLS mutants via two-step gene replacement. The recipients for two-step gene replacement, strain MH11131 [*gpd(p)areA^{HA} pyroA4 ΔnkuA::argB*] or MH11457 [*gpd(p)areA^{HA,Δ60-423} pyroA4 ΔnkuA::Bar*], were constructed by meiotic crossing to introduce *ΔnkuA* (82).

(i) Mutation of the bipartite NLS. The R685A,R686A,R720A,R722A (R685A is the R-to-A change at position 685) bipartite NLS mutation (*bip^{ALA}*) construct was made in two inverse PCR steps using pCW7273 [wild-type JFareA1-JFareA2 *areA* in pBluescript SK(+)] as

TABLE 2 Oligonucleotides used in this study

Oligonucleotide	Sequence ^a	Coordinates ^b
JFareA1	5'-CGACTCGGATGTTGAAGATG-3'	+1591–+1610
areANLS4-InvR	5'-GTCTTGATCCCGATTGCGCACCTCGC-3'	+1885–+1860
RTareANLS5Del	5'-CAGAGGCCTTTCCAGAGCCACCTGTA-3'	+2525–+2510, +2491–+2481
JFareA2	5'-GCGTCACTCGTAACCATCAA-3'	+2881–+2862
areANLS4-invF	5'-CGCACCTCGTCCACTCCAAACACAGC-3'	+1907–+1932
DeltaZnF3	5'-AACAGCGCAATAGCCTTGC-3'	+2006–+2012, +2235–+2257
AreAR720AR722A	5'-GGCGTTAGCCTTCTTGATCA-3'	+2227–+2208
newAreAR685AR686A	5'-GTTAGCCGCCACAGCGG-3'	+2122–+2105
newAreA688invF	5'-CCTGAAGGTCAGCCGCTGT-3'	+2123–+2141
NotIT7	5'-TTGCGGCCGCTAATACGACTCACTATAGGG-3'	N/A
T3	5'-AATTAACCCTCACTAAAGGG-3'	N/A
CCHNLS123F1	5'-AAAAGCTTCACAACGAAAGCCTCCGAAGCC-3'	+670–+691
CCHNLS123R1	5'-AAGGATCCGACACAGGCGGTACGTGAG-3'	+922–+903
KSNLS4F	5'-AAAAGCTTCAGCGAGGTGCGCAATCGG-3'	+1859–+1876
KSNLS4R	5'-AAGGATCCGCTCTGGCGTAGTAGTTGG-3'	+1951–+1933
CCHNLS4BglIIF	5'-AAAGATCTAGCGAGGTGCGCAATCGG-3'	+1859–+1876
KSNLS5F	5'-AAAAGCTTAAACAACGGTGTGGTGCGGT-3'	+2461–+2481
KSNLS5R	5'-AAGGATCCCGCCATATCAACATCAGAG-3' G	+2520–+2539
CCHNLS5BglIIF	5'-AAAAGATCTAACAACGGTGTGGTGCG-3'	+2462–+2479
KSareAzfF	5'-TTAAGCTTGTGCGGTCTAAACAGCGC-3'	+1996–+2013
KSareAzfR	5'-TTGGATCCGGATGTCGTATTGCTTTGG-3'	+2353–+2335
whitecodF	5'-TATGGTGCCAATCCACGG-3'	N/A
whitecodR	5'-TGATGGAAGATCTGCGC-3'	N/A

^a Mismatches with the wild-type *areA* sequence are underlined in *areA* oligonucleotides.

^b The coordinates are relative to the A of the *areA* ATG at position +1. N/A, not applicable.

the template. In the first inverse PCR, primers DeltaZnF3 and AreAR720AR722A were used. The PCR product was gel purified, phosphorylated, and ligated, and the resultant plasmid (pSL7199) was sequenced to confirm the presence of the R720A R722A mutation. The second inverse PCR used primers newAreAR685AR686A and newAreA688invF to amplify using pSL7199 as the template. The 1.2-kb Sall-NotI fragment from the resulting plasmid was subcloned into pSM6363 digested with Sall and NotI to generate pRT7309. pRT7309 was transformed into strain MH11131, and transformants were selected for pyridoxine prototrophy. One transformant was selfed, and the progeny were screened for loss of *AfpyroA* and *areA* loss of function on nitrate to identify the two-step gene replacement strain RT49 [*gpd(p)areA*^{HA.R685A,R686A,R720A,R722A} *pyroA4*].

(ii) **NLS mutant combinations.** The Δ NLS4,R685A,R686A,R720A,R722A, Δ NLS5 (NLS4 Δ -bip^{ALA}-NLS5 Δ) construct (pRT145) was made similarly to the bipartite NLS mutation construct in two inverse PCR steps followed by subcloning into the *AfpyroA* vector pSM6363, except the NLS4 Δ NLS5 Δ plasmid pCW6609 was used as the primary template to generate pSL7200, which was used as the template in the second step. pRT145 was transformed into strain MH11131, and pyridoxine prototrophs were selected. One transformant was selfed, and the progeny were screened for pyridoxine auxotrophs that had lost the *AfpyroA* selectable marker and were *areA* loss-of-function mutants, i.e., two-step gene replacements. Depending on the position of the crossovers in the first and second steps, different outcomes are possible in the two-step gene replacement progeny. Sequence analysis of JFareA1-JFareA2 PCR amplicons from genomic DNA of second-step pRT145 gene replacement progeny identified two different gene replacements: NLS4 Δ bip^{ALA} [RT1 [*gpd(p)areA*^{HA. Δ 609-615.R685A,R686A,R720A,R722A} *pyroA4*]] and NLS4 Δ bip^{ALA} NLS5 Δ [RT2 [*gpd(p)areA*^{HA. Δ 609-615.R685A,R686A,R720A,R722A. Δ 811-816} *pyroA4*]]. For bip^{ALA}NLS5 Δ , the bip^{ALA}NLS5 Δ region of pRT145 was separated from NLS4 Δ by amplification with areANLS4-InvF and JFareA2 and cloned into the SmaI site of pSM6363 to generate pKS138. pKS138 was transformed into strain MH11131, and transformants were selected for pyridoxine prototrophy. One transformant was selfed, and the progeny were screened for loss of *AfpyroA* and *areA* loss-of-function on nitrate to identify strain RT231 [*gpd(p)areA*^{HA.R685A,R686A,R720A,R722A. Δ 811-816} *pyroA4*].

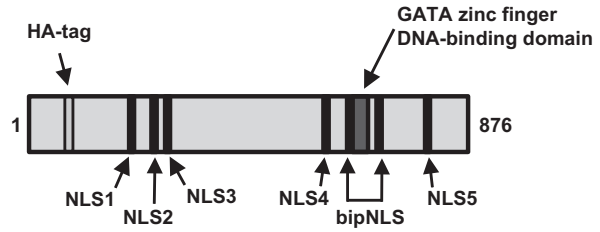
NLS mutants that contained Δ 60-423 (i.e., Δ NLS1,2,3) were made by two-step gene replacement in a MH11457 [*gpd(p)areA*^{HA. Δ 60-423} *pyroA4* *AnkuA::Bar*] recipient isolated from a cross of MH10041 \times MH11072. In each case, the constructs contained *areA* sequences in the *AfpyroA* vector pSM6363, and transformants were selected for pyridoxine prototrophy. One transformant was selfed, and the progeny were screened for loss of pyridoxine prototrophy. The second step of the gene replacement was confirmed by sequencing the PCR products amplified with JFareA1 and JFareA2. Strain RT175 [*gpd(p)areA*^{HA. Δ 60-423.609-615} *pyroA4*] was made by transformation with the construct pCH225 which carried a JFareA1-JFareA2 PCR product from strain MH11099 (NLS4 Δ) genomic DNA cloned into the SmaI site of pSM6363. Strain RT168 [*gpd(p)areA*^{HA. Δ 60-423. Δ 811-816} *pyroA4*] was made by transformation with the construct pKS139, which carried a JFareA1-JFareA2 PCR product from a pSL7191 (NLS5 Δ) template cloned into the SmaI site of pSM6363. RT46 [*gpd(p)areA*^{HA. Δ 60-423. Δ 609-615. Δ 811-816} *pyroA4*] was made by transformation with the construct pKS19, which carried a JFareA1-JFareA2 PCR product from pCW6607 cloned into the SmaI site of pSM6363. Strain RT147 [*gpd(p)areA*^{HA. Δ 60-423.R685A,R686A,R720A,R722A} *pyroA4*] was made by transformation with the construct pRT7309. Strains RT30 [*gpd(p)areA*^{HA. Δ 60-423. Δ 609-615.R685A,R686A,R720A,R722A} *pyroA4*] and RT37 [*gpd(p)areA*^{HA. Δ 60-423. Δ 609-615.R685A,R686A,R720A,R722A. Δ 811-816} *pyroA4*] were made by transformation with the construct pRT145. The positions of the crossovers were different in RT30 and RT37 as revealed by sequencing. Strain RT237 [*gpd(p)areA*^{HA. Δ 60-423.R685A,R686A,R720A,R722A. Δ 811-816} *pyroA4*] was made by transformation with the construct pKS138.

Construction of GFP-NLS fusions. (i) **Constructs.** We constructed *gfp-NLS* fusions in *wA*-targeting vectors in two steps. First, pDFC6917, which was derived by filling in the ends of the unique BglII site in the polylinker of the *gpd(p)gfp* fusion plasmid pALX213 (pAA4362 [83]), was used to construct *gfp-NLS* fusions expressed from the *gpdA* promoter. The NLSs were amplified with primers containing BamHI or HindIII sites, and the amplicons were digested with BamHI and HindIII and ligated into the BamHI and HindIII sites of pDFC6917. Second, the *gpd(p)gfpNLS* sequence was PCR amplified with primers NotIT7 and T3, and the NotI-BamHI restriction fragment was subcloned into the NotI and BamHI sites of the *wA*-targeting vector pCW6500, which was constructed by insertion

A

NLS	Amino acid coordinates	Sequence
NLS1	216 – 222	PIKARRD
NLS2	252 – 258	PRRVKRT
NLS3	271 – 277	PSRKRPA
NLS4	609 – 615	PRRQKIA
NLS5	811 – 816	PKRQRRL
Classical NLS consensus		PKKKRKV
bipNLS		RRX ₃₃ RXR

B



C

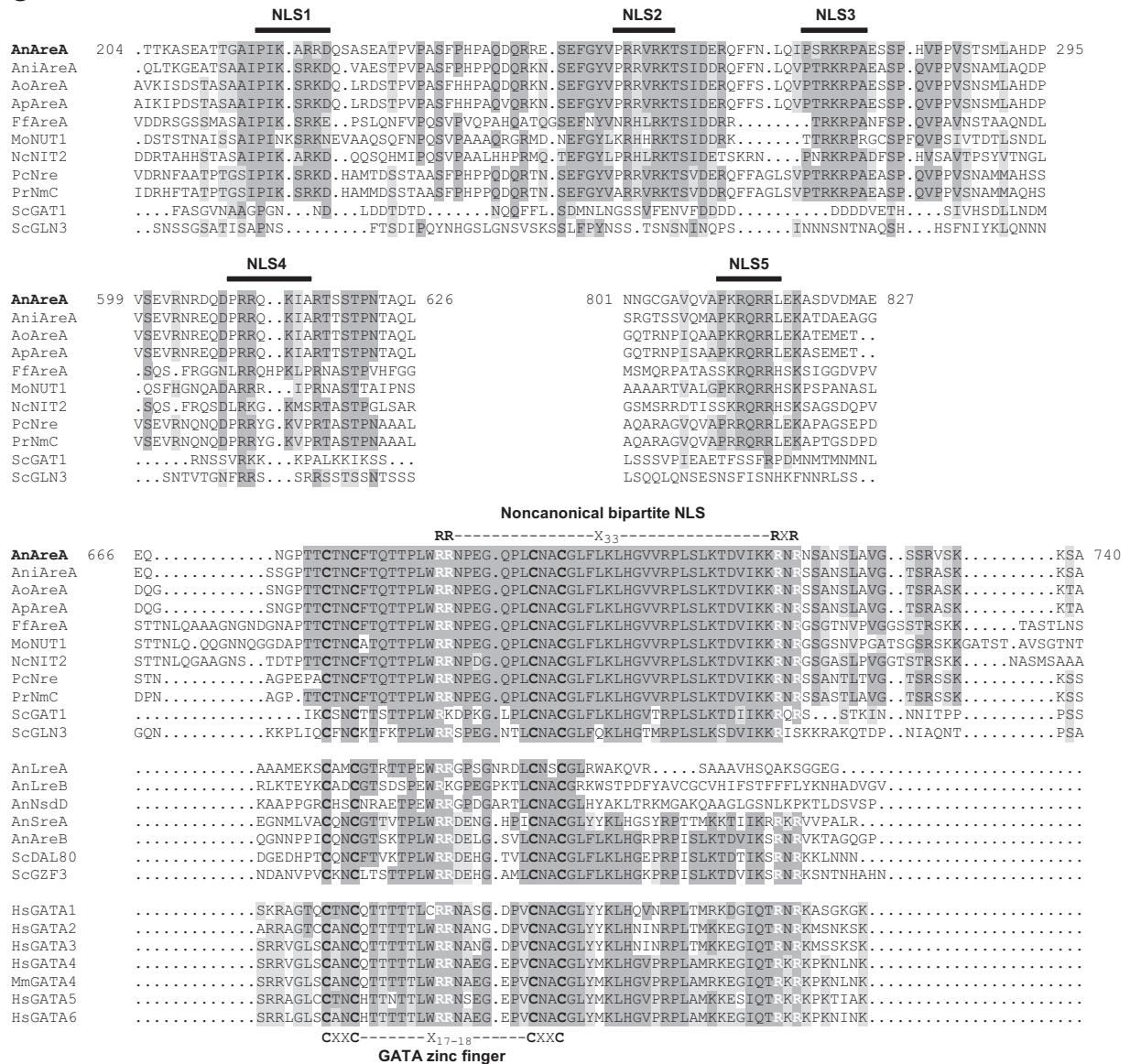


FIG 1 Nuclear localization signals in AreA. (A) Sequences of the five classical NLSs identified by similarity to the consensus sequence PKKKRKV using PSORTII analysis. The bipartite NLS (bipNLS) conforms to the noncanonical bipartite arginine NLS RRX₃₃RXR. (B) Positions of the NLSs in the AreA protein. The NLSs are indicated as black bars, the GATA zinc finger DNA-binding domain is indicated as a dark gray box, and the HA tag is indicated as an open box. (C) Partial protein sequence alignment of AreA homologs showing the conservation of the nuclear localization signals across species. The first two or three letters indicate

of an internal 2.15-kbp EcoICRI fragment of the *wA* (white) gene, amplified with primers whitecodF and whitecodR, into the NruI site of pSM6363. For the GFP control, *gpd(p)gfp* was PCR amplified from pDFC6917 and subcloned into pCW6500 to generate pCH183. For GFP-NLS1,2,3, *areA* codons 204 to 287 were amplified from MH1 genomic DNA using CCHNLS123F1 and CCHNLS123R1 primers, cut with BamHI and HindIII, and ligated into pDFC6917. The *gpd(p)gfpNLS123* sequence was subcloned into pCW6500 to generate pCH62. For GFP-NLS4, KSNLS4F and KSNLS4R primers were used to amplify *areA* codons 600 to 630 using the pKS5 [JFareA1-JFareA2 *areA* amplified from MH1 genomic DNA cloned into the SmaI site of pBluescript SK(+)] template. The *gpd(p)gfpNLS4* sequence was subcloned into pCW6500 to generate pCH212. For GFP-NLS5, KSNLS5F and KSNLS5R primers were used to amplify *areA* codons 801 to 826 from the pKS5 template. The *gpd(p)gfpNLS5* sequence was transferred into pCW6500 to generate pCH62. For GFP-bipNLS, KSareAzfF and KSareAzfR primers were used to amplify *areA* codons 646 to 764 from the pKS5 template. The *gpd(p)gfpbipNLS* sequence was transferred into pCW6500 to generate pCH64. For GFP-bip^{ALA}NLS, KSareAzfF and KSareAzfR primers were used to amplify *areA* codons 646 to 746 from pRT7309. The *gpd(p)gfpbip^{ALA}NLS* sequence was transferred into pCW6500 to generate pCH65. For GFP-NLS1,2,3,5, the NLS5 encoding codons 801 to 826 were amplified with primers CCHNLS5BglIIF and KSNLS5R using the pKS5 template, digested with BglII and BamHI, and ligated into the BamHI site of pCH59 to generate pCH180. For GFP-NLS1,2,3,4, the NLS4 encoding codons 600 to 630 were amplified with primers CCHNLS4BglIIF and KSNLS4R using pKS5 as the template, digested with BglII and BamHI, and ligated into the BamHI site of pCH59 to generate pCH227. For GFP-NLS4,5, the NLS5 encoding codons 801 to 826 were amplified with primers CCHNLS5BglIIF and KSNLS5R using the pCH62 template, digested with BglII and BamHI, and ligated into the BamHI site of pCH212 to generate pCH226. For GFP-NLS1,2,3,4,5, the NLS4 and NLS5 encoding codons 600 to 630 and 801 to 826 were amplified with primers CCHNLS4BglIIF and KSNLS5R using pCH226 as the template, digested with BglII and BamHI, and ligated into the BamHI site of pCH59 to generate pCH228.

(ii) **GFP strains.** The *gpd(p)-gfp-NLS* plasmids pCH59, pCH212, pCH62, pCH64, pCH65, pCH180, pCH226, pCH227, and pCH228 and the *gpd(p)gfp* control pCH183 were transformed into strain RT96 [*pyroA4 nuka::Bar*]. Transformants were selected for pyridoxine prototrophy, and transformants with targeted integration at the *wA* gene by the internal *wA* fragment in the vector were visible as white-colored colonies. Single-copy integration was confirmed by Southern blot analysis (data not shown).

Immunostaining, immunofluorescence, and GFP microscopy. Immunostaining was conducted as described previously (46). Indirect UV immunofluorescence microscopy was performed using an Olympus BX51 upright biological reflected fluorescence microscope equipped with Nomarski differential interference contrast (DIC), an EXFO X-Cite 120 Q fluorescence illumination system and a UPlanFLN Plan Semi Apochromat (field number FN26.5) Fluorite 100× oil objective with a numerical aperture of 1.30. Alexa Fluor 488 immunofluorescence was detected using a BrightLine fluorescein isothiocyanate (FITC) filter set (excitation wavelength band pass, 482/35 nm; dichroic mirror, 506 nm; emission, 536/40 nm; ZPIXEL). DAPI (4',6"-diamidino-2-phenylindole) fluorescence was detected using a BrightLine DAPI Hi Contrast filter set (excitation wavelength band pass, 387/11 nm; dichroic mirror, 409 nm; ZPIXEL). For direct visualization of GFP, germlings were prepared for UV fluorescence microscopy as described previously (83). GFP fluorescence was detected

in fixed cells with the same microscope and camera as used for immunofluorescence but using a BrightLine GFP filter set (excitation wavelength band pass, 473/31 nm; dichroic mirror, 495 nm; emission 483/32 nm; ZPIXEL). At least 30 nuclei from each of two independent experiments were analyzed for each growth condition. Photomicrographs were captured using an Olympus DP72 12.8 Megapixel digital color camera and DP2-BSW digital camera software. Images were manipulated similarly within and between experiments using Adobe Photoshop CS4. Images were cropped, and the tonal range was increased by adjusting highlights and shadows without altering the color balance. GFP or α -hemagglutinin (α -HA) fluorescence was quantified with ImageJ (W. S. Rasband, ImageJ, U.S. National Institutes of Health, Bethesda, Maryland, USA; <http://imagej.nih.gov/ij/>; 1997 to 2012) using representative raw images. The nuclear fluorescence to cytoplasmic fluorescence ratio per unit area was calculated using the mean of 25 randomly paired ratios of nuclear to cytoplasmic regions, allowing the standard error of the mean (SEM) to be calculated. Significance was tested with a two-sample, unequal variance *t* test (*P* value of <0.025).

β -Galactosidase assays. Strains for *fmdS-lacZ* assays were constructed by meiotic crossing (48). β -Galactosidase assays were performed as described previously (84). Specific activity is expressed as $A_{420} \times 10^3 \text{ min}^{-1} \text{ mg}^{-1}$ of soluble protein. Protein concentrations were calculated as described previously (85) using Bio-Rad protein assay reagent (Bio-Rad) following the manufacturer's instructions. Significance was tested using a two-sample, unequal variance *t* test (*P* value of <0.05). *t* tests were done comparing the wild type and each mutant for each condition, within each strain comparing NH_4 to either alanine (ALA) or nitrogen-free medium (-N), as well as within strains comparing ALA to -N.

RESULTS

AreA has multiple conserved nuclear localization signals. The *A. nidulans* AreA sequence was analyzed for nuclear localization signals using the PSORTII program (51), which identifies sequences with similarity to consensus targeting signals. Five classical NLSs were identified within AreA by their adherence to the PKKKRKV classical simian virus 40 (SV40) large T-antigen-type NLS consensus sequence (86): NLS1 (residues 216 to 222), NLS2 (residues 252 to 258), NLS3 (residues 271 to 277), NLS4 (residues 609 to 615), and NLS5 (residues 811 to 816) (Fig. 1A and B).

We aligned the protein sequences of AreA orthologs (Fig. 1C). NLS1, NLS2, NLS3, and NLS5 were strongly conserved in most ascomycete homologs of AreA. NLS4 was conserved in many ascomycetes but showed poor conservation with *F. fujikuroi* AreA, *M. oryzae* NUT1, and *N. crassa* NIT2. None of the classical NLSs were conserved in either Gln3p or Gat1p from *S. cerevisiae*. Gln3p contains two predicted NLSs, only one of which is required for nuclear localization (20). Neither of these sequences corresponds in position with any of the classical NLSs in the AreA orthologs.

Effects of mutation of AreA classical NLSs on AreA activity. We constructed a battery of hemagglutinin (HA) epitope-tagged AreA mutant strains by direct selection or by two-step gene replacement (see Materials and Methods) in order to determine the effects of the loss of NLSs on AreA function and localization. The AreA^{HA} variants were expressed from the constitutive *gpdA* pro-

the species as follows: An, *A. nidulans*; Ani, *Aspergillus niger*; Ao, *Aspergillus oryzae*; Ap, *Aspergillus parasiticus*; Ff, *F. fujikuroi*; Mo, *M. oryzae*; Nc, *N. crassa*; Pc, *Penicillium chrysogenum*; Pr, *Penicillium roqueforti*; Sc, *Saccharomyces cerevisiae*; Hs, *Homo sapiens*; Mm, *Mus musculus*. For the fungal NLSs including the noncanonical bipartite NLS, dark gray shading represents >60% identity and light gray shading represents >60% similarity. Gaps within the aligned sequences are indicated as periods. The arginine-based bipartite NLS has the arginine residues shown in bold white type and the cysteine residues for the GATA zinc finger binding domain shown in bold black type. For the human and mouse GATA transcription factors, dark gray shading represents identity with the fungal amino acids, and light gray shading represents identity within the mammalian GATA factors but not with the fungal zinc finger-binding domain. Coordinates are shown for *A. nidulans* AreA.

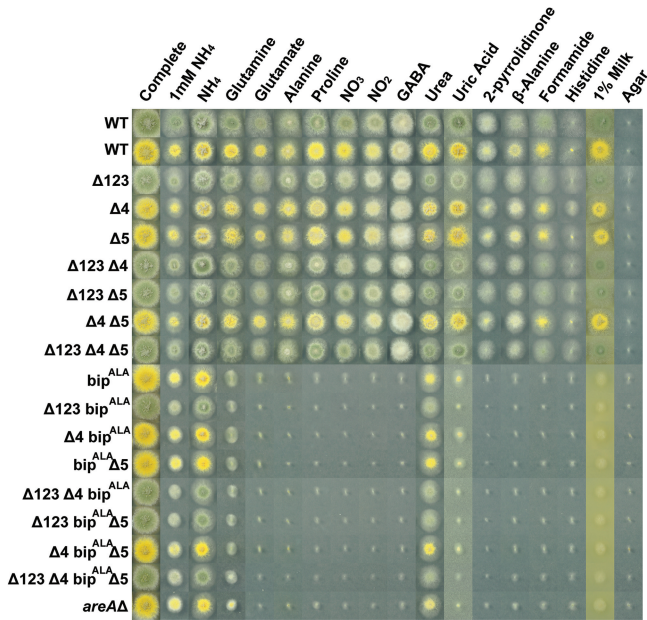


FIG 2 Effects of mutation of AreA NLSs on AreA activity. The various nuclear localization signal mutant strains and green and yellow conidial-colored wild-type (WT) strains were grown on complete medium or minimal medium containing a range of nitrogen sources at 10 mM, except where otherwise indicated, for 2 days at 37°C. GABA, gamma-aminobutyric acid.

motor [*gpd(p)*] to uncouple any effects of the mutations on auto-genous control of *areA* transcript levels (46). We deleted NLS1, NLS2, and NLS3 together in a single deletion mutation of residues 60 to 423 (Δ NLS1,2,3). NLS4 (residues 609 to 615) and NLS5

(residues 811 to 816) were deleted individually to generate the NLS4 Δ and NLS5 Δ mutations. We also made all of the possible double and triple combinations of the Δ NLS1,2,3, Δ NLS4, and Δ NLS5 mutations. The seven mutants, with wild-type and *areA* Δ controls, were tested for growth on a range of sole nitrogen sources, including the preferred nitrogen sources ammonium and glutamine, and various alternative nitrogen sources (Fig. 2). Mutation of the classical NLSs in all combinations, including all the mutations together, resulted in growth comparable to the wild-type controls for all nitrogen sources tested.

In order to determine the effects of these mutations on AreA-dependent gene expression, the *fmdS-lacZ* reporter gene (87) was introduced into the NLS mutants by meiotic crossing. We assayed β -galactosidase activity of the *gpd(p)areA*^{HA}-NLS mutant *fmdS-lacZ* progeny grown on ammonium or grown on ammonium and then transferred to either alanine medium or nitrogen-free medium (Fig. 3). The wild-type *gpd(p)areA*^{HA} control showed low levels of gene expression when grown on ammonium, increased AreA-dependent expression on the alternative nitrogen source alanine, and even higher AreA-dependent expression following transfer to medium lacking nitrogen, as observed previously (46). Deletion of the classical NLSs (NLS1,2,3, NLS4, and NLS5) in all combinations had no effect on the expression of FmdS-LacZ.

Analysis of the effects of mutations in AreA classical NLSs on nuclear accumulation. The wild-type AreA^{HA} protein accumulates in the nucleus after nitrogen starvation but not after growth in nitrogen-sufficient or nitrogen-limiting conditions (46). To determine which of the NLSs was necessary for nuclear accumulation of AreA, we immunostained the HA epitope-tagged AreA NLS mutant strains (Fig. 4). Deletion of the five classical NLSs individually (Δ NLS1,2,3, Δ NLS4, or Δ NLS5), in combinations

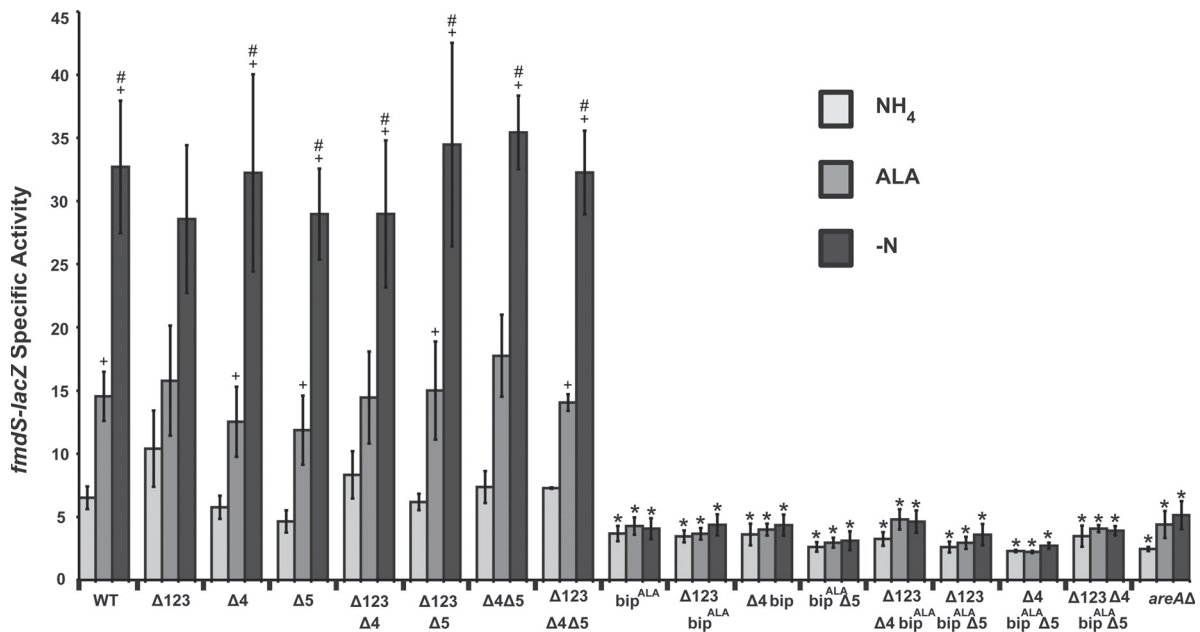


FIG 3 Effects of mutation of AreA NLSs on AreA-dependent gene expression. Wild-type (WT) and *areA* NLS mutation or deletion strains carrying the *fmdS-lacZ* reporter gene were grown in supplemented minimal medium for 16 h with 10 mM ammonium tartrate (NH₄) as a nitrogen source. The mycelia were then harvested or washed with supplemented liquid medium without nitrogen and transferred for 4 h to 10 mM alanine (ALA) minimal medium or nitrogen-free (-N) minimal medium. Soluble protein extracts were prepared from the harvested mycelia and assayed for β -galactosidase specific activity. Values are means \pm standard errors of the means (SEMs) (error bars) (≥ 3 experiments). Values that are significantly different are indicated as follows: *, *P* value of <0.05 between WT and mutants of the same nitrogen condition; +, *P* value <0.05 between NH₄ and either ALA or -N within a strain; #, *P* value of <0.05 between ALA and -N within a strain.

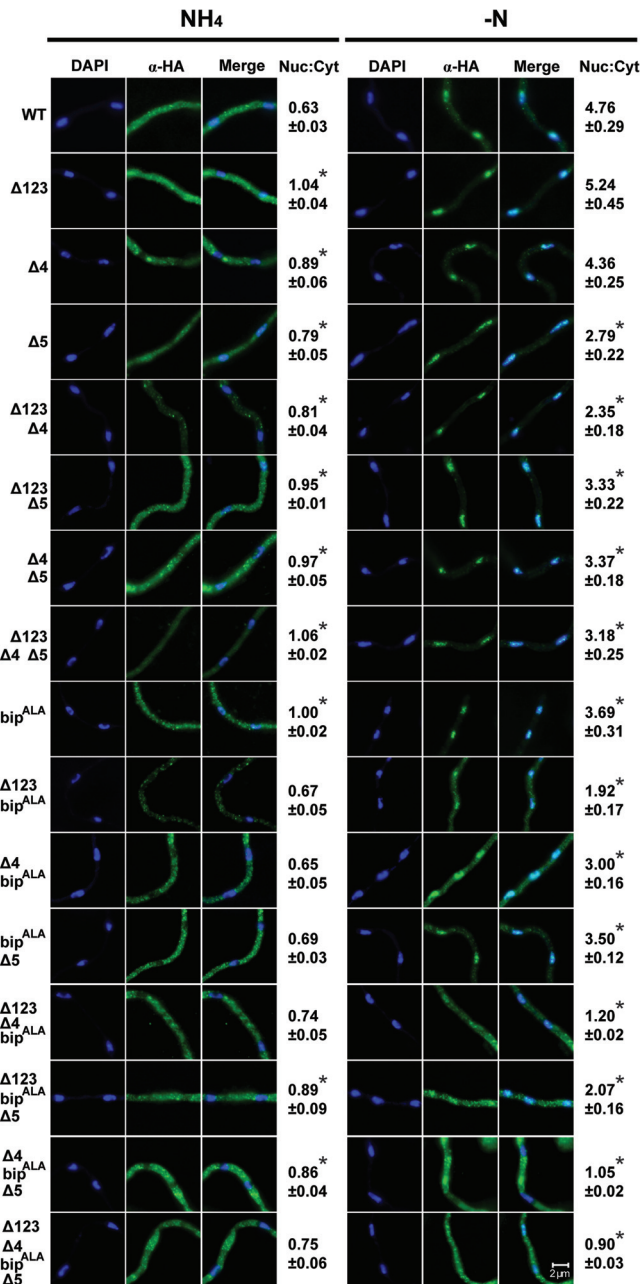


FIG 4 Effects of mutation of AreA NLSs on AreA^{HA} nuclear accumulation. The subcellular distribution of AreA^{HA} (α-HA) in gene-replaced *gpd(p)areA^{HA}* variants after 14-h growth on 10 mM ammonium and 4-h transfer to minimal medium containing 10 mM ammonium (NH₄) or no nitrogen source (-N) was visualized by UV fluorescence microscopy following immunostaining with α-HA (3F10) and Alexa Fluor 488-conjugated goat anti-rat antibodies. A representative image of at least 100 nuclei is shown. Nuclei are stained with DAPI. Nuc:Cyt indicates the mean α-HA nuclear fluorescence to cytoplasmic fluorescence ratio with SEMs for 25 randomly paired nuclear and cytoplasmic regions. Values that are significantly different (*P* value < 0.025) for the WT and mutants grown under the same nitrogen condition are indicated by an asterisk.

(ΔNLS1,2,3-ΔNLS4, ΔNLS1,2,3-ΔNLS5, or ΔNLS4-ΔNLS5), or together (ΔNLS1,2,3-ΔNLS4-ΔNLS5) did not abolish nuclear accumulation of AreA, indicating that other nonclassical nuclear localization signals are involved in AreA nuclear import.

A noncanonical bipartite NLS in AreA is conserved with mammalian GATA-4. The mouse transcription factor GATA-4 has a noncanonical arginine-based bipartite NLS RRX₃₃RXR within the GATA zinc finger DNA-binding domain (10). As the PSORTII algorithm does not include this noncanonical bipartite NLS, we identified by manual inspection an RRX₃₃RXR motif within the AreA zinc finger domain at residues 685 to 722 as a sixth bipartite NLS (bip) (Fig. 1A and B). The AreA bipartite NLS is highly conserved within the zinc finger across most fungal AreA homologs, with *S. cerevisiae* Gln3p and Gat1p being the notable exceptions showing only partial conservation of this motif (RRX₃₃RXS and RKX₃₃RXR, respectively). The bipartite NLS is also conserved in the *A. nidulans* GATA factors AreB, the C-terminal zinc finger of *A. nidulans* SreA, the *S. cerevisiae* GATA factors Dal80p and Gzf3p, and the C-terminal zinc finger of all six mammalian GATA factors, suggesting that this NLS is ancient in origin (Fig. 1C). The bipartite NLS was not conserved in the other *A. nidulans* GATA factors, LreA, LreB, or NsdD. An additional RRX₃₃RXR motif separated from the zinc finger is also found in SreA.

As the bipartite NLS spans the GATA zinc finger, we mutated the bipartite NLS by point mutation of the four key arginine residues R685A, R686A, R720A, R722A (bip^{ALA}). We also made all of the possible double, triple, and quadruple combinations of bip^{ALA} with the ΔNLS1,2,3, ΔNLS4, and ΔNLS5 mutations. Deletion of all five classical NLSs in conjunction with the bip^{ALA} bipartite NLS mutation (ΔNLS1,2,3-ΔNLS4-bip^{ALA}-ΔNLS5) prevented nuclear accumulation of AreA during nitrogen starvation (Fig. 4), implicating the bipartite NLS as a major nuclear localization sequence. However, the bip^{ALA} single mutant strain showed nuclear accumulation (Fig. 4), indicating that the five classical NLSs together can mediate AreA nuclear import without the bipartite NLS. The bip^{ALA} mutant alone or in combination with any of the classical NLSs showed a loss-of-function phenotype with growth comparable to growth of the *areAΔ* strain (Fig. 2). Furthermore, mutation of the bipartite NLS affected FmdS-LacZ activity as severely as *areAΔ*, indicating that the four arginine residues comprising the bipartite NLS are critical for AreA function, presumably for AreA DNA binding (Fig. 3). We found that the ΔNLS1,2,3-bip^{ALA}-ΔNLS5 mutant AreA protein lacking all NLSs except NLS4 weakly accumulated in the nucleus, showing that NLS4 is able to direct AreA nuclear accumulation by itself. NLS1,2,3 (i.e., in the ΔNLS4-bip^{ALA}-ΔNLS5 mutant) and NLS5 (i.e., in the ΔNLS1,2,3-ΔNLS4-bip^{ALA} mutant) did not individually confer AreA nuclear accumulation, but in the ΔNLS4-bip^{ALA} mutant, which has NLS1,2,3 and NLS5 intact, we observed strong nuclear accumulation. Therefore, although NLS1,2,3 and NLS5 are separately insufficient for nuclear accumulation, they appear to work together to signal AreA nuclear localization.

Identification of AreA nuclear localization signals sufficient for nuclear localization. The mutational analysis above strongly suggests that all the identified NLSs in AreA are functional and show redundancy. In order to dissect the nuclear import function of the six NLSs, we fused the AreA NLSs to the C terminus of GFP expressed from the constitutive *gpdA* promoter in a *wa*-targeting vector. The *gpd(p)gfp*-NLS constructs and a *gpd(p)gfp* control construct lacking sequences encoding a NLS were targeted in single copy at the *A. nidulans wa* gene (see Materials and Methods). Subcellular localization of the GFP-NLS fusion proteins was determined by direct UV fluorescence microscopy. Similar patterns

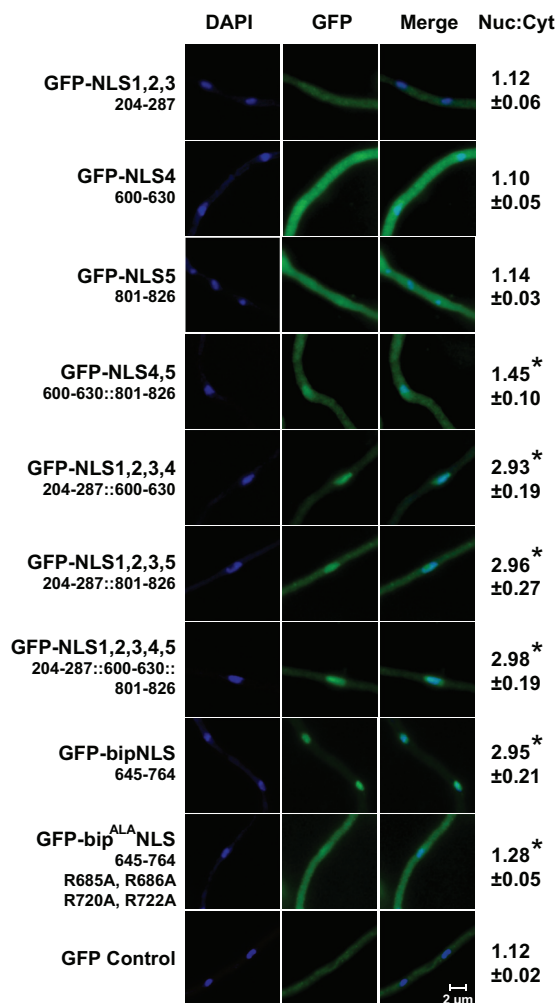


FIG 5 Subcellular distribution of GFP-NLS proteins. Direct UV fluorescence GFP microscopy of germlings of *gpdA(p)gfp-NLS* transformants after 14-h growth in minimal medium containing 10 mM ammonium and then a 4-h transfer to nitrogen-free (–N) minimal medium. A representative image of at least 100 nuclei is shown. Nuclei are stained with DAPI. Nuc:Cyt indicates the mean GFP nuclear fluorescence to cytoplasmic fluorescence ratio with SEMs for 25 randomly paired nuclear and cytoplasmic regions. The coordinates of AreA sequences included in the GFP fusion proteins are shown. Values that are significantly different (P value < 0.005) for the GFP control and GFP-NLS fusion proteins are indicated by an asterisk.

of subcellular distribution were observed for each fusion protein after growth for 14 h on 10 mM ammonium (data not shown) and after 4 h of nitrogen starvation (Fig. 5). The GFP control was distributed throughout the hyphae and not directed specifically to the nucleus, similar to previous observations for GFP expressed from randomly integrated constructs (16, 83, 88). The GFP-zinc finger region fusion protein containing the bipartite NLS (GFP-bipNLS) was strongly localized to the nucleus. The GFP-zinc finger bip^{ALA} mutant fusion protein (GFP-bip^{ALA}NLS) showed markedly reduced nuclear accumulation compared to the wild-type GFP-zinc finger fusion. Therefore, the bipartite NLS alone acts as a strong nuclear localization signal. Neither GFP fused to NLS1, NLS2, and NLS3 together, nor GFP fused separately to NLS4 or NLS5 accumulated in the nucleus. For NLS1,2,3 and NLS5, this is consistent with our NLS deletions in AreA. However,

the lack of nuclear accumulation of GFP-NLS4 coupled with the weak nuclear accumulation we observed for the Δ NLS1,2,3-bip^{ALA}- Δ NLS5 mutant suggests that NLS4 has weak or context-dependent activity. We tested whether the classical NLSs might be separately weak NLSs that could function in combination. GFP was fused to both NLS4 and NLS5, to NLS1, NLS2, NLS3 and either NLS4 or NLS5, and fused to all five classical NLSs. These combinations of NLSs in the context of a single fusion protein conferred nuclear accumulation of GFP. NLS4 and NLS5 together weakly conferred nuclear accumulation, whereas NLS1, NLS2, and NLS3 fused to NLS4 and/or NLS5 conferred strong nuclear accumulation. Taken together, these results strongly indicate that the five classical NLSs and the bipartite NLS can cooperatively target AreA to the nucleus.

DISCUSSION

The presence of sequences capable of interacting with nuclear transport machinery is a vital component for nuclear entry of most transcription factors. We have now shown that AreA has multiple functional NLSs. The RRX₃₃RXR bipartite NLS is conserved in filamentous fungal AreA orthologs, in the *A. nidulans* GATA factors AreB and SreA, *S. cerevisiae* negative-acting GATA factors Dal80p and Gzf3p, and in mammalian GATA factors. *S. cerevisiae* Gat1p has a conservative substitution of one of the bipartite NLS arginines for lysine, and it is conceivable that this sequence may act as an NLS. In *S. cerevisiae* Gln3p, however, there is a nonconservative substitution in one of the key arginine residues, and evidence that this region does not serve as a functional NLS (20). The five classical NLSs found in AreA are conserved across most of the filamentous fungi but not in the *S. cerevisiae* nitrogen GATA factors. These NLSs appear to work together in various combinations to mediate nuclear import, and the bipartite NLS is independently able to localize AreA to the nucleus. The four arginine residues in the bipartite NLS are critical for AreA-dependent gene expression as seen in growth tests on a range of nitrogen nutrients and in *fmdS-lacZ* reporter gene assays. This is likely due to the fact that they are DNA contact residues in the AreA zinc finger, and the arginine-to-alanine mutations likely disrupt AreA DNA binding (89). Mutation of these four arginine residues simultaneously in the GATA-4 bipartite NLS abolishes nuclear localization, and mutation of any of the four residues abolishes or severely inhibits DNA binding and transcriptional activation (10). Although mutation of the bipartite NLS abolishes AreA function, the bipartite NLS mutant AreA protein accumulates in the nucleus during nitrogen starvation. However, when we deleted all five of the classical NLSs and mutated the bipartite NLS simultaneously, AreA was not functional and did not accumulate in the nucleus.

There is a stark mechanistic difference in the localization of *A. nidulans* AreA compared with its *S. cerevisiae* homolog Gln3p. In *S. cerevisiae*, nuclear import is the regulated step, as Gln3p is held in the cytoplasm by a cytoplasmic anchor Ure2p during nitrogen-sufficient conditions (28). During nitrogen limitation, dephosphorylation of Gln3p and Ure2p leads to release of Gln3p, and Gln3p is imported into the nucleus (20, 28). Gln3p has only one functional classical NLS that is inactivated by cytoplasmic anchoring (20). A second potential NLS in Gln3p was found to be dispensable for nuclear import (20). In contrast, AreA nuclear localization is regulated primarily by nuclear export via CrmA, as the export in response to the addition of nitrogen nutrients of AreA is

rapid (46). The kinetics of AreA nuclear accumulation, however, are slow, and we have found no evidence for differential regulation of AreA nuclear import.

AreA is unusual in the large number of NLSs it contains. Nuclear localization signals in other transcription factors are quite variable in both type and number. For many transcription factors, a single NLS mediates nuclear import. For example, *A. nidulans* PrnA, the constitutively nuclear transcriptional activator for proline utilization pathway genes, has a tripartite NLS located in its N-terminal region (15). A single NLS is also found in other *A. nidulans* transcription factors: AlcR, NirA and AmyR each have a tripartite NLS (16, 17, 31), and VeA and PacC have a classical bipartite NLS (32, 90, 91). There are many examples of nuclear proteins containing multiple NLSs; however, there are usually no more than three (24, 26). *A. nidulans* HapB has two monopartite NLSs located in the C-terminal domain (18, 19). One of these NLSs is conserved in fungal, yeast, and human HapB orthologs, and is functional in *A. nidulans* HapB, *S. cerevisiae* Hap2p, and human NF-YA proteins expressed in *S. cerevisiae* (19). The other NLS is found only in the aspergilli, but it is required for nuclear localization of HapB in *A. nidulans* (19). Both NLSs are functional in *Aspergillus oryzae* HapB (92). The AreA NLSs show apparent redundancy in their ability to promote localization of AreA and GFP to the nucleus. If these sequences share truly redundant functions, we might expect them to be lost over time in different lineages. However, all of the NLSs are conserved across most fungal species, suggesting that each NLS has an important and unique function. One possibility is that AreA may use alternative importins for nuclear import under different growth conditions due to differential expression of importins. *A. nidulans* has 17 nuclear importins, but the expression of these across different growth conditions has not been determined (12). Alternatively, multiple NLSs could allow for more-efficient nuclear import. The cooperativity we observed for the AreA classical NLSs suggests low binding affinities of individual NLSs to nuclear importin(s). α -Importin binds to different NLSs, including classical NLSs, via either of two NLS-binding grooves (93). Binding of multiple AreA NLSs to different binding grooves of importin(s) may confer stronger binding affinity and more-efficient nuclear import. The RRR₃₃RXR bipartite NLS of GATA-4 interacts with β -importin, but not α -importin (10). If the interaction with β -importin is conserved for AreA, the AreA NLSs may mediate interaction with both importins of the α -importin- β -importin complex.

The presence of multiple NLSs has been proposed to allow for multiple regulatory steps for import to mediate a gradation of nuclear protein levels under different conditions compared with having only a single strong NLS, which could function more like an on/off switch (24). None of our observations suggest that nuclear import of AreA is differentially regulated or that the six AreA NLSs allow varied levels of nuclear import depending on nitrogen conditions. We have demonstrated a high degree of redundancy of the NLSs in AreA. Either the bipartite NLS alone or the classical NLSs together can strongly promote protein accumulation into the nucleus. What is unclear is why this functional redundancy has not been curtailed by evolution. This hints to the possibility of various importins recognizing AreA to ensure import during constantly changing environmental conditions and nitrogen nutrient availability.

ACKNOWLEDGMENTS

This work was supported by the Australian Research Council's Discovery Projects funding scheme project DP0558002 (M.A.D. and R.B.T.), a K-INBRE ARRA Scholarship supported by award P20RR016475 from the National Center for Research Resources (NCRR) (C.C.H.), Kansas NSF EPSCoR First Award EPS-0903806 (R.B.T.), Kansas State University Plant Biotechnology Center (R.B.T.), and the Johnson Center for Basic Cancer Research (R.B.T.).

The content of this article is solely the responsibility of the authors and does not necessarily represent the official views of the NCRR or the National Institutes of Health.

We acknowledge the expert technical assistance of K. Nguyen, M. Wallis, M. Ghosn, K. Smith, J. Bowne, S. Murray, G. Y. Busot, and B. T. Pfannenstiel and preliminary GFP fusion analysis by M. C. Zanker.

REFERENCES

- Feldherr CM, Kallenbach E, Schultz N. 1984. Movement of a karyophilic protein through the nuclear pores of oocytes. *J. Cell Biol.* 99:2216–2222. <http://dx.doi.org/10.1083/jcb.99.6.2216>.
- Tran EJ, Bolger TA, Wente SR. 2007. Snapshot: nuclear transport. *Cell* 131:420. <http://dx.doi.org/10.1016/j.cell.2007.10.015>.
- Mattaj JW, Englmeier L. 1998. Nucleocytoplasmic transport: the soluble phase. *Annu. Rev. Biochem.* 67:265–306. <http://dx.doi.org/10.1146/annurev.biochem.67.1.265>.
- De Souza CP, Horn KP, Masker K, Osmani SA. 2003. The SONB- (NUP98) nucleoporin interacts with the NIMA kinase in *Aspergillus nidulans*. *Genetics* 165:1071–1081.
- De Souza CP, Osmani AH, Hashmi SB, Osmani SA. 2004. Partial nuclear pore complex disassembly during closed mitosis in *Aspergillus nidulans*. *Curr. Biol.* 14:1973–1984. <http://dx.doi.org/10.1016/j.cub.2004.10.050>.
- Osmani AH, Davies J, Liu HL, Nile A, Osmani SA. 2006. Systematic deletion and mitotic localization of the nuclear pore complex proteins of *Aspergillus nidulans*. *Mol. Biol. Cell* 17:4946–4961. <http://dx.doi.org/10.1091/mbc.E06-07-0657>.
- Jans DA, Xiao CY, Lam MH. 2000. Nuclear targeting signal recognition: a key control point in nuclear transport? *Bioessays* 22:532–544. [http://dx.doi.org/10.1002/\(SICI\)1521-1878\(200006\)22:6<532::AID-BIES6>3.0.CO;2-O](http://dx.doi.org/10.1002/(SICI)1521-1878(200006)22:6<532::AID-BIES6>3.0.CO;2-O).
- Dingwall C, Sharnick SV, Laskey RA. 1982. A polypeptide domain that specifies migration of nucleoplasm into the nucleus. *Cell* 30:449–458. [http://dx.doi.org/10.1016/0092-8674\(82\)90242-2](http://dx.doi.org/10.1016/0092-8674(82)90242-2).
- Kalderon D, Roberts BL, Richardson WD, Smith AE. 1984. A short amino acid sequence able to specify nuclear location. *Cell* 39:499–509. [http://dx.doi.org/10.1016/0092-8674\(84\)90457-4](http://dx.doi.org/10.1016/0092-8674(84)90457-4).
- Philips AS, Kwok JC, Chong BH. 2007. Analysis of the signals and mechanisms mediating nuclear trafficking of GATA-4. Loss of DNA binding is associated with localization in intranuclear speckles. *J. Biol. Chem.* 282:24915–24927.
- Araujo-Bazan L, Dhingra S, Chu J, Fernandez-Martinez J, Calvo AM, Espeso EA. 2009. Importin alpha is an essential nuclear import carrier adaptor required for proper sexual and asexual development and secondary metabolism in *Aspergillus nidulans*. *Fungal Genet. Biol.* 46:506–515. <http://dx.doi.org/10.1016/j.fgb.2009.03.006>.
- Markina-Inarrairaegui A, Etxebeste O, Herrero-Garcia E, Araujo-Bazan L, Fernandez-Martinez J, Flores JA, Osmani SA, Espeso EA. 2011. Nuclear transporters in a multinucleated organism: functional and localization analyses in *Aspergillus nidulans*. *Mol. Biol. Cell* 22:3874–3886. <http://dx.doi.org/10.1091/mbc.E11-03-0262>.
- Robbins J, Dilworth SM, Laskey RA, Dingwall C. 1991. Two interdependent basic domains in nucleoplasmic nuclear targeting sequence: identification of a class of bipartite nuclear targeting sequence. *Cell* 64:615–623. [http://dx.doi.org/10.1016/0092-8674\(91\)90245-T](http://dx.doi.org/10.1016/0092-8674(91)90245-T).
- El Alami M, Feller A, Pierard A, Dubois E. 2000. Characterisation of a tripartite nuclear localisation sequence in the regulatory protein Lys14 of *Saccharomyces cerevisiae*. *Curr. Genet.* 38:78–86. <http://dx.doi.org/10.1007/s002940000134>.
- Pokorska A, Drevet C, Scazzocchio C. 2000. The analysis of the transcriptional activator PrnA reveals a tripartite nuclear localisation sequence. *J. Mol. Biol.* 298:585–596. <http://dx.doi.org/10.1006/jmbi.2000.3666>.
- Nikolaev I, Cochet MF, Felenbok B. 2003. Nuclear import of zinc binuclear cluster proteins proceeds through multiple, overlapping transport

- pathways. *Eukaryot. Cell* 2:209–221. <http://dx.doi.org/10.1128/EC.2.2.209-221.2003>.
17. Berger H, Pachlinger R, Morozov I, Goller S, Narendja F, Caddick M, Strauss J. 2006. The GATA factor AreA regulates localization and in vivo binding site occupancy of the nitrate activator NirA. *Mol. Microbiol.* 59:433–446. <http://dx.doi.org/10.1111/j.1365-2958.2005.04957.x>.
 18. Steidl S, Tuncher A, Goda H, Guder C, Papadopoulou N, Kobayashi T, Tsukagoshi N, Kato M, Brakhage AA. 2004. A single subunit of a heterotrimeric CCAAT-binding complex carries a nuclear localization signal: piggy back transport of the pre-assembled complex to the nucleus. *J. Mol. Biol.* 342:515–524. <http://dx.doi.org/10.1016/j.jmb.2004.07.011>.
 19. Tuncher A, Sprote P, Gehrke A, Brakhage AA. 2005. The CCAAT-binding complex of eukaryotes: evolution of a second NLS in the HapB subunit of the filamentous fungus *Aspergillus nidulans* despite functional conservation at the molecular level between yeast, *A. nidulans* and human. *J. Mol. Biol.* 352:517–533. <http://dx.doi.org/10.1016/j.jmb.2005.06.068>.
 20. Carvalho J, Zheng XF. 2003. Domains of Gln3p interacting with karyopherins, Ure2p, and the target of rapamycin protein. *J. Biol. Chem.* 278:16878–16886. <http://dx.doi.org/10.1074/jbc.M300429200>.
 21. Burich R, Lei M. 2003. Two bipartite NLSs mediate constitutive nuclear localization of Mcm10. *Curr. Genet.* 44:195–201. <http://dx.doi.org/10.1007/s00294-003-0443-y>.
 22. Chen CF, Li S, Chen Y, Chen PL, Sharp ZD, Lee WH. 1996. The nuclear localization sequences of the BRCA1 protein interact with the importin- α subunit of the nuclear transport signal receptor. *J. Biol. Chem.* 271:32863–32868. <http://dx.doi.org/10.1074/jbc.271.51.32863>.
 23. Yano K, Morotomi K, Saito H, Kato M, Matsuo F, Miki Y. 2000. Nuclear localization signals of the BRCA2 protein. *Biochem. Biophys. Res. Commun.* 270:171–175. <http://dx.doi.org/10.1006/bbrc.2000.2392>.
 24. Luo M, Pang CW, Gerken AE, Brock TG. 2004. Multiple nuclear localization sequences allow modulation of 5-lipoxygenase nuclear import. *Traffic* 5:847–854. <http://dx.doi.org/10.1111/j.1600-0854.2004.00227.x>.
 25. Xiao SJ, Wang LY, Kimura M, Kojima H, Kunimoto H, Nishiumi F, Yamamoto N, Nishio K, Fujimoto S, Kato T, Kitagawa S, Yamane H, Nakajima K, Inoue A. 2013. S1-1/RBM10: multiplicity and cooperativity of nuclear localisation domains. *Biol. Cell* 105:162–174. <http://dx.doi.org/10.1111/boc.201200068>.
 26. Reisenauer MR, Wang SW, Xia Y, Zhang W. 2010. Dot1a contains three nuclear localization signals and regulates the epithelial Na⁺ channel (ENaC) at multiple levels. *Am. J. Physiol. Renal Physiol.* 299:F63–F76. <http://dx.doi.org/10.1152/ajprenal.00105.2010>.
 27. Li SJ, Qi Y, Zhao JJ, Li Y, Liu XY, Chen XH, Xu P. 2013. Characterization of nuclear localization signals (NLSs) and function of NLSs and phosphorylation of serine residues in subcellular and subnuclear localization of transformer-2beta (Tra2beta). *J. Biol. Chem.* 288:8898–8909. <http://dx.doi.org/10.1074/jbc.M113.456715>.
 28. Beck T, Hall MN. 1999. The TOR signalling pathway controls nuclear localization of nutrient-regulated transcription factors. *Nature* 402:689–692. <http://dx.doi.org/10.1038/45287>.
 29. De Vit MJ, Waddle JA, Johnson M. 1997. Regulated nuclear translocation of the Mig1 glucose repressor. *Mol. Biol. Cell* 8:1603–1618. <http://dx.doi.org/10.1091/mbc.8.8.1603>.
 30. Peleg Y, Addison R, Aramayo R, Metzberg RL. 1996. Translocation of *Neurospora crassa* transcription factor NUC-1 into the nucleus is induced by phosphorus limitation. *Fungal Genet. Biol.* 20:185–191. <http://dx.doi.org/10.1006/fgbi.1996.0034>.
 31. Makita T, Katsuyama Y, Tani S, Suzuki H, Kato N, Todd RB, Hynes MJ, Tsukagoshi N, Kato M, Kobayashi T. 2009. Inducer-dependent nuclear localization of a Zn(II)(2)Cys(6) transcriptional activator, AmyR, in *Aspergillus nidulans*. *Biosci. Biotechnol. Biochem.* 73:391–399. <http://dx.doi.org/10.1271/bbb.80654>.
 32. Mingot JM, Espeso EA, Diez E, Penalva MA. 2001. Ambient pH signaling regulates nuclear localization of the *Aspergillus nidulans* PacC transcription factor. *Mol. Cell. Biol.* 21:1688–1699. <http://dx.doi.org/10.1128/MCB.21.5.1688-1699.2001>.
 33. Poon IK, Jans DA. 2005. Regulation of nuclear transport: central role in development and transformation? *Traffic* 6:173–186. <http://dx.doi.org/10.1111/j.1600-0854.2005.00268.x>.
 34. Bertram PG, Choi JH, Carvalho J, Ai W, Zeng C, Chan TF, Zheng XF. 2000. Tripartite regulation of Gln3p by TOR, Ure2p, and phosphatases. *J. Biol. Chem.* 275:35727–35733. <http://dx.doi.org/10.1074/jbc.M004235200>.
 35. Scazzocchio C. 2000. The fungal GATA factors. *Curr. Opin. Microbiol.* 3:126–131. [http://dx.doi.org/10.1016/S1369-5274\(00\)00063-1](http://dx.doi.org/10.1016/S1369-5274(00)00063-1).
 36. Kudla B, Caddick MX, Langdon T, Martinez-Rossi NM, Bennett CF, Sibley S, Davies RW, Arst HN, Jr. 1990. The regulatory gene *areA* mediating nitrogen metabolite repression in *Aspergillus nidulans*. Mutations affecting specificity of gene activation alter a loop residue of a putative zinc finger. *EMBO J.* 9:1355–1364.
 37. Langdon T, Sheerins A, Ravagnani A, Gielkens M, Caddick MX, Arst HN, Jr. 1995. Mutational analysis reveals dispensability of the N-terminal region of the *Aspergillus* transcription factor mediating nitrogen metabolite repression. *Mol. Microbiol.* 17:877–888. http://dx.doi.org/10.1111/j.1365-2958.1995.mmi_17050877.x.
 38. Morozov IY, Galbis-Martinez M, Jones MG, Caddick MX. 2001. Characterization of nitrogen metabolite signalling in *Aspergillus* via the regulated degradation of *areA* mRNA. *Mol. Microbiol.* 42:269–277.
 39. Morozov IY, Martinez MG, Jones MG, Caddick MX. 2000. A defined sequence within the 3' UTR of the *areA* transcript is sufficient to mediate nitrogen metabolite signalling via accelerated deadenylation. *Mol. Microbiol.* 37:1248–1257. <http://dx.doi.org/10.1046/j.1365-2958.2000.02085.x>.
 40. Platt A, Langdon T, Arst HN, Jr, Kirk D, Tollervey D, Sanchez JM, Caddick MX. 1996. Nitrogen metabolite signalling involves the C-terminus and the GATA domain of the *Aspergillus* transcription factor AREA and the 3' untranslated region of its mRNA. *EMBO J.* 15:2791–2801.
 41. Andrianopoulos A, Kourambas S, Sharp JA, Davis MA, Hynes MJ. 1998. Characterization of the *Aspergillus nidulans* *nmrA* gene involved in nitrogen metabolite repression. *J. Bacteriol.* 180:1973–1977.
 42. Lamb HK, Ren J, Park A, Johnson C, Leslie K, Cocklin S, Thompson P, Mee C, Cooper A, Stammers DK, Hawkins AR. 2004. Modulation of the ligand binding properties of the transcription repressor NmrA by GATA-containing DNA and site-directed mutagenesis. *Protein Sci.* 13:3127–3138.
 43. Kotaka M, Johnson C, Lamb HK, Hawkins AR, Ren J, Stammers DK. 2008. Structural analysis of the recognition of the negative regulator NmrA and DNA by the zinc finger from the GATA-type transcription factor AreA. *J. Mol. Biol.* 381:373–382. <http://dx.doi.org/10.1016/j.jmb.2008.05.077>.
 44. Wong KH, Hynes MJ, Todd RB, Davis MA. 2007. Transcriptional control of *nmrA* by the bZIP transcription factor MeaB reveals a new level of nitrogen regulation in *Aspergillus nidulans*. *Mol. Microbiol.* 66:534–551. <http://dx.doi.org/10.1111/j.1365-2958.2007.05940.x>.
 45. Zhao X, Hume SL, Johnson C, Thompson P, Huang J, Gray J, Lamb HK, Hawkins AR. 2010. The transcription repressor NmrA is subject to proteolysis by three *Aspergillus nidulans* proteases. *Protein Sci.* 19:1405–1419. <http://dx.doi.org/10.1002/pro.421>.
 46. Todd RB, Fraser JA, Wong KH, Davis MA, Hynes MJ. 2005. Nuclear accumulation of the GATA factor AreA in response to complete nitrogen starvation by regulation of nuclear export. *Eukaryot. Cell* 4:1646–1653. <http://dx.doi.org/10.1128/EC.4.10.1646-1653.2005>.
 47. Michielse CB, Pfannmuller A, Macios M, Rengers P, Dzikowska A, Tudzynski B. 29 November 2013. The interplay between the GATA transcription factors AreA, the global nitrogen regulator and AreB in *Fusarium fujikuroi*. *Mol. Microbiol.* <http://dx.doi.org/10.1111/mmi.12472>.
 48. Todd RB, Davis MA, Hynes MJ. 2007. Genetic manipulation of *Aspergillus nidulans*: meiotic progeny for genetic analysis and strain construction. *Nat. Protoc.* 2:811–821. <http://dx.doi.org/10.1038/nprot.2007.112>.
 49. Downes DJ, Davis MA, Kreutzberger SD, Taig BL, Todd RB. 2013. Regulation of the NADP-glutamate dehydrogenase gene *gdhA* in *Aspergillus nidulans* by the Zn(II)2Cys6 transcription factor LeuB. *Microbiology* 159:2467–2480. <http://dx.doi.org/10.1099/mic.0.071514-0>.
 50. Cove DJ. 1966. The induction and repression of nitrate reductase in the fungus *Aspergillus nidulans*. *Biochim. Biophys. Acta* 113:51–56. [http://dx.doi.org/10.1016/S0926-6593\(66\)80120-0](http://dx.doi.org/10.1016/S0926-6593(66)80120-0).
 51. Nakai K, Horton P. 1999. PSORT: a program for detecting sorting signals in proteins and predicting their subcellular localization. *Trends Biochem. Sci.* 24:34–36. [http://dx.doi.org/10.1016/S0968-0004\(98\)01336-X](http://dx.doi.org/10.1016/S0968-0004(98)01336-X).
 52. Thompson JD, Gibson TJ, Higgins DG. 2002. Multiple sequence alignment using ClustalW and ClustalX. *Curr. Protoc. Bioinformatics Chapter 2:Unit 2.3*. <http://dx.doi.org/10.1002/0471250953.bi0203s00>.
 53. Arnaud MB, Cerqueira GC, Inglis DO, Skrzypek MS, Binkley J, Chibucos MC, Crabtree J, Howarth C, Orvis J, Shah P, Wymore F, Binkley G, Miyasato SR, Simison M, Sherlock G, Wortman JR. 2012. The *Aspergillus* Genome Database (AspGD): recent developments in comprehensive multispecies curation, comparative genomics and community resources. *Nucleic Acids Res.* 40:D653–D659. <http://dx.doi.org/10.1093/nar/gkr875>.
 54. MacCabe AP, Vanhanen S, Sollewign Gelpke MD, van de Vondervoort

- PJ, Arst HN, Jr, Visser J. 1998. Identification, cloning and sequence of the *Aspergillus niger* *areA* wide domain regulatory gene controlling nitrogen utilisation. *Biochim. Biophys. Acta* 1396:163–168. [http://dx.doi.org/10.1016/S0167-4781\(97\)00212-1](http://dx.doi.org/10.1016/S0167-4781(97)00212-1).
55. Christensen T, Hynes MJ, Davis MA. 1998. Role of the regulatory gene *areA* of *Aspergillus oryzae* in nitrogen metabolism. *Appl. Environ. Microbiol.* 64:3232–3237.
56. Chang PK, Yu J, Bhatnagar D, Cleveland TE. 2000. Characterization of the *Aspergillus parasiticus* major nitrogen regulatory gene, *areA*. *Biochim. Biophys. Acta* 1491:263–266. [http://dx.doi.org/10.1016/S0167-4781\(00\)00004-X](http://dx.doi.org/10.1016/S0167-4781(00)00004-X).
57. Tudzynski B, Homann V, Feng B, Marzluf GA. 1999. Isolation, characterization and disruption of the *areA* nitrogen regulatory gene of *Gibberella fujikuroi*. *Mol. Gen. Genet.* 261:106–114. <http://dx.doi.org/10.1007/s004380050947>.
58. Froeliger EH, Carpenter BE. 1996. *NUT1*, a major nitrogen regulatory gene in *Magnaporthe grisea*, is dispensable for pathogenicity. *Mol. Gen. Genet.* 251:647–656. <http://dx.doi.org/10.1007/BF02174113>.
59. Fu YH, Marzluf GA. 1990. *nit-2*, the major nitrogen regulatory gene of *Neurospora crassa*, encodes a protein with a putative zinc finger DNA-binding domain. *Mol. Cell. Biol.* 10:1056–1065.
60. Haas H, Bauer B, Redl B, Stoffer G, Marzluf GA. 1995. Molecular cloning and analysis of *nre*, the major nitrogen regulatory gene of *Penicillium chrysogenum*. *Curr. Genet.* 27:150–158. <http://dx.doi.org/10.1007/BF00313429>.
61. Gente S, Poussereau N, Fevre M. 1999. Isolation and expression of a nitrogen regulatory gene, *nmc*, of *Penicillium roqueforti*. *FEMS Microbiol. Lett.* 175:291–297. <http://dx.doi.org/10.1111/j.1574-6968.1999.tb13633.x>.
62. Coffman JA, Rai R, Cunningham T, Svetlov V, Cooper TG. 1996. Gat1p, a GATA family protein whose production is sensitive to nitrogen catabolite repression, participates in transcriptional activation of nitrogen-catabolic genes in *Saccharomyces cerevisiae*. *Mol. Cell. Biol.* 16:847–858.
63. Minehart PL, Magasanik B. 1991. Sequence and expression of *GLN3*, a positive nitrogen regulatory gene of *Saccharomyces cerevisiae* encoding a protein with a putative zinc finger DNA-binding domain. *Mol. Cell. Biol.* 11:6216–6228.
64. Cunningham TS, Cooper TG. 1991. Expression of the *DAL80* gene, whose product is homologous to the GATA factors and is a negative regulator of multiple nitrogen catabolic genes in *Saccharomyces cerevisiae*, is sensitive to nitrogen catabolite repression. *Mol. Cell. Biol.* 11:6205–6215.
65. Soussi-Boudekou S, Vissers S, Urrestarazu A, Jauniaux JC, Andre B. 1997. Gzf3p, a fourth GATA factor involved in nitrogen-regulated transcription in *Saccharomyces cerevisiae*. *Mol. Microbiol.* 23:1157–1168. <http://dx.doi.org/10.1046/j.1365-2958.1997.3021665.x>.
66. Conlon H, Zadra I, Haas H, Arst HN, Jr, Jones MG, Caddick MX. 2001. The *Aspergillus nidulans* GATA transcription factor gene *areB* encodes at least three proteins and features three classes of mutation. *Mol. Microbiol.* 40:361–375. <http://dx.doi.org/10.1046/j.1365-2958.2001.02399.x>.
67. Purschwitz J, Muller S, Kastner C, Schoser M, Haas H, Espeso EA, Atoui A, Calvo AM, Fischer R. 2008. Functional and physical interaction of blue- and red-light sensors in *Aspergillus nidulans*. *Curr. Biol.* 18:255–259. <http://dx.doi.org/10.1016/j.cub.2008.01.061>.
68. Haas H, Zadra I, Stoffer G, Angermayr K. 1999. The *Aspergillus nidulans* GATA factor SREA is involved in regulation of siderophore biosynthesis and control of iron uptake. *J. Biol. Chem.* 274:4613–4619. <http://dx.doi.org/10.1074/jbc.274.8.4613>.
69. Han KH, Han KY, Yu JH, Chae KS, Jahng KY, Han DM. 2001. The *nsdD* gene encodes a putative GATA-type transcription factor necessary for sexual development of *Aspergillus nidulans*. *Mol. Microbiol.* 41:299–309. <http://dx.doi.org/10.1046/j.1365-2958.2001.02472.x>.
70. Trainor CD, Evans T, Felsenfeld G, Boguski MS. 1990. Structure and evolution of a human erythroid transcription factor. *Nature* 343:92–96. <http://dx.doi.org/10.1038/343092a0>.
71. Zon LI, Tsai SF, Burgess S, Matsudaira P, Bruns GA, Orkin SH. 1990. The major human erythroid DNA-binding protein (GF-1): primary sequence and localization of the gene to the X chromosome. *Proc. Natl. Acad. Sci. U. S. A.* 87:668–672. <http://dx.doi.org/10.1073/pnas.87.2.668>.
72. Dorfman DM, Wilson DB, Bruns GA, Orkin SH. 1992. Human transcription factor GATA-2. Evidence for regulation of preproendothelin-1 gene expression in endothelial cells. *J. Biol. Chem.* 267:1279–1285.
73. Lee ME, Temizer DH, Clifford JA, Quertermous T. 1991. Cloning of the GATA-binding protein that regulates endothelin-1 gene expression in endothelial cells. *J. Biol. Chem.* 266:16188–16192.
74. Ko LJ, Yamamoto M, Leonard MW, George KM, Ting P, Engel JD. 1991. Murine and human T-lymphocyte GATA-3 factors mediate transcription through a cis-regulatory element within the human T-cell receptor delta gene enhancer. *Mol. Cell. Biol.* 11:2778–2784.
75. Ho IC, Vorhees P, Marin N, Oakley BK, Tsai SF, Orkin SH, Leiden JM. 1991. Human GATA-3: a lineage-restricted transcription factor that regulates the expression of the T cell receptor alpha gene. *EMBO J.* 10:1187–1192.
76. Huang WY, Cukerman E, Liew CC. 1995. Identification of a GATA motif in the cardiac alpha-myosin heavy-chain-encoding gene and isolation of a human GATA-4 cDNA. *Gene* 155:219–223. [http://dx.doi.org/10.1016/0378-1119\(94\)00893-W](http://dx.doi.org/10.1016/0378-1119(94)00893-W).
77. Gao X, Sedgwick T, Shi YB, Evans T. 1998. Distinct functions are implicated for the GATA-4, -5, and -6 transcription factors in the regulation of intestine epithelial cell differentiation. *Mol. Cell. Biol.* 18:2901–2911.
78. Suzuki E, Evans T, Lowry J, Truong L, Bell DW, Walsh K. 1996. The human GATA-6 gene: structure, chromosomal location, and regulation of expression by tissue-specific and mitogen-responsive signals. *Genomics* 38:283–290. <http://dx.doi.org/10.1006/geno.1996.0630>.
79. Arceci RJ, King AA, Simon MC, Orkin SH, Wilson DB. 1993. Mouse GATA-4: a retinoic acid-inducible GATA-binding transcription factor expressed in endodermally derived tissues and heart. *Mol. Cell. Biol.* 13:2235–2246.
80. Sambrook J, Russell DW. 2001. *Molecular cloning: a laboratory manual*, 3rd ed. Cold Spring Harbor Laboratory Press, Cold Spring Harbor, NY.
81. Oakley CE, Weil CF, Kretz PL, Oakley BR. 1987. Cloning of the *riboB* locus of *Aspergillus nidulans*. *Gene* 53:293–298. [http://dx.doi.org/10.1016/0378-1119\(87\)90019-9](http://dx.doi.org/10.1016/0378-1119(87)90019-9).
82. Nayak T, Szewczyk E, Oakley CE, Osmani A, Ukil L, Murray SL, Hynes MJ, Osmani SA, Oakley BR. 2006. A versatile and efficient gene-targeting system for *Aspergillus nidulans*. *Genetics* 172:1557–1566.
83. Small AJ, Todd RB, Zanker MC, Delimitrou S, Hynes MJ, Davis MA. 2001. Functional analysis of TamA, a coactivator of nitrogen-regulated gene expression in *Aspergillus nidulans*. *Mol. Genet. Genomics* 265:636–646. <http://dx.doi.org/10.1007/s004380100456>.
84. Davis MA, Cobbett CS, Hynes MJ. 1988. An *amdS-lacZ* fusion for studying gene regulation in *Aspergillus*. *Gene* 63:199–212. [http://dx.doi.org/10.1016/0378-1119\(88\)90525-2](http://dx.doi.org/10.1016/0378-1119(88)90525-2).
85. Bradford MM. 1976. A rapid and sensitive method for the quantitation of microgram quantities of protein utilizing the principle of protein-dye binding. *Anal. Biochem.* 72:248–254. [http://dx.doi.org/10.1016/0003-2697\(76\)90527-3](http://dx.doi.org/10.1016/0003-2697(76)90527-3).
86. Hicks GR, Raikhel NV. 1995. Nuclear localization signal binding proteins in higher plant nuclei. *Proc. Natl. Acad. Sci. U. S. A.* 92:734–738. <http://dx.doi.org/10.1073/pnas.92.3.734>.
87. Fraser JA, Davis MA, Hynes MJ. 2001. The formamidase gene of *Aspergillus nidulans*: regulation by nitrogen metabolite repression and transcriptional interference by an overlapping upstream gene. *Genetics* 157:119–131.
88. Suelmann R, Sievers N, Fischer R. 1997. Nuclear traffic in fungal hyphae: in vivo study of nuclear migration and positioning in *Aspergillus nidulans*. *Mol. Microbiol.* 25:757–769. <http://dx.doi.org/10.1046/j.1365-2958.1997.5131873.x>.
89. Starich MR, Wikstrom M, Arst HN, Jr, Clore GM, Gronenborn AM. 1998. The solution structure of a fungal AREA protein-DNA complex: an alternative binding mode for the basic carboxyl tail of GATA factors. *J. Mol. Biol.* 277:605–620. <http://dx.doi.org/10.1006/jmbi.1998.1625>.
90. Stinnett SM, Espeso EA, Cobeno L, Araujo-Bazan L, Calvo AM. 2007. *Aspergillus nidulans* VeA subcellular localization is dependent on the importin alpha carrier and on light. *Mol. Microbiol.* 63:242–255. <http://dx.doi.org/10.1111/j.1365-2958.2006.05506.x>.
91. Fernandez-Martinez J, Brown CV, Diez E, Tilburn J, Arst HN, Jr, Penalva MA, Espeso EA. 2003. Overlap of nuclear localisation signal and specific DNA-binding residues within the zinc finger domain of PacC. *J. Mol. Biol.* 334:667–684. <http://dx.doi.org/10.1016/j.jmb.2003.09.072>.
92. Goda H, Nagase T, Tanoue S, Sugiyama J, Steidl S, Tuncher A, Kobayashi T, Tsukagoshi N, Brakhage AA, Kato M. 2005. Nuclear translocation of the heterotrimeric CCAAT binding factor of *Aspergillus oryzae* is dependent on two redundant localising signals in a single subunit. *Arch. Microbiol.* 184:93–100. <http://dx.doi.org/10.1007/s00203-005-0014-3>.
93. Kosugi S, Hasebe M, Matsumura N, Takashima H, Miyamoto-Sato E, Tomita M, Yanagawa H. 2009. Six classes of nuclear localization signals specific to different binding grooves of importin alpha. *J. Biol. Chem.* 284:478–485. <http://dx.doi.org/10.1074/jbc.M807017200>.